A Theory for Modified Conservation Principles Optimization of CFD Algorithm Fidelity

A dissertation

Presented for the

Doctor of Philosophy Degree

The University of Tennessee, Knoxville

Sunil Sahu

August, 2006

This research is dedicated to the memory of my father Late Shri C. L. Sahu whose principled life has been a guiding force for many including myself

Acknowledgment

I would like to thank my major professor Dr. Allen J. Baker for his help, encouragement, advice and financial support that was rendered during my PhD program. This dissertation was possible only because of the exceptional learning environment provided by him. I would also like to thank my dissertation committee, Profs. Charles Collins, Suzanne Lenhart and Mohamed Mahfouz, for their assistance rendered during my dissertation research. In addition I would like to thank my colleagues Shawn Ericson, Joe Orzechowski and Marcel Grubert for their countless hours of valuable discussion and technical help.

I owe a debt of gratitude to my Mother Smt. Rukmani Sahu and Brothers Mr. Satish and Mr. Sanjay, who were always there for me. Their warm support and optimism kept me on track during these past few years and made the completion of this dissertation a reality when it looked almost impossible.

Abstract

A theory is developed in one and two space dimensions that successfully predicts optimal algorithm constructions for the convection operator intrinsic to unsteady Navier-Stokes (NS) problem statements. The analysis statement is parameterized via a Taylor series (TS) modification to the parent NS conservation principles statements. Phase velocity and amplification factor error analyses are enabled via weak form discretized implementations assembled at the generic node. The parameterized error statement is then resolved into a Taylor series expansion in non-dimensional wave number space, admitting identifications that progressively annihilate lowest order error terms. The theory computational implementation is via a Galerkin weak statement on the TS modified formulation, discretely implemented using linear and bi-linear finite element basis functions for one and two dimensions respectively.

The theory is extended to one dimension FE quadratic basis. A general formulation for TWS class of algorithms enabling analysis for phase accuracy is derived. Matrix stability analysis approach pertinent to TWS algorithms is presented. Theory suggested results are ported to other verification and validation problems and analyzed for solution fidelity. One dimensional space test cases include advection-diffusion and non-linear Burgers equation. Two-dimensional space test cases include a pure advection verification problem, an advection-diffusion-source verification problem and 8x1 full Navier-Stokes validation-class thermal cavity problem. Algorithm predictability is also

compared for the selected algorithms on non-uniform Cartesian and regular but non-Cartesian triangular mesh.

A computational approach to obtain progressively higher order phase accurate solutions using a Matlab enabled optimization theory has also been examined. The unusual behavior algorithms thus generated are analyzed under the anomalous behavior topic generated by this approach.

Contents

Chapter **Page**

1. Introduction 1

1.1. Motivation and history 1

1.2. Fourier modal analysis 3

1.3. This dissertation 7

2. Modified Conservation Principles Formulation 9

2.1. Problem statement 9

2.2. The modified conservation principles parameterization 10

3. Taylor Weak Statement Finite Element Implementation 12

3.1. TWS algorithm formulation 12

3.2. TWS formulation for one-dimensional linear problems 14

3.3. TWS formulation for one-dimensional non-linear Burgers equation 16

3.4. TWS formulation for two-dimensional advection-diffusion-source problem 18

3.5. TWS formulation for two-dimensional NS thermal cavity problem 19

4. Theoretical Development and Analysis 20

4.1. One-dimension 20

4.2 Two-dimensions 37

4.3 Matrix stability analysis 41

5. Discussion and Results 43

5.1. Pure advection, one dimensional scalar transport 43

5.2. Algorithm automated optimization 45

5.3. Advection-diffusion in one dimension 46

5.4. One dimensional Burgers equation 48

5.5. Pure advection two dimensional scalar transport 51

5.6. Gaussian plume advection-diffusion with source 53

5.7. Thermal cavity Navier-Stokes problem 55

5.8. Identified algorithm anomalous behavior 59

6. Conclusions and Recommendations 62

Bibliography 65

Appendices 71

Appendix I 72

Tables 72

Appendix II 81

Figures 81

Appendix III 125

TS expansion of amplification factor modulus error in orders of non-D wave number for TWS^h + θTS algorithms for 1D pure advection 125

Appendix IV 127

Matlab script for computing relative phase velocity spectral distribution for FE quadratic basis 127

Appendix V 129

TS expansion of amplification factor for TWS^h + θTS algorithms in orders of non-D wave number for 2D pure advection 129

Appendix VI 134

TS expansion of amplification factor phase error for TWS^h + θTS algorithms in orders of non-D wave number for 2D pure advection 134

Appendix VII 144

Matlab script for the 1D advection-diffusion 144

Appendix VIII 148

Matlab script for the 1D Burgers equation 148

Appendix IX 152

Matlab script for the rotating cone 152

Appendix X 158

aPSE model and template file for the NS thermal cavity problem 158

Vita 180

List of Tables

Table **Page**

Table 1.1. TWS formulation categorization of independently derived CFD algorithms. 73

Table 5.1. Summary of tested algorithms. 74

Table 5.2. Solution nodal extrema after 3-wavelength translation, Gaussian IC, 1-D pure advection. 75

Table 5.3. Amplification factor TS expansion coefficients in wavenumber space. 76

Table 5.4. Solution nodal extrema after 25 time-steps, Gaussian IC, 1-D advection-diffusion, Pe=10, 1000; C=1, M=40. 77

Table 5.5. 2D pure advection, algorithm nodal extrema after one rotation, $|\mathbf{C}| = 0.3$ at IC centroid. 78

Table 5.6. Temperature global energy norm, Ra = 3.4E+07 and 3.4E+08. 79

Table 5.7. Stream-function extrema, Ra = 3.4 E+07. 80

List of Figures

Figure **Page**

Figure 1.1. Wave number vector and phase velocity in the Cartesian continuum..... 82

Figure 4.1. FE basis nodalization, (a) linear1D (b) quadratic 1D, (c) linear, 2D. 83

Figure 4.2. TWS algorithm discrete solution TS coefficients in non-D wave-number space, 1D pure advection. a) C =0.25, b) C = 0.5, c) C = 1.0. 84

Figure 4.3. Phase velocity and amplification factor modulus error, 1D pure advection, C = 0.5, k =1, θ = 0.5 (except for TG)..... 86

Figure 4.4. Phase velocity error, 1D pure advection, C = 0.5, k =2, θ = 0. 87

Figure 4.5. Phase velocity error, 1D pure advection, C = 0.5, k =2, θ = 0.5. 88

Figure 4.6. Sample space of wave vector angles for TS theoretical error quantization. 89

Figure 4.7. Theoretical Taylor series wave number dependence for TWS^h + θTS algorithms, 2D pure advection, η = 3π/4, 0.19 < C < 0.41. 90

Figure 4.8. Theoretical Taylor series wave number dependence for TWS^h + θTS algorithms, 2D pure advection, η = 5π/8, 0.19 < C < 0.41. 92

Figure 4.9. Theoretical Taylor series wave number dependence for GWS^h, TWS^h + θTS algorithms, 2D pure advection, η = π/2, 5π/8, 3π/4, |**C**| = 0.41. 94

Figure 5.1. 1D pure advection of a Gaussian IC, C = 0.5, dashed line is exact solution, following 3 IC wavelength translation. 95

Figure 5.2. 1D pure advection of a Gaussian initial distribution, C = 1.0, dashed line is exact solution following 3-wavelength translation. 96

Figure 5.3. 1D pure advection of a square wave IC for TWS-γ, C = 1.0, dashed line is exact solution following 7-wavelength translation. 97

Figure 5.4. 1D pure advection of a Gaussian initial distribution for CN and CNm, C = 1.0, dashed line is exact solution following 3-wavelength translation. 98

Figure 5.5 Time evolution of Gaussian IC, optimization code suggested parameter sets and various C. 99

Figure 5.6. 1D advection-diffusion, solution after 25 time-steps, Pe=10, C=1. 100

Figure 5.7. 1D advection-diffusion, solution after 25 time-steps, Pe=1000, C=1. 101

Figure 5.8. Burgers Equation, semi-implicit β, time = 0, 0.2, 0.6, 1.0, 1.4, 2.0, M=200. 102

Figure 5.9. Burgers equation, fully-implicit β, time = 0, 0.2, 0.6, 1.0, 1.4, 2.0, M=200. 106

Figure 5.10 Gaussian IC and exact solution for the 2D rotating cone verification problem 108

Figure 5.11. 2D pure advection rotating cone verification problem, discrete solutions after one revolution, uniform Cartesian mesh, |**C**| = 0.3 at IC centroid..... 109

Figure 5.12. 2D pure advection rotating cone verification problem, discrete solutions after one revolution, non-uniform Cartesian mesh, |**C**| = 0.3 at IC centroid..... 110

Figure 5.13. 2D pure advection rotating cone verification problem, uniform-triangular mesh and discrete solutions after one revolution, uniform triangular mesh, |**C**| = 0.3 at IC centroid, M = 2048. 111

Figure 5.14. Advection-diffusion with source, M= 20x20, M = 80x80. 112

Figure 5.15. Thermal cavity set, 8x1 aspect ratio. 113

Figure 5.16. M=41x201, non-uniform mesh, a) full-mesh, b) close-up. 114

Figure 5.17. Temperature distribution after 1500 time steps for GWS and TWS-γ, Ra=3.4E+07, M=41x201. 115

Figure 5.18. Close-up of the temperature distribution after 1500 time steps for GWS and TWS-γ, Ra=3.4E+07, M=41x201. 116

Figure 5.19. Temperature energy norm distribution after 1500 time steps for GWS and TWS-γ, Ra=3.4E+07, M=41x201. 117

Figure 5.20. Stream function distribution after 1500 time steps for GWS and TWS-γ, Ra=3.4E7. M=41x201. 118

Figure 5.21. Temperature distribution after 1500 time steps for GWS and TWS-γ, Ra=3.4E+08. 119

Figure 5.22. Temperature energy norm distribution after 1500 time steps for GWS and TWS-γ, Ra=3.4E+08. 120

Figure 5.23. Stream-function distribution after 1500 time steps for GWS and TWS-γ, Ra=3.4E+08, M=41x201. 121

Figure 5.24. 1D pure advection of a Gaussian initial distribution, C = 1.0, RGm with α=100=β, dashed line is exact solution following 3-wavelength translation. 122

Figure 5.25. Phase velocity and amplification factor modulus error, C = 1.0, θ = 0.5. 123

Figure 5.26. Phase velocity and amplification factor modulus error, C=0.5, θ=1.0..... 124

List of Symbols

c_p	mass-specific heat capacity
$\hat{g}_i$	gravity vector
u_i	velocity vector
h	mesh size
k	FE basis degree
m	non-dimensional wave number
n	dimensionality
s	source
t	time
G^h	Numerical amplification factor
T	temperature
C	Courant number
Gr	Grashof number
Ra	Rayleigh number
Re	Reynolds number
Pr	Prandtl number

Greek symbols

α	Thermal diffusivity
α	Taylor weak statement correction parameter
β	coefficient of thermal expansion
β	Taylor weak statement correction parameter
γ	Taylor weak statement correction parameter

μ	Taylor weak statement correction parameter
υ	kinematic viscosity
ρ_0	constant reference density
θ	Implicit parameter
κ	wave number
ω	Cylic frequency
ϕ	Amplitude, ratio of non-vertex node to vertex node
Θ	Potential temperature

Chapter 1

1. Introduction

1.1. Motivation and history

Computational fluid dynamics (CFD) is the name of the field given to generation of approximate numerical solutions to fluid-thermal flow problems. In the past decade CFD has matured to significantly enhance and complement the classical theoretical and experimental understanding of the problem class. The ultimate goal of CFD is to incorporate it into the engineering design phase, and hence to moderate the need for experimental testing. Hence, the fundamental CFD quest is to obtain best possible solution. The multitude of numerical techniques proposed by numerous researchers to solve fluid-thermal flow problems exhibit far from satisfactory performance. This research is an effort in the direction of generating more mathematically precise, hence more predictable performance algorithms.

CFD in one form or an other attempts to “solve” the fundamental conservation principles of mass, momentum and energy, which define the physics of the fluid-thermal problem [1]. It is a process in which approximate solutions are obtained to the resultant partial differential equation (PDE) system. The most commonly used approximation procedure employ domain discretization via finite difference, finite volume and finite element methodology. This research uses the finite element implementation, as perceived

by this author for the mathematical elegance purely defined by calculus, and the ability of its theory to precisely qualify approximation error in intrinsic norms.

This research uses the standard Galerkin weak form theory approach, applied to modified conservation equation, which has its roots in the pioneering work of Donea [2]. He published the original modified conservation principle approach to weak form algorithm performance optimization, the time-explicit Taylor-Galerkin algorithm, and applied it to convective transport problems. Baker and Kim [3] generalized the approach, including the option for an implicit time formulation, in developing the parameterized Taylor weak statement (TWS) modified hyperbolic conservation law theory, and documented improved performance opportunities over the classical Galerkin (GWS) algorithm as well as TWS recovery of a dozen or more alternatively-derived algorithms

The TWS Taylor series (TS) analysis framework produces a modified restatement of fluid-thermal conservation principles PDE systems, *in the continuum*, parameterized by a set of algebraic coefficients associated with arbitrariness in the TS process, [3-4]. Upon theory completion, the error associated with generation of an approximate solution to the TS-modified conservation principle is rendered orthogonal to the approximation trial space in a Galerkin weak form construction, producing the genuine (optimal) constraint.

Superior performance of TWS over many algorithms has been documented for 1D and 2D pure advection problems, [3-6]. Furthermore, the TWS formulation process has

admitted generation of over a dozen independently derived CFD algorithms, simply by selecting appropriate values for the TS-generated parameter set $\{\alpha, \beta, \gamma, \mu, \theta\}$. Table 1.1[§] summarizes this observation for the one-dimensional, scalar advection-diffusion problem statement, for the linear finite element basis TWS discrete implementation, as augmented from the original publication, [3].

Chaffin and Baker [4] document TWS algorithm applications to the incompressible Navier-Stokes (INS) equations using a linear FE basis implementation with implicit time integration. Kolesnikov and Baker [5] developed the TS conservation principles modification approach to the steady INS system, which identified the identical tensor product *continuum term* associated with β of the unsteady theory in the limit of large Reynolds number. An added caveat of this TWS construction was prediction, and computational validation, of the linear FE basis implementation asymptotic convergence rate improvement to that associated with the quadratic basis implementation of a GWS algorithm for a INS benchmark problem.

1.2. Fourier modal analysis

For incisive comparative performance assessment of CFD algorithms, Fourier analysis is a preferred approach, admitting detailed phase velocity and amplitude error spectral distribution characterization. Vichnevetsky [7,8] reports on the results of Fourier analysis predicting phase and group velocity distributions for hyperbolic problem

§ All tables and figures are located in the appendix

statement algorithms implemented using both finite difference and finite element methods. Comparative phase and amplitude error analysis for finite difference schemes is reported by Morton and Mayers [9]. Shakib and Hughes [10] employ Fourier analysis to investigate the stability and accuracy of the space-time Galerkin-Least Squares method applied to advection-diffusion problems. Christon [11] studied the influence of the finite element mass matrix dispersive characteristics for a second-order wave equation. Belytschko and Mullen [12] used a generalized Fourier analyses approach to study the effects of consistent and lumped mass matrices on the phase speed for linear and quadratic finite element basis formulations. Christon et al [13,14] report on a generalized Fourier analyses approach and present a very detailed procedure for estimation of error in phase and group speeds, discrete diffusivity, and artificial diffusivity in 1D and 2D advection-diffusion problems.

Comparison of numerically generated solutions to an available analytical solution, classed as a verification problem, to 1D and 2D unsteady scalar transport problems underlies the analysis process. Due to the use of a mesh of measure h to support the discrete approximate solution process, it is well understood that the capability of an algorithm to resolve, hence propagate, solution spectral content of measure the order $2h$ is typically thoroughly compromised. This lack of resolution fidelity results in the cascading of solution short wave length content into longer wavelength spurious solution oscillations and is termed dispersion error. This dispersive error mechanism can be

moderated by embedding numerical diffusion, which then generates artificial dissipation error.

The mathematical analysis framework for characterizing dispersive and diffusive error mechanisms is briefly reviewed. Referring to Figure 1.1, the phase velocity **c** is the velocity of propagation of a solution component (called a "wave") of velocity **u** in the direction of the wave number vector **κ,** [15]. Mathematically,

$$\mathbf{c} = \frac{(\mathbf{u} \cdot \boldsymbol{\kappa})\boldsymbol{\kappa}}{\kappa^2} \tag{1.1}$$

where $\kappa \equiv |\boldsymbol{\kappa}|$ is the wave number, which quantifies the number of wave crests existing in the interval 2π in the direction of the wave vector angle η, [17]. Thereby, $\kappa=2\pi/\lambda$, where λ is the length of the wave between crests, i.e., wavelength, and $\boldsymbol{\kappa}$ is orthogonal to wave crests. In one dimension, the phase velocity becomes the scalar *c* identical with the magnitude of the imposed velocity of magnitude *u*. In the discretized solution process, *c* is no longer equal to *u*, but instead becomes a complex variable with only the real component related to *u*. Hence, any numerical approximation procedure should seek to minimize this error.

Group velocity is defined as the velocity with which sinusoidal waves propagate energy in a dispersive medium. Mathematically, in two dimensional rectangular Cartesian coordinates

$$\mathbf{G(\kappa)} = \nabla_{\kappa}\omega = \begin{bmatrix} \dfrac{\partial\omega}{\partial\kappa_1}\hat{\mathbf{i}} \\ \dfrac{\partial\omega}{\partial\kappa_2}\hat{\mathbf{j}} \end{bmatrix} \tag{1.2}$$

where ω represents the cyclic frequency, and $\kappa_1 = \kappa\cos\eta$ and $\kappa_2 = \kappa\sin\eta$ is wave number resolution in the *x* and *y* directions respectively. In the continuum, group velocity is independent of $\boldsymbol{\kappa}$ and is simply the fluid velocity. However, in the numerical approximation, phase and group velocity will differ due to wave number dependence. Further, in the discrete or dispersive case, the group velocity is not always aligned with the wave vector, but instead has a propagation direction φ defined by

$$\varphi = \tan^{-1}\left(\frac{G_y}{G_x}\right) = \tan^{-1}\left(\frac{\partial\omega/\partial\kappa_1}{\partial\omega/\partial\kappa_2}\right) \tag{1.3}$$

Reverting to one dimension, from (1) – (3)

$$G(\kappa) = \frac{\partial\omega(\kappa)}{\partial\kappa} = \frac{\partial\left(c(\kappa)\kappa\right)}{\partial\kappa} = c(\kappa) + \kappa\frac{\partial\left(c(\kappa)\right)}{\partial\kappa} \tag{1.4}$$

Hence, if phase speed *c* is independent of wave number κ, then group speed is equal to the phase speed. This is true in the continuum; however, in a discrete approximation, phase speed is typically wave number dependent, the theoretical characterization of which leads to the analysis opportunity.

1.3. This dissertation

This dissertation research aims to generate a theoretical foundation for optimization of a modified conservation principles CFD algorithm. An error extremization theory based on generation of an analysis statement amenable to optimization is developed. The mathematical foundation is phase velocity error characterization, with the theory results ultimately expressed in a Taylor series cast in non-dimensional wave number space. The theory is developed in completeness in one and two space dimensions, and verification employs available analytical solutions for the pure advection problem. The theory is analytically expressible only for spaces spanned by uniform discretization in rectangular Cartesian coordinates. Hence, numerical experiments are performed on non-uniform Cartesian and regular but non-Cartesian triangular meshes to characterize solution fidelity dependence on mesh organization.

Optimal linear and bi-linear FE basis algorithms are identified using the developed theory for the INS problem class. Their performance is compared to other algorithms of the "TWS-type" including Crank-Nicolson finite difference (CN), Raymond-Garder (RG), Jiang Least Squares (JLS), Taylor-Galerkin (TG) and classical Galerkin Weak Statement (GWS). The results generated from these comparative performance assessments are tested for optimal FE algorithm construction for the 1D advection-diffusion, 1D non-linear Burgers equation, 2D advection-diffusion with source and a 2D NS thermal cavity problem.

The theory is extended to TWS implementation using the FE one dimensional quadratic basis. The methodologies available for analytical determination of phase velocity for the complete TWS class of algorithms proved intractable, however numerical experiments did confirm existence of an optimal-γ algorithm. In addition, a Matlab enabled optimization theory is used to automate algorithm error extremization for FE linear basis. The resultant anomalous behavioral algorithms are identified, which expands the theoretical characterization envelope.

Chapter 2

2. Modified Conservation Principles Formulation

2.1. Problem statement

The focus is on the convection operator associated with the famous Navier-Stokes PDE system characterizing unsteady flow of a viscous, incompressible fluid including thermal effects. The incompressible Navier-Stokes (INS) conservation principles for mass, momentum and energy in non-dimensional tensor index form are

D*M*: $$\mathcal{L}(\rho_0) = \frac{\partial u_i}{\partial x_i} = 0 \tag{2.1}$$

D**P**: $$\mathcal{L}\left(u_i\right) = \frac{\partial u_i}{\partial t} + \frac{\partial}{\partial x_j}\left(u_i u_j + P\delta_{ij} - \mathrm{Re}^{-1}\frac{\partial u_i}{\partial x_j}\right) + \frac{\mathrm{Gr}\hat{g}_i}{\mathrm{Re}^2} = 0 \tag{2.2}$$

D*E*: $$\mathcal{L}(\Theta) = \frac{\partial \Theta}{\partial t} + u_i\frac{\partial \Theta}{\partial x_i} - \frac{1}{\mathrm{Re}\,\mathrm{Pr}}\frac{\partial^2 \Theta}{\partial x_i^{\,2}} - s = 0 \tag{2.3}$$

In (2.1)-(2.3), u_i is the velocity vector, $P = p/\rho_o$ is the kinematic pressure for ρ_o the constant density, Θ is the potential temperature and s is a heat source. The non-dimensional groups parameterizing solutions to (2.1)-(2.3) are

Grashoff number $$\mathrm{Gr} = \frac{g\beta\Delta T L^3}{\nu^2} \tag{2.4}$$

Reynolds number $$\mathrm{Re} = \frac{UL}{\nu} \tag{2.5}$$

Prandtl number $$\mathrm{Pr} = \frac{\rho_o \nu c_p}{k} \tag{2.6}$$

where β is thermal expansion coefficient associated with the Boussinesq approximation, [18], ν is kinematic viscosity, c_p is the heat capacity at constant pressure and k is the thermal conductivity.

The PDE system (2.2)-(2.3) constitutes an initial-value, elliptic boundary value (EBV) problem statement, solutions to which are subject to the differential constraint (2.1). Solutions to (2.1)-(2.3) are dominantly parameterized by Re, which is of order $10^4 \leq \mathrm{Re} \leq 10^6$ for realistic flow problems.

2.2. The modified conservation principles parameterization

The formulation for the Taylor series (TS) modified conservation principles construction is detailed in [3]. The resultant TS modified INS statement for D**P** generates the arbitrary parameter set $\{\alpha, \beta, \gamma, \mu\}$ of the form

$$\mathcal{L}^m(u_\mathrm{i}) = \mathcal{L}(u_\mathrm{i}) - \frac{\Delta t}{2}\frac{\partial}{\partial x_\mathrm{j}}\left(\alpha u_\mathrm{j}\frac{\partial u_\mathrm{i}}{\partial t} + \beta u_\mathrm{j}u_\mathrm{k}\frac{\partial u_\mathrm{i}}{\partial x_\mathrm{k}}\right) - \frac{\Delta t^2}{6}\frac{\partial}{\partial x_\mathrm{j}}\left[\gamma u_\mathrm{j}u_\mathrm{k}\frac{\partial}{\partial x_\mathrm{k}}\frac{\partial u_\mathrm{i}}{\partial t} + \mu u_\mathrm{j}u_\mathrm{k}\frac{\partial}{\partial x_\mathrm{k}}\left(u_\mathrm{m}\frac{\partial u_\mathrm{i}}{\partial x_\mathrm{m}}\right)\right] + O(\Delta t^3) = 0 \tag{2.7}$$

where $\mathcal{L}(u_\mathrm{i})$ remains (2.2) in completeness. The non-linearity in (2.7) severely limits theoretical analysis, which is not the case for scalar transport, e.g., (2.3). The corresponding TS-modified transport equation for any scalar variable $q(x_j,t)$ is

$$\mathcal{L}^m(q) = \mathcal{L}(q) - \frac{\Delta t}{2}\frac{\partial}{\partial x_\mathrm{j}}\left(\alpha u_\mathrm{j}\frac{\partial q}{\partial t} + \beta u_\mathrm{j}u_\mathrm{k}\frac{\partial q}{\partial x_\mathrm{k}}\right) - \frac{\Delta t^2}{6}\frac{\partial}{\partial x_\mathrm{j}}\left[\gamma u_\mathrm{j}u_\mathrm{k}\frac{\partial}{\partial x_\mathrm{k}}\frac{\partial q}{\partial t} + \mu u_\mathrm{j}u_\mathrm{k}\frac{\partial}{\partial x_\mathrm{k}}\left(u_\mathrm{m}\frac{\partial q}{\partial x_\mathrm{m}}\right)\right] + O(\Delta t^3) = 0 \tag{2.8}$$

which is amenable to the exacting theoretical analysis presented herein.

Chapter 3

3. Taylor Weak Statement Finite Element Implementation

3.1. TWS algorithm formulation

Any approximation solution q^N to (2.7)-(2.8) is defined as an inner product of a set of trial space functions $\Psi_\alpha(\mathbf{x})$ with a set of time-dependent expansion coefficients, specifically

$$q(\mathbf{x},t) \approx q^N(\mathbf{x},t) = \sum_{\alpha}^{N} \Psi_\alpha(\mathbf{x}) Q_\alpha(t) \tag{3.1}$$

Extremization of the error associated with the definition (3.1) accrues to a weak form construction with the Galerkin criterion that the test function space is identically the trial function space. This renders the associated error $e^N(\mathbf{x},t) = q(\mathbf{x},t) - q^N(\mathbf{x},t)$ orthogonal to the trial function set $\Psi_\alpha(\mathbf{x})$ which is optimal. Thereby, the "Taylor" weak form is

$$\mathrm{TWS}^N \equiv \int_\Omega \Psi_\beta \mathcal{L}^m(q^N) \mathrm{d}\tau \equiv \{0\}, \; \textit{for all } \beta \tag{3.2}$$

Assuming the integrals defined in (3.2) can be evaluated, all **x**-dependence vanishes yielding a large system of ordinary differential equations of the form

$$\mathrm{TWS}^N = [\mathrm{M}] \frac{\mathrm{d}\{Q\}}{\mathrm{d}t} + \{\mathrm{RES}\} = \{0\} \tag{3.3}$$

where [M] is the TWS parameter augmented "mass matrix" and {RES} contains all other contributions from (3.2). The single stage Euler TS with implicitness parameter θ is

$$\theta\text{TS:}\;\; Q_{n+1} = Q_n + \Delta t\left(\theta Q'_{n+1} + (1-\theta)Q'_n\right) + O(\Delta t^2, \Delta t^3) \tag{3.4}$$

From (3.3), $d\{Q\}/dt = \{Q\}' = -[M]^{-1}\{RES\}$, hence substituting into (3.4) and multiplying through by [M] yields the algebraic statement

$$TWS^h + \theta TS \Rightarrow [JAC(\alpha,\beta,\gamma,\mu,\theta,Re)]\{\Delta Q\} = -\{RES(Q,\alpha,\beta,\gamma,\mu,\theta,Re)\} \tag{3.5}$$

with solution essence

$$\{\Delta Q\} = [JAC]^{-1}\{RES\} \tag{3.6}$$

where [JAC] is the algorithm jacobian matrix and {RES} remains as originally defined.

The $TWS^h+\theta TS$ weak form theory is thus complete. What remains is to implement (3.2) - (3.6) in computable form, which invariably amounts to definition of $q^N(\mathbf{x},t)$ in a spatially discrete form, herein denoted $q^h(\mathbf{x},t)$. For this purpose, select the finite element trial space basis function set $\{N_k(\mathbf{x})\}$ containing a set of polynomials complete to degree k. Thereby, the classical asymptotic convergence theory, [19] predicts that for 1/Re > 0, i.e., viscous effects remain important, that the associated semi-discrete approximate solution error under mesh refinement is bounded at time t as,

$$\left\|e^h(t)\right\|_E \le C h_e^{2\gamma} \left\|\text{data}\right\|_{\Omega,\partial\Omega} + C_t \Delta t^{f(\theta)} \left\|q(\mathbf{x},0)\right\|^2_{H^1} \;,\; \gamma = \min(k, r\text{-}1) \tag{3.7}$$

where r is a smoothness measure of the exact solution and C is a constant independent of h, the measure of the computational mesh Ω^h associated with the FE basis discretization formed for $\{N_k(\mathbf{x})\}$. Also, the error contribution from the time-step Δt, as a function of θ is identified. In the instance of negligible viscous effect contribution, i.e., $1/\mathrm{Re} \Rightarrow 0$, the mesh measure exponent in (3.7) degenerates to $\gamma = \min(1, r-1)$, hence the asymptotic convergence rate is independent of the FE basis completeness degree k.

3.2. TWS formulation for one-dimensional linear problems

The TS modified scalar transport equation (2.8) simplified to one-dimension is

$$\begin{aligned}\mathcal{L}^m(q) = \frac{\partial q}{\partial t} + u\frac{\partial q}{\partial x} - \frac{1}{\mathrm{Pa}}\frac{\partial^2 q}{\partial x^2} - \frac{\Delta t}{2}\frac{\partial}{\partial x}\left(\alpha u\frac{\partial q}{\partial \mathrm{t}} + \beta u^2\frac{\partial q}{\partial x}\right) \\ - \frac{\Delta t^2}{6}\frac{\partial}{\partial x}\left[\gamma u^2\frac{\partial}{\partial x}\frac{\partial q}{\partial t} + \mu u^2\frac{\partial}{\partial x}\left(u\frac{\partial q}{\partial x}\right)\right] + O(\Delta t^3) = 0\end{aligned} \tag{3.8}$$

where Pa is the placeholder for the non-D parameter appropriate for q. (For (7), Pa = RePr, while for mass transport Pa = ReSc, for Sc the Schmidt number for binary diffusion.)

From (3.2) and (3.8), for FE basis such that test and trial functions are same the weak statement can be written as

$$\mathrm{TWS}^{N} = \int_{\Omega_e} \{\mathrm{N}_k\}\{\mathrm{N}_k^T\}\,\mathrm{dx}\,\{\mathrm{Q}'\} + \mathrm{u}\int_{\Omega_e} \{\mathrm{N}_k\}\frac{\partial\{\mathrm{N}_k^T\}}{\partial \mathrm{x}}\,\mathrm{dx}\,\{\mathrm{Q}\}$$
$$-\frac{\alpha \mathrm{u}\Delta \mathrm{t}}{2}\int_{\Omega_e} \{\mathrm{N}_k\}\frac{\partial\{\mathrm{N}_k^T\}}{\partial \mathrm{x}}\,\mathrm{dx}\,\{\mathrm{Q}'\} - \frac{\beta \mathrm{u}^2\Delta \mathrm{t}}{2}\int_{\Omega_e} \{\mathrm{N}_k\}\frac{\partial^2\{\mathrm{N}_k^T\}}{\partial \mathrm{x}^2}\,\mathrm{dx}\,\{\mathrm{Q}\} \tag{3.9}$$
$$-\frac{\gamma \mathrm{u}^2\Delta \mathrm{t}^2}{6}\int_{\Omega_e} \{\mathrm{N}_k\}\frac{\partial^2\{\mathrm{N}_k^T\}}{\partial \mathrm{x}^2}\,\mathrm{dx}\,\{\mathrm{Q}'\} \equiv \{0\}$$

Applying integration by parts on the integrands associated with the β and γ terms yields

$$\mathrm{TWS}^{N} = \int_{\Omega_e} \{\mathrm{N}_k\}\{\mathrm{N}_k^T\}\,\mathrm{dx}\,\{\mathrm{Q}'\} + \mathrm{u}\int_{\Omega_e} \{\mathrm{N}_k\}\frac{\partial\{\mathrm{N}_k^T\}}{\partial \mathrm{x}}\,\mathrm{dx}\,\{\mathrm{Q}\}$$
$$-\frac{\alpha \mathrm{u}\Delta \mathrm{t}}{2}\int_{\Omega_e} \{\mathrm{N}_k\}\frac{\partial\{\mathrm{N}_k^T\}}{\partial \mathrm{x}}\,\mathrm{dx}\,\{\mathrm{Q}'\} + \frac{\beta \mathrm{u}^2\Delta \mathrm{t}}{2}\int_{\Omega_e} \frac{\partial\{\mathrm{N}\}}{\partial \mathrm{x}}\frac{\partial\{\mathrm{N}_k^T\}}{\partial \mathrm{x}}\,\mathrm{dx}\,\{\mathrm{Q}\} \tag{3.10}$$
$$+\frac{\gamma \mathrm{u}^2\Delta \mathrm{t}^2}{6}\int_{\Omega_e} \frac{\partial\{\mathrm{N}_k\}}{\partial \mathrm{x}}\frac{\partial\{\mathrm{N}_k^T\}}{\partial \mathrm{x}}\,\mathrm{dx}\,\{\mathrm{Q}'\} \equiv \{0\}$$

Finally, from (3.5) the TWS^{h} + θTS algebraic form to (3.10) is

$$\left[[\mathrm{A200}d] - \frac{\alpha \mathrm{C}}{2}[\mathrm{A201}d] + \frac{\gamma \mathrm{C}^2}{6}[\mathrm{A211}d] + \theta \mathrm{C}[\mathrm{A201}d] + \frac{\theta\beta \mathrm{C}^2}{2}[\mathrm{A211}d]\right]\{\Delta \mathrm{Q}\}$$
$$= -\left[\mathrm{C}[\mathrm{A201}d] + \frac{\beta \mathrm{C}^2}{2}[\mathrm{A211}d]\right]\{\mathrm{Q}\}_n \tag{3.11}$$

where *d* is a label, e.g., L or Q, representing linear and quadratic basis implementation respectively. The symbolically represented FE linear basis matrices are

$$[\mathrm{A200L}]=\frac{1}{6}\begin{bmatrix}2 & 1\\ 1 & 2\end{bmatrix},\ [\mathrm{A211L}]=\begin{bmatrix}1 & -1\\ -1 & 1\end{bmatrix}$$
$$[\mathrm{A201L}]=\frac{1}{2}\begin{bmatrix}-1 & 1\\ -1 & 1\end{bmatrix} \tag{3.12}$$

and for FE quadratic basis the matrices are

$$[\mathrm{A200Q}]=\frac{1}{30}\begin{bmatrix}4 & 2 & -1\\ 2 & 16 & 2\\ -1 & 2 & 4\end{bmatrix},\ [\mathrm{A211Q}]=\frac{1}{30}\begin{bmatrix}70 & -80 & 10\\ -80 & 160 & -80\\ 10 & -80 & 70\end{bmatrix}$$
$$[\mathrm{A201Q}]=\frac{1}{6}\begin{bmatrix}-3 & 4 & -1\\ -4 & 0 & 4\\ 1 & -4 & 3\end{bmatrix} \tag{3.13}$$

3.3. TWS formulation for one-dimensional non-linear Burgers equation

The TS modified 1D momentum principle model, called the Burgers equation, from (2.7) is

$$\text{D}\mathbf{P}:\quad \mathcal{L}^m(q)=\frac{\partial u}{\partial t}+u\frac{\partial u}{\partial x}-\frac{1}{\mathrm{Re}}\frac{\partial^2 u}{\partial x^2}-\frac{\Delta t}{2}\frac{\partial}{\partial x}\left(\alpha u\frac{\partial u}{\partial t}+\beta u^2\frac{\partial u}{\partial x}\right)$$
$$-\frac{\Delta t^2}{6}\frac{\partial}{\partial x}\left(\gamma u^2\frac{\partial}{\partial x}\left(\frac{\partial u}{\partial t}\right)\right)+O(\Delta t^3)=0 \tag{3.14}$$

The weak statement formulation process is similar to as identified in previous section. The computable algebraic statement is {FQ}, which is a place holder for TWS^h + θTS, and is given as

$$
\begin{aligned}
\{\mathrm{FQ}\} = & \left[\begin{array}{l}
[\mathrm{A200}d] + \dfrac{\alpha\Delta t}{2}\left\{\bar{\mathrm{U}}\right\}^T [\mathrm{A3010}d] \\
+\dfrac{\gamma\Delta t^2}{6}\left\{\bar{\mathrm{U}}^2\right\}^T [\mathrm{A3011}d] + \dfrac{\theta\Delta t}{\mathrm{Re}}[\mathrm{A211}d]
\end{array}\right]\{\Delta \mathrm{U}\} \\
& + \theta\Delta t \{\mathrm{U}\}_{\mathrm{n+1}}^T [\mathrm{A3001}d]\{\mathrm{U}\}_{\mathrm{n+1}} + \frac{\theta\beta\Delta t^2}{2}\left\{\mathrm{U}^2\right\}_{\mathrm{n+1}}^T [\mathrm{A3011}d]\{\mathrm{U}\}_{\mathrm{n+1}} \\
& + \frac{\Delta t}{\mathrm{Re}}[\mathrm{A211}d]\{\mathrm{U}\}_{\mathrm{n}} + (1-\theta)\Delta t \{\mathrm{U}\}_n^T [\mathrm{A3001}d]\{\mathrm{U}\}_{\mathrm{n}} \\
& + \frac{(1\text{-}\theta)\beta\Delta t^2}{2}\left\{\mathrm{U}^2\right\}_n^T [\mathrm{A3011}d]\{\mathrm{U}\}_{\mathrm{n+1}} \equiv \{0\}
\end{aligned}
\tag{3.15}
$$

FE linear basis matrices A200L and A211L remains as given in (3.12). The hyper-matrices A3(·) are evaluated as

$$
\begin{aligned}
[\mathrm{A3010L}] &= \frac{1}{6}\begin{bmatrix} -2 & -1 \\ -1 & -2 \\ 2 & 1 \\ 1 & 2 \end{bmatrix}, \quad [\mathrm{A3011L}] = \frac{1}{2}\begin{bmatrix} 1 & -1 \\ 1 & -1 \\ -1 & 1 \\ -1 & 1 \end{bmatrix} \\
[\mathrm{A3001L}] &= \frac{1}{6}\begin{bmatrix} -2 & 2 \\ -1 & 1 \\ -1 & 1 \\ -2 & 2 \end{bmatrix}
\end{aligned}
\tag{3.16}
$$

[JAC] remains as defined in (3.5), which is $\partial\{\mathrm{FQ}\}/\partial\{\mathrm{Q}\}$, yielding

$$
\begin{aligned}
[\mathrm{JAC}] = & \left[\begin{array}{l} [\mathrm{A200}d] + \dfrac{\alpha\Delta \mathrm{t}}{2} \left\{ \bar{\mathrm{U}} \right\}^T [\mathrm{A3010}d] \\ + \dfrac{\gamma\Delta \mathrm{t}^2}{6} \left\{ \bar{\mathrm{U}}^2 \right\}^T [\mathrm{A3011}d] + \dfrac{\theta\Delta \mathrm{t}}{\mathrm{Re}} [\mathrm{A211}d] \end{array} \right] \{\mathrm{ONE}\} \\
& + \theta\Delta \mathrm{t} \{\mathrm{U}\}_{\mathrm{n+1}}^T [\mathrm{A3001}d] \{\mathrm{ONE}\} + \theta\Delta \mathrm{t} \{\mathrm{U}\}_{\mathrm{n+1}}^T [\mathrm{A3100}d] \{\mathrm{ONE}\} \\
& + \frac{\theta\beta\Delta \mathrm{t}^2}{2} \left\{ \mathrm{U}^2 \right\}_{\mathrm{n+1}}^T [\mathrm{A3011}d] \{\mathrm{ONE}\} + \theta\beta\Delta \mathrm{t}^2 \{\mathrm{U}\}_{\mathrm{n+1}}^T [\mathrm{A3110}d] \{\mathrm{U}\}_{n+1} \\
& + \frac{\gamma\Delta \mathrm{t}^2}{6} \{\Delta \mathrm{U}\}^T [\mathrm{A3110}d] \{\bar{\mathrm{U}}\} + \frac{\alpha\Delta \mathrm{t}}{4} \{\Delta \mathrm{U}\}^T [\mathrm{A3010}d] \{\mathrm{ONE}\}
\end{aligned}
\tag{3.17}
$$

Additional hyper-matrices identified in (3.17) are

$$
[\mathrm{A3100L}] = \frac{1}{6} \begin{bmatrix} -2 & -1 \\ 2 & 1 \\ -1 & -2 \\ 1 & 2 \end{bmatrix}, \quad [\mathrm{A3110L}] = \frac{1}{2} \begin{bmatrix} 1 & 1 \\ -1 & -1 \\ -1 & -1 \\ 1 & 1 \end{bmatrix} \tag{3.18}
$$

3.4. TWS formulation for two-dimensional advection-diffusion-source problem

A steady state advection-diffusion-source problem with the TWS modified restatement of the continuum as identified by Kolesnikov [20] is given as

D**P**: $$\mathcal{L}(q) = u_{\mathrm{j}} \frac{\partial q}{\partial x_{\mathrm{j}}} - \frac{1}{\mathrm{Pe}} \left(\frac{\partial^2 q}{\partial x_{\mathrm{j}}^2} \right) - \frac{h^2 \mathrm{Pe}}{12} \frac{\partial}{\partial x_{\mathrm{j}}} \left(\frac{\partial q}{\partial x_{\mathrm{k}}} \right) - s_{ij} = 0 \tag{3.19}$$

where *h* remains the mesh length, and Pe is the Peclet number. For a Gaussian plume with uni-directional velocity in the x-direction and diffusion only in the y-direction, (3.19) reduces to

D**P**: $$\mathcal{L}(q) = u\frac{\partial q}{\partial x} - \frac{1}{\text{Pe}}\left(\frac{\partial^2 q}{\partial y^2}\right) - \frac{h^2\text{Pe}}{12}\left(\frac{\partial^2 q}{\partial x^2}\right) - s = 0 \tag{3.20}$$

The weak statement formulation procedure remains same as defined in Section (3.1), and the computable TWS^h + θTS algebraic form is

$$\{\text{FQ}\} = \left[\text{u[B201L]} + \frac{1}{\text{Pe}}[\text{B222L}] + \frac{h^2\text{Pe}}{12}[\text{B211L}]\right]\{\text{Q}\} \tag{3.21}$$

The matrices [B201L], [B222L] and [B211L] are given in [32]. Again as identified in (3.5), [JAC] remains $\partial\{\text{FQ}\}/\partial\{\text{Q}\}$.

3.5. TWS formulation for two-dimensional NS thermal cavity problem

The physical problem is governed by (2.1)-(2.6) with TWS theory TS modification leading to (2.7). TWS^h + θTS weak statement formulation process remains as identified in Section (3.1). But now because of multi-dimensionality and incorporation of energy equation (2.3), the process is more involved and the number of terms has increased significantly. Hence, easily readable six-point template identifying the computational algebraic form is supplied in Appendix X.

Chapter 4

4. Theoretical Development and Analysis

4.1. One-dimension

The TS modified scalar transport equation (2.8) simplified to one-dimension is

$$\begin{aligned}\mathcal{L}^m(q) = \frac{\partial q}{\partial t} + u\frac{\partial q}{\partial x} - \frac{1}{\mathrm{Pa}}\frac{\partial^2 q}{\partial x^2} - \frac{\Delta t}{2}\frac{\partial}{\partial x}\left(\alpha u\frac{\partial q}{\partial \mathrm{t}} + \beta u^2\frac{\partial q}{\partial x}\right) \\ -\frac{\Delta t^2}{6}\frac{\partial}{\partial x}\left[\gamma u^2\frac{\partial}{\partial x}\frac{\partial q}{\partial t} + \mu u^2\frac{\partial}{\partial x}\left(u\frac{\partial q}{\partial x}\right)\right] + O(\Delta t^3) = 0\end{aligned} \tag{4.1}$$

where Pa is the placeholder for the non-D parameter appropriate for q. (For (2.3), Pa = RePr, while for mass transport Pa = ReSc. Sc is the Schmidt number for binary diffusion.)

4.1.1. Linear Basis

The amplification factor G^h associated with the discrete approximate solution $q^h(x,t)$ is determined by assembling TWS^h + θTS, (3.5), for (4.1) at the generic mesh node X_j, ref. Figure 4.1(a). The resultant form for the linear FE basis implementation is the recursion stencil

$$\begin{bmatrix} a_{j-1} & a_j & a_{j+1} \end{bmatrix} \begin{bmatrix} Q_{j-1}^{n+1} \\ Q_j^{n+1} \\ Q_{j+1}^{n+1} \end{bmatrix} = \begin{bmatrix} b_{j-1} & b_j & b_{j+1} \end{bmatrix} \begin{bmatrix} Q_{j-1}^{n} \\ Q_j^{n} \\ Q_{j+1}^{n} \end{bmatrix} \tag{4.2}$$

where coefficients a_j and b_j contain all mesh constants as well as the parameter set defined in (3.5). Recalling the Fourier representations

$$Q_{j-1} = Q\,(x-\Delta x) = Q_j e^{-im} \tag{4.3}$$

$$Q_{j+1} = Q\,(x+\Delta x) = Q_j e^{+im} \tag{4.4}$$

where $m = \kappa h$ is the non-dimensional wave number, and $\Delta x = h$ is the measure of the (assumed) uniform mesh. Substituting into (4.2), the solution for the TWS algorithm amplification factor is

$$G^h = \frac{b_{j-1}e^{-im} + b_j + b_{j+1}e^{im}}{a_{j-1}e^{-im} + a_j + a_{j+1}e^{im}} \tag{4.5}$$

Inserting data pertinent to the linear FE basis implementation of (3.5) for the restriction (4.1), neglecting the μ term as requiring more derivatives than supported by the linear FE basis, produces (4.5) as the rational polynomial of complex functions

$$G^h_{FE(k=1)} = \frac{\left(2+\gamma C^2-3(1-\theta)\beta C^2-6(1-\theta)D\right)+\left(1-\gamma C^2+3(1-\theta)\beta C^2+6(1-\theta)D\right)\cos m - i3C\left(\frac{1}{2}\alpha+(1-\theta)\right)\sin m}{\left(2+\gamma C^2+3\theta\beta C^2+6D\theta\right)+\left(1-\gamma C^2-3\theta\beta C^2-6D\theta\right)\cos m - i3C\left(\frac{1}{2}\alpha-\theta\right)\sin m} \tag{4.6}$$

where $C = U\Delta t/h$ is the Courant number, equivalent to the non-dimensional time step, and $D \equiv \Delta t/\ Pah^2$ is the placeholder for the action of physical diffusion.

The clear statement of discrete approximation error accrues to multiplying (4.6) through by the complex conjugate and clearing the denominator via a sufficiently high-order Taylor series (TS). The resultant form is $G^h = p + iq$, and the resultant TS to order seven in m is (4.7).

$$
\begin{aligned}
G^{h}_{\mathrm{FE}(k=1)} = {} & 1\text{-}\mathrm{i}Cm+\left[\frac{1}{2}(\alpha\text{-}\beta\text{-}D)\text{-}\theta\right]C^2m^2+\mathrm{i}\left[\begin{array}{l}\left(\frac{1}{4}\alpha(\alpha\text{-}\beta)+\frac{\gamma}{6}+(\text{-}\alpha+\beta)\theta+\theta^2\right)C^3\\ +CD\left(\text{-}\frac{\alpha}{2}+2\theta\right)\end{array}\right]m^3\\
& +C^2\left[\begin{array}{l}\text{-}\frac{\beta}{24}+C^2\left(\frac{\alpha^2}{8}(\text{-}\alpha+\beta)+\frac{\gamma}{6}\left(\text{-}\alpha+\frac{\beta}{2}\right)+\left(\alpha\left(\frac{3}{4}\alpha\text{-}\beta\right)+\frac{1}{4}\beta^2+\frac{1}{3}\gamma\right)\theta+\frac{3}{2}(\text{-}\alpha+\beta)\theta^2+\theta^3\right)\\ D\left(\frac{\text{-}1}{12C^2}+\frac{\theta D}{C^2}+\left(\frac{\alpha^2}{4}+\frac{\gamma}{6}\text{-}2\alpha\theta+\beta\theta+3\theta^2\right)\right)\end{array}\right]m^4\\
& +\mathrm{i}C\left[\begin{array}{l}\frac{1}{180}+C^2\left(\frac{\text{-}\alpha\beta}{48}+\frac{\gamma}{72}+\frac{\beta\theta}{12}\right)+C^4\left\{\frac{\text{-}\alpha^3}{16}(\alpha\text{-}\beta)\text{-}\frac{\alpha\gamma}{4}\left(\frac{\alpha}{2}\text{-}\frac{\beta}{3}\right)\text{-}\frac{\gamma^2}{36}\right\}\\ +C^4\left\{\theta\left(\frac{\alpha^3}{2}\text{-}\frac{\alpha\beta}{4}(3\alpha\text{-}\beta)+\gamma\left(\frac{\alpha}{2}\text{-}\frac{\beta}{3}\right)\right)\right\}+C^4\theta^2\left\{\frac{\text{-}3\alpha}{2}\left(\alpha\text{-}\frac{3\beta}{2}\right)\text{-}\frac{3\beta^2}{4}\text{-}\frac{\gamma}{2}\right\}\\ +C^4\left(2\theta^3(\alpha\text{-}\beta)\text{-}\theta^4\right)\\ +D\left(\frac{\text{-}\alpha}{24}+\frac{\theta}{6}+(\alpha\text{-}3\theta)\theta D+C^2\left(\frac{\alpha^3}{8}+\frac{\alpha\gamma}{6}+(\text{-}\frac{3}{2}\alpha+\beta)\alpha\theta\text{-}\frac{2}{3}\gamma\theta+(\frac{9}{2}\alpha\text{-}3\beta\text{-}4\theta)\theta^2\right)\right)\end{array}\right]m^5\\
& +C^2\left[\begin{array}{l}\frac{\text{-}\alpha}{180}\text{-}\frac{\beta}{720}+\frac{\theta}{90}+C^2\left\{\frac{\alpha\beta}{12}\left(\frac{\alpha}{8}\text{-}\theta\right)\text{-}\frac{\gamma}{72}(\alpha\text{-}\beta)+\frac{\gamma\theta}{36}+\frac{\beta\theta}{8}\left(\frac{\beta}{3}+\theta\right)\right\}\\ +C^4\left\{\frac{\alpha^5}{32}\text{-}\frac{\alpha^4\beta}{32}+\frac{\alpha^2\gamma}{4}\left(\frac{\alpha}{3}\text{-}\frac{\beta}{4}\right)+\frac{\gamma^2}{24}\left(\alpha\text{-}\frac{\beta}{3}\right)\right\}\\ +C^4\theta\left\{\frac{\text{-}5\alpha^4}{16}+\frac{\alpha^2\beta}{2}\left(\alpha\text{-}\frac{3\beta}{16}\right)+\frac{\gamma}{2}\left(\text{-}\alpha(\alpha\text{-}\beta)\text{-}\frac{1}{6}(\beta^2+\gamma)\right)\right\}\\ +\theta^2C^4\left\{\frac{5\alpha^3}{4}+9\alpha\beta\left(\text{-}\frac{\alpha}{4}+\frac{\beta}{8}\right)\text{-}\frac{\beta^3}{8}+\gamma\left(\alpha\text{-}\frac{3\beta}{4}\right)\right\}\\ +C^4\theta^3\left\{\frac{\text{-}1}{2}(5\alpha^2+3\beta^2)+4\alpha\beta\text{-}\frac{2}{3}\gamma+\frac{5}{2}\theta(\alpha\text{-}\beta)\right\}\text{-}C^4\theta^5\\ +D\left(\begin{array}{l}\frac{1}{C^2}\left(\frac{\text{-}1}{360}+\frac{1}{6}D\theta\text{-}D^2\theta^2\right)+\frac{\alpha^2}{48}+\frac{\gamma}{36}\text{-}\frac{1}{6}\alpha\theta\text{-}\frac{3}{4}D\alpha^2\theta+\frac{1}{6}\beta\theta\text{-}\frac{1}{3}D\gamma\theta\\ +\frac{\theta^2}{4}+\frac{9}{2}D\alpha\theta^2\text{-}\frac{3}{2}D\beta\theta^2\text{-}6D\theta^3\end{array}\right)\end{array}\right]m^6\\
& +C^2\left[DC^2\left(\begin{array}{l}\text{-}\frac{\alpha^4}{16}\text{-}\frac{1}{8}\alpha^2\gamma\text{-}\frac{\gamma^2}{36}+\alpha^3\theta\text{-}\frac{3}{4}\alpha^2\beta\theta+\alpha\gamma\theta\text{-}\frac{1}{3}\beta\gamma\theta\text{-}\frac{9}{2}\alpha^2\theta^2+\frac{9}{2}\alpha\beta\theta^2\text{-}\frac{3}{4}\beta^2\theta^2\\ \text{-}\frac{3}{2}\gamma\theta^2+8\alpha\theta^3\text{-}6\beta\theta^3\text{-}5\theta^4\end{array}\right)\right]m^6 \qquad (4.7)\\
& +O(m^7)
\end{aligned}
$$

The exact solution for a 1-D advection-diffusion problem is

$$q(x,t) = \exp\left[\mathrm{i}\kappa(x - \mathrm{u}t) - \kappa^2 \mathrm{D}t \right] \tag{4.8}$$

The corresponding amplification factor is the ratio of solutions at two successive times computed at location x

$$\mathrm{G} = \frac{q(x,(\mathrm{n}+1)t)}{q(x,\mathrm{n}t)} = \exp(-\mathrm{i}\mathrm{C}m - \mathrm{D}m^2) \tag{4.9}$$

and the associated TS is

$$\begin{aligned} \mathrm{G} = 1 - \mathrm{i}\mathrm{C}m - \left(\frac{\mathrm{C}^2}{2} + \mathrm{D} \right) m^2 + \mathrm{i}\mathrm{C}\left(\frac{\mathrm{C}^2}{6} + \mathrm{D} \right) m^3 + \left[\mathrm{C}^2 \left(\frac{\mathrm{C}^2}{24} + \frac{\mathrm{D}}{2} \right) + \frac{\mathrm{D}^2}{2} \right] m^4 \\ - \mathrm{i}\mathrm{C}\left(\frac{\mathrm{C}^4}{120} + \frac{\mathrm{D}\mathrm{C}^2}{6} + \frac{\mathrm{D}^2}{2} \right) m^5 - \left[\mathrm{C}^2 \left(\frac{\mathrm{C}^4}{720} + \frac{\mathrm{D}\mathrm{C}^2}{24} + \frac{\mathrm{D}^2}{4} \right) + \frac{\mathrm{D}^3}{6} \right] m^6 + O(m^7) \end{aligned} \tag{4.10}$$

Thereby, the linear FE basis approximate solution phase error $e^h = \mathrm{G} - \mathrm{G}^h$ for any $\mathrm{TWS}^h + \theta\mathrm{TS}$ algorithm construction is analytically the difference between the exact and approximate solution TS expansions (4.10) and (4.7). Neglecting the D terms for the moment, as the theoretical focus is role of the TWS parameter set α, β, γ, θ and C in the absence of physical diffusion, any approximate solution phase error in non-dimensional wave number m space to seventh order is

$$
\begin{aligned}
e^{h}_{\mathrm{FE}(k=1)} = &-\left[1\text{-}2\theta+(\alpha\text{-}\beta)\right]\frac{C^2m^2}{2}+\mathrm{i}\left[\frac{1}{6}\text{-}\frac{1}{4}\alpha(\alpha\text{-}\beta)\text{-}\frac{\gamma}{6}\text{-}(\text{-}\alpha+\beta)\theta\text{-}\theta^2\right]C^3m^3 \\
&+C^2\left[\frac{C^2}{24}+\frac{\beta}{24}\text{-}C^2\left(\frac{\alpha^2}{8}(\text{-}\alpha+\beta)+\frac{\gamma}{6}\left(\text{-}\alpha+\frac{\beta}{2}\right)+\left(\alpha\left(\frac{3}{4}\alpha\text{-}\beta\right)+\frac{1}{4}\beta^2+\frac{1}{3}\gamma\right)\theta+\frac{3}{2}(\text{-}\alpha+\beta)\theta^2+\theta^3\right)\right]m^4 \\
&+\mathrm{i}C\left[\begin{array}{l}
-\frac{C^4}{120}-\frac{1}{180}\text{-}C^2\left(\frac{\text{-}\alpha\beta}{48}+\frac{\gamma}{72}+\frac{\beta\theta}{12}\right)\text{-}C^4\left\{\frac{\text{-}\alpha^3}{16}(\alpha\text{-}\beta)\text{-}\frac{\alpha\gamma}{4}\left(\frac{\alpha}{2}\text{-}\frac{\beta}{3}\right)\text{-}\frac{\gamma^2}{36}\right\} \\
\text{-}C^4\left\{\theta\left(\frac{\alpha^3}{2}\text{-}\frac{\alpha\beta}{4}(3\alpha\text{-}\beta)+\gamma\left(\frac{\alpha}{2}\text{-}\frac{\beta}{3}\right)\right)\right\}\text{-}C^4\theta^2\left\{\frac{\text{-}3\alpha}{2}\left(\alpha\text{-}\frac{3\beta}{2}\right)\text{-}\frac{3\beta^2}{4}\text{-}\frac{\gamma}{2}\right\} \\
\text{-}C^4\left(2\theta^3(\alpha\text{-}\beta)\text{-}\theta^4\right)
\end{array}\right]m^5 \\
&+C^2\left[\begin{array}{l}
-\frac{C^4}{720}+\frac{\alpha}{180}+\frac{\beta}{720}\text{-}\frac{\theta}{90}\text{-}C^2\left\{\frac{\alpha\beta}{12}\left(\frac{\alpha}{8}\text{-}\theta\right)\text{-}\frac{\gamma}{72}(\alpha\text{-}\beta)+\frac{\gamma\theta}{36}+\frac{\beta\theta}{8}\left(\frac{\beta}{3}+\theta\right)\right\} \\
\text{-}C^4\left\{\frac{\alpha^5}{32}\text{-}\frac{\alpha^4\beta}{32}+\frac{\alpha^2\gamma}{4}\left(\frac{\alpha}{3}\text{-}\frac{\beta}{4}\right)+\frac{\gamma^2}{24}\left(\alpha\text{-}\frac{\beta}{3}\right)\right\} \\
\text{-}C^4\theta\left\{\frac{\text{-}5\alpha^4}{16}+\frac{\alpha^2\beta}{2}\left(\alpha\text{-}\frac{3\beta}{16}\right)+\frac{\gamma}{2}\left(\text{-}\alpha(\alpha\text{-}\beta)\text{-}\frac{1}{6}(\beta^2+\gamma)\right)\right\} \\
\text{-}\theta^2C^4\left\{\frac{5\alpha^3}{4}+9\alpha\beta\left(\text{-}\frac{\alpha}{4}+\frac{\beta}{8}\right)\text{-}\frac{\beta^3}{8}+\gamma\left(\alpha\text{-}\frac{3\beta}{4}\right)\right\} \\
\text{-}C^4\theta^3\left\{\frac{\text{-}1}{2}(5\alpha^2+3\beta^2)+4\alpha\beta\text{-}\frac{2}{3}\gamma+\frac{5}{2}\theta(\alpha\text{-}\beta)\right\}\text{-}C^4\theta^5
\end{array}\right]m^6+\mathrm{O}(m^7)
\end{aligned}
\tag{4.11}
$$

Since the first order in m term is missing in (4.11), any choice for the TWS^h+θTS parameter set α, β, γ, θ, C will produce a discrete solution at least first-order phase-accurate for D ≡ 0. For guaranteed second-order phase accuracy, the m^2 term coefficient [1+2θ+(α-β)] must vanish. For θ = 0.5, this accrues for any α = β and for all C. For this restriction on θ, third-order phase accuracy results upon setting -γ/6 – 1/12 = 0, hence the optimal choice is γ = -0.5. For these θ and γ constraints, a fourth-order phase accurate solution results for α(1-C^2)/24 = 0, which requires C = 1 or α = 0 = β.

The theory predicts the optimally phase-accurate TWS^h + θTS algorithm for linear FE basis implementation, herein denoted TWS-γ, accrues to the selections α = 0 = β, θ = 0.5 and γ = -1/2. Solutions generated with this TWS-γ algorithm are always fourth-order phase-accurate on a uniform mesh, independent of C. Actual TWS^h + θTS solution accuracy is of course a function of C and mesh non-uniformity.

As stated, the TWS^h + θTS construction readily admits recovery of independently derived algorithms, be they finite element, finite difference or finite volume in the original derivation. Recalling Table 1.1, the Donea TG algorithm is obtained by the substitutions α = 0 = θ and β = 1 = γ in (4.1). From (4.11), solution optimal phase accuracy thus requires $(1-C^2)/24 = 0$, which implies that greater than third-order accuracy occurs *only* for C = 1. The Raymond-Garder (RG) and Jiang least squares (JLS) algorithms both result via non-zero α and β with γ = 0 and θ = ½. The original RG construction defined α ≡ β and their semi-discrete (only) theoretical analysis [21] determined optimal phase accuracy accrued to $\alpha = 2/(C\sqrt{15})$. Any JLS construction is recovered for the definition α = 2θ = β. These choices result in the third-order term coefficient fixed at –1/12, hence both original algorithms produce solutions that are at best second-order phase accurate.

Figure 4.2 summarizes wave-number order dependence of the theory TS coefficients for Courant numbers C = 0.25, 0.5 and 1.0. For C = 0.25 and 0.5 the predicted performance order is TWS-γ, TG, GWS, JLS, RG and CN. For C = 1.0, the

performance order is TWS-γ, TG, RG, JLS, GWS and CN. Clearly then, TWS-γ is the predicted optimal linear basis FE implementation of the TWS + θTS theory.

Existence of the established TWS^h + θTS theory admits the opportunity to optimize phase accuracy for published algorithms. For example, one can minimize the fourth-order truncation error coefficient $C^2(\alpha\text{-}2C^2)/24$ while keeping $\alpha = \beta$ for RG and JLS. The results remain Courant number dependent, e.g., for C = 1, optimal $\alpha = \beta = 2$, while for C = ½ the value is ½. A third example is the famous Crank-Nicolson (CN) FD algorithm, [22], the solution phase accuracy of which can be improved via TWS^h + θTS. The fundamental distinguishing characteristic between linear basis TWS^h + θTS FE implementation and CN is the FE non-diagonal mass matrix [M] in (3.3). Diagonalizing [M], then proceeding through the amplification factor process produces

$$G^{h}_{CNm-FD} = 1 + \frac{3\beta C^2\left(\cos m + 1\right) - i3C\sin m}{\left(3 + \gamma C^2 + 3\theta\beta C^2\right) - C^2\left(\gamma + 3\theta\beta\right)\cos m + i3C\left(\frac{-\alpha}{2} + \theta\right)\sin m} \tag{4.12}$$

for the “modified” CN algorithm (CNm). The corresponding CNm algorithm phase error TS through third order is

$$
\begin{aligned}
e^{h}_{\text{CNm-FD}} &= -2(C^2\beta)\ -iC\left[1+\left(1+C^2\alpha\beta-2C^2\beta\theta\right)\right]m \\
&+C^2\left[-\frac{1}{2}-\frac{1}{2}(\alpha-\beta)-\frac{1}{3}C^2\beta\gamma+\theta\left(1-C^2\beta^2\right)-2\beta C^2\left(-\frac{\alpha^2}{4}-\frac{\gamma}{3}+\theta(\alpha-\beta-\theta)\right)\right]m^2 \\
&+i\left[\frac{C^3}{6}-\left(\frac{C}{6}+C^3\left(-\frac{5}{12}\alpha\beta-\frac{\gamma}{6}+\frac{1}{3}\beta\theta\right)\right)-C^2\left(-C+C^3\beta(\alpha-2\theta)\right)\left(-\frac{\alpha^2}{4}-\frac{\gamma}{3}+\theta(\alpha-\beta-\theta)\right)\right]m^3 \\
&+O(m^4)
\end{aligned}
\tag{4.13}
$$

Viewing (4.13), to obtain even first-order phase accuracy requires $\beta = 0$, whereupon the second-order TS coefficient becomes $C^2(-1/2+\theta)$ which defines $\theta = ½$, as in the original CN formulation. With these determinations, the third-order coefficient becomes $C^3(-1/12-\gamma/3) - C(1-C\gamma)/6$ which will not vanish for any γ or C. Optimal γ can be chosen for select C, e.g., for C = 1 optimal γ is –1/2, while for C = ½ third-order phase accuracy is independent of γ.

Finally, any TWS^h + θTS algorithm when optimized for phase accuracy exhibits discrete approximation error e^h that is a function of non-dimensional wave number *m*. Recalling (1.1), the relative phase velocity of the analytical solution is unity for all wave numbers. The wave number dependence of the relative phase velocity is computable in terms of the real and imaginary components of the amplification factor as

$$
\Phi^h = \frac{1}{-m\mathrm{C}}\tan^{-1}\left(\frac{\mathrm{Imag}(\mathrm{G}^h)}{\mathrm{Real}(\mathrm{G}^h)}\right) \tag{4.14}
$$

For the six TWS^h + θTS algorithms considered, the solutions (4.14) are graphed in Figure 4.3 (a) for C = 0.5. Note the use of a semi-log abscissa scale to expand

resolution in the all-important short wavelength region. Except for TG, which exhibits zero dependence on wavelength λ, all TWS^h + θTS algorithms exhibit lagging phase error over all λ and 100% error at $\lambda = 2h$. In the interval $2h < \lambda \leq 3h$, JLS and RG exhibit the minimal error but thereafter lose comparative superiority. CN exhibits the largest phase error throughout, and the TWS-γ phase error is minimal for all $\lambda > 4h$ (except for TG).

The terminal theoretical issue is algorithm stability, which requires $|G^h| \leq 1$. For the exact solution $|G| = 1$. Appendix III details the determined spectral distribution of the TWS^h + θTS algorithm error modulus $|e^h| = |G^h| - |G|$. Figure 4.3 (b) graphs the solutions for amplification factor modulus error for the considered algorithms. GWS, TWS-γ and CN exhibit zero error for all wavelengths, since they possess no numerical diffusion. At $\lambda = 2h$ the modulus error for TG is 100% and 87% for JLS and RG. Thereby, the superior short wavelength phase error character of these algorithms comes at the expense of a very large level of numerical diffusion.

To further validate the theory, error analysis is extended for the 1D advection-diffusion problem. TS error statement in the orders of m is obtained from (4.7) and (4.10). Interestingly, m^2 error term is independent of D and is equal to $C^2[\ ½ + ½(\alpha-\beta)-\theta]$. Clearly, to obtain second order phase accurate solution requires $\alpha = \beta$, for $\theta = ½$. Substitution of these values to third order error term gives a requirement of $\gamma = -1/2$ for error annihilation. Hence, again as in 1D pure advection, $\gamma = -1/2$ is the optimal value for

1D advection-diffusion and suggests direct extension of the theory to the advection-diffusion class of problems.

4.1.2. Quadratic Basis

Theoretical analysis using one dimensional FE quadratic basis is much more complex because due consideration is required for the non-vertex node, c.f. Figure 4.1(b). The procedure followed is given by Gresho [15]. For non-vertex nodes seek a solution in the form

$$Q_j = \phi e^{i\kappa(jh-ct)} \tag{4.15}$$

that is similar to (4.3)-(4.4), where j represents the nodal location as shown in Figure 4.1(b), and ϕ is the ratio of amplitude at non-vertex node to vertex node. For vertex nodes seek a solution in the form of

$$Q_j = e^{i\kappa(jh-ct)} \tag{4.16}$$

Distinct matrix elements for (3.5), assembled at generic node X_j and dividing by a factor 1/3 to convert into finite difference form for vertex nodes are

$$[\text{A200Q}] \Rightarrow \frac{1}{10}\left|-1 \quad 2 \quad 8 \quad 2 \quad -1\right|$$

$$[\mathrm{A201Q}] \Rightarrow \frac{1}{2}\left|1 \quad -4 \quad 0 \quad 4 \quad -1\right|$$

$$[\mathrm{A211Q}] \Rightarrow \frac{1}{10}\left|10 \quad -80 \quad 140 \quad -80 \quad 10\right| \tag{4.17}$$

Similarly, for non-vertex nodes assembling at generic node X_j and dividing by a factor 2/3 to convert into finite difference form gives

$$[\mathrm{A200Q}] \Rightarrow \frac{1}{10}\left|1 \quad 8 \quad 1\right|$$

$$[\mathrm{A201Q}] \Rightarrow \left|-1 \quad 0 \quad 1\right|$$

$$[\mathrm{A211Q}] \Rightarrow \left|-4 \quad 8 \quad -4\right| \tag{4.18}$$

From (3.5), writing the algebraic statement explicitly

$$\begin{aligned}
[\mathrm{JAC}] &= [\mathrm{A200Q}] - \frac{\alpha C}{2}[\mathrm{A201Q}] + \frac{\gamma C^2}{6}[\mathrm{A211Q}] + \theta C[\mathrm{A201Q}] + \frac{\theta\beta C^2}{2}[\mathrm{A211Q}] \\
[\mathrm{RES}] &= -C[\mathrm{A201Q}] - \frac{\beta C^2}{2}[\mathrm{A211Q}]
\end{aligned} \tag{4.19}$$

Computing phase velocity requires inserting the trial solution (4.15)-(4.16) into TWS^h + θTS algebraic formulation (4.19), for (4.1), at the generic mesh node X_j. For vertex nodes nodes, coefficients of [JAC] in (4.15), herein referred LHS identifying left hand side in (3.5), for a semi-discrete TWS^h algorithm is

$$
\begin{aligned}
\text{LHS} = &-\frac{i\omega}{10}\left[-e^{-i2m} + 2\phi e^{-im} + 8 + 2\phi e^{+im} - e^{+i2m}\right] \\
&+\frac{i\omega\alpha C}{4}\left[e^{-i2m} - 4\phi e^{-im} + 4\phi e^{+im} - e^{+i2m}\right] \\
&-\frac{i\omega\gamma C^2}{6}\left[e^{-i2m} - 8\phi e^{-im} + 14 - 8\phi e^{+im} + e^{+i2m}\right] \\
&-\frac{i\omega\theta C}{2}\left[e^{-i2m} - 4\phi e^{-im} + 4\phi e^{+im} - e^{+i2m}\right] \\
&-\frac{i\omega\theta\beta C^2}{2}\left[e^{-i2m} - 8\phi e^{-im} + 14 - 8\phi e^{+im} + e^{+i2m}\right]
\end{aligned}
\tag{4.20}
$$

where ω is cyclic frequency. Similarly, coefficients of [RES] in (4.19), herein referred as RHS, identifying right hand side in (3.5) is

$$
\begin{aligned}
\text{RHS} = &-\frac{C}{2}\left[e^{-i2m} - 4\phi e^{-im} + 4\phi e^{+im} - e^{+i2m}\right] \\
&-\frac{\beta C^2}{2}\left[e^{-i2m} - 8\phi e^{-im} + 14 - 8\phi e^{+im} + e^{+i2m}\right]
\end{aligned}
\tag{4.21}
$$

Rewriting (4.20) – (4.21) in terms of trigonometric functions, cosines and sines, yields

$$
\begin{aligned}
\text{LHS} = &-\frac{i\omega}{10}\left[-2\cos(2m) + 4\phi\cos(m) + 8\right] \\
&+\frac{i\omega\alpha C}{4}\left[-i2\sin(2m) + i8\phi\sin(m)\right] \\
&-\frac{i\omega\gamma C^2}{6}\left[2\cos(2m) - 16\phi\cos(m) + 14\right] \\
&-\frac{i\omega\theta C}{2}\left[-i2\sin(2m) + i8\phi\sin(m)\right] \\
&-\frac{i\omega\theta\beta C^2}{2}\left[2\cos(2m) - 16\phi\cos(m) + 14\right]
\end{aligned}
\tag{4.22}
$$

and,

$$\begin{aligned} RHS = &-iC\left[-i\sin(2m)+4\phi\sin(m)\right] \\ &-\beta C^2\left[\cos(2m)-8\phi\cos(m)+7\right] \end{aligned} \tag{4.23}$$

Since LHS = RHS, combining (4.22) and (4.23), and dividing by "i=$\sqrt{-1}$", gives

$$\begin{aligned} &-\frac{\omega}{10}\left[-2\cos(2m)+4\phi\cos(m)+8\right]+\frac{\omega\alpha C}{4}\left[-i2\sin(2m)+i8\phi\sin(m)\right] \\ &-\frac{\omega\gamma C^2}{6}\left[2\cos(2m)-16\phi\cos(m)+14\right]-\frac{\omega\theta C}{2}\left[-i2\sin(2m)+i8\phi\sin(m)\right] \\ &-\frac{\omega\theta\beta C^2}{2}\left[2\cos(2m)-16\phi\cos(m)+14\right] \\ &=-C\left[-i\sin(2m)+4\phi\sin(m)\right]+i\beta C^2\left[\cos(2m)-8\phi\cos(m)+7\right] \end{aligned} \tag{4.24}$$

Similarly, for non-vertex nodes, inserting the trial solution (4.15)-(4.16) into (4.19) gives the coefficients of [JAC] identified by LHS as

$$\begin{aligned} LHS = &-\frac{i\omega}{10}\left[e^{-im}+8\phi+e^{+im}\right] \\ &+\frac{i\omega\alpha C}{2}\left[-e^{-im}+e^{+im}\right] \\ &-\frac{i\omega\gamma C^2}{6}\left[-4e^{-im}+8\phi e^{+im}-4e^{+im}\right] \\ &-i\omega\theta C\left[-e^{-im}+e^{+im}\right] \\ &-\frac{i\omega\theta\beta C^2}{2}\left[-4e^{-im}+8\phi-4e^{+im}\right] \end{aligned} \tag{4.25}$$

and coefficients of [RES] identified by RHS are

$$\begin{aligned} \text{RHS} &= -C\left[-e^{-im}+e^{+im}\right] \\ &-\frac{\beta C^2}{2}\left[-4e^{-im}+8\phi-4e^{+im}\right] \end{aligned} \tag{4.26}$$

Writing (4.25) – (4.26) in terms of trigonometric functions, cosines and sines, gives

$$\begin{aligned} \text{LHS} &= -\frac{i\omega}{10}\left[2\cos(m)+8\phi\right] \\ &+\frac{i\omega\alpha C}{2}\left[i2\sin(m)\right] \\ &-\frac{i\omega\gamma C^2}{6}\left[-8\cos(m)+8\phi\right] \\ &-i\omega\theta C\left[i2\sin(m)\right] \\ &-\frac{i\omega\theta\beta C^2}{2}\left[-8\cos(m)+8\phi\right] \end{aligned} \tag{4.27}$$

and,

$$\begin{aligned} \text{RHS} &= -C\left[i2\sin(m)\right] \\ &-\beta C^2\left[-4\cos(m)+4\phi\right] \end{aligned} \tag{4.28}$$

Since, LHS = RHS, equating (4.27) and (4.28), gives

$$\begin{aligned} -i\omega&\left[\begin{aligned} &\frac{1}{5}\cos(m)+\frac{4}{5}\phi-i\alpha C\sin(m)-\frac{4}{3}\gamma C^2\cos(m)+\frac{4}{3}\gamma C^2\phi \\ &+i\theta C2\sin(m)-4\theta\beta C^2\cos(m)+4\theta\beta C^2\phi \end{aligned}\right] \\ &= -i2C\sin(m)+4\beta C^2\cos(m)-4\beta C^2\phi \end{aligned} \tag{4.29}$$

Rearranging (4.29), gives

$$\phi = \frac{\left[\begin{array}{l} 2C\sin(m) + i4\beta C^2\cos(m) \\ -\omega\left[\frac{1}{5}\cos(m) - i\alpha C\sin(m) - \frac{4}{3}\gamma C^2\cos(m) + i2\theta C\sin(m) - 4\theta\beta C^2\cos(m)\right] \end{array}\right]}{4\left(\frac{1}{5} + \frac{1}{3}\gamma C^2 + \theta\beta C^2\right)\omega + i4\beta C^2} \tag{4.30}$$

To compute cyclic frequency ω, (4.30) is substituted into (4.24), and is solved in Mathematica, a symbolic toolbox. The resultant relation is some hundreds of lines of output and hence becomes mathematically intractable. Substituting $\alpha=0=\beta$ considerably simplifies the issue, but of course destroys the sought full theory. Substituting (4.30) in (4.24) results in a quadratic relation for ω, hence two roots exist. The principal root has a negative sign and the other is identified as spurious by Gresho [15], and Vichnevetsky and De Schutter [16]. The principal root as obtained using Mathematica is,

$$\begin{aligned} \omega = & (15\,(24\,Co\,Cos[m]\,Sin[m] - 40\,Co^3\,\gamma\,Cos[m]\,Sin[m] + 120\,i\,Co^2\,\theta\,Sin[m]^2 + \\ & 12\,Co\,Sin[2\,m] + 5\,Co^3\,\gamma\,Sin[2\,m] - \\ & \sqrt{(4608\,Co^2\,Sin[m]^2 + 5280\,Co^4\,\gamma\,Sin[m]^2 + 1400\,Co^6\,\gamma^2\,Sin[m]^2 - \\ & 1152\,Co^2\,Cos[2\,m]\,Sin[m]^2 + 200\,Co^6\,\gamma^2\,Cos[2\,m]\,Sin[m]^2 + \\ & 576\,Co^2\,Cos[m]\,Sin[m]\,Sin[2\,m] - \\ & 720\,Co^4\,\gamma\,Cos[m]\,Sin[m]\,Sin[2\,m] - \\ & 400\,Co^6\,\gamma^2\,Cos[m]\,Sin[m]\,Sin[2\,m] + 144\,Co^2\,Sin[2\,m]^2 + \\ & 120\,Co^4\,\gamma\,Sin[2\,m]^2 + 25\,Co^6\,\gamma^2\,Sin[2\,m]^2)))\,/ \\ & (-576 - 660\,Co^2\,\gamma - 175\,Co^4\,\gamma^2 + 72\,Cos[m]^2 - 240\,Co^2\,\gamma\,Cos[m]^2 + \\ & 200\,Co^4\,\gamma^2\,Cos[m]^2 + 144\,Cos[2\,m] - 25\,Co^4\,\gamma^2\,Cos[2\,m] + \\ & 720\,i\,Co\,\theta\,Cos[m]\,Sin[m] - 1200\,i\,Co^3\,\gamma\,\theta\,Cos[m]\,Sin[m] - \\ & 1800\,Co^2\,\theta^2\,Sin[m]^2 + 360\,i\,Co\,\theta\,Sin[2\,m] + 150\,i\,Co^3\,\gamma\,\theta\,Sin[2\,m]) \end{aligned} \tag{4.31}$$

For a semi-discrete algorithm (time remains continuous), phase velocity can be directly computed by dividing ω by κ, the wave number. For a finite time-step, the fully discrete phase velocity analysis is required, which is determined by computing G^h, the

numerical amplification factor. For a fully discrete scheme, $G^h = 1\text{-}i\omega\Delta t$, and is obtained directly from (4.31). Relative phase velocity is obtained by separating real and imaginary parts of G^h and using (4.14). Appendix IV shows the Matlab script for computing G^h and plotting the relative phase velocity spectral distribution. For explicit time integration, $\theta=0$ in (4.31) the relative phase velocity definition is

$$\Phi^h = \frac{1}{Cm}\tan^{-1}\left[\frac{-C\sin(2m)+C\sin(m)\sqrt{9+\sin^2(m)}}{1+\sin^2(m)}\right] \tag{4.32}$$

Figure 4.4 shows the relative phase velocity spectral error distribution for the $\theta = 0$ explicit time scheme at C=0.5 for $\gamma = 0$. The error is 100% at $\lambda = 2h$ because of the inability of the mesh to resolve $2h$ wavelength spectral content. The error as expected asymptotes to zero for $\lambda\rightarrow\infty$.

Figure 4.5 graphs the phase velocity spectral error distribution for the GWS and TWS-γ for $\theta = ½$ and various C and γ. Figure 4.5 (a) shows 100% error at $\lambda=2h$, as expected, and on $2h \le \lambda \le 6h$, a smaller phase error results for TWS-γ than GWS, which is again expected . But for $\lambda > 6h$ GWS phase error is less than TWS-γ, which is contrary to what has been seen from numerical experiments. Also, when $\lambda\rightarrow\infty$, the phase error remains in the range from 10-20%, which is obviously an error.

Another set of comparisons for the TWS-γ algorithm with γ = -0.2, -0.4 and -0.5 at C=0.5 and C=1.0, are shown in Figure 4.5 (b)-(c). Numerical experiments indeed

determined that γ = -0.4 is optimal, but no definitive trend is seen from these relative phase velocity error analysis. Therefore, the approach of Gresho [15], when applied to TWS class of algorithms implemented with FE quadratic basis, possesses an apparently fatal restriction. Therefore, the state of the TWS-γ theory reported by Chaffin [23] remains the most general prediction available.

4.2 Two-dimensions

The TWS modified conservation principle for a 2D pure advection problem, in a rectangular Cartesian resolution, neglecting the μ term and assuming $Pa^{-1} = 0$ is

$$\begin{aligned}\mathcal{L}^m(q) = {} & \frac{\partial q}{\partial t} + u\frac{\partial q}{\partial x} + v\frac{\partial q}{\partial y} - \frac{\alpha\Delta t}{2}\left[\frac{\partial}{\partial x}\left(u\frac{\partial q}{\partial \mathrm{t}}\right) + \frac{\partial}{\partial y}\left(v\frac{\partial q}{\partial t}\right)\right] \\ & -\frac{\beta\Delta t}{2}\left[\frac{\partial}{\partial x}\left(u^2\frac{\partial q}{\partial x}\right) + \frac{\partial}{\partial x}\left(uv\frac{\partial q}{\partial y}\right) + \frac{\partial}{\partial y}\left(vu\frac{\partial q}{\partial x}\right) + \frac{\partial}{\partial y}\left(v^2\frac{\partial q}{\partial y}\right)\right] \\ & -\frac{\gamma\Delta t^2}{6}\left[\frac{\partial}{\partial x}\left(u^2\frac{\partial}{\partial x}\frac{\partial q}{\partial t}\right) + \frac{\partial}{\partial x}\left(uv\frac{\partial}{\partial y}\frac{\partial q}{\partial t}\right) + \frac{\partial}{\partial y}\left(vu\frac{\partial}{\partial x}\frac{\partial q}{\partial t}\right) + \frac{\partial}{\partial y}\left(v^2\frac{\partial}{\partial y}\frac{\partial q}{\partial t}\right)\right] + O(\Delta t^3) = 0\end{aligned} \tag{4.33}$$

The amplification factor G^h for the discrete solution $q^h(x,y,t)$ for (4.16) is again determined via assembly of the TWS^h + θTS algorithm at the generic mesh node X_j, Y_k (ref. Figure 4.1(c)). The Fourier representations analogous to (4.3)-(4.4) are

$$Q_{j-1,k-1} = Q\,(x-\Delta x, y-\Delta y) = Q_{j,k}e^{-i\Delta x\kappa_1}e^{-i\Delta y\kappa_2} \tag{4.34}$$

$$Q_{j+1,k+1} = Q\,(x+\Delta x, y+\Delta y) = Q_{j,k} e^{+i\Delta x \kappa_1} e^{+i\Delta y \kappa_2} \tag{4.35}$$

where κ_1 and κ_2 are the non-D wave numbers in the x and y directions respectively. The resultant TWS algorithm 2D amplification factor, for the bilinear FE basis implementation is

$$G^h = \frac{\left(b_{j-1}e^{-i\kappa_1} + b_j + b_{j+1}e^{+i\kappa_1}\right)e^{-i\kappa_2} + \left(b_{j-1}e^{-i\kappa_1} + b_j + b_{j+1}e^{+i\kappa_1}\right) + \left(b_{j-1}e^{-i\kappa_1} + b_j + b_{j+1}e^{+i\kappa_1}\right)e^{+i\kappa_2}}{\left(a_{j-1}e^{-i\kappa_1} + a_j + a_{j+1}e^{+i\kappa_1}\right)e^{-i\kappa_2} + \left(a_{j-1}e^{-i\kappa_1} + a_j + a_{j+1}e^{+i\kappa_1}\right) + \left(b_{j-1}e^{-i\kappa_1} + b_j + b_{j+1}e^{+i\kappa_1}\right)e^{+i\kappa_2}} \tag{4.36}$$

for wave number definitions $\kappa_1 = \kappa\cos\eta$ and $\kappa_2 = \kappa\sin\eta$, recall Figure 1.1.

The theoretical analysis is tractable only for the uniform mesh case, hence $\kappa_1\Delta x = m = \kappa_2\Delta y$, thereby $\Delta x \equiv h \equiv \Delta y$ in (4.34)-(4.35), and m remains the non-dimensional wave number. The resultant Taylor series expansion for G^h to order m^4 is detailed in Appendix V. The exact solution for a 2D pure advection problem is

$$q(x,y,t) = \exp\left[-i\left\{\kappa_1\left(x - u_x t\right) + \kappa_2\left(y - u_y t\right)\right\}\right] \tag{4.37}$$

for advection velocity vector resolved into Cartesian scalar components. The analytical amplification factor remains the ratio of two successive time interval solutions

$$G = \frac{q(x,y,t_{n+1})}{q(x,y,t_n)} \tag{4.38}$$

Alternatively, since $\kappa_1 = \kappa\cos\eta$ and $\kappa_2 = \kappa\sin\eta$

$$G = \exp\left[-im\left(C_x \cos\eta + C_y \sin\eta\right)\right] \tag{4.39}$$

where C_x and C_y denote the Cartesian resolution of the Courant number vector. The resulting TS expansion to the first three terms in order m is

$$\begin{aligned} G = 1 - i[C_x\cos(\eta)+C_y\sin(\eta)]m - \frac{1}{2}[C_x\cos(\eta)+C_y\sin(\eta)]^2 m^2 \\ + \frac{i}{6}[C_x\cos(\eta)+C_y\sin(\eta)]^3 m^3 + O(m^4) \end{aligned} \tag{4.40}$$

The TWS^h + θTS algorithm phase-dependent error remains $e^h \equiv G - G^h$, which is readily computed from the TS expansions, and is detailed in Appendix VI to the order m^4. As before, stability accrues to bounding of $|e^h| = |G| - |G^h|$ by unity. Since $|G| = 1$, then $|e^h| = 1 - |G^h|$ and the resultant solution to order m^2 is

$$|e^h| = \left(\frac{C_x^2}{2} + C_x C_y + \frac{C_y^2}{2} - \frac{1}{2}(\alpha+\beta)\left(C_x^2 + C_y^2\right) - \alpha C_x C_y - C_x^2\theta - 2C_x C_y\theta - C_y^2\theta\right) m^2 \tag{4.41}$$

From (4.41), it is clear that the phase-dependent error for *any* TWS^h + θTS algorithm with definitions $\alpha = 0 = \beta$ and $\theta = ½$ will be order m^3 or better.

It remains to probe the TS analysis to quantify phase angle dependence, recall Figure 1.1, hence Courant vector dependence. Figure 4.6 presents the sample space of wave vector angles $\eta = \pi/2$, $5\pi/8$, $3\pi/4$, π, $5\pi/4$ and $11\pi/8$, along with geometric

coordinates, as determined definitive in spanning the Courant vector magnitude range $0.19 \leq |\mathbf{C}| \leq 0.41$ associated with a validation problem, discussed later.

The theory predicts that solution error is angular quadrant independent, even though $\mathbf{C} = (r\omega\Delta t/h)\hat{\mathbf{e}}$ is indeed a vector, where ω is angular velocity and $\hat{\mathbf{e}}$ is the unit vector tangent to the η direction. This prediction is in agreement with observations by Christon et. al. [13]. Figure 4.7(a)-(c) graphs the comparative TS coefficients in orders of non-dimensional wave number *m*, as predicted for the range of TWS^h + θTS algorithms evaluated, at $\eta = 3\pi/4$ and for $0.19 \leq |\mathbf{C}| \leq 0.41$. Figure 4.8 (a)-(c) present similar data for $\eta = 5\pi/8$. The lead error terms for RG, JLS and TG are order m^2 for all η and $|\mathbf{C}|$. The lead error terms for GWS, CN and TWS-γ are all order m^3, as predicted.

Since such a large disparity exists on order m^3 TS coefficient magnitude for CN versus GWS and TWS-γ, Figures 4.7 (d) and 4.8 (d) graph only these data for direct comparison. As algorithm solution fidelity is dominated by the lowest order in *m* non-vanishing TS coefficient, the theory predicts the TWS-γ algorithm optimal, as this coefficient is from 1/2 to 1/5 that of GWS. The same comment holds for the m^4 coefficients, while the m^5 coefficient being small and nominally identical is of marginal practical impact. As the final caveat, both TWS-γ and TG algorithm TS order m^3 coefficients vanish for η aligned with a coordinate axis.

TWS-γ exhibits the minimum TS coefficient for all *m*, η, $|\mathbf{C}|$ and coordinates tested. Thereby, the theory again predicts that TWS-γ algorithm solutions will be

optimally accurate among those of the group, hence there exists little incentive to further consider RG, JLS or CN. As a final comparison, Figure 4.9 quantifies the TS phase accuracy order distinction predictions for GWS versus TWS-γ on $\pi/2 \le \eta \le 3\pi/4$ and extremum $|\mathbf{C}|$. Note the zero TS coefficients for orders m^3 and m^4 for the TWS-γ algorithm for $\eta=\pi/2$. Predicted solution fidelity dependence on $|\mathbf{C}|$ is clearly evident, comparing the data in Figures 4.7 – 4.9, with the lead order TS coefficient magnitude roughly three times larger at $|\mathbf{C}| = 0.41$ than at $|\mathbf{C}| = 0.19$.

4.3 Matrix stability analysis

Any CFD algorithm produces the matrix statement

$$[A]\{Q\}^{n+1} = [B]\{Q\}^{n} \tag{4.42}$$

For the TWS 1D pure advection problem, writing (3.11) in the form of (4.41) gives

$$\begin{aligned}&\left\{[A200d]-\frac{\alpha C}{2}[A201d]+\frac{\gamma C^2}{6}[A211d]+\theta C[A201d]+\frac{\theta\beta C^2}{2}[A211d]\right\}\{Q^{n+1}\}\\&=\left\{[A200d]-\frac{\alpha C}{2}[A201d]+\frac{\gamma C^2}{6}[A211d]-(1-\theta)\left(C[A201d]+\frac{\beta C^2}{2}[A211d]\right)\right\}\{Q^{n}\}\end{aligned} \tag{4.43}$$

Assembling at the node common to two elements, and using the matrices as identified in (3.12), gives [A] as

$$\begin{bmatrix} \frac{1}{3}+\frac{\alpha C}{4}+\frac{\theta\beta C^2}{2}+\frac{\gamma C^2}{6}-\frac{\theta C}{2} & \frac{1}{6}-\frac{\alpha C}{4}-\frac{\theta\beta C^2}{2}-\frac{\gamma C^2}{6}+\frac{\theta C}{2} & 0 \\ \frac{1}{6}+\frac{\alpha C}{4}-\frac{\theta\beta C^2}{2}-\frac{\gamma C^2}{6}-\frac{\theta C}{2} & \frac{2}{3}+\theta\beta C^2+\frac{\gamma C^2}{3} & \frac{1}{6}-\frac{\theta\beta C^2}{2}-\frac{\gamma C^2}{6}+\frac{\theta C}{2} \\ 0 & \frac{1}{6}+\frac{\alpha C}{4}-\frac{\theta\beta C^2}{2}-\frac{\gamma C^2}{6}-\frac{\theta C}{2} & \frac{1}{3}-\frac{\alpha C}{4}+\frac{\theta\beta C^2}{2}+\frac{\gamma C^2}{6}+\frac{\theta C}{2} \end{bmatrix}$$

and matrix [B] is

$$\begin{bmatrix} \frac{1}{3}+\frac{\alpha C}{4}-\frac{(1-\theta)\beta C^2}{2}+\frac{\gamma C^2}{6}+\frac{(1-\theta)C}{2} & \frac{1}{6}-\frac{\alpha C}{4}+\frac{(1-\theta)\beta C^2}{2}-\frac{\gamma C^2}{6}-\frac{(1-\theta)C}{2} & 0 \\ \frac{1}{6}+\frac{\alpha C}{4}+\frac{(1-\theta)\beta C^2}{2}-\frac{\gamma C^2}{6}+\frac{(1-\theta)C}{2} & \frac{2}{3}-(1-\theta)\beta C^2+\frac{\gamma C^2}{3} & \frac{1}{6}-\frac{\alpha C}{4}+\frac{(1-\theta)\beta C^2}{2}-\frac{\gamma C^2}{6}-\frac{(1-\theta)C}{2} \\ 0 & \frac{1}{6}+\frac{\alpha C}{4}+\frac{(1-\theta)\beta C^2}{2}-\frac{\gamma C^2}{6}+\frac{(1-\theta)C}{2} & \frac{1}{3}-\frac{\alpha C}{4}-\frac{(1-\theta)\beta C^2}{2}+\frac{\gamma C^2}{6}-\frac{(1-\theta)C}{2} \end{bmatrix}$$

If [A] is invertible, then $\{Q\}^{n+1} = [A]^{-1}\,[B]\{Q\}^{n}$. Stability analysis can now be performed by determining the spectral radius, c.f., Ames [24], and Wait and Mitchell [25], defined as the largest eigenvalue of the matrix $[A]^{-1}\,[B]$. Also, if each eigenvalue of the matrix has magnitude less than unity then the algorithm will produce stable results.

Chapter 5

5. Discussion and Results

A list of tested algorithms is given in Table 5.1. All algorithms are derived from TWS theory by choosing appropriate identifications for α, β, γ and θ, except CN, which requires the mass matrix to be diagonalized. TWS represents a Taylor weak statement algorithm with extensions TWS-$\alpha/\beta/\gamma$ to identify the specific constructions.

5.1. Pure advection, one dimensional scalar transport

The *m*-dependent spectral distribution of phase velocity and amplification factor modulus errors has been determined for TWS^h + θTS algorithms; namely, GWS, RG, JLS, TG, TWS-γ and CN, for $0.25 \leq C \leq 1.0$ and time integration implicitness factor θ = 0.5, except TG for which the original $\theta = 0$ definition is retained. Algorithm relative actual performance is assessed for the verification problem of propagation of smooth and non-smooth initial conditions (IC) by a constant imposed velocity. The smooth IC is a Gaussian while the non-smooth IC is a square wave.

For the Gaussian propagated over three IC wavelengths, TWS^h + θTS algorithm solutions are compared to the exact solution in Figure 5.1 for $C = 0.5 = \theta$, except TG which retains $\theta = 0$. Clearly, the best solution in the visual *eyeball norm* is TWS-γ,

followed in order by TG, GWS, RG, JLS and CN respectively. Note that even though TG possesses zero phase error, it performs just poorer than TWS-γ due to its large level of numerical diffusion. RG and JLS phase velocity and amplitude error distributions are very similar, hence also is their performance. The developed theory, detailed in Section 4.1, precisely predicts this relative performance.

The theory predicts that solution quality improves/degrades for solution propagation at Courant numbers lesser/greater than C=0.5. Figure 5.2 summarizes Gaussian IC propagation compared to the exact solution for C = 1. Except for TWS-γ and TG, solution fidelity for the remaining algorithms indeed degenerates in the *eyeball norm*, with CN the worst performer. The theory predicts higher order phase accuracy for both TWS-γ and TG at C=1, and while not herein detailed, the TS process predicts at least tenth-order phase accuracy at C=1. Factually, both algorithms generate nodally exact solutions at C=1; this also occurs for the IC a (non-smooth) square wave, Figure 5.3, or for that matter any other IC.

To quantify the visual results of Figures 5.1-5.2, Table 5.2 lists the computed nodal extrema for each algorithm tested for C = 0.5 and C = 1.0. Except TWS-γ and TG, algorithm performance degrades at larger C with additional loss of peak value and larger dispersion error-induced lagging phase error. Note that solutions generated via the TWS theory-optimized CNm algorithm are improvements over those generated by classical CN, Figure 5.4. Although the improvement is truly modest, that it is theoretically predicted is the key result.

5.2. Algorithm automated optimization

The derived amplification factor error theory dependence on non-dimensional wave number *m* admits exploring automated optimization. The approach uses a fuzzy logic concept for a single-objective function, as enabled by an existing MATLAB optimization code, [26]. Only the first three coefficients in the theory TS expansion (4.11), for D = 0, are considered denoted as E^h_{m2}, E^h_{m3} and E^h_{m4} in Table 5.3. The objective is to minimize these terms subject to the constraint $E^h_{m2} < E^h_{m3} < E^h_{m4}$ since lowest order in *m* error annihilation is the primary objective. The code requires initial values for each parameter and the search seeks the nearest values to these that satisfy the objective function. Thereby, an endless set of determinations for α, β, γ, θ and C is possible.

Figure 5.5 summarizes solutions for smooth IC propagation as obtained using parameter set coefficients produced by the optimization code. All exhibit small phase and amplitude error, but none is an improvement over that of TWS-γ. The very practical constraint on optimization code execution is the convergence limit set for the objective function. The requirement cannot be zero, and computer time is directly proportional to use of tighter limits. The selected convergence criteria were 1E-12, 1E-04 and 1E-03 respectively, for E^h_{m2}, E^h_{m3} and E^h_{m4} for the results graphed in Figure 5.5.

Clearly, generating candidate optimal TWS solution parameter sets using optimization techniques depends totally on optimization code robustness. However, the truly interesting aspect of this exercise was code prediction of very large optimal coefficients α, β with values of $\theta < 0.5$, which theoretically is unstable integration. For example, for C = 1 and initial guess $\alpha = 100 = \beta$, $\gamma = 0$, $\theta = 0.5$, the optimization process returned $\alpha = 100.048$, $\beta = 100.0532$, $\gamma = 0.27067$, $\theta = 0.49743$. Substituting these values into (4.11), the modest difference between α and β is compensated by the shift in $\theta < 0.5$, which minimizes the m^2 TS coefficient. For these values, $\gamma = 0.27067$ minimizes the m^3 TS coefficient. This parameter choice basically constitutes a modified RG and/or JLS algorithm.

5.3. Advection-diffusion in one dimension

The one-dimensional advection-diffusion equation with constant velocity u and Peclet number Pe is

D**P**:
$$\mathcal{L}(q) = \frac{\partial q}{\partial t} + u\frac{\partial q}{\partial x} - \frac{1}{\text{Pe}}\frac{\partial^2 q}{\partial x^2} = 0 \tag{5.1}$$

This is a verification class problem with the analytical solution, for a smooth IC Gaussian distribution, given by Gresho [15] as,

$$q(x,t) = \frac{\exp[-(x - x_0 - t)^2 / 2(1 + 2t/\mathrm{Pe})]}{\sqrt{(1 + 2t/\mathrm{Pe})}} \tag{5.2}$$

Figure 5.6 shows the Pe = 10 solution for the algorithms tested at time = 25 for C = 1. GWS and RG exhibit small amounts of lagging phase error. JLS in comparison to RG for C = 1, completely annihilates the dispersion error. Of significance both have contributions from the α and β terms, except that the coefficient values are larger for JLS, ref. Table 1.1. The TG solution is unstable and high frequency oscillations can be seen at time = 25. CN exhibits the largest dispersion error and a lagging phase error. TWS-γ and JLS are the best performing among the selected algorithms. The TWS-γ solution slightly over-predicts whereas JLS slightly under-predicts the peak compared to the exact value.

Figure 5.7 compares the solutions for Pe=1000, hence the problem is advection dominated making it numerically more challenging. Mathematically, the problem is gaining hyperbolic character, smaller Pe being parabolic. As detailed in the developed theory, Section 4.1, and the corresponding results in Section 5.1, we expect TWS-γ, (γ=–0.5), to exhibit optimum solution fidelity, as is clearly validated in Figure 5.7. Table 5.4 compares the extremum of the selected algorithms after 25 time-steps. For Pe=10, the performance order is TWS-γ/JLS, RG, GWS, CN and TG, whereas, for Pe=1000, the performance order is TWS-γ, TG, GWS, RG, JLS and CN. This is identically the trend observed for pure advection problem, as expected.

Numerical experiments were also performed for Pe = 10 and 1000 at C=0.5. All algorithms, as expected show an improved performance, hence the results are not shown. Notably, TG which was unstable for C=1.0 and Pe =10, now performs second to TWS-γ. These experiments highlight the limitation of the TG algorithm being time explicit.

5.4. One dimensional Burgers equation

The non-linear Burgers equation is a standard verification model for characterizing CFD algorithm candidates for the INS system. The number of grid points required to resolve a steep front for a GWS algorithm is directly proportional to the $O(\mathrm{Re})$ [31]. For Re = 1E4, number of elements required are of $O(10^4)$, which is not practical. Hence, an alternative algorithm to GWS is required with the range of those tested to date as candidates. The goal is to choose a problem specification that serves as a good example for testing the robustness of any candidate algorithm. D**P** and the selected smooth IC and Dirichlet BCs for one such verification case in 1D are

$$\begin{aligned} \mathrm{D}\mathbf{P}: \quad & \mathcal{L}(u) = \frac{\partial u}{\partial t} + u\frac{\partial u}{\partial x} - \frac{1}{\mathrm{Re}}\frac{\partial^2 u}{\partial x^2} = 0, \quad 0 < x < 1, \ t > 0, \\ & \left\{ \begin{array}{lll} \mathrm{IC}: & \mathrm{u}(x,0) = 0.5\sin(\pi x) + \sin(2\pi x), & 0 \le x \le 1 \\ \mathrm{BC}: & \mathrm{u}(0,t) = 0 = \mathrm{u}(1,t), & t \ge 0 \end{array} \right\} \end{aligned} \tag{5.3}$$

Equation (5.3) is explicitly non-linear with viscous term impact controlled by Re The solution to (5.3) is a wave that steepens and forms a sharp front at time = 0.2. The wave

moves to the right as time advances and ultimately decays to zero because of the Dirichlet BCs. This Burgers specification has served as a validation case for many authors [27-29], especially for the computational scientists working on moving mesh techniques.

Analytical solution to (5.3) involves very complex mathematics [30], hence in order to get a reference solution a GWS simulation is done with M = 2000 and Δt = 0.00035. The resultant solution replicates the exact result but with over and under-shoots for the nodes near the steep front, Figure 5.8 (a). For clarity of TWS algorithm solution comparisons, these oscillations are smoothed when graphed as the "exact solution", Figure 5.8 (b) in the following discussion.

The candidate algorithms are GWS, JLS, TWS-β, TWS-$\beta\gamma$, TWS-$\alpha\beta$ and TWS-$\alpha\beta\gamma$. The choice of TWS-$\alpha\beta$ algorithm originated from analyzing the TS expansion coefficients of numerical amplification factor (4.7). Coefficients of m^2 term suggest a possible choice of optimal α/β as a function of physical diffusion parameter D. Figure 5.8 (c)-(h)compares the solutions obtained for these linear basis algorithms for Re = 1E4 for an M = 200 uniform mesh, time-step = 0.05, θ = 0.5 and at times = 0, 0.2 0.6, 1.4, 2.0s. In each graph, the smoothed reference solution is shown as dashed lines.

GWS fails completely in resolving the problem and the solution blows up, Figure 5.8 (c). Similarly, JLS, TWS-$\beta\gamma$ and TWS-$\alpha\beta\gamma$ Figures 5.8 (d)-(f) are unable to resolve

the steep front developed after time = 0.2 and this inadequacy completely pollutes the solution for times greater than 0.2.

TWS-β for β=1, and TWS-αβ, for β=1, α=-0.25 at θ = 0.5, Figures 5.8 (f), (g) are much more successful in resolving the steep front but dispersion error oscillations remain. Notable also is that these algorithms under-predict the speed of the steep front for $t > 0.2$, which is due to the under-prediction of the upstream wave velocity on this coarse mesh. The TWS numerical diffusion β-term is essential for damping the dispersive oscillations, which persist even for β=1. Combining β with α = -0.25 and the optimal γ=-0.5 term worsens the solution, Figure 5.8 (h). But when combined only with the α-term, oscillations are damped and hence yield an improved solution. Note that α and γ terms are both corrections to the TWS mass matrix, with α term an altered convection matrix whereas the γ term is associated with a diffusion matrix.

These TWS-β and TWS-αβ, θ = 0.5 algorithms gave the best solutions, but residual oscillations remained. Hence, a set of computational experiments were made to assess options for annihilating these residual oscillations. The end result was a newly developed numerical technique, which uses the standard θ = 0.5 formulation for the physical, and α and γ terms in the modified equation (2.7), but it uses θ = 1.0 (fully-implicit) formulation for the TWS-β term.

The results for select TWS algorithm tests are summarized in Figure 5.9 for the progression a) α = 0 = γ, β = 1, b) α = 0, β = 1, γ = -0.5, c) α = -0.25, β = 1, γ = 0 and d)

α = -0.25, β = 1, γ = -0.5. These numerical experiments indicate the "best" values for β and γ are 1 and -0.5 respectively with θ = 1.0. TWS-γ (γ = -0.5) when combined with TWS-β (β = 1) smoothens the slight over-shoot predicted by TWS-β and sharpens the steep front in closer agreement with the exact solution. The α-term has the similar effect as the γ-term on steepening the front but appears comparatively less effective for the tested range. This modified TWS-$\alpha\beta\gamma$ formulation still under-predicts the steep front velocity for all time > 0.2, which remains the consequence of use of the coarse M = 200 uniform mesh.

5.5. Pure advection two dimensional scalar transport

The classic 2D verification is the rotating cone, [32], a pure advection problem defined on a square solution domain Ω. On domain boundary segments $\partial\Omega$ experiencing inflow, the BC is $q(\mathbf{x}_b) = q_b = 0$. Conversely, on segments with outflow the BC is the homogeneous Neumann constraint $\hat{\mathbf{n}} \cdot \nabla q = 0$. The IC is $q(\mathbf{x},t_o) = 0 = q(\mathbf{x}_b)$ everywhere on $\Omega \cup \partial\Omega$ except for an isolated gaussian distribution of mass fraction. Figure 5.10 presents the IC in perspective view, which is advected along a circular path by imposition of the solid body rotation velocity vector field $\mathbf{u}(x,y) = \mathbf{u}(r) = r\omega\hat{\mathbf{e}}_\theta$. Here, r is the radial coordinate with origin at the center of Ω, ω is the angular velocity and $\hat{\mathbf{e}}_\theta$ is the unit vector tangent to the angular direction. The corresponding Courant vector $\mathbf{C}$ =

$C\hat{\mathbf{e}}_\theta = \sqrt{(C^2_x + C^2_y)}\ \hat{\mathbf{e}}_\theta$ is a linear function of radius *r*; the Cartesian resolution C_x, C_y of which are linear functions of the opposing Cartesian coordinate.

For the rotating cone, the IC is identically the analytical solution following any translation by the solid body rotation. Figure 5.11 graphs in perspective the various TWS^h + θTS algorithm solutions, as generated for the FE bilinear basis implementation, after the precise time required for the analytical solution to complete one revolution. In each graph, the '×' denotes the analytical solution peak after one revolution. The magnitude of Courant vector at the centroid of the IC is $|\mathbf{C}| = 0.3$ and the mesh is uniform rectangular Cartesian. In the *eyeball norm* the best performer is TWS-γ regarding peak preservation with minimal dispersion error-induced wake magnitude. The GWS and TG solutions follow with both suffering considerable peak loss, GWS due to dispersion error and TG due to numerical diffusion. The RG and JLS algorithms generate complete distortion of the IC due to the combination of dispersion and diffusion errors. The CN solution suffers rampant dispersion error due to its low order phase accuracy.

As confirmed by these data, only TWS-γ, GWS and TG, in that order, remain relevant algorithms. An algorithm is robust only when it maintains its predictability for different types of meshes. Hence, further analysis based on eyeball assessment is performed with non-uniform Cartesian mesh and a regular triangular mesh. Figure 5.12 graphs the non-uniform Cartesian mesh of M=32x32 and the results for TWS-γ, GWS and TG algorithms. There was a significant degradation in the performance of all algorithms. But TWS-γ remains the best with an extrema of 91.8 and -15.0 after one

complete rotation. GWS performance followed TWS-γ and TG was the worst in terms of peak value extrema. Recall the theory predicts that TG has a very small dispersion error, which is totally compromised by excessive artificial diffusion.

Next, algorithm robustness is tested on uniform triangular mesh. Finite element domain of the Figure 5.11 rectangular Cartesian mesh was uniformly bisected into two triangles, which enabled TWS^h + θTS algorithm implementation using the FE linear natural coordinate basis. Figure 5.13 graphs the associated solutions in perspective following the time for one IC revolution. Each algorithm suffers a modest degradation in accuracy, as detailed in Table 5.5 in terms of extrema nodal values. In both the tabulated data, and in the *eyeball norm,* the theoretically predicted optimal TWS-γ algorithm remains the best performer.

5.6. Gaussian plume advection-diffusion with source

A verification problem for computing the dispersion of air pollution from a single point source is the Gaussian plume model, originally proposed by Sutton [33]. The PDE defining the physics in 2D with uni-directional diffusion along the y-axis and constant imposed velocity along the x-axis is

$$\mathcal{L}(q) = u\frac{\partial q}{\partial x} - \frac{1}{\mathrm{Pe}}\frac{\partial}{\partial y}\left(\frac{\partial q}{\partial y}\right) - s = 0 \tag{5.4}$$

The analytical solution is given by Heines and Peters [34] for an infinite line source

$$q(x,y) = \frac{s}{\sqrt{\pi \nu u x}} \exp\left(\frac{-u y^2}{4\nu x}\right) \tag{5.5}$$

Dobbins [35] has given the Gaussian model for the turbulent dispersion and for multiple point sources with arbitrary velocity. Mayhoub et. al. [36] have developed analytical models for different atmospheric conditions. To derive the point source relation from the line source (5.5), a factor was chosen for source based on mesh size. For M = 20x20, a factor of 40 is chosen, whereas for M = 80x80, a factor of 86.4 is chosen.

Steady state GWS algorithm solutions are obtained for (5.4) on a unit square ($0 \le x \le 1$, $-0.5 \le y \le 0.5$). The point source is applied on first node off (x,y) = (0,0). The parameter values chosen are s = 0.00375, Pe = 100 and u = 1. Figure 5.14 shows the GWS solutions for M = 20x20 and 80x80 meshes and the TWS solution for M = 20x20. The analytical solution is overlaid at the boundary (1,y). With M = 20x20 a GWS error of 2.25% is predicted whereas M=80x80 predicts 0.04% error at the center, i.e., at coordinate (1,0), when compared with the analytical solution. The simulation is repeated with TWS-β (β=1) for M = 20x20. An error of 0.0446% is obtained at coordinate location (1,0), which is close to GWS solution of M = 80x80, and clearly demonstrates the improved solution accuracy of TWS-β algorithm for a steady problem. A very small amount of dispersion error is also present near the point source. The minimum values for

the two algorithm solutions for M = 20x20 is -0.0028 for the GWS and -0.003 for TWS, both of which are considered of no practical significance.

5.7. Thermal cavity Navier-Stokes problem

Final assessment of the TWS theory employs a full NS validation problem. Selected is the 8x1 aspect ratio thermal cavity enclosure, Figure 5.15, since significant multi-scale spectral content accrues to laminar flow as a function of Rayleigh number, Ra. Experimental data confirm this problem transitions from steady to unsteady [37] at a critical Rayleigh number, the occurence of which is computationally validated [38]. Christon et. al. [39] collected the results of various numerical models, confirming the critical Rayleigh number in the vicinity of $Ra_c \approx 3.1E+05$. A flow-field with $Ra > Ra_c$ gives unsteady flow with interesting flow features like vertical and horizontal boundary layers, corner structures, and shedding and multi-scale eddies, and hence is considered an excellent test case for the moderation of dispersion error via the TWS-γ algorithm.

Numerical experiments were performed for Ra = 3.4E+07 and Ra = 3.4E+08 to analyze the γ-term effect. $TWS^h + \theta TS$ applied on (2.8) gives the algebraic computable form, with the algorithm template given in Appendix X. The thermal cavity enclosure, Figure 5.15, is eight unit lengths tall and one unit length wide. The left and right walls are kept at a constant temperature T_{hot} and T_{cold} respectively, while the top and bottom of the cavity are insulated. The enclosure is subjected to the gravitational body force operating

in the y direction. This natural convection problem is driven by buoyancy, hence it is appropriate to non-dimensionalize the PDE system (2.1)-(2.3) with a reference velocity based on the temperature difference between the two walls. Hence U_r is defined as, [40]

$$U_r = \sqrt{\beta g \Delta T_r W} \tag{5.6}$$

where $\Delta T_r = T_{hot} - T_{cold}$, and W is the width of the cavity This definition relates the Reynolds number directly proportional to the square root of Ra [39], defined as,

$$\mathrm{Ra} = \frac{g\beta \Delta T W^3}{\mathrm{Pr}\,\alpha^2} \tag{5.7}$$

where α is the thermal diffusivity. The Prandtl number for all numerical experiments is constant at $\mathrm{Pr} = 0.71$.

A non-uniform Cartesian mesh of M = 41x201 elements, Figure 5.16, consists a coarser mesh in the domain center transitioning to a finer mesh near the boundaries. A finer mesh near the boundaries is required to capture the boundary layer formation induced due to buoyancy driven flow. The initial condition for the simulation was the solution obtained after 8000 GWS algorithm integration time steps, t = 148 sec at Ra = 3.4E+06. Since the objective was to quantitatively assess the γ-term effect this solution was then restarted at a fixed constant time-step of Δt = 0.02, for both the GWS and TWS-γ algorithms.

Figure 5.17 compares a snapshot of the unsteady solution temperature distribution after 1500 time steps, time = 168 sec for the GWS and TWS-γ (γ=-0.5) solutions at Ra = 3.4E+07, hence Re = 6850. The flow-field is unsteady and can be seen from the large number of eddy structures. Large number of eddies are concentrated near the center region. The thermal boundary layer is very thin, and wall shedding in the boundary layer is clearly visible above the mid-plane region. The GWS and TWS-γ solutions appear very similar. But on a closer look at the associated vortex structure the γ-term smoothning effect is clearly visible. Figure 5.18 graphs a close-up with mesh overlaid for the comparison of a recirculation region in the upper part of the domain and clearly visualizes the dispersion modulation characteristic of the TWS-γ algorithm.

This information can be quantified both theoretically, via the available asymptotic error estimate, (3.7), and in terms of the strength of the vortex structures, as measured by the span of the stream function. Figure 5.19 graphs the temperature energy norm distribution, with extrema near the wall boundaries in response to the thermal boundary layer, Figure 5.18. Mathematically notable is that just one order of magnitude difference in the extrema exist, identifying the equalization distribution of energy norm as suggesting the optimality of the mesh. The total scalar (Global) temperature energy norm values are compared, and tabulated in Table 5.6. TWS-γ solution results in the larger norm, a mathematical measure of moderation of dispersion error in this solution.

The close-up of the vortex structure for the re-circulation region in the lower part of the domain, as visualized by the stream-function distribution is presented in Figure

5.20. The γ term solution extremizes the stream-function range, as identified from the larger spread at the lower contour level, in this enlarged view. The stream-function extremization effect of the TWS-γ solution during time evolution is summarized in node point extremum values tabulated at select times in Table 5.7. At each time point, the TWS-γ solution extremizes the stream-function range. The point norm data are indeed small in magnitude, but importantly confirm independently, the temperature energy norm data.

The GWS and TWS-γ (γ=-0.5) temperature solutions at time = 168 sec for Ra = 3.4E+08 and Re = 19,932 are compared in Figure 5.21. When compared with Ra = 3.4E+07 solution, Figure 5.17, the number of small eddies have significantly decreased. The thermal boundary layer has become even thinner and wall shedding in the boundary layer occurs at a much shorter distance from the lower part of the domain. This pattern is also clearly identified in the temperature energy norm distribution, Figure 5.22. In comparison to the Ra = 3.4E+07 case, two new re-circulation regions have appeared near the upper left and lower right part of the domain, Figure 5.23. The measurable impact of the γ term on the Ra = 3.4E+08 temperature solution is less significant. Of fundamental importance however, small but definite increase in the global norm results, Table 5.6. The stream-function nodal extrema difference data are inconclusive for this Ra solution.

5.8. Identified algorithm anomalous behavior

Select results presented in the Sections (5.1)-(5.2) identify what might be termed anomalous behavior for certain algorithms. Theoretical insight into these odd performers accrues to detailing the associated TWS^h + θTS stencils. Recalling (4.1) as the general statement, both the TWS-γ and TG linear basis algorithms, when assembled at the generic node X_j for C = 1, produce (4.2) in the specific form

$$\left(Q_j + Q_{j+1}\right)_{n+1} = \left(Q_j + Q_{j-1}\right)_n \tag{5.8}$$

where n is the time-step index. Equation (5.8) states precise transport of nodal data exactly one mesh point at each time step on a uniform mesh for C=1 and for any IC.

Repeating this process for the RGm algorithm parameter set determination of the optimization process is similarly informative. Retaining arbitrary α = β, assuming γ small and setting θ = 0.5 yields (4.2) in the form

$$-\frac{1}{12}Q_{j-1}{}^{n+1} + \left(\frac{\alpha}{2} + \frac{2}{3}\right)Q_j{}^{n+1} + \left(-\frac{\alpha}{2} + \frac{5}{12}\right)Q_{j+1}{}^{n+1} = \left(\frac{\alpha}{2} + \frac{5}{12}\right)Q_{j-1}{}^{n} + \left(-\frac{\alpha}{2} + \frac{2}{3}\right)Q_j{}^{n} - \frac{1}{12}Q_{j+1}{}^{n} \tag{5.9}$$

For sufficiently large α (5.9) can be approximated as

$$-\frac{1}{12}Q_{j-1}{}^{n+1} + \left(\frac{\alpha}{2}\right)Q_j{}^{n+1} + \left(-\frac{\alpha}{2}\right)Q_{j+1}{}^{n+1} \approx \left(\frac{\alpha}{2}\right)Q_{j-1}{}^{n} + \left(-\frac{\alpha}{2}\right)Q_j{}^{n} - \frac{1}{12}Q_{j+1}{}^{n} \tag{5.10}$$

which, upon term cancellation, predicts exact propagation of nodal data at C=1. Figure 5.24 confirms this occurrence for $\alpha=100=\beta$; the RGm and exact solutions are indistinguishable.

It is informative to generate the RGm, as well as all TWS^h + θTS algorithm phase velocity and amplification factor modulus error distributions for C = 1. The TWS-γ, TG and RGm algorithms exactly propagate nodal data at C=1, and they each exhibit substantial leading phase error on $2h < \lambda \leq 4h$, which abruptly shifts to lagging at near zero levels for all wavelengths $\lambda > 4h$, Figure 5.25. The RG and JLS algorithms also exhibit this phenomenon, while GWS and CN exhibit lagging phase error at all wavelengths, none of which exactly propagate nodal data.

Any algorithm using a time-implicitness factor $\theta > 0.5$ inherits stability due to the associated inherent numerical dissipation mechanism. An interesting case is C = 0.5 and $\theta = 1$, for which the phase velocity and amplification factor modulus error distributions are graphed in Figure 5.26. The absolutely minimal phase error accrues to RGm; thereafter, in order of increasing phase error across the wavelength spectrum is TWS-γ, GWS, JLS, RG, TGm and CN. (For this comparison only, the original TG definition θ = 0 has been replaced with $\theta = 1$ yielding TGm.) The phase error distribution for TGm is equivalent to CN, which exhibits the minimal amplitude error. TG shows large amplitude error even at long wavelengths, while the GWS and TWS-γ amplitude errors are nearly

identical over the wavelength spectrum. It is quite apparent that these algorithm forms will not perform optimally.

Chapter 6

6. Conclusions and Recommendations

The TWS^h + θTS algorithm spectral theory, developed in completeness for the linear and bilinear FE basis implementations, provides a predictive framework for identifying optimal algorithm constructions belonging to the class. The generated TS expansion in non-dimensional wave number space is precisely predictive of actual computational performance, as verified for the selected scalar transport test cases. The computed spectral distributions of phase velocity and amplification factor modulus error further confirmed the developed theory fidelity. The influence of Courant vector magnitude on solution quality is included in the theory, also wave vector angle dependency and angular quadrant independence.

A general formulation for the analysis of phase velocity for one dimensional FE quadratic basis for TWS class of algorithms is derived. The cyclic frequency was successfully determined for TWS algorithms. Subsequent computation for phase velocity becomes mathematically intractable because of the huge number of terms involved. Further, the approach available in the literature to determine phase velocity for FE quadratic basis has fatal restrictions when applied to TWS approach. TWS-γ relative phase velocity and its spectral distribution as determined from the available approach are documented for various γ and Courant number. Hence, there is no incentive to pursue theoretical analysis for TWS α/β algorithm optimization.

The theory predicted, and test case results for FE linear basis confirmed the superiority of the TWS-γ algorithm over other selected candidate algorithms for one and two dimensional advection-diffusion problems. It is fair to assume that this conclusion would hold for three dimensional pure advection-diffusion problems as well.

The theory suggested results are tested for one dimensional FE linear basis verification problems that include linear advection-diffusion and non-linear unsteady Burgers equation. The Burgers equation analyses lead to the potential for determination of optimal TWS-$\alpha/\beta/\gamma$ algorithms. Various improved performance results are documented with TWS-β (β=1), TWS-$\beta\gamma$ (β=1, γ=-0.5), and TWS-$\alpha\beta$ (α=-0.25, β=1). A new algorithm based on the standard TWS implicit formulation, except for β-term being fully-implicit was developed, and its superior performance for the Burgers equation solution is documented for TWS-$\alpha/\beta/\gamma$ algorithms. In addition, TWS-β results for steady-state 2D advection-diffusion-source are presented showing improved solutions over GWS.

The theory predicted optimal TWS-γ results are tested on NS validation thermal cavity problem for above critical Rayleigh numbers and compared with GWS solutions. The results confirmed solution improvement and validated the TWS-γ algorithm dispersion error modulation characteristic. The scalar temperature energy norm was found to be quantitatively definitive for solution quality assessment with a larger value for TWS-γ algorithm. In addition, temperature energy norm equalization distribution

suggested the suitability of this mesh. Finally, TWS-γ algorithm solution also extremized the velocity field distribution as quantified by stream-function range.

TWS algorithm robustness and performance superiority over other algorithms on non-uniform Cartesian mesh and a regular triangular mesh is documented for two-dimensional pure advection problem. It is reasonable to assume that mesh-independent relative performance superiority of the TWS-γ algorithm will be maintained for scalar transport associated with full NS problem statments.

Analysis of the numerical amplification factor TS expansion of the advection-diffusion problem in non-dimensional wave-number suggests an interplay of α, β, θ, C and Re in solution quality. Numerical experiments with Burgers equation have confirmed a significant potential role of the α-term. Since, further analysis was beyond the scope of current work it is suggested that future research directions should look into the role of {α, β, Re, θ, C} parameters in solution improvement for the problem with physical diffusion. Further, the TWS standard implicit formulation with β-term fully implicit should be investigated for the full NS class of problems for minimizing residual oscillations, hence improving predictability for solutions exhibiting non-smooth behavior.

Bibliography

1. J.D. Anderson, Jr, Computational fluid dynamics: The basics with applications, McGraw-Hill, New York, NY, 1995.
2. J. Donea, A Taylor-Galerkin algorithm for hyperbolic conservation laws. Int J. Numer. Methods Engr. Vol. 20, (1984) 101-119.
3. A.J. Baker, J.W. Kim, A Taylor weak statement for hyperbolic conservation laws, Int. J. Numer. Methods Fluids Vol. 7 (1987) 489-520.
4. D.J. Chaffin, A.J. Baker, On Taylor weak statement finite element methods for computational fluid dynamics, Int. J. Numer. Methods Fluids Vol. 21 (1995) 273-294.
5. A. Kolesnikov, A. J. Baker, An efficient high order Taylor weak statement formulation for the Navier-Stokes equations, J. Comp. Physics, Vol. 173 (2001) 549-574.
6. S. Sahu, A.J. Baker, A modified conservation law approach to improved finite element incompressible Navier-Stokes algorithms, K.-J. Bathe, Ed, Proceedings 3rd MIT conference on computational fluid and solid mechanics, Cambridge, MA, 2005, pp. 824-827.
7. R. Vichnevetsky, Wave propagation analysis of difference schemes for hyperbolic equations: A review, Int. J. Numer. Methods Fluids Vol. 7 (1987) 409-452.
8. R. Vichnevetsky, J.B. Bowles, Fourier Analysis of Numerical Approximations of hyperbolic problems, SIAM, Philadelphia, PA, 1982.

9. K.W. Morton, D.F. Mayers, *Numerical Solution of Partial Differential Equations*, Cambridge Univ. Press, Cambridge, England, 1994.
10. F. Shakib, T.J.R Hughes, A new finite element formulation for computational fluid dynamics: IX Fourier analysis of space-time Galerkin/Least-squares algorithms, Comput. Methods Appl. Mech. Engrg. Vol. 87 (1991) 35-58.
11. M.A. Christon, The influence of the mass matrix on the dispersive nature of the semi-discrete, second-order wave equation, Comp. Methods Appl. Mech. Engrg. Vol. 173 (1999) 147-166.
12. T. Belytschko, R. Mullen, On dispersive properties of finite element solutions, in Milovitz J, Achenbach, JD (eds), *Modern Problems in Elastic Wave Propagation*. John Wiley: New York, 1978, pp. 67-82.
13. M. A. Christon, M.J. Martinez, T.E. Voth, Generalized Fourier Analyses of the advection-diffusion equation – part I: one-dimensional domains, Int. J. Numer. Methods Fluids Vol 45 (2004) 889-887.
14. T.E. Voth, M.J. Martinez, M.A. Christon, Generalized Fourier Analyses of the advection-diffusion equation – part II: two-dimensional domains, Int. J. Numer. Methods Fluids Vol. 45 (2004) 889-920.
15. P. M. Gresho, R. L. Sani, *Incompressible Flow and the Finite Element Method*, Vol. I, John Wiley, Chicester, England, 2000.
16. R. Vichnevetsky and F De. Schutter. A Frequency analysis of finite difference and finite element methods for initial value problems, Proceedings of the AICA

international symposium on computer methods for partial differential equations, Lehigh University, Pennsylvania, 1975.

17. R. Haberman, *Elementary Applied Partial Differential Equations*, Third edition, Prentice-Hall Inc. 1998.
18. F.P. Incropera, D.P. Dewitt, *Fundamentals of Heat and Mass Transfe*r, John Wiley, Fifth Edition, New York, 2002.
19. J.T. Oden, J.N. Reddy, *An Introduction to the Mathematical Theory of Finite Elements*, John Wiley, New York, 1976.
20. A. Kolesnikov, Efficient Implementation of High Order Methods in Computational Fluid Dynamics, Dissertation Research, University of Tennessee, 2000.
21. W.H. Raymond, A. Garder, Selective damping in a Galerkin method for solving wave problems with variable grids. Monthly Weather Review Vol. 104 (1976) 1583-1591.
22. J. Crank, P. Nicolson, A practical method for numerical evaluation of solutions of partial differential equations of the heat conduction type. Advances in Computational Math. Vol. 6 (1) (1996) 207-226.
23. D. Chaffin, A Taylor weak statement finite element method for computational fluid dynamics, Ph.D. Dissertation, University of Tennessee, Knoxville, TN, 1997.
24. W.F. Ames, Numerical methods for partial differential equations. Barnes & Noble, New York, 1969.

25. R. Wait, A.R. Mitchell, *Finite Element Analysis and Applications*, John Wiley, New York, 1985.
26. M.B. Trabia, X.B. Lu, A fuzzy adaptive simplex search optimization algorithm. J. Mechanical Design, Vol. 123 (2001) 216-225.
27. J.M. Hyman, S. Li, An adaptive moving mesh method with locally refined nested grids for partial differential equations. Los Alamos National Lab, UR-98-5460.
28. R.M. Furzeland, J.G. Verwer and P.A. Zegeling, A numerical study of three moving grid methods for one-dimensional partial differential equations which are based on the method of lines, J. Comp. Physics. 89 (1990), 349-388.
29. R.J. Gelinas, S.K. Doss, K. Miller, The moving finite element method-Applications to general partial differential equations with multiple large gradients, J. Comp. Physics. 40 (1981), 202-249.
30. F. Calogero, S.D. Lillo, The Burgers equation on the semi-infinite and finite intervals, Nonlinearity. 2 (1989), 37-43.
31. J. Donea, A. Huerta, *Finite Element Methods for Flow Problems*, Wiley, Chichester, England, 2003.
32. A. J. Baker, *Finite Element Computational Fluid Mechanics*, Taylor and Francis, Washington DC, 1983.
33. O.G. Sutton, A theory of eddy diffusion in the atmosphere. Proc. R. Soc. Lond. 135 A, (1932), 143-165.

34. T.S. Heines, L.K. Peters, The effect of a horizontal impervious layer caused by a temperature inversion aloft on the dispersion of pollutants in the atmosphere. Atmospheric Environment, Vol. 7 (1973), 39-48.
35. R.A. Dobbins, *Atmospheric motion and air pollution: an introduction for students*. Wiley, New York, 1979.
36. A.B. Mayhoub, S.M. Khaled, A. Sherif, Atmospheric form of pollutants dispersion for different atmospheric conditions. Romanian Reports in Physics, Vol. 55, No. 1, 94-101, 2003.
37. L. P. Quere, Onset of unsteadiness, routes to chaos and simulations of chaotic flows in cavities heated from the side: a review of present status, Proceeding of the 10th Int. Heat Transfer Conference, Brighton, UK, pp. 281-296, 1994
38. M. Grubert, Development of a Potentially Accurate and Efficient LES CFD Algorithm to Predict Heat and Mass Transport in Inhabited Spaces, Ph.D Dissertation, University of Tennessee, Knoxville, TN, 2006.
39. M. Christon, P.M. Gresho, S.B. Sutton, Computational predictability of time-dependent natural convection flows in enclosures, Int. J. Numer. Methods Fluids, Vol. 40: 953-980, 2002.
40. P.T. Williams, A Three-Dimensional, Time-Accurate, Incompressible Navier-Stokes, Finite Element CFD Algorithm, Ph.D. Dissertation, University of Tennessee, Knoxville, TN, 1993.

Appendices

Appendix I

Tables

Table 1.1. TWS formulation categorization of independently derived CFD algorithms.

Algorithm name	θ	α	β	γ	μ
$TWS^h+\theta TS$	all	arbitrary	arbitrary	arbitrary	arbitrary
(Bubnov) Galerkin	all	0	0	0	0
Donor cell FD	0	0	u/C	$1/C^2$	0
Lax-Wendroff FD	0	0	sgn(u)	0	0
Euler Taylor Galerkin	0	0	1	1	0
CN Taylor Galerkin	0.5	0	0.5	1	0
Euler Char. Galerkin	0	0	1	0	1
Swansea Tay Galerkin	0	0	1	0	0
Wahlbin	0	sgn(u)	2sgn(u)	0	0
Dendy	0	$\Delta x \cdot sgn(u)$	$\Delta x \cdot sgn(u)$	0	0
Raymond-Garder	0.5	$2v_o sgn(u)/C$	$2v_o sgn(u)/C$	0	0
Hughes SUPG	---	0	sgn(u)	0	0
Euler Petrov Galerkin	0	0	0	(1-ν)	0
CN Petrov Galerkin	0.5	sgn(u)	$\nu \cdot sgn(u)$	-ν/2	0
Warming-Beam FD	0	0	1	0	-3(1-C)
VanLeer MUSCL	1	0	sgn(u)	0	-3
Jiang Least Squares	all	2θ	2θ	0	0
Note: sgn(u) is the sign of u, $v_o = 1/\sqrt{15}$, $C \leq \nu \leq 1$, C is Courant number					

Table 5.1. Summary of tested algorithms.

Verification and Validation Problems	Algorithms tested
1D transient pure advection	GWS, CN, JLS, RG, TG, TWS-γ, CNm, RGm
1D transient advection-diffusion	GWS, CN, JLS, RG, TG, TWS-γ
1D transient non-linear Burgers equation	GWS, CN, JLS, RG, TG, TWS-β, TWS-$\beta\gamma$, TWS-$\alpha\beta\gamma$
2D transient pure advection	GWS, CN, JLS, RG, TG, TWS-γ
2D transient advection-diffusion with source	GWS
2D transient NS thermal cavity	GWS, TWS-$\beta\gamma$

Table 5.2. Solution nodal extrema after 3-wavelength translation, Gaussian IC, 1-D pure advection.

		Max	Min
C = 0.5	GWS	0.9938	-0.0767
	RG	0.9385	-0.0508
	JLS	0.9398	-0.0516
	TG	0.9608	-0.0207
	TWS-γ	1.0087	-0.0210
	CN	0.8397	-0.3374
	CNm	0.8556	-0.3207
C = 1.0	GWS	0.9496	-0.1765
	RG	0.9194	-0.1458
	JLS	0.8988	-0.1171
	TG	1.0	0.0
	TWS- γ	1.0	0.0
	CN	0.7989	-0.3649
	CNm	0.8640	-0.3104

Table 5.3. Amplification factor TS expansion coefficients in wavenumber space.

Error	TS Coefficients
E^{h}_{m2}	$-\frac{C^2}{2}\left[1+2\theta+\left(\alpha-\beta\right)\right]$
E^{h}_{m3}	$\left[\frac{1}{6}-\frac{1}{4}\alpha\left(\alpha-\beta\right)-\frac{\gamma}{6}-\left(-\alpha+\beta\right)\theta-\theta^2\right]C^3$
E^{h}_{m4}	$C^2\left[\frac{C^2}{24}+\frac{\beta}{24}-C^2\left(\frac{\alpha^2}{8}\left(-\alpha+\beta\right)+\frac{\gamma}{6}\left(-\alpha+\frac{\beta}{2}\right)-\left(\alpha\left(\frac{3}{4}\alpha-\beta\right)+\frac{1}{4}\beta^2+\frac{1}{3}\gamma\right)\theta-\frac{3}{2}\left(-\alpha+\beta\right)\theta^2-\theta^3\right)\right]$

Table 5.4. Solution nodal extrema after 25 time-steps, Gaussian IC, 1-D advection-diffusion, Pe=10, 1000; C=1, M=40.

	C = 1			
	Pe = 10		Pe = 1000	
	Max	Min	Max	Min
GWS	0.679990	-1.422E-02	0.966789	-1.4810E-01
RG	0.674538	-5.207E-03	0.931993	-1.1942E-01
JLS	0.681359	-9.816E-04	0.908791	-9.8639E-02
TG	4.362461	-4.523E+00	0.996144	-5.8300E-06
TWS-γ	0.689254	-6.042E-05	0.995248	-5.4484E-10
CN	0.645886	-1.058E-01	0.833308	-3.4159E-01
Exact	0.684000	0	0.995090	0

Table 5.5. 2D pure advection, algorithm nodal extrema after one rotation, |**C**| = 0.3 at IC centroid.

						Uniform Cartesian Mesh		Uniform non-Cartesian triangular Mesh	
	α	β	γ	θ	**|C|**	Max	Min	Max	Min
TWS-γ	0	0	-0.5	0.5	0.3	0.996	-0.052	0.984	-0.095
GWS	0	0	0	0.5	0.3	0.960	-0.120	0.934	-0.148
TG	0	1	1	0	0.3	0.863	-0.026	0.806	-0.039
						Non-uniform Cartesian Mesh			
	α	β	γ	θ	**|C|**	Max	Min		
TWS-γ	0	0	-0.5	0.5	0.3	91.8	15.0		
GWS	0	0	0	0.5	0.3	88.1	19.6		
TG	0	1	1	0	0.3	76.4	-6.1		

Table 5.6. Temperature global energy norm, Ra = 3.4E+07 and 3.4E+08.

		Temperature Energy Norm
Ra = 3.4 E+07, Re = 6850	$\gamma = 0$	6.63116E-05
Ra = 3.4 E+07, Re = 6850	$\gamma = -0.5$	3.33277E-04
Ra = 3.4 E+08, Re = 19,932	$\gamma = 0$	2.086058E-07
Ra = 3.4 E+08, Re = 19,932	$\gamma = -0.5$	2.086188E-07

Table 5.7. Stream-function extrema, Ra = 3.4 E+07.

Ra = 3.4 E+07, Re = 6850			
Time(s)		Min	Max
1.40E+02	$\gamma = 0$	-0.0795979	0.0011473**7**
	$\gamma = -0.5$	-0.0795983	0.0011480**7**
1.49E+02	$\gamma = 0$	-0.0808421	0.00**28**06
	$\gamma = -0.5$	-0.08**10**310	0.00**33**54
1.50E+02	$\gamma = 0$	-0.079**57**9	0.001**14**73
	$\gamma = -0.5$	-0.079**78**6	0.001**85**10
1.63E+02	$\gamma = 0$	-0.0**68**7447	0.00**04**458
	$\gamma = -0.5$	-0.0**70**4804	0.00**12**224

Appendix II

Figures

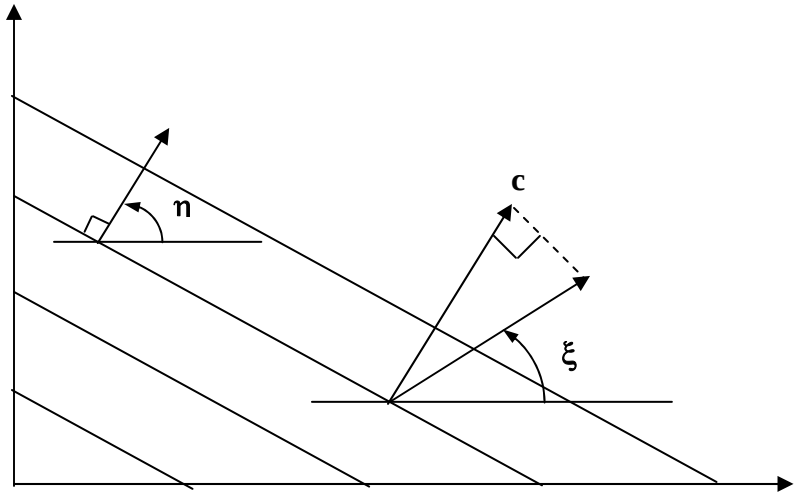

Figure 1.1. Wave number vector and phase velocity in the Cartesian continuum.

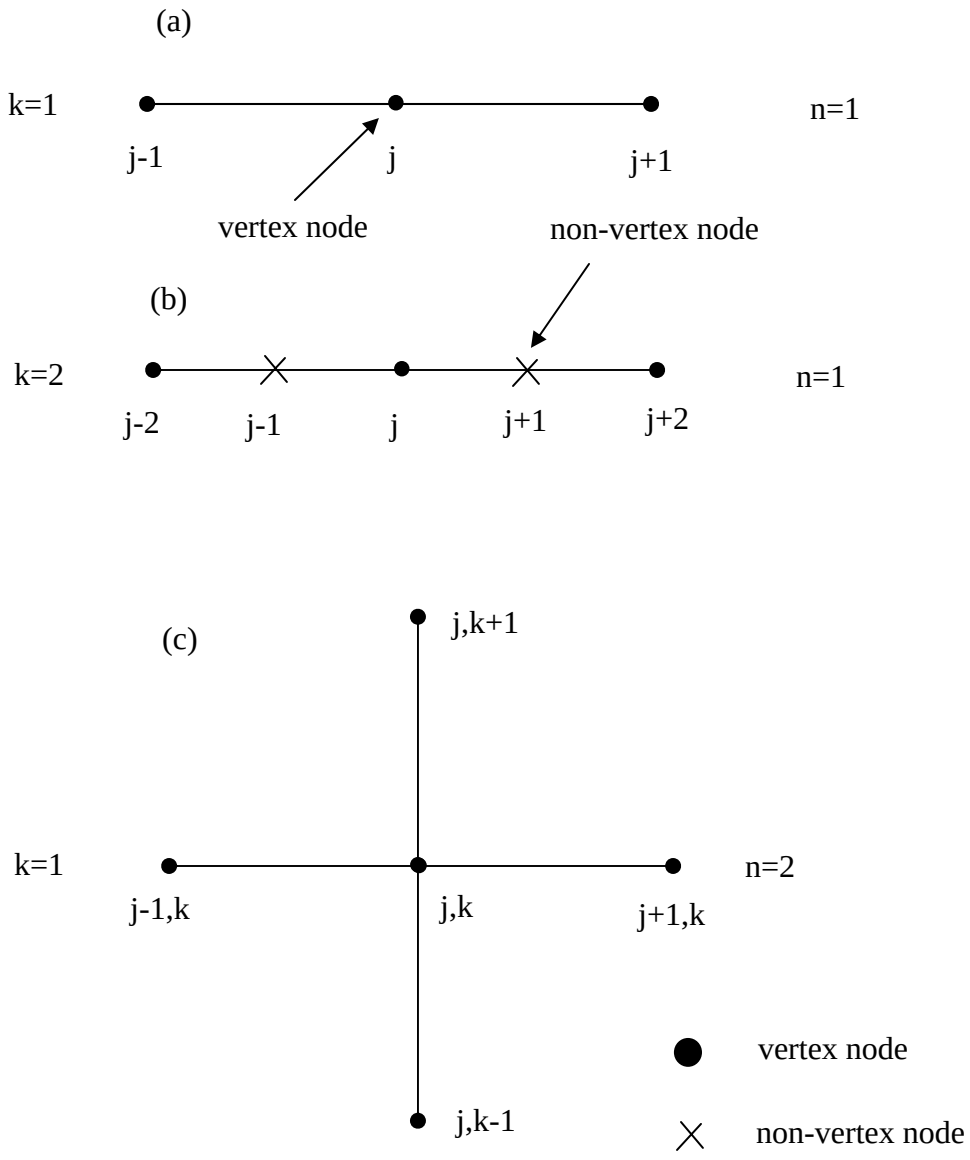

Figure 4.1. FE basis nodalization, (a) linear1D (b) quadratic 1D, (c) linear, 2D.

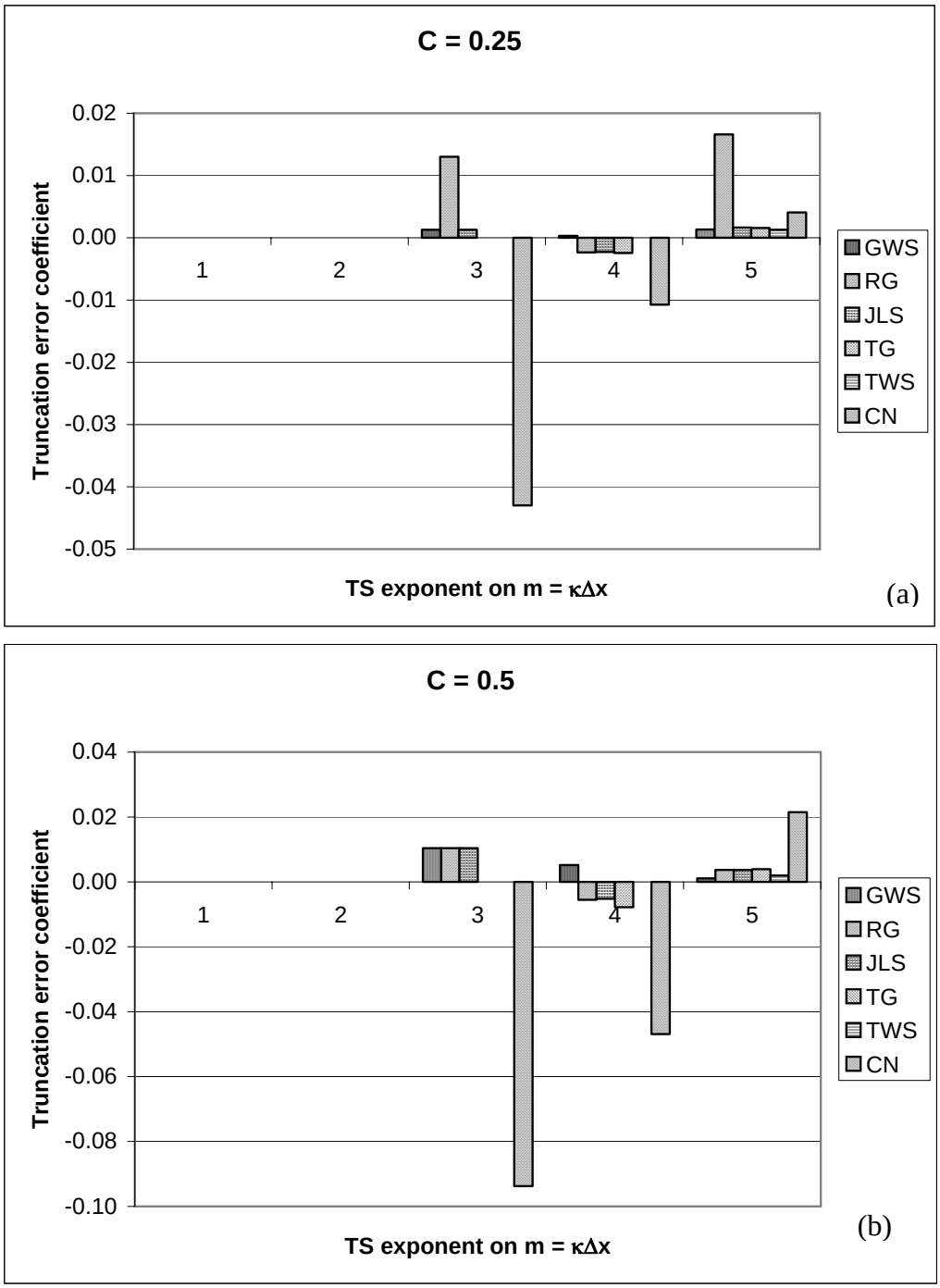

Figure 4.2. TWS algorithm discrete solution TS coefficients in non-D wave-number space, 1D pure advection. a) C =0.25, b) C = 0.5, c) C = 1.0.

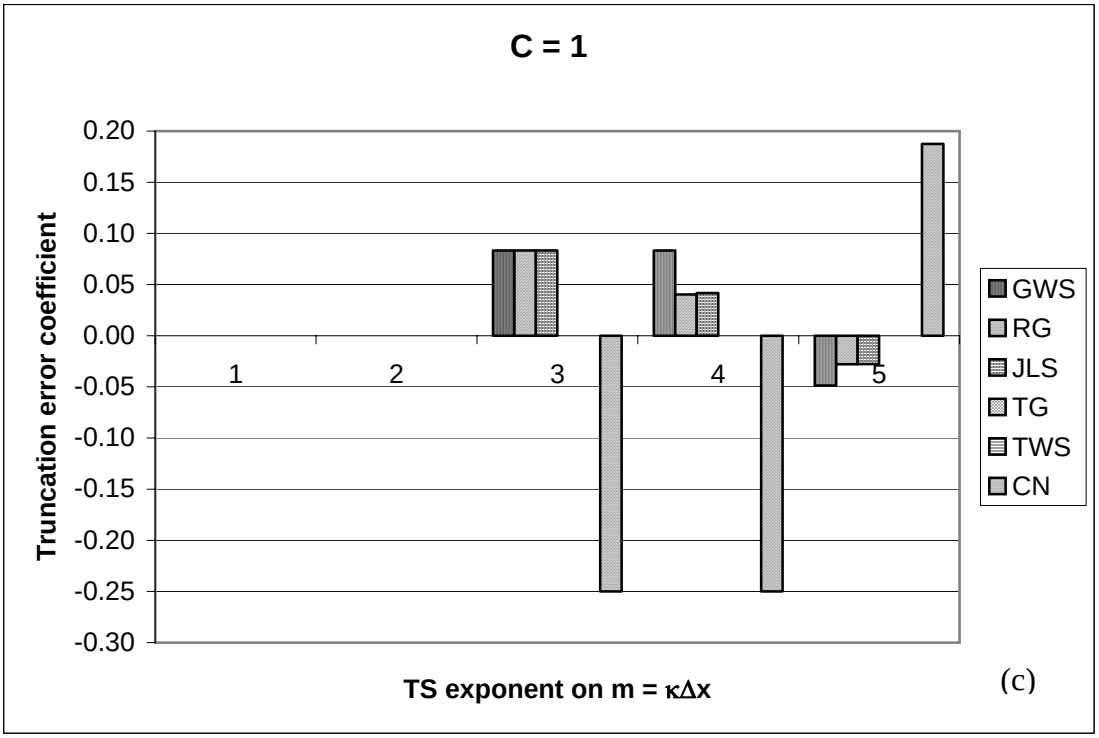

Figure 4.2. Continued

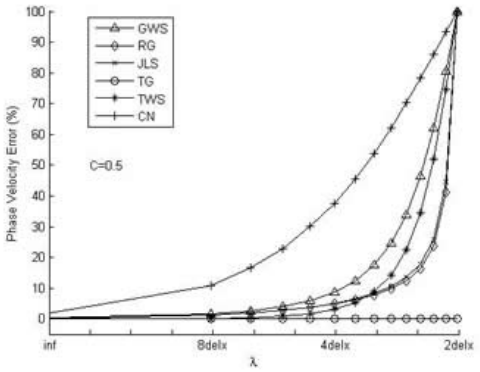

(a)

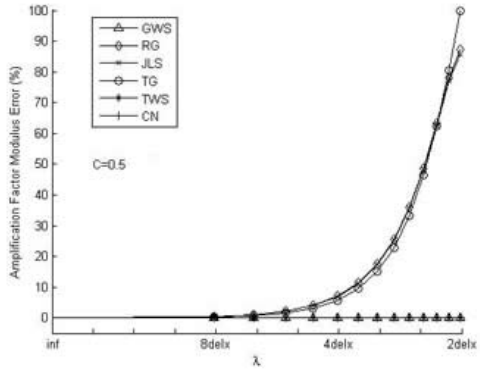

(b)

Figure 4.3. Phase velocity and amplification factor modulus error, 1D pure advection, C = 0.5, k =1, θ = 0.5 (except for TG).

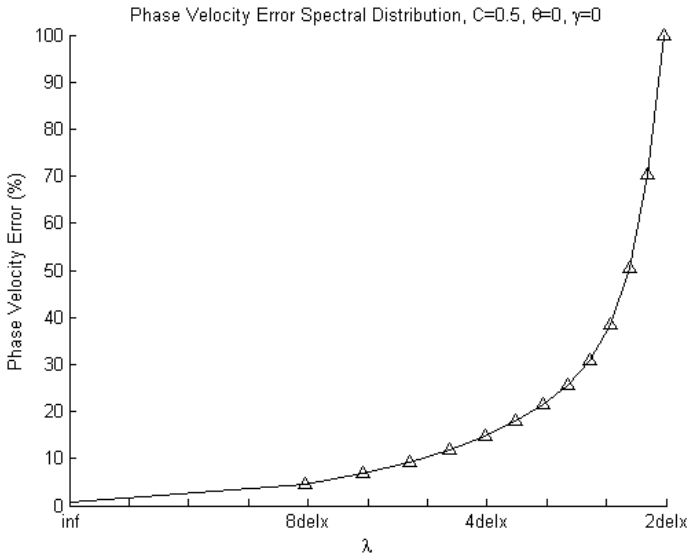

Figure 4.4. Phase velocity error, 1D pure advection, C = 0.5, k =2, θ = 0.

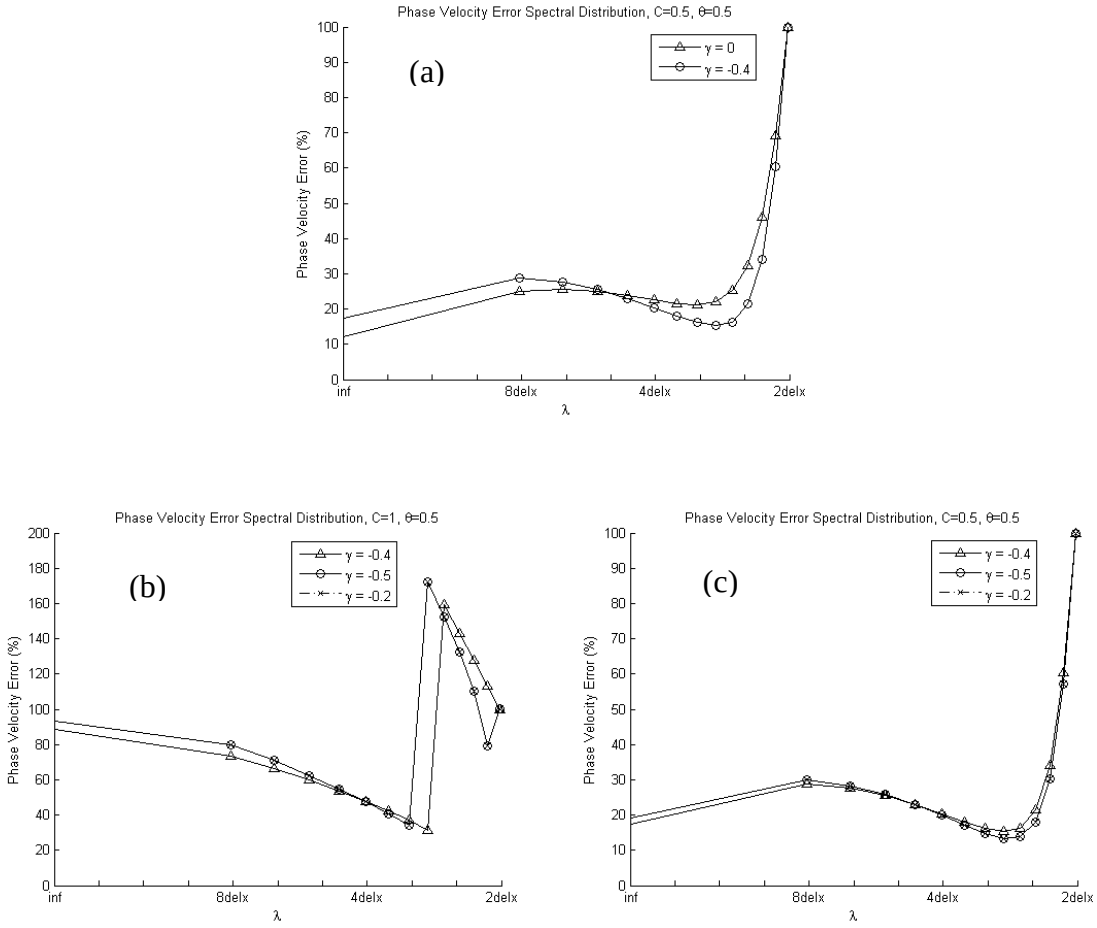

Figure 4.5. Phase velocity error, 1D pure advection, C = 0.5, k =2, θ = 0.5.

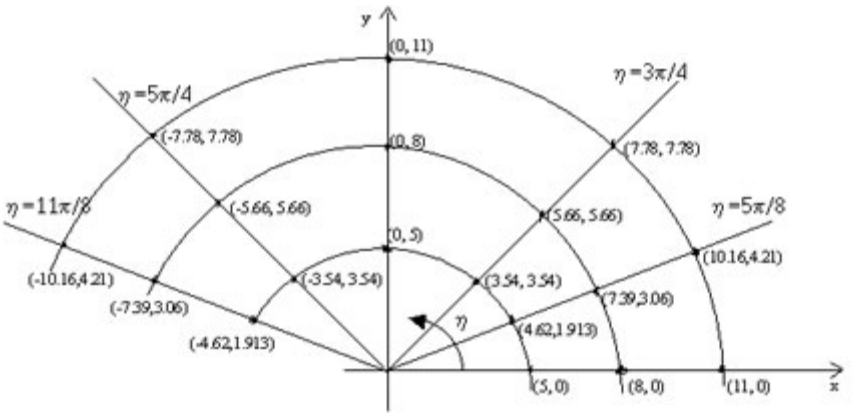

Figure 4.6. Sample space of wave vector angles for TS theoretical error quantization.

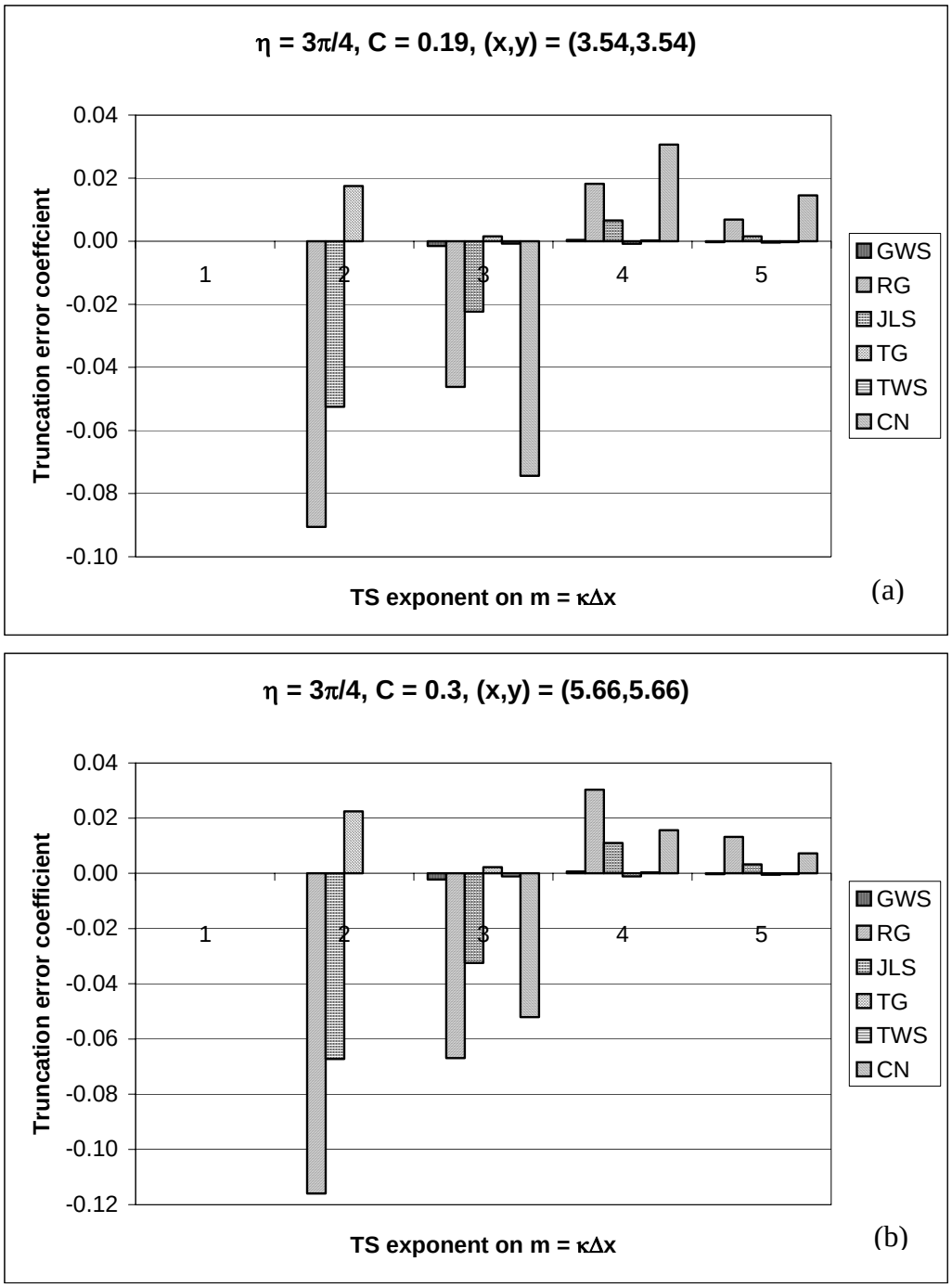

Figure 4.7. Theoretical Taylor series wave number dependence for TWS^h + θTS algorithms, 2D pure advection, $\eta = 3\pi/4$, $0.19 < C < 0.41$.

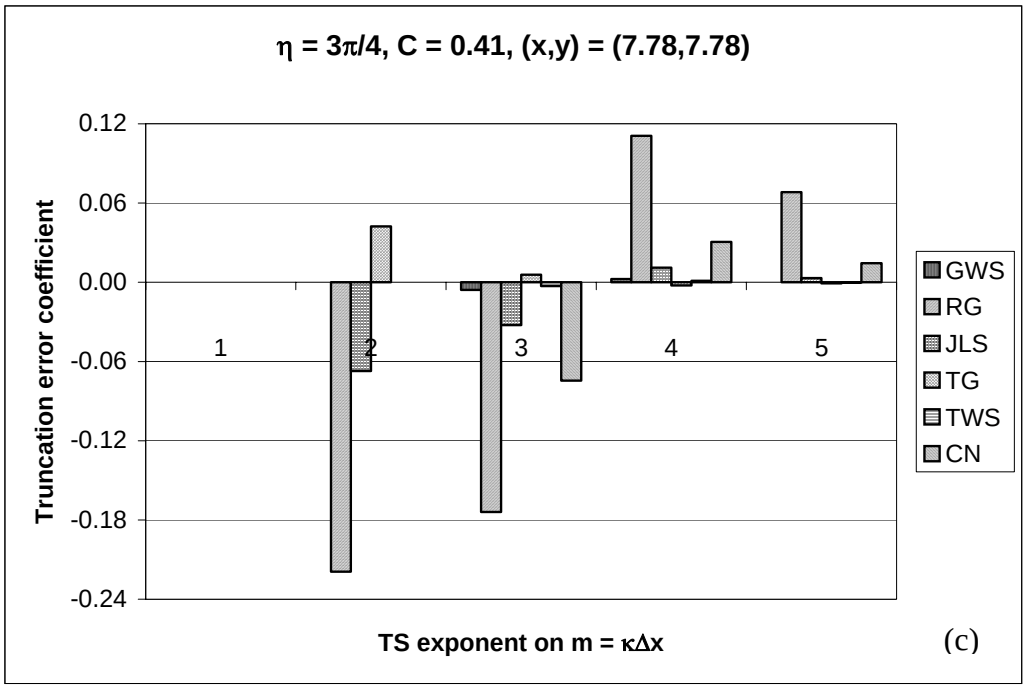

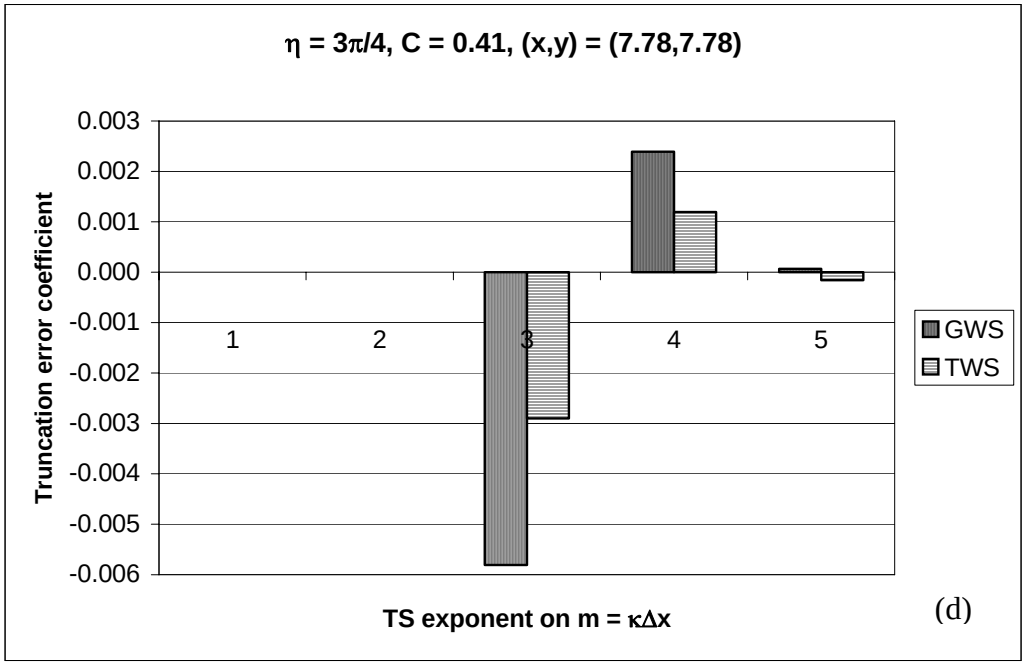

Figure 4.7. Continued

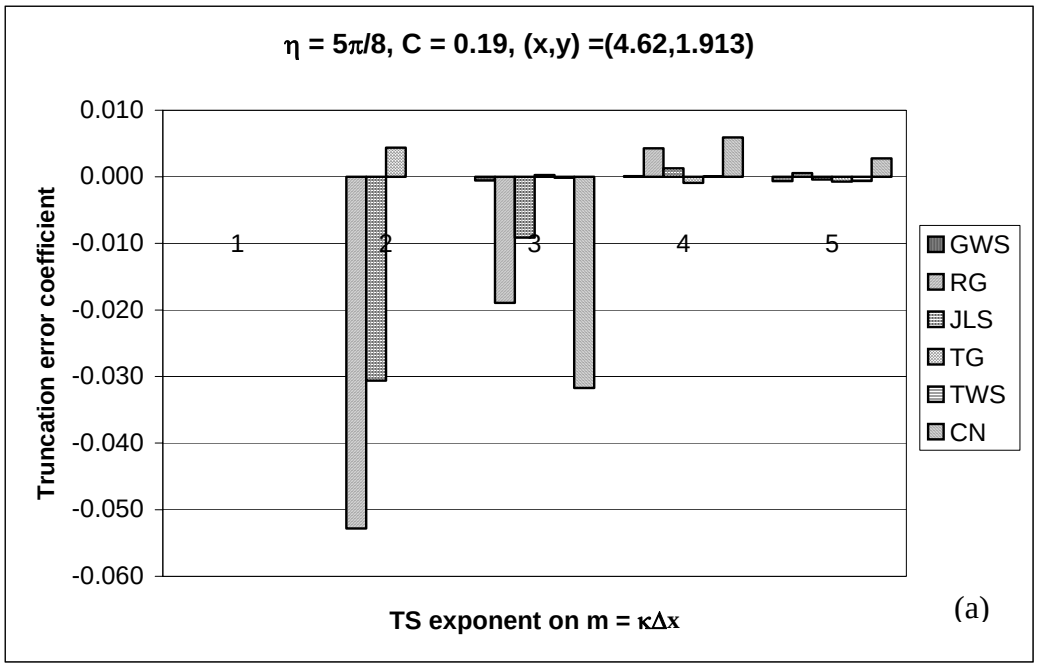

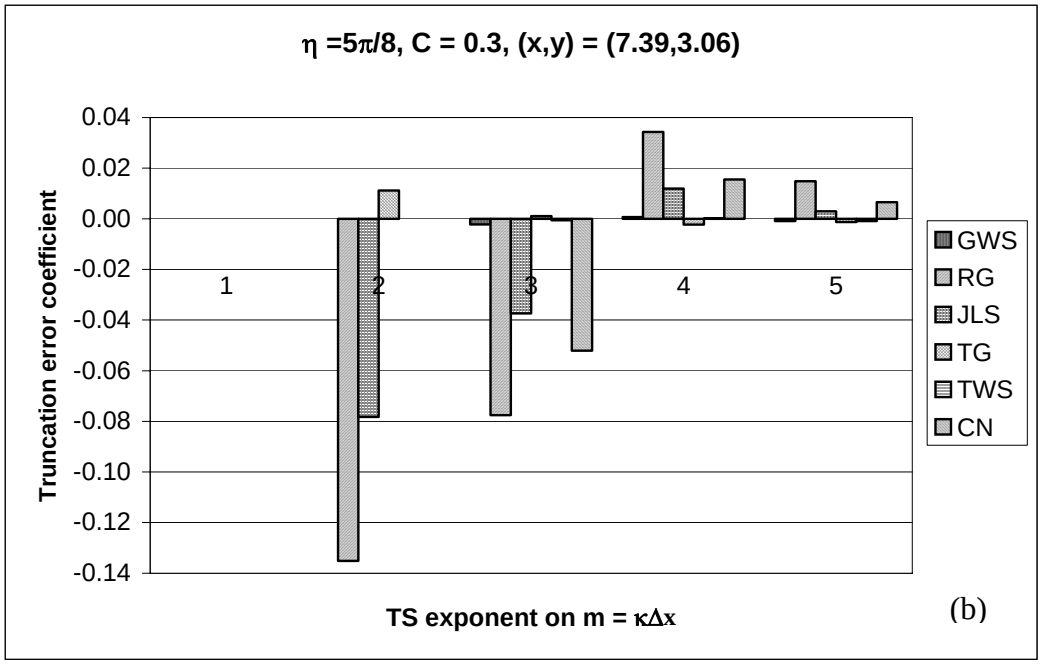

Figure 4.8. Theoretical Taylor series wave number dependence for TWS^h + θTS algorithms, 2D pure advection, $\eta = 5\pi/8$, $0.19 < C < 0.41$.

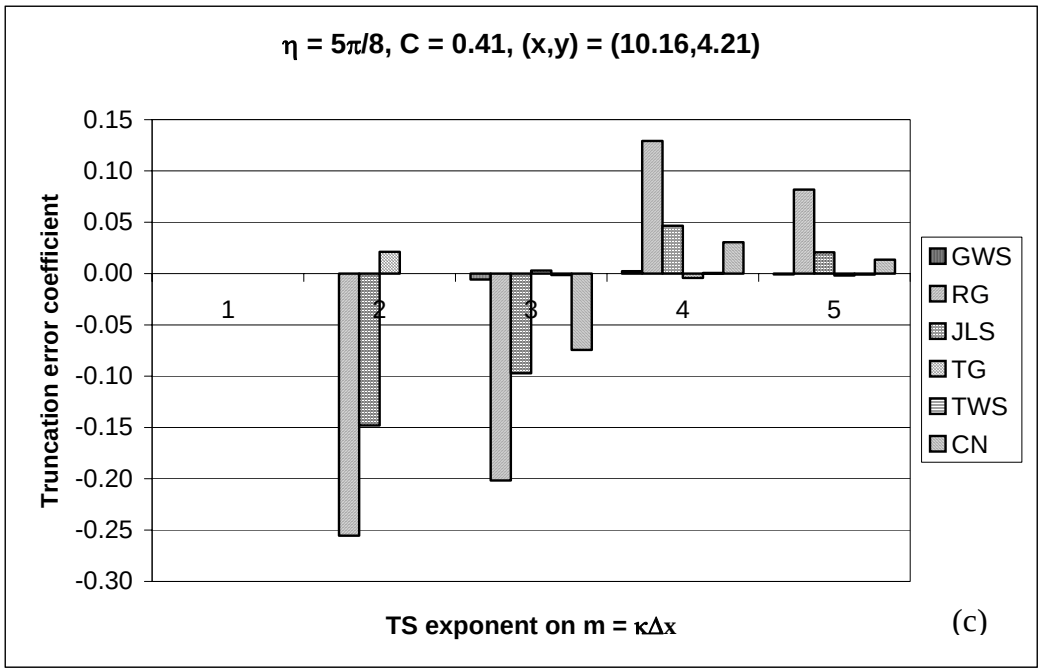

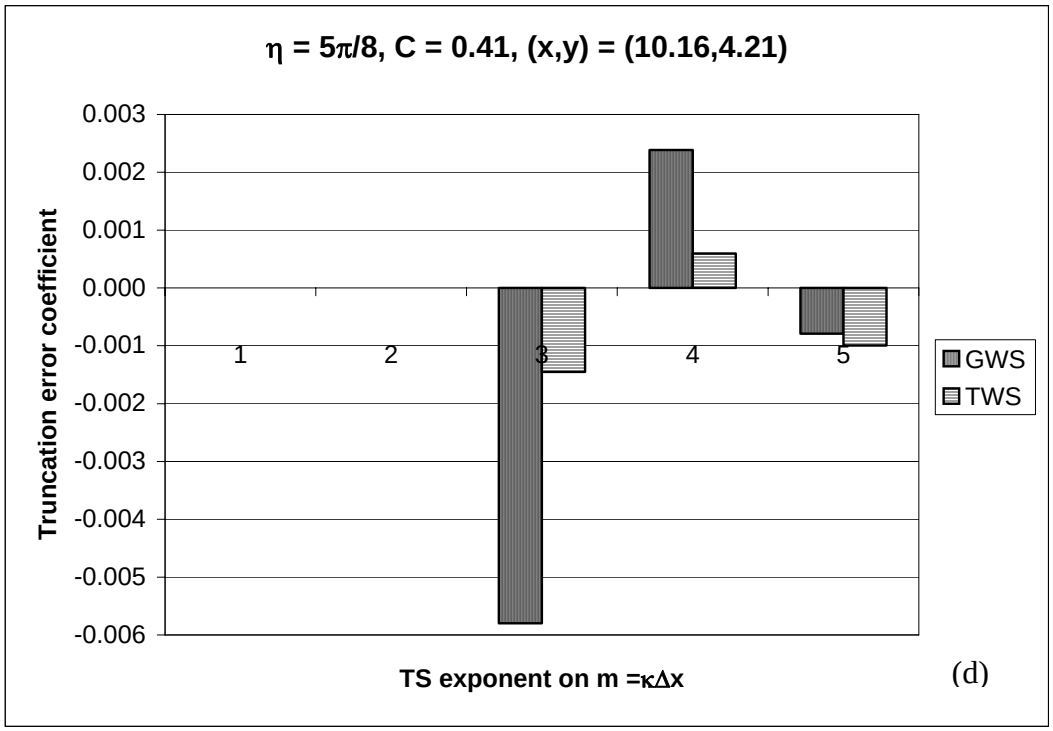

Figure 4.8. Continued

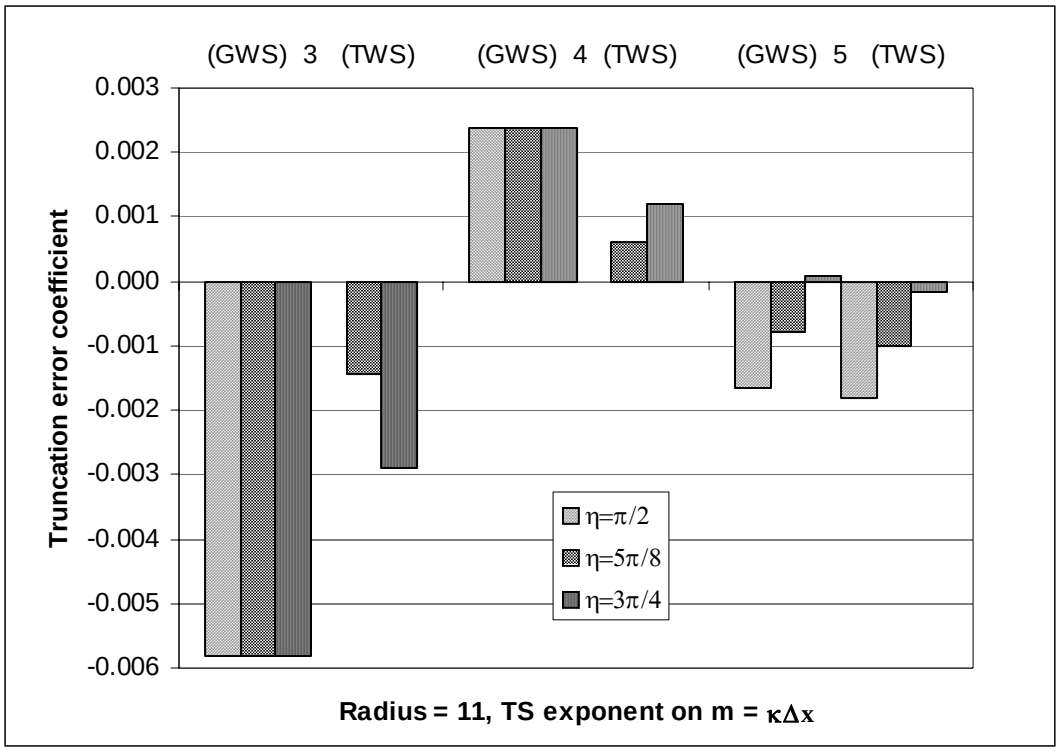

Figure 4.9. Theoretical Taylor series wave number dependence for GWS^h, TWS^h + θTS algorithms, 2D pure advection, $\eta = \pi/2, 5\pi/8, 3\pi/4$, $|\mathbf{C}| = 0.41$.

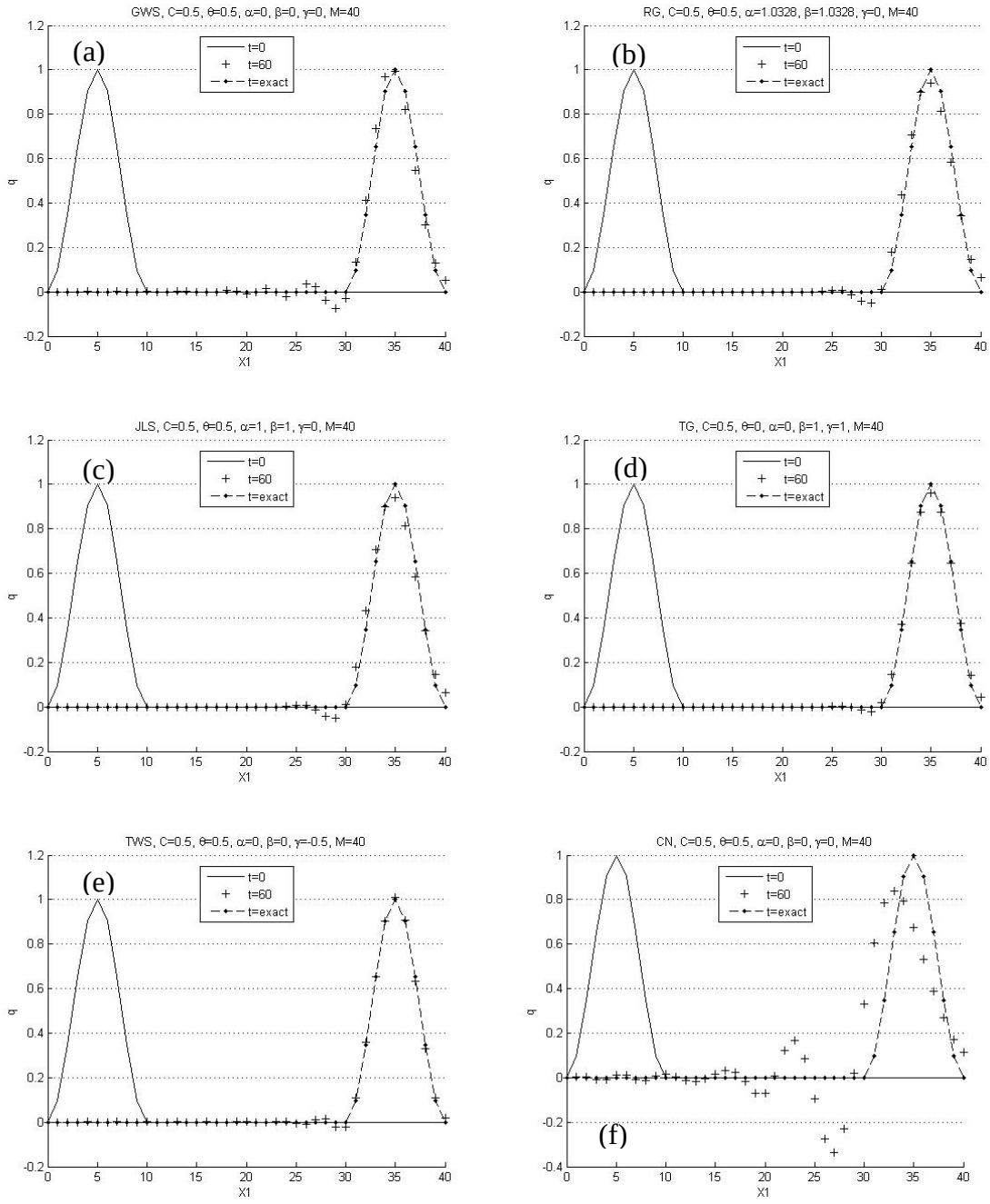

Figure 5.1. 1D pure advection of a Gaussian IC, C = 0.5, dashed line is exact solution, following 3 IC wavelength translation.

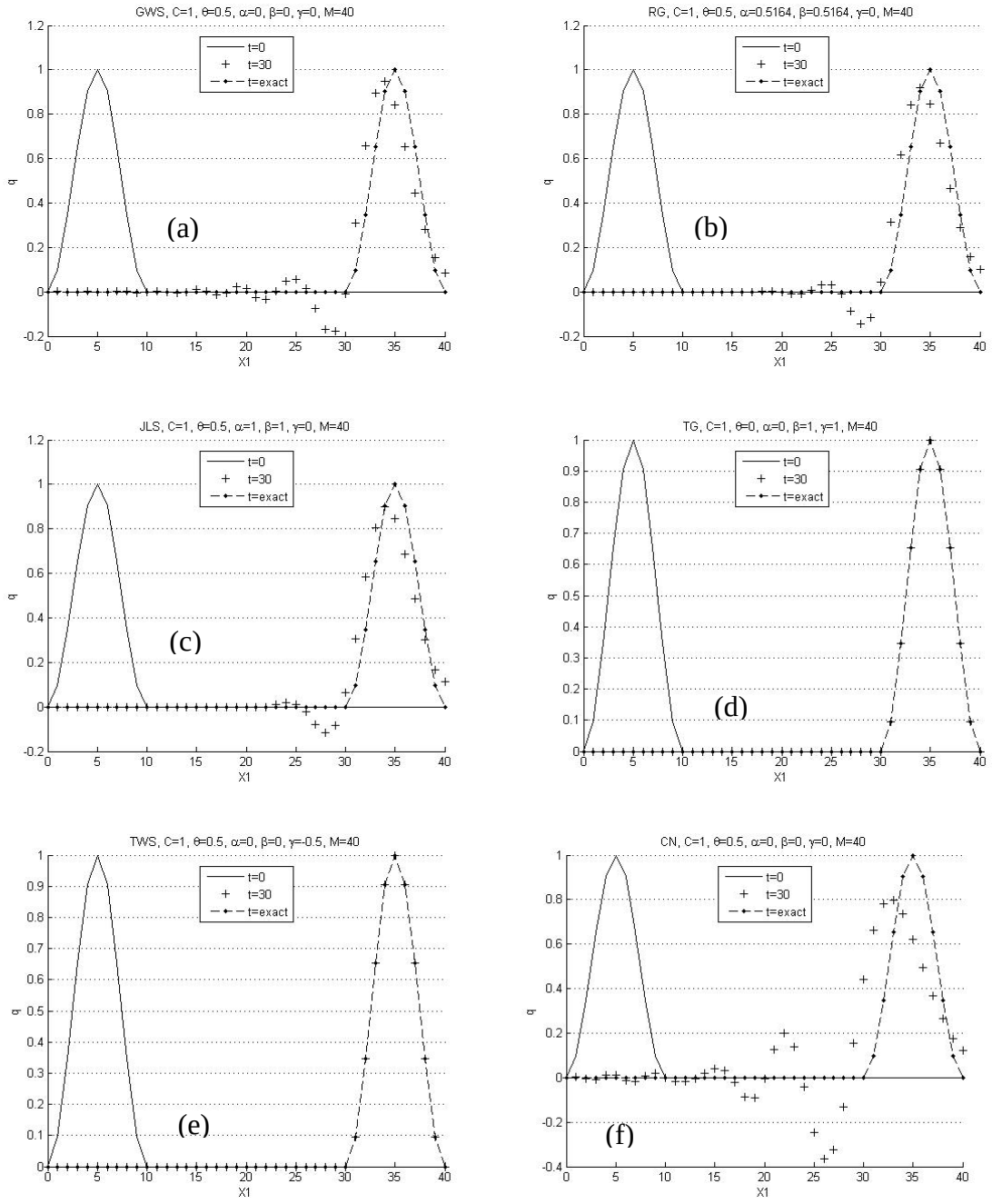

Figure 5.2. 1D pure advection of a Gaussian initial distribution, C = 1.0, dashed line is exact solution following 3-wavelength translation.

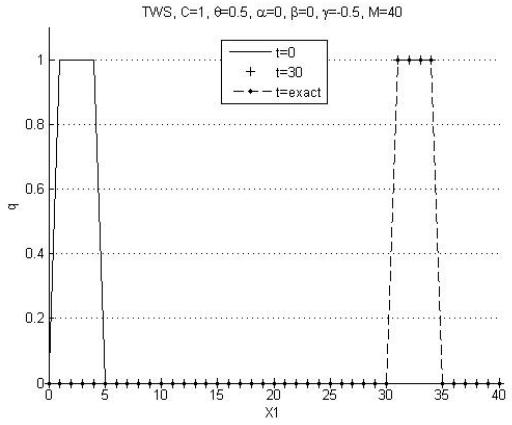

Figure 5.3. 1D pure advection of a square wave IC for TWS-γ, C = 1.0, dashed line is exact solution following 7-wavelength translation.

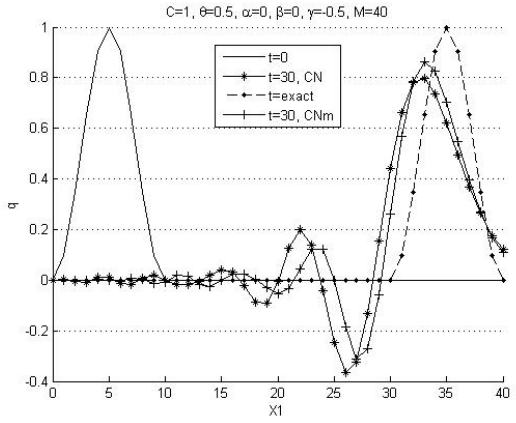

Figure 5.4. 1D pure advection of a Gaussian initial distribution for CN and CNm, C = 1.0, dashed line is exact solution following 3-wavelength translation.

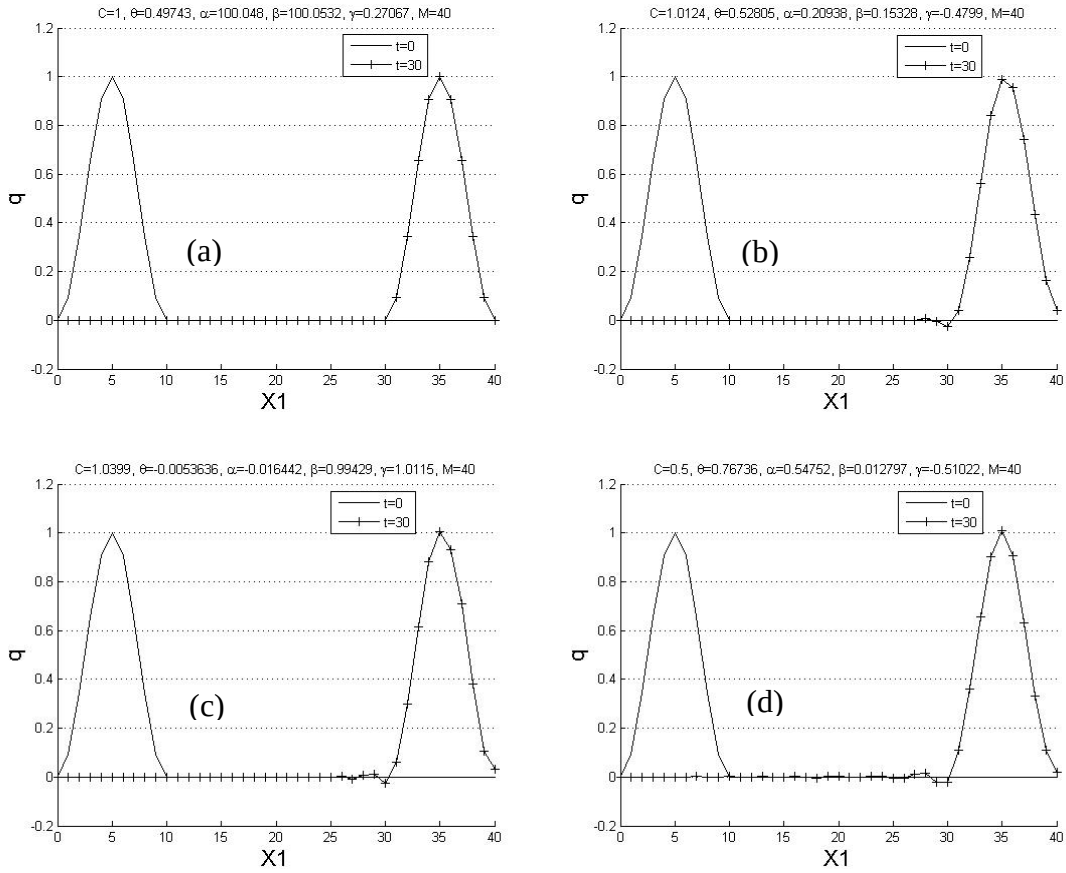

Figure 5.5 Time evolution of Gaussian IC, optimization code suggested parameter sets and various C.

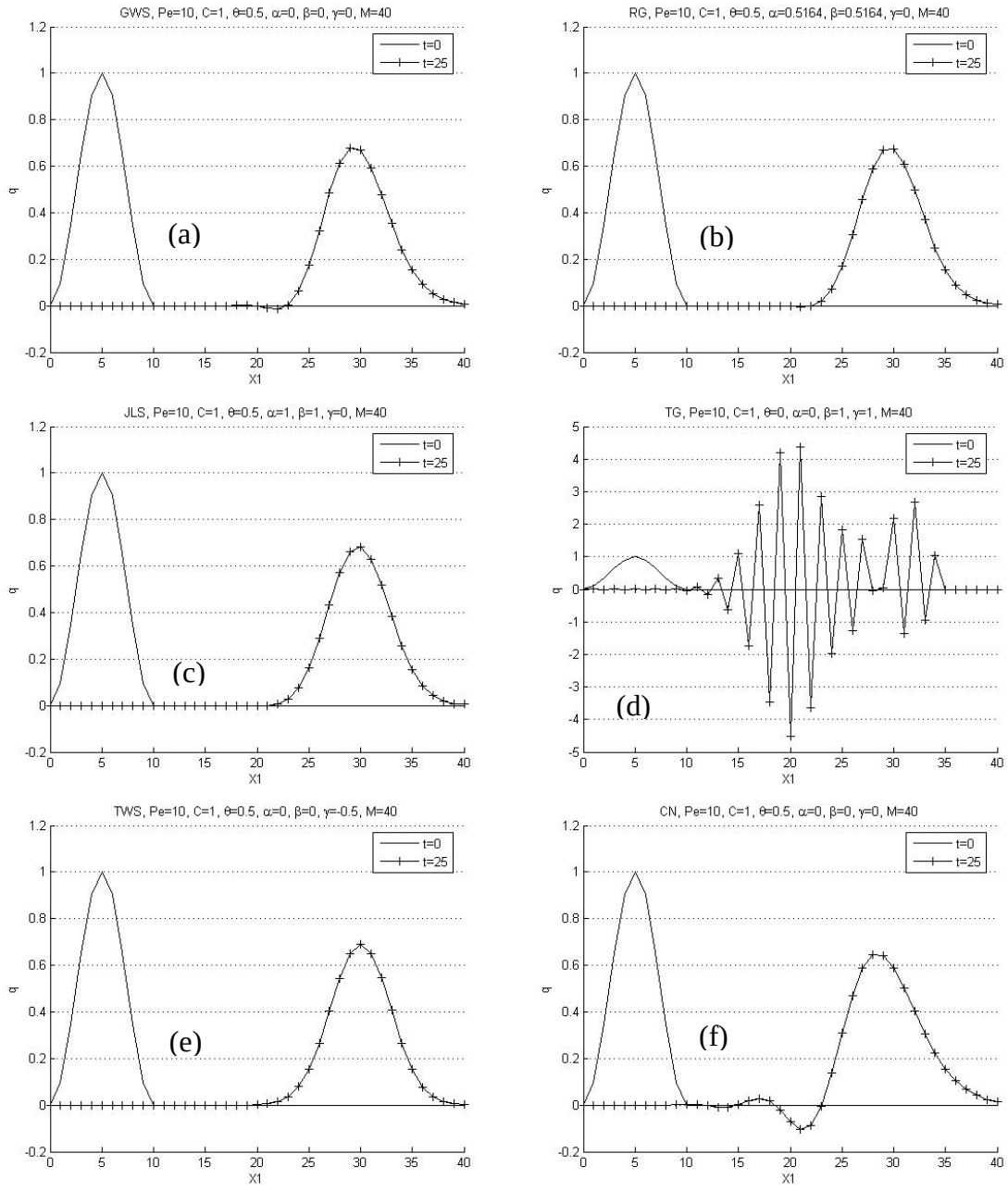

Figure 5.6. 1D advection-diffusion, solution after 25 time-steps, Pe=10, C=1.

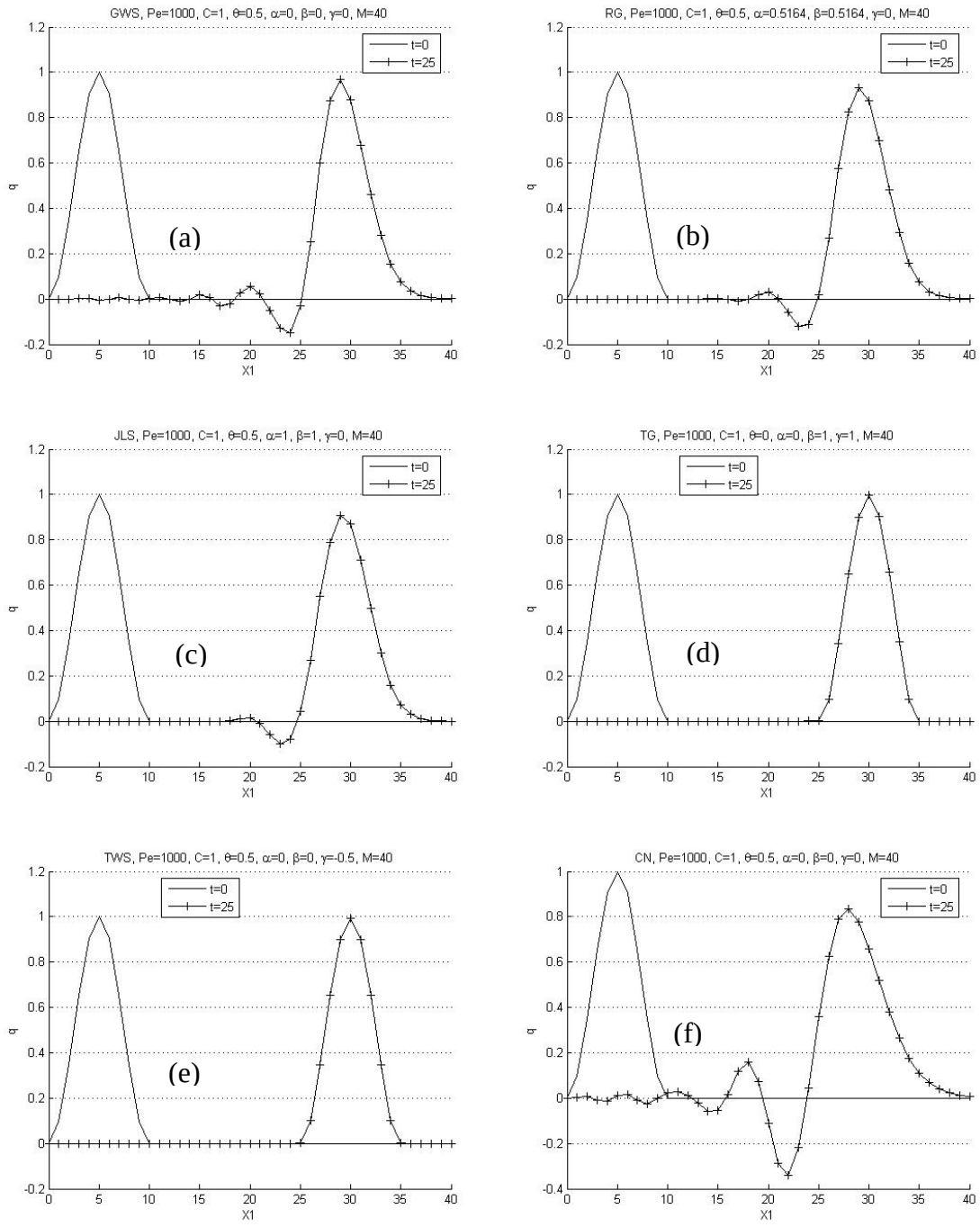

Figure 5.7. 1D advection-diffusion, solution after 25 time-steps, Pe=1000, C=1.

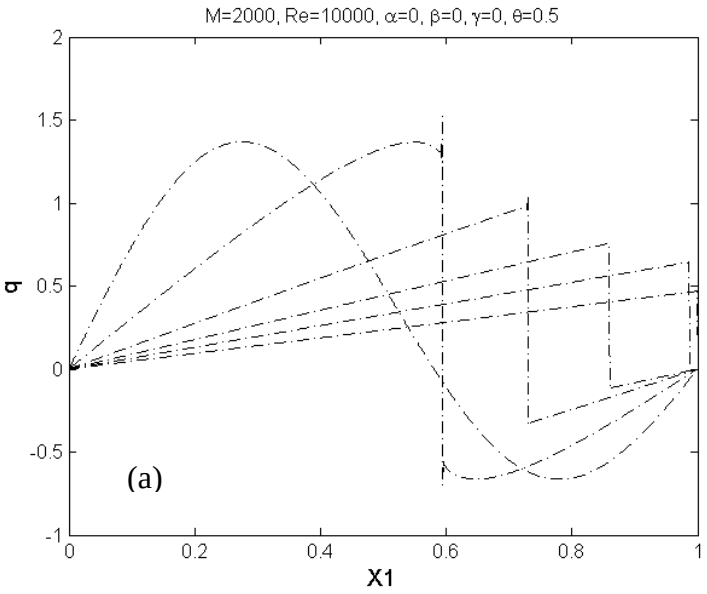

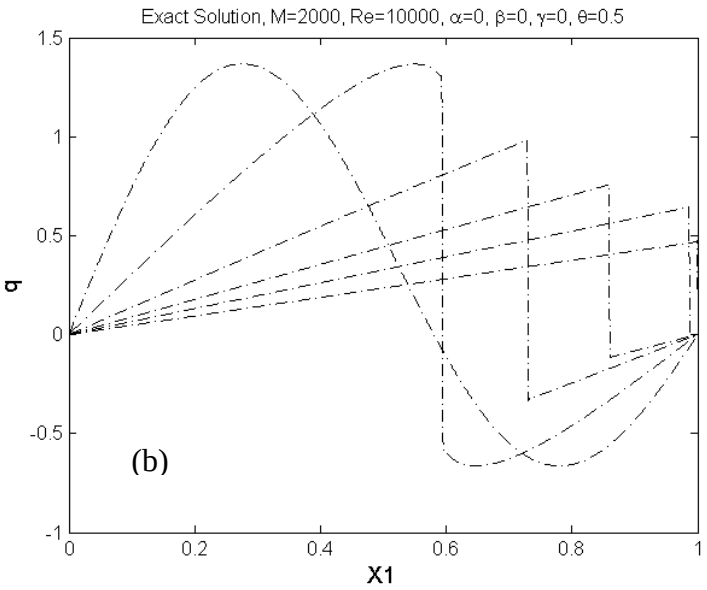

Figure 5.8. Burgers Equation, semi-implicit β, time = 0, 0.2, 0.6, 1.0, 1.4, 2.0, M=200.

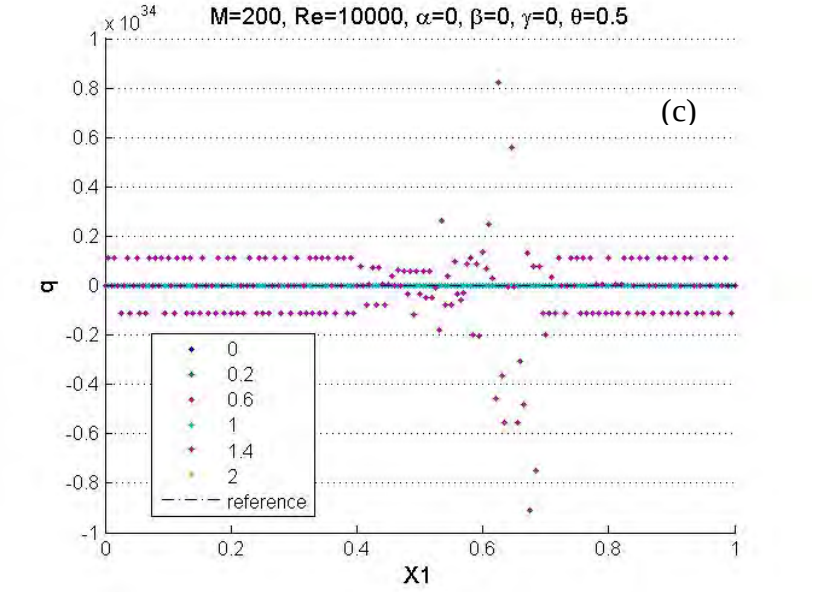

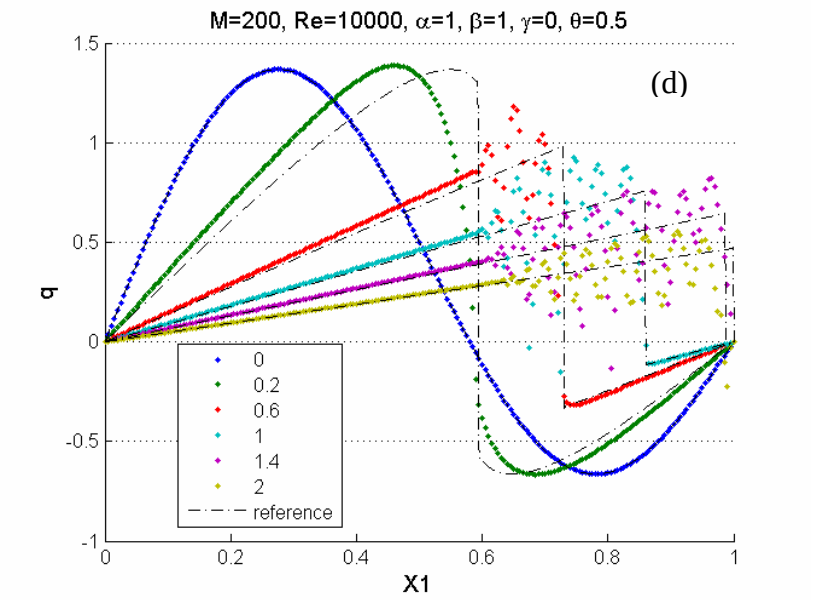

Figure 5.8. Continued

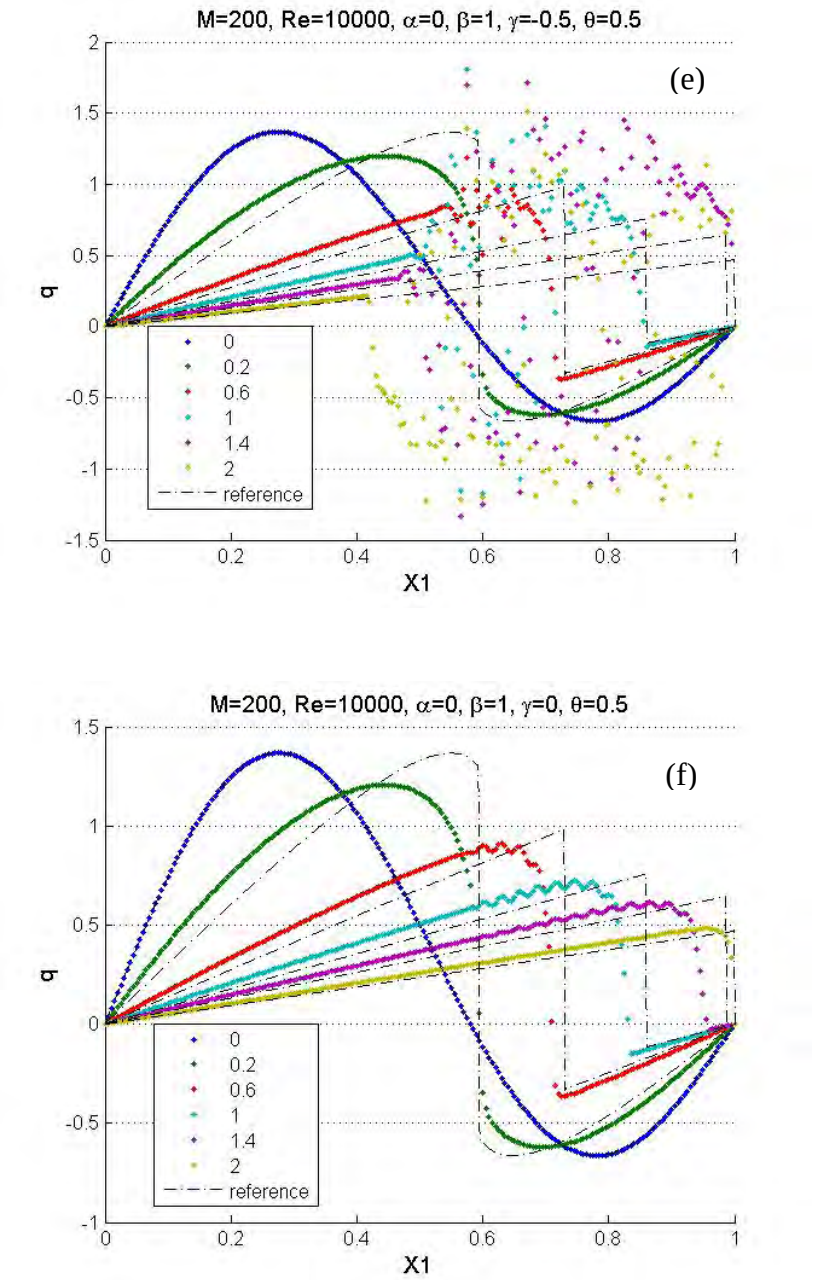

Figure 5.8. Continued

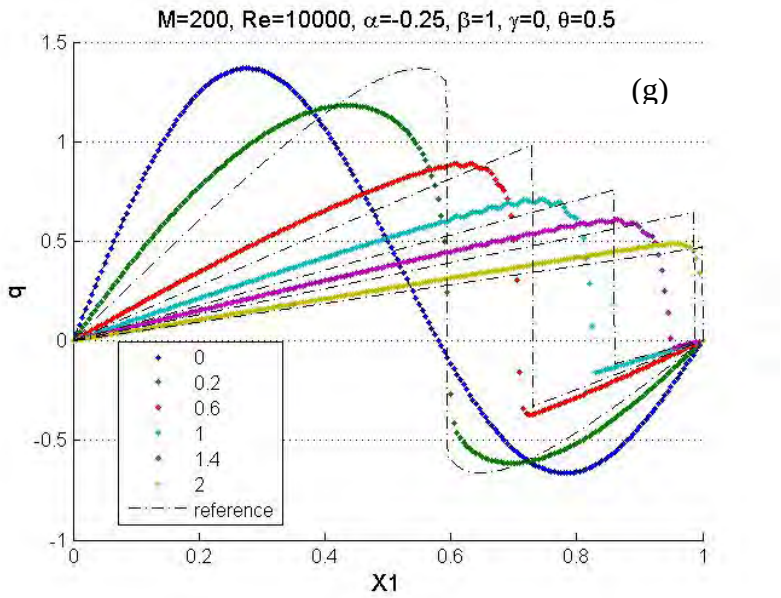

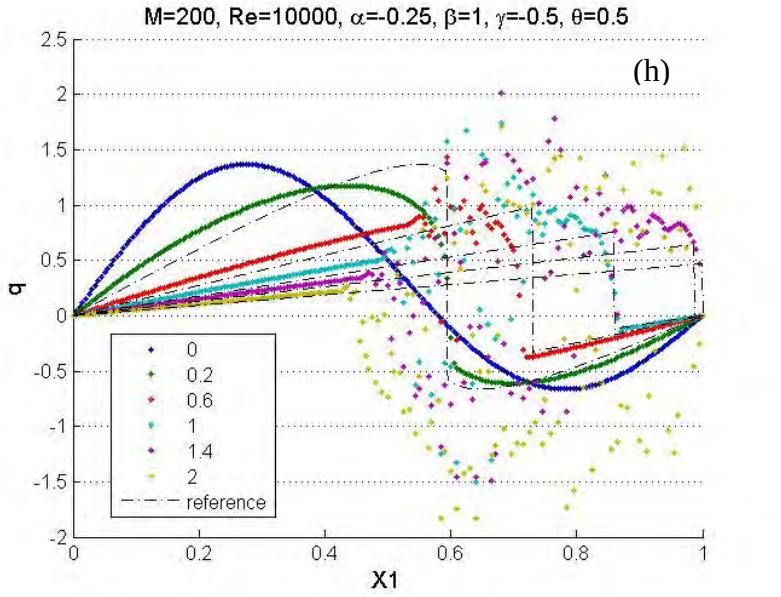

Figure 5.8. Continued

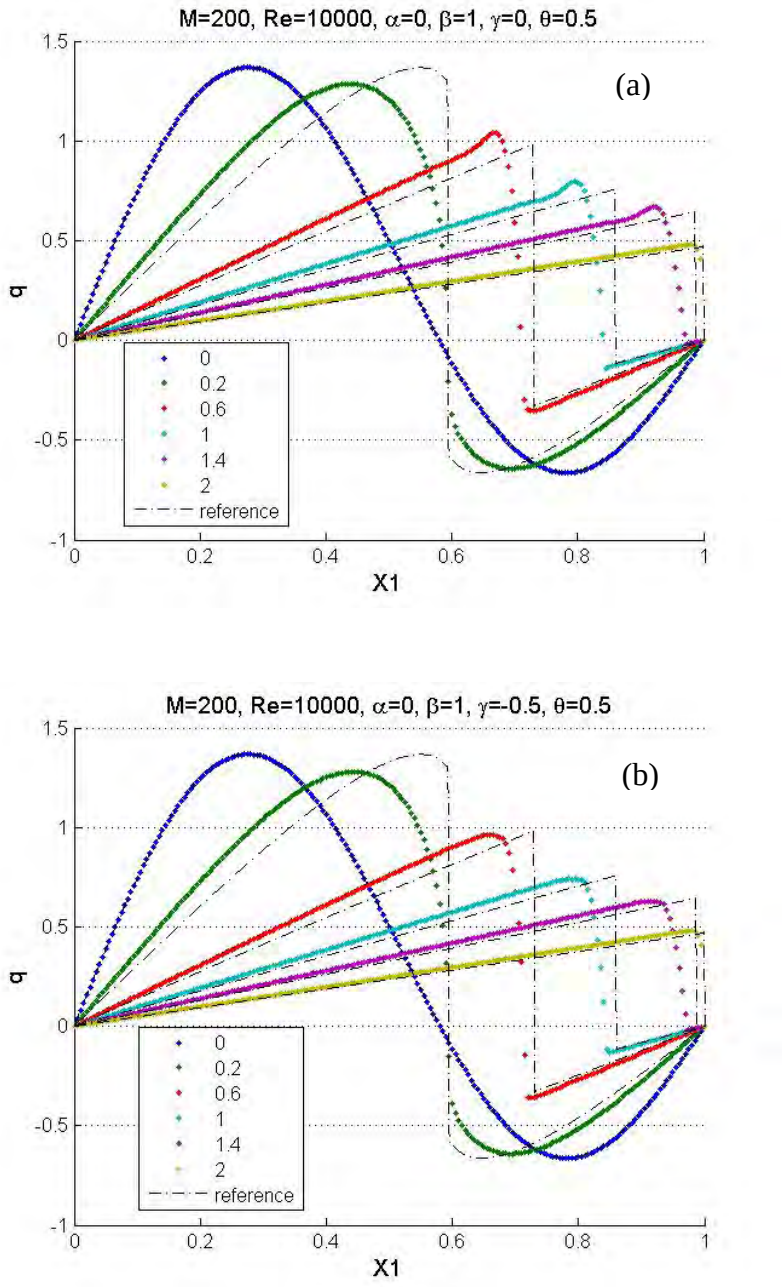

Figure 5.9. Burgers equation, fully-implicit β, time = 0, 0.2, 0.6, 1.0, 1.4, 2.0, M=200.

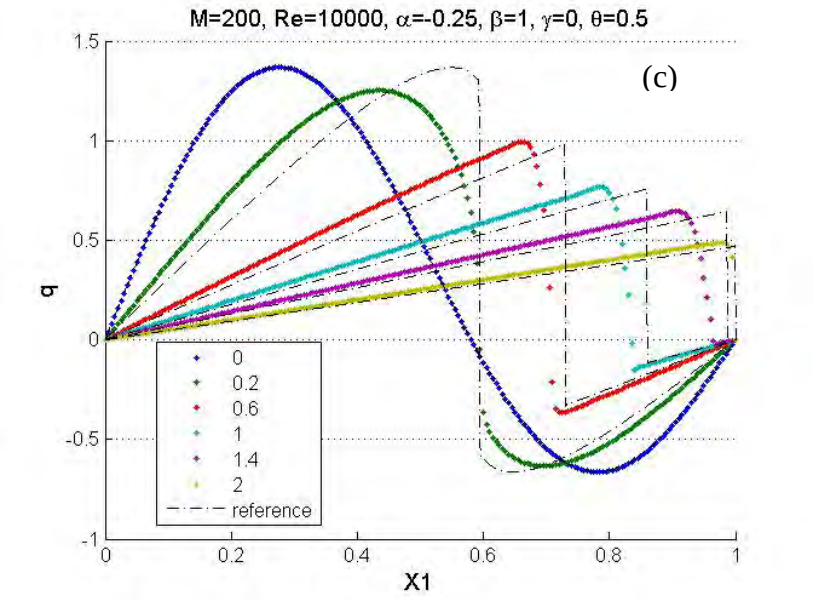

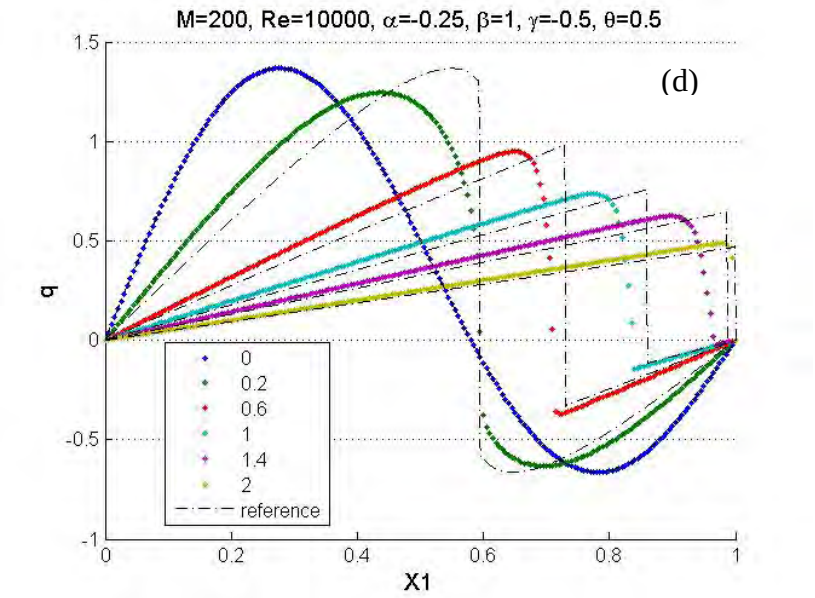

Figure 5.9. Continued

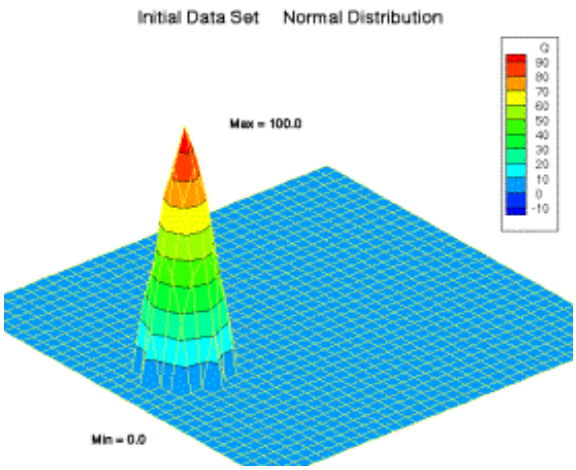

Figure 5.10 Gaussian IC and exact solution for the 2D rotating cone verification problem

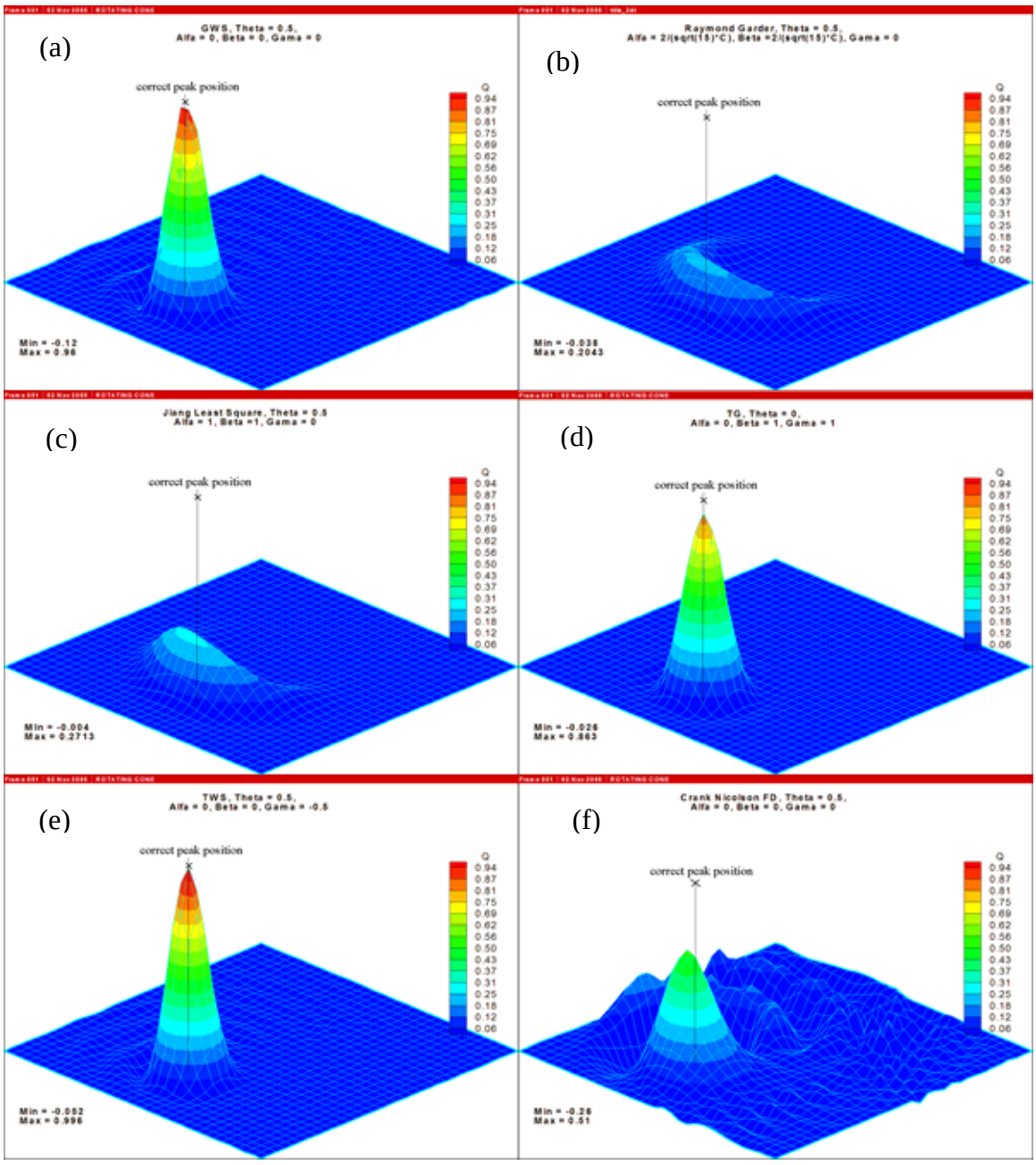

Figure 5.11. 2D pure advection rotating cone verification problem, discrete solutions after one revolution, uniform Cartesian mesh, $|\mathbf{C}| = 0.3$ at IC centroid.

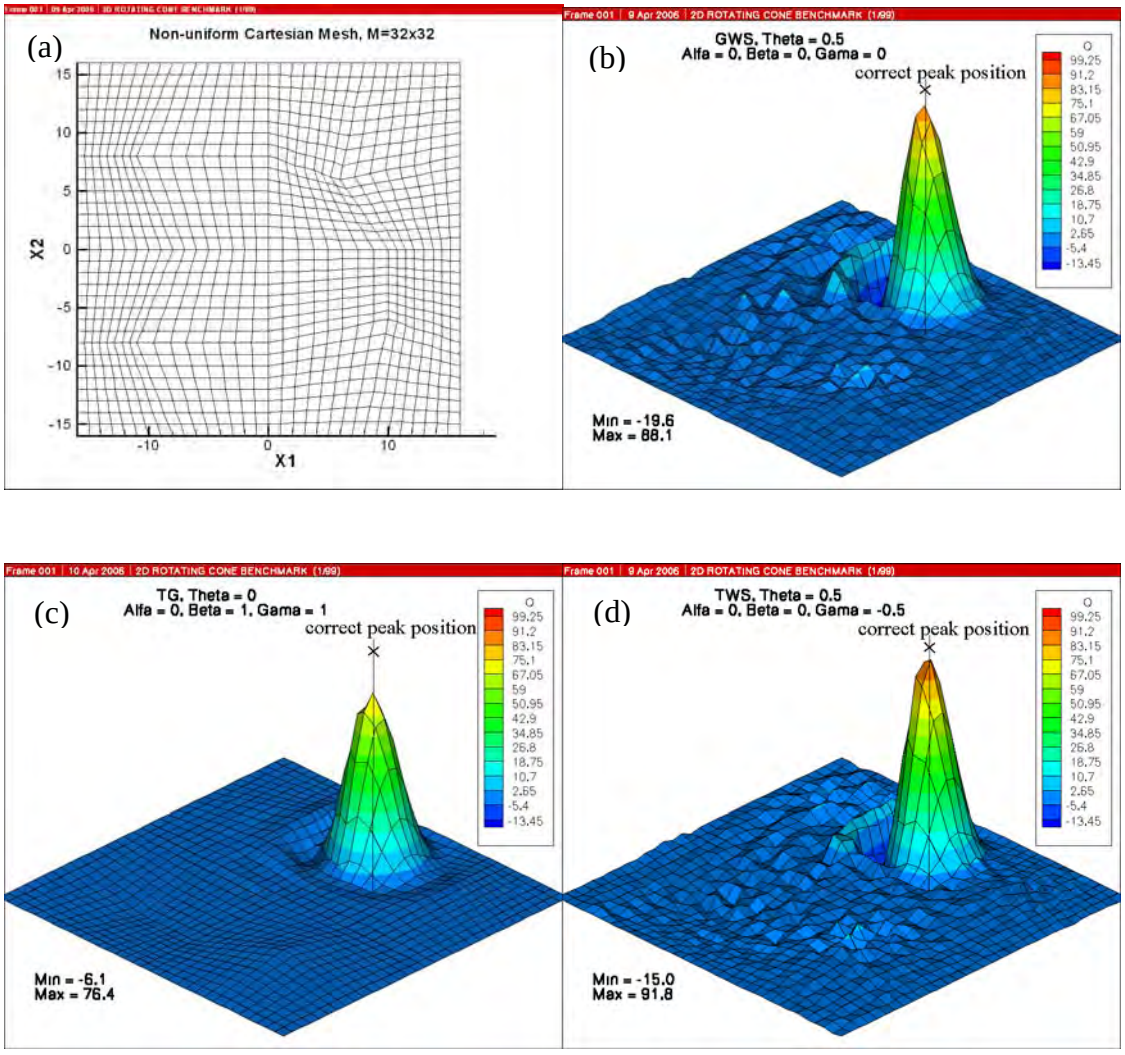

Figure 5.12. 2D pure advection rotating cone verification problem, discrete solutions after one revolution, non-uniform Cartesian mesh, $|\mathbf{C}| = 0.3$ at IC centroid.

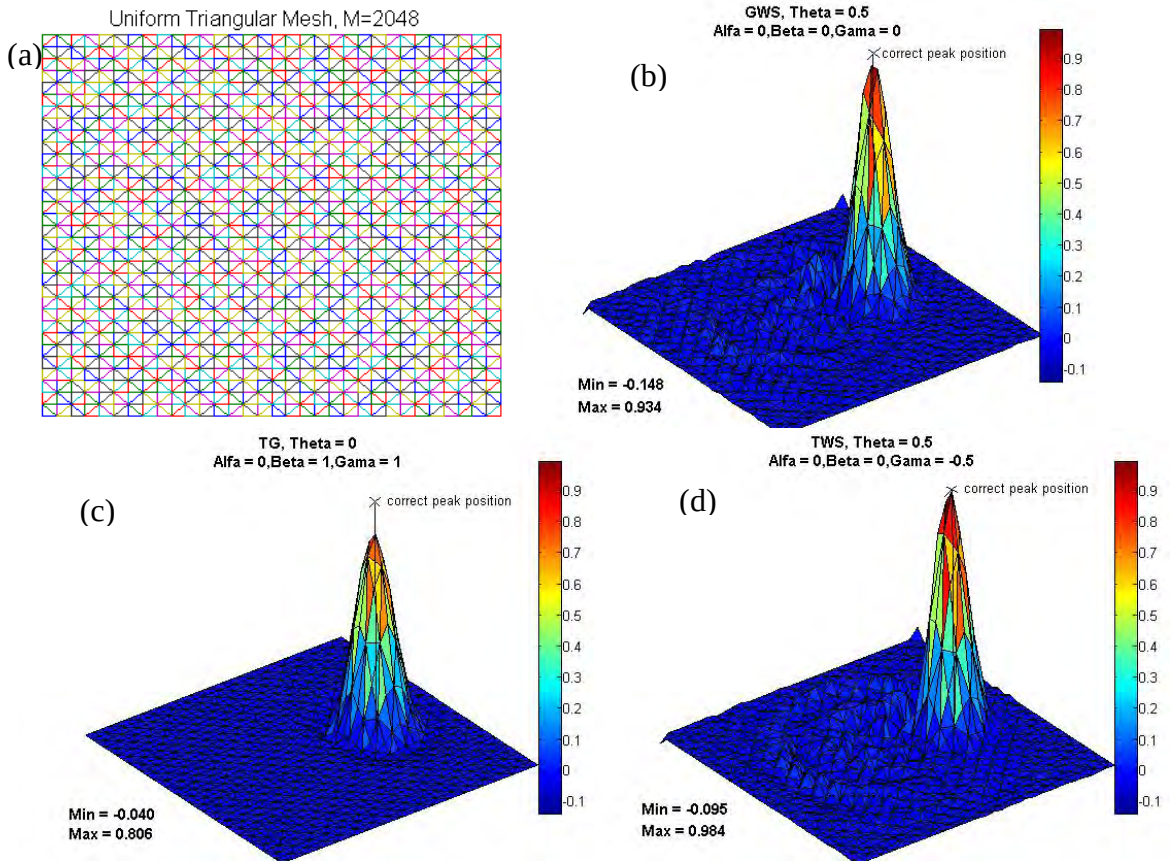

Figure 5.13. 2D pure advection rotating cone verification problem, uniform-triangular mesh and discrete solutions after one revolution, uniform triangular mesh, |**C**| = 0.3 at IC centroid, M = 2048.

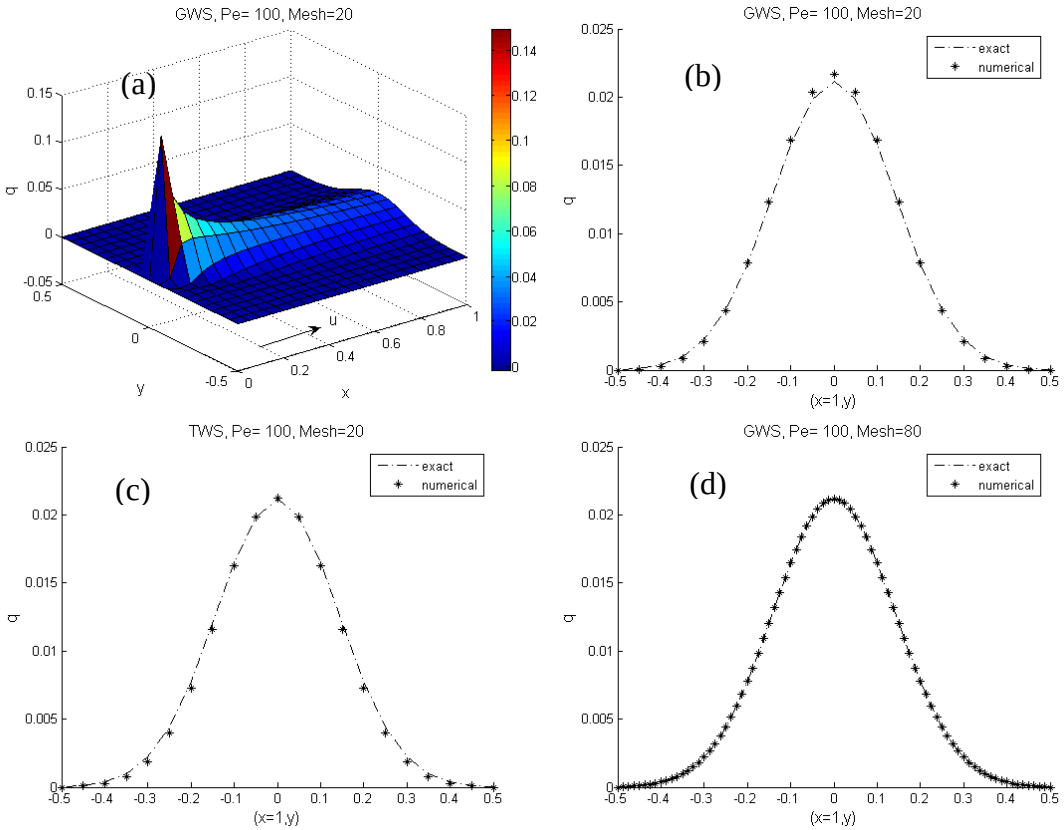

Figure 5.14. Advection-diffusion with source, M= 20x20, M = 80x80.

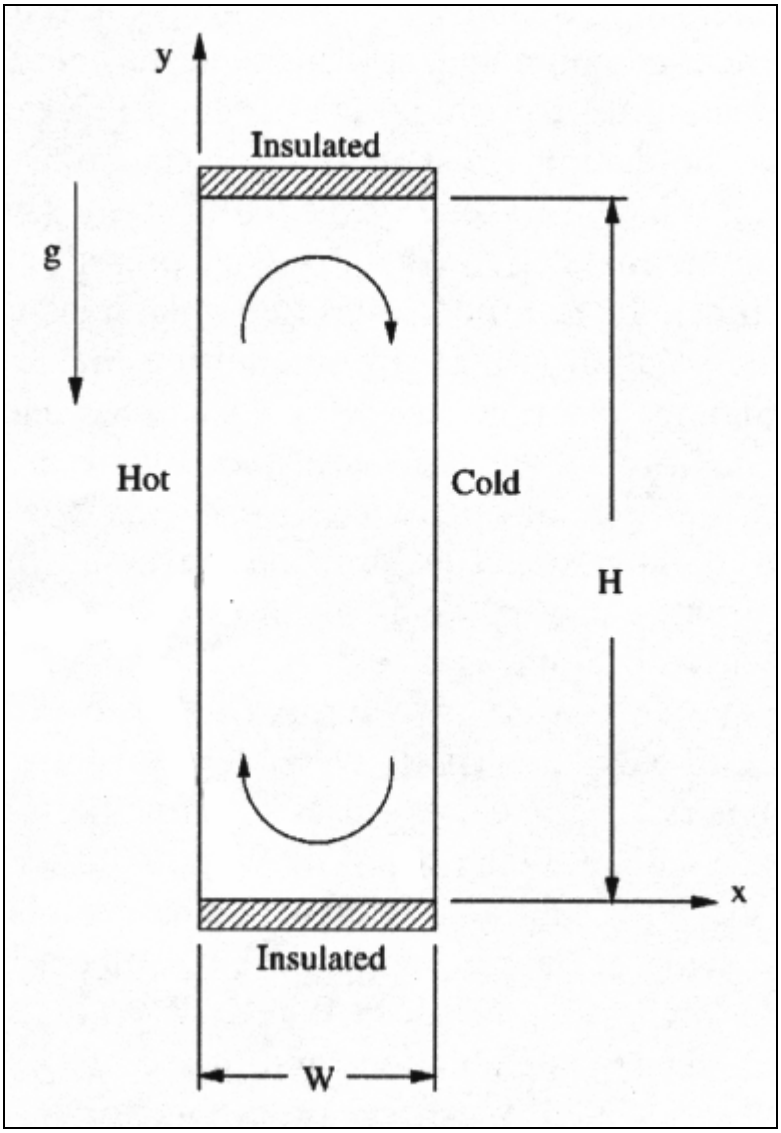

Figure 5.15. Thermal cavity set, 8x1 aspect ratio.

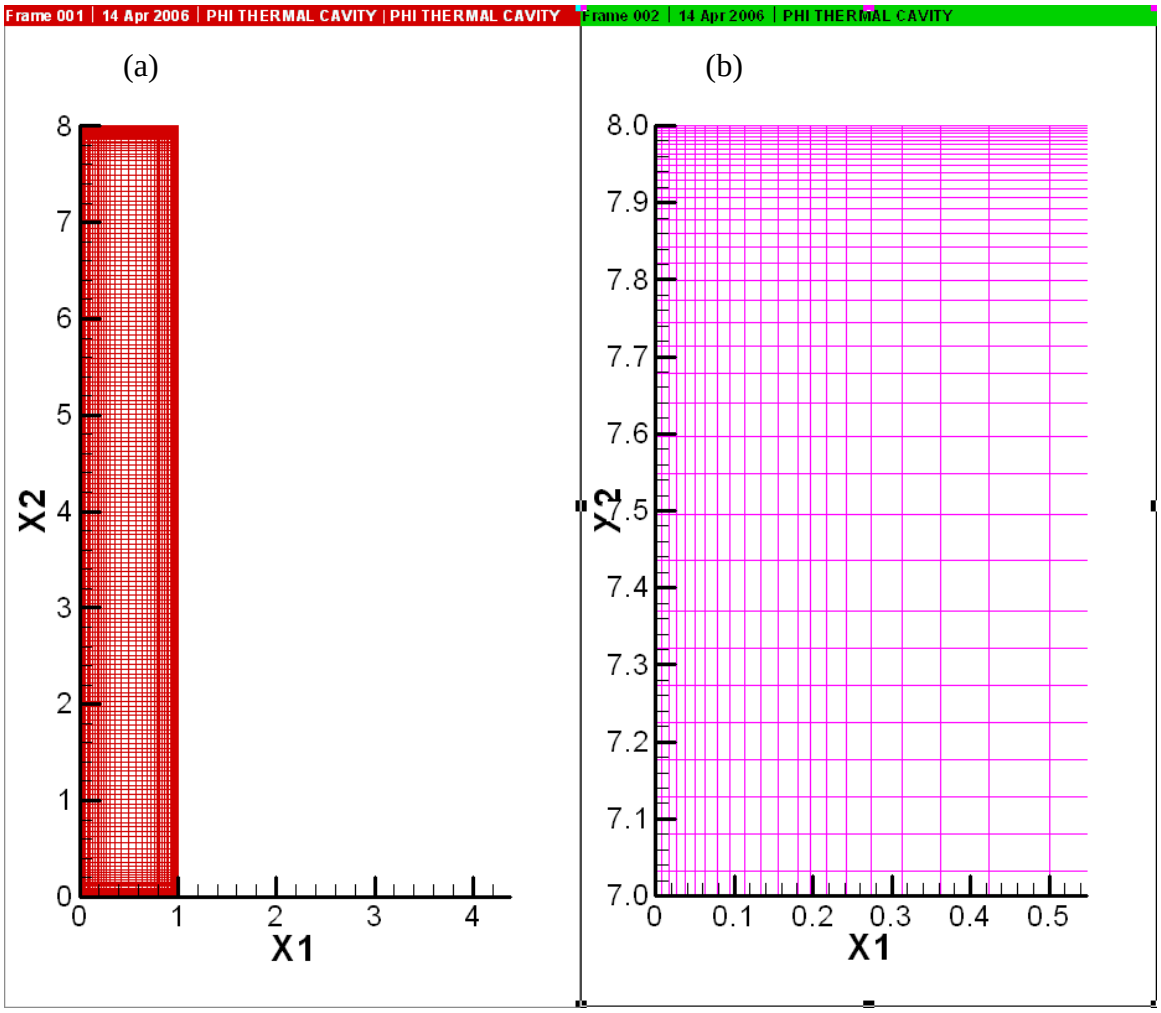

Figure 5.16. M=41x201, non-uniform mesh, a) full-mesh, b) close-up.

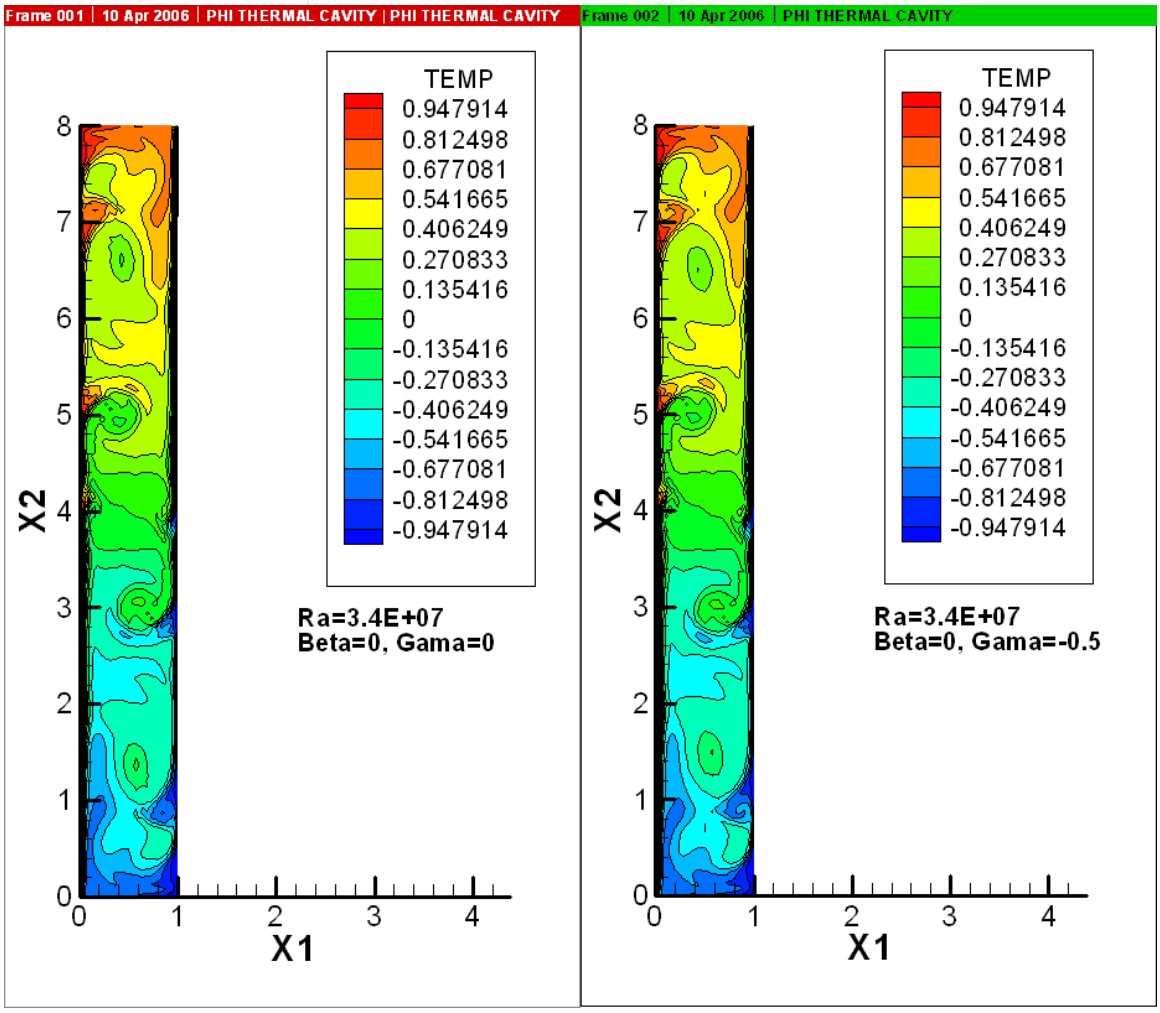

Figure 5.17. Temperature distribution after 1500 time steps for GWS and TWS-γ, Ra=3.4E+07, M=41x201.

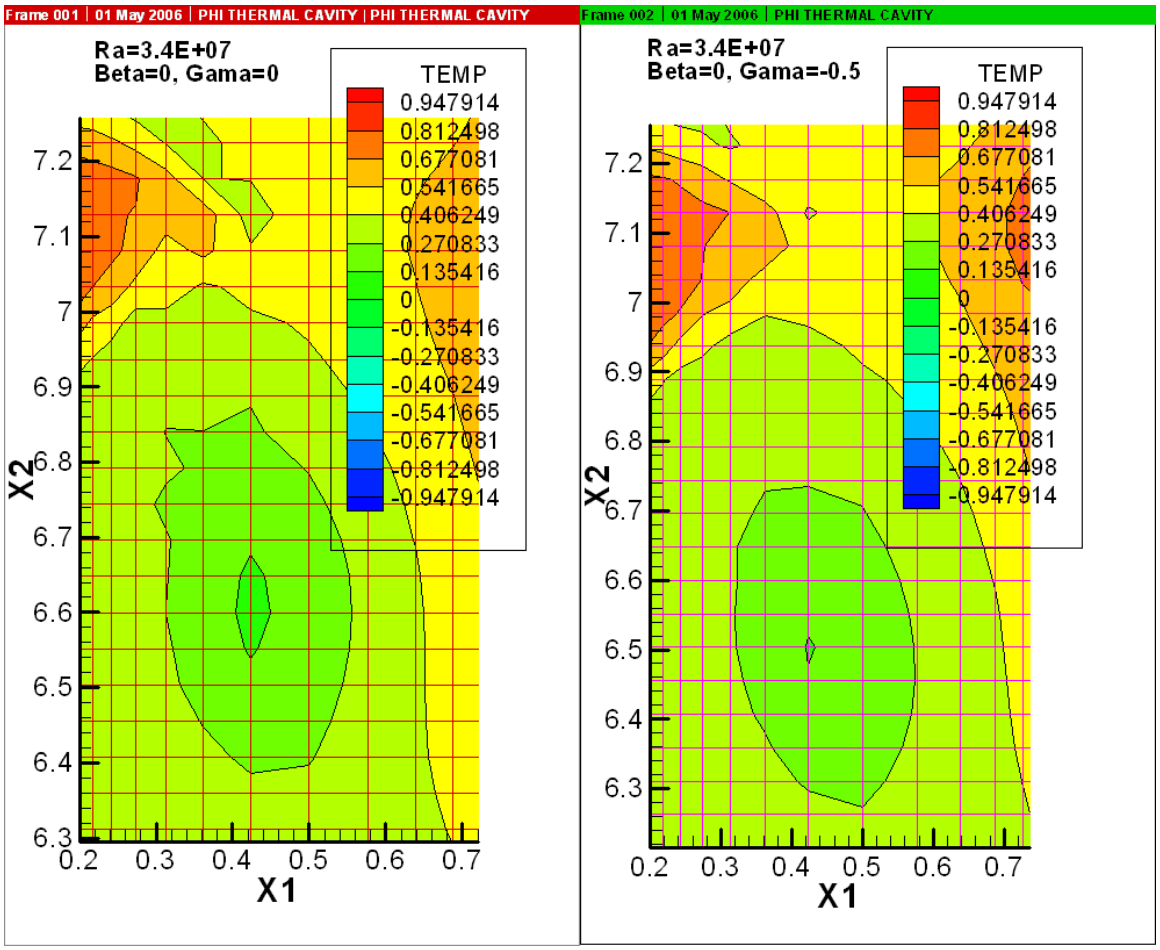

Figure 5.18. Close-up of the temperature distribution after 1500 time steps for GWS and TWS-γ, Ra=3.4E+07, M=41x201.

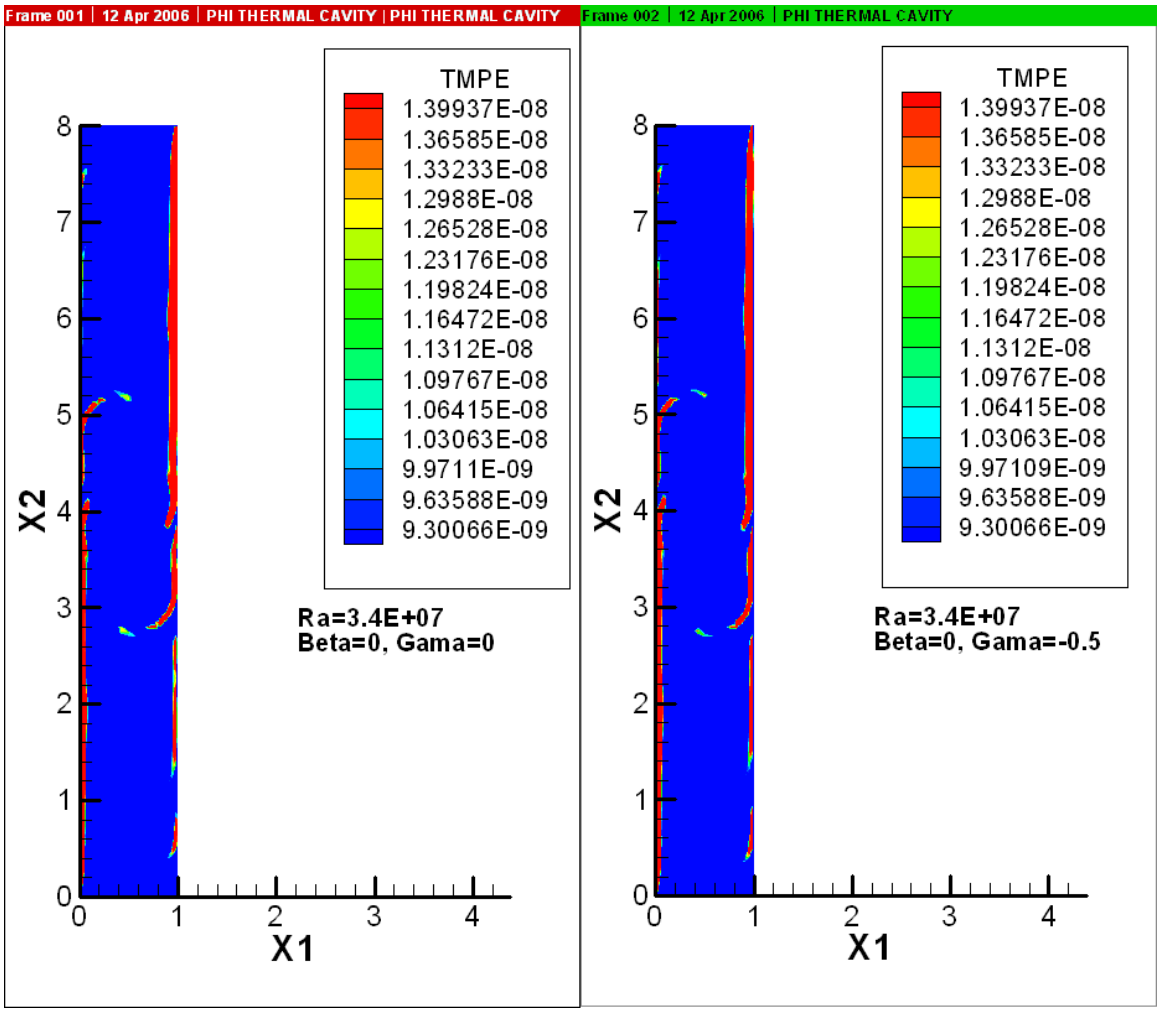

Figure 5.19. Temperature energy norm distribution after 1500 time steps for GWS and TWS-γ, Ra=3.4E+07, M=41x201.

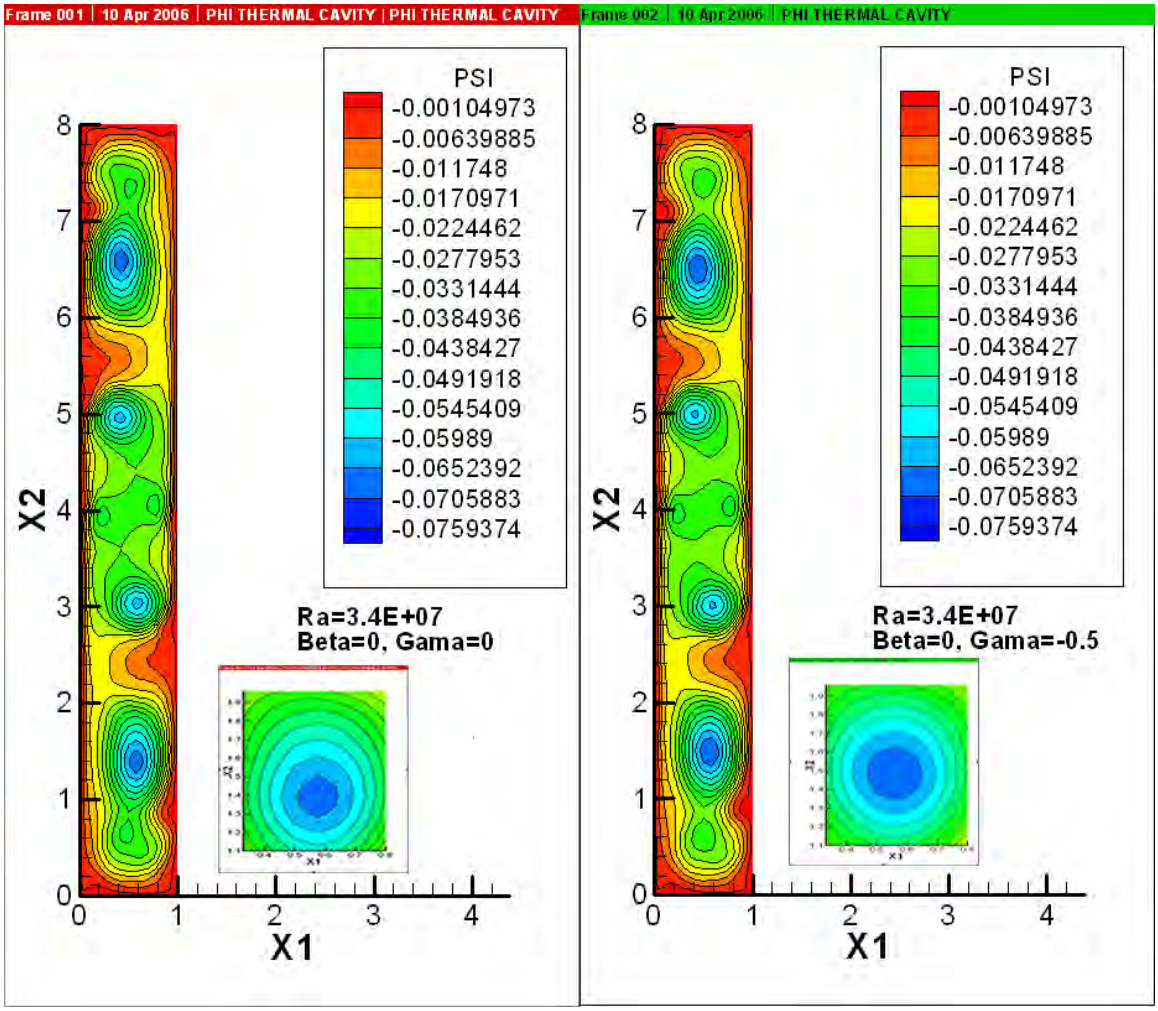

Figure 5.20. Stream function distribution after 1500 time steps for GWS and TWS-γ, Ra=3.4E7. M=41x201.

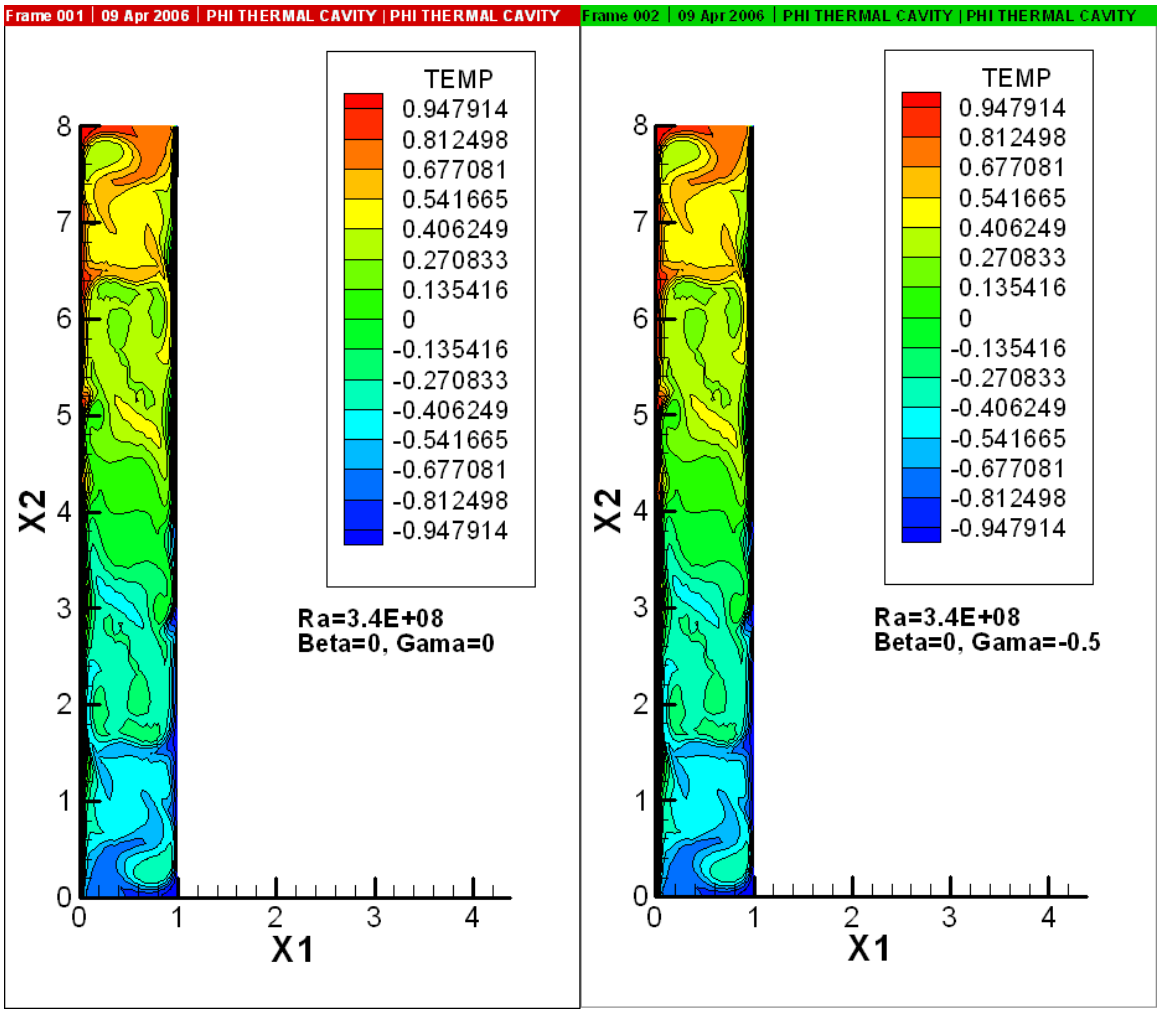

Figure 5.21. Temperature distribution after 1500 time steps for GWS and TWS-γ, Ra=3.4E+08.

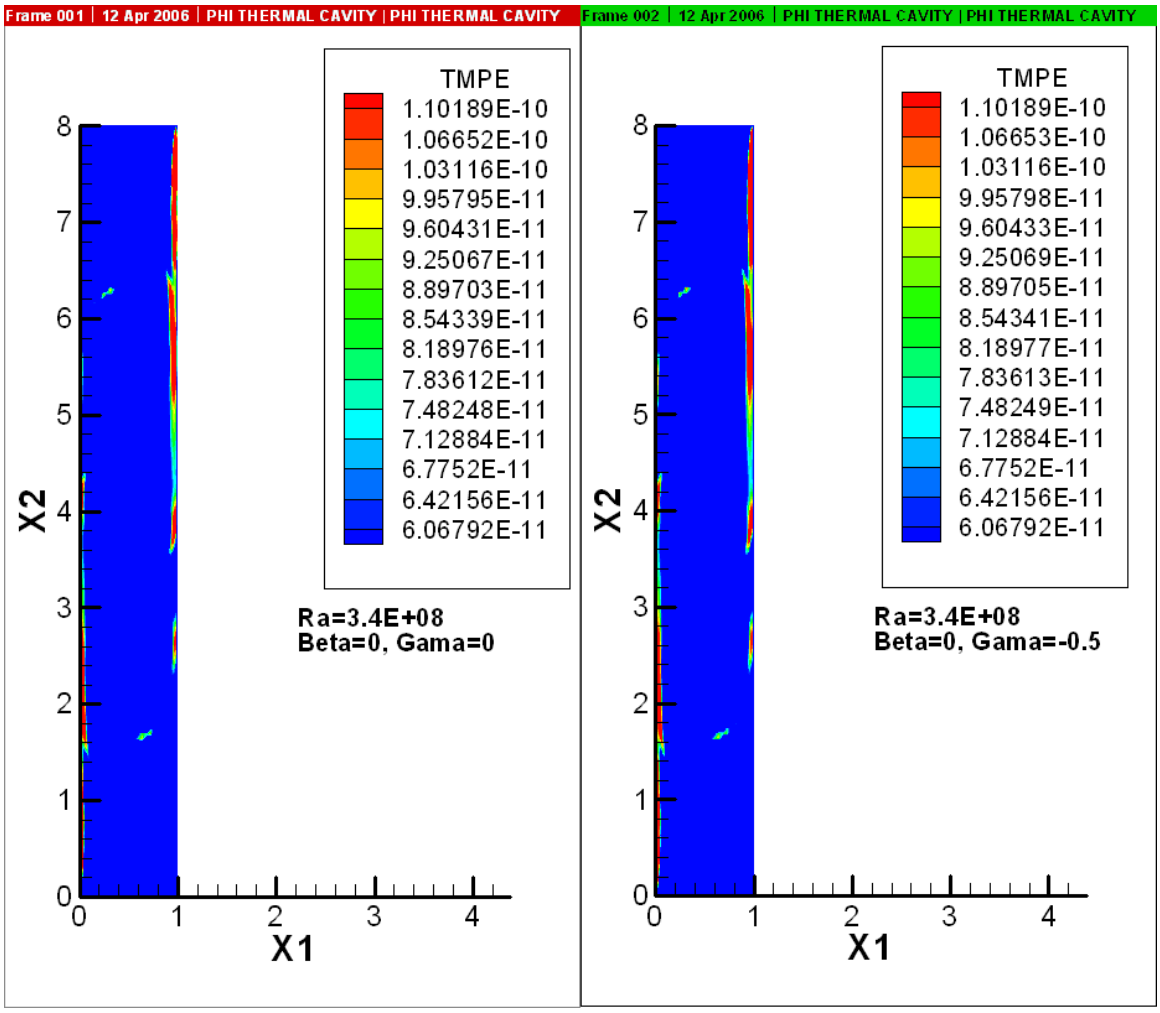

Figure 5.22. Temperature energy norm distribution after 1500 time steps for GWS and TWS-γ, Ra=3.4E+08.

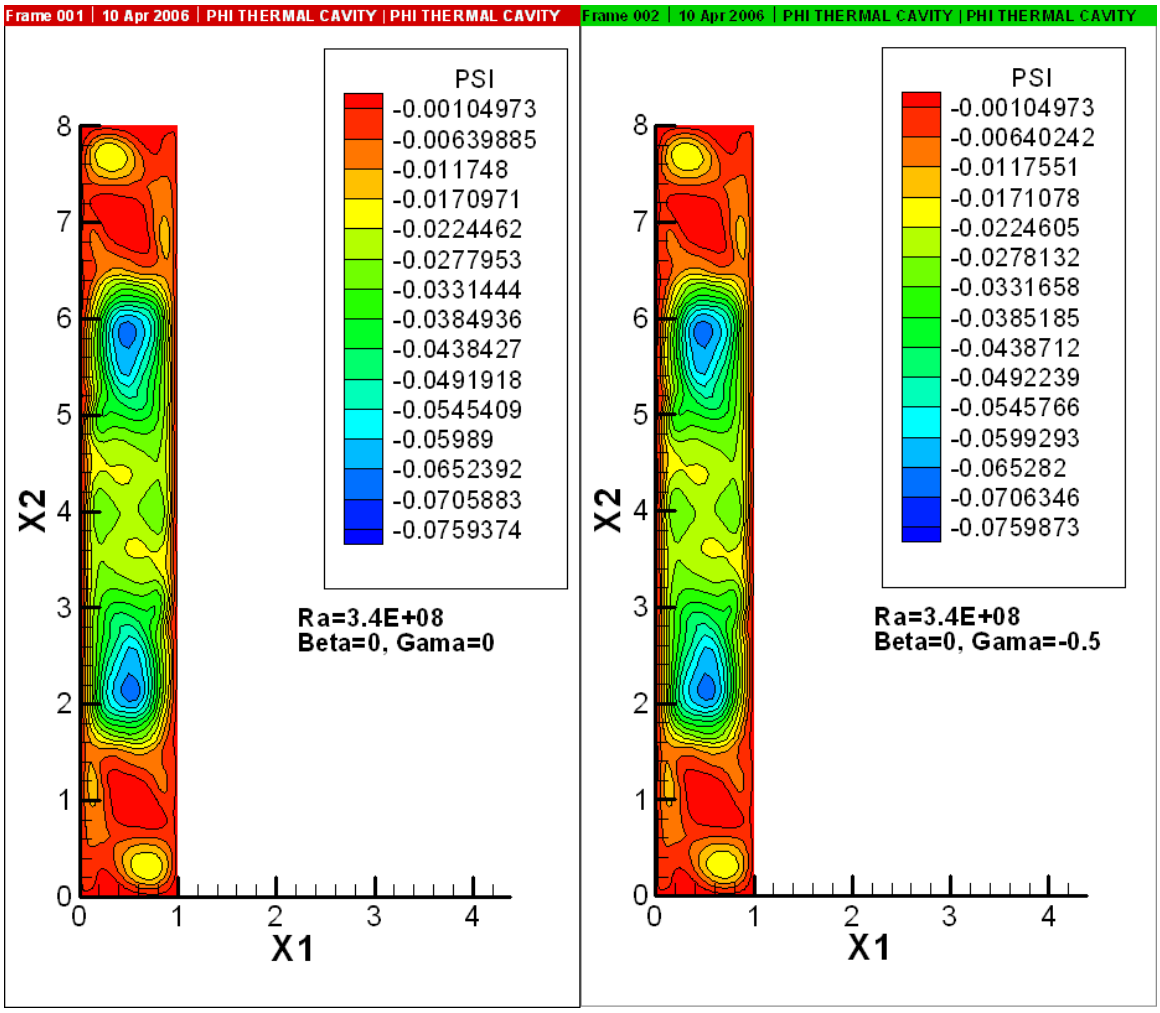

Figure 5.23. Stream-function distribution after 1500 time steps for GWS and TWS-γ, Ra=3.4E+08, M=41x201.

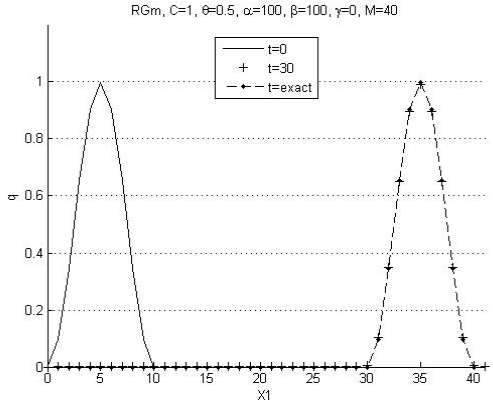

Figure 5.24. 1D pure advection of a Gaussian initial distribution, C = 1.0, RGm with $\alpha=100=\beta$, dashed line is exact solution following 3-wavelength translation.

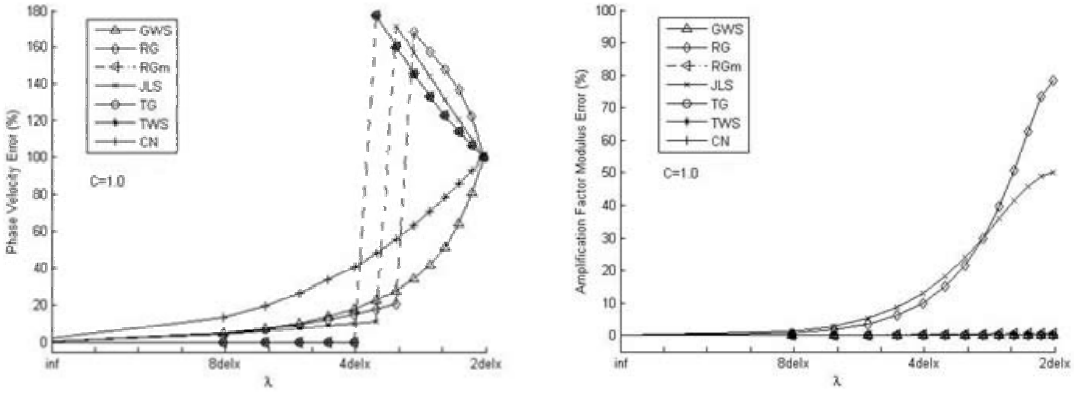

Figure 5.25. Phase velocity and amplification factor modulus error, C = 1.0, θ = 0.5.

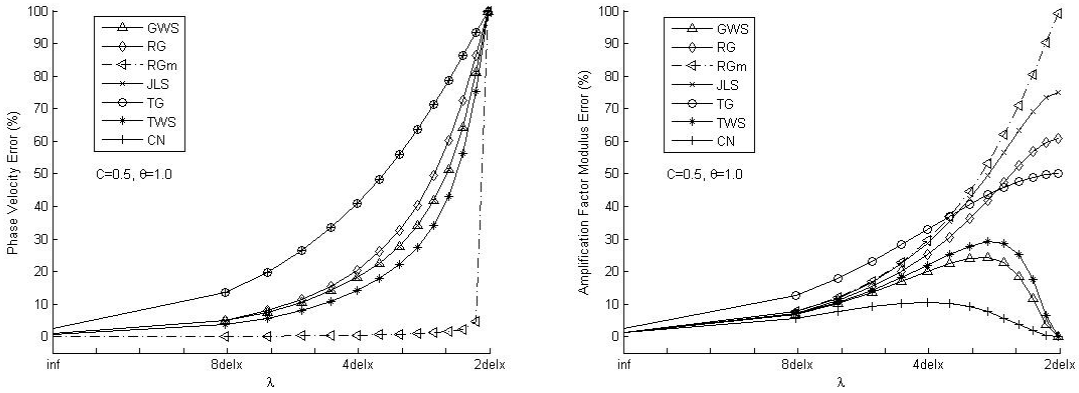

Figure 5.26. Phase velocity and amplification factor modulus error, C=0.5, θ=1.0.

Appendix III

TS expansion of amplification factor modulus error in orders of non-D wave number for TWS^{h} + θTS algorithms for 1D pure advection

$$
\begin{aligned}
\left|e^{h}\right| = {} & \frac{c^2}{2}\,(1+\alpha-\beta-2\theta)\,m^2 + \\
& c^4\left(-\frac{1}{8} - \frac{1}{4}\,\alpha - \frac{1}{4}\,\alpha^2 - \frac{1}{8}\,\alpha^3 - \frac{1}{24}\,\frac{\beta}{c^2} + \frac{1}{4}\,\beta + \frac{1}{4}\,\alpha\beta + \frac{1}{8}\,\alpha^2\beta - \frac{1}{6}\,\gamma - \frac{1}{6}\,\alpha\gamma + \right. \\
& \left. \frac{1}{12}\,\beta\gamma + \frac{1}{2}\,\theta + \alpha\theta + \frac{3}{4}\,\alpha^2\theta - \beta\theta - \alpha\beta\theta + \frac{1}{4}\,\beta^2\theta + \frac{1}{3}\,\gamma\theta - \theta^2 - \frac{3}{2}\,\alpha\theta^2 + \frac{3}{2}\,\beta\theta^2 + \theta^3\right)m^4 + \\
& c^6\left(\frac{1}{c^4}\left(-\frac{1}{180} - \frac{1}{180}\,\alpha - \frac{1}{720}\,\beta + \frac{1}{90}\,\theta\right) + \right. \\
& \frac{1}{c^2}\left(\frac{1}{48}\,c^4\,\beta + \frac{1}{48}\,c^4\,\alpha\beta + \frac{1}{96}\,c^4\,\alpha^2\beta + \frac{1}{36}\,c^4\,\gamma\theta - \frac{1}{72}\,c^4\,\gamma - \frac{1}{72}\,c^4\,\alpha\gamma + \frac{1}{72}\,c^4\beta\gamma - \right. \\
& \left.\left. \frac{1}{12}\,c^4\,\beta\theta - \frac{1}{12}\,c^4\,\alpha\beta\theta + \frac{1}{24}\,c^4\,\beta^2\theta + \frac{1}{8}\,c^4\beta\theta^2\right) + \frac{1}{16} + \frac{3}{16}\,\alpha + \frac{1}{4}\,\alpha^2 + \right. \\
& \frac{3}{16}\,\alpha^3 + \frac{3}{32}\,\alpha^4 + \frac{1}{32}\,\alpha^5 - \frac{3}{16}\,\beta - \frac{3}{8}\,\alpha\beta - \frac{5}{16}\,\alpha^2\beta - \frac{1}{8}\,\alpha^3\beta - \frac{1}{32}\,\alpha^4\beta + \frac{1}{8}\,\beta^2 + \\
& \frac{1}{8}\,\alpha\beta^2 + \frac{1}{32}\,\alpha^2\beta^2 + \frac{1}{12}\,\gamma + \frac{1}{6}\,\alpha\gamma + \frac{1}{6}\,\alpha^2\gamma + \frac{1}{12}\,\alpha^3\gamma - \frac{1}{8}\,\beta\gamma - \frac{1}{8}\,\alpha\beta\gamma - \frac{1}{16}\,\alpha^2\beta\gamma + \\
& \frac{1}{24}\,\gamma^2 + \frac{1}{24}\,\alpha\gamma^2 - \frac{1}{72}\,\beta\gamma^2 - \frac{3}{8}\,\theta - \alpha\theta - \frac{9}{8}\,\alpha^2\theta - \frac{3}{4}\,\alpha^3\theta - \frac{5}{16}\,\alpha^4\theta + \beta\theta + \\
& \frac{7}{4}\,\alpha\beta\theta + \frac{5}{4}\,\alpha^2\beta\theta + \frac{1}{2}\,\alpha^3\beta\theta - \frac{5}{8}\,\beta^2\theta - \frac{1}{2}\,\alpha\beta^2\theta - \frac{3}{16}\,\alpha^2\beta^2\theta - \frac{1}{3}\,\gamma\theta - \frac{2}{3}\,\alpha\gamma\theta - \\
& \frac{1}{2}\,\alpha^2\gamma\theta + \frac{1}{2}\,\beta\gamma\theta + \frac{1}{2}\,\alpha\beta\gamma\theta - \frac{1}{12}\,\beta^2\gamma\theta - \frac{1}{12}\,\gamma^2\theta + \theta^2 + \frac{9}{4}\,\alpha\theta^2 + \frac{9}{4}\,\alpha^2\theta^2 + \\
& \frac{5}{4}\,\alpha^3\theta^2 - \frac{9}{4}\,\beta\theta^2 - \frac{7}{2}\,\alpha\beta\theta^2 - \frac{9}{4}\,\alpha^2\beta\theta^2 + \frac{5}{4}\,\beta^2\theta^2 + \frac{9}{8}\,\alpha\beta^2\theta^2 - \frac{1}{8}\,\beta^3\theta^2 + \\
& \frac{2}{3}\,\gamma\theta^2 + \alpha\gamma\theta^2 - \frac{3}{4}\,\beta\gamma\theta^2 - \frac{3}{2}\,\theta^3 - 3\,\alpha\theta^3 - \frac{5}{2}\,\alpha^2\theta^3 + 3\,\beta\theta^3 + 4\,\alpha\beta\theta^3 - \frac{3}{2}\,\beta^2\theta^3 - \\
& \left.\frac{2}{3}\,\gamma\theta^3 + \frac{3}{2}\,\theta^4 + \frac{5}{2}\,\alpha\theta^4 - \frac{5}{2}\,\beta\theta^4 - \theta^5\right)m^6
\end{aligned}
$$

Appendix IV

Matlab script for computing relative phase velocity spectral distribution for FE quadratic basis

```
clear all; clc
theta=0.5; u=1; h=1; delta_t=1; C=0.5;%(u*delta_t)/(2*h);
gamaV = [-0.4]
% Phase velocity diagram using log plot
for j=1:13
   Piv(j)=(17-j)*pi/16;
end
Piv(14)=pi/10;
for ii =1:14
   m0(ii)=Piv(ii);
   AA(ii) = 15*(cos(m0(ii))*sin(m0(ii))*(24*C-40*C^3*gama)...
      +sin(2*m0(ii))*(12*C+5*C^3*gama));
CC(ii) = 15*sqrt((sin(m0(ii)))^2*(4608*C^2 + 5280*C^4*gama+1400*C^6*gama^2)...
    + cos(2*m0(ii))*(sin(m0(ii)))^2*(-1152*C^2+200*C^6*gama^2)...
    + cos(m0(ii))*sin(m0(ii))*sin(2*m0(ii))*(576*C^2-720*C^4*gama-
400*C^6*gama^2)...
    + (sin(2*m0(ii)))^2*(144*C^2 + 120*C^4*gama+25*C^6*gama^2));
BB(ii) = (sin(m0(ii)))^2*120*C^2*theta;
DD(ii) = (-576-660*C^2*gama-175*C^4*gama^2 ...
   +(cos(m0(ii)))^2*(72-240*C^2*gama+200*C^4*gama^2) ...
   +cos(2*m0(ii))*(144-25*C^4*gama^2) ...
   +(sin(m0(ii)))^2*(-1800*C^2*theta^2));
EE(ii) = cos(m0(ii))*sin(m0(ii))*(720*C*theta-1200*C^3*gama*theta)...
      + sin(2*m0(ii))*theta*(360*C+150*C^3*gama);
Re11(ii) = DD(ii)^2+EE(ii)^2+BB(ii)*DD(ii);
Re22(ii) = -EE(ii)*(AA(ii)-CC(ii));
Im11(ii) = (AA(ii)-CC(ii))*DD(ii);
Im22(ii) = BB(ii)*EE(ii);
RPV(ii) = atan((Im11(ii)+Im22(ii))/(Re11(ii)+Re22(ii)))/(m0(ii)*C);
pv_error(ii) = (1-RPV(ii))*100;
end
figure(3)
hold all
set(0,'DefaultAxesColorOrder',[0 0 0 ],...
     'DefaultAxesLineStyleOrder','-^|-o|-.x|-<|-d|-*|:')
plot(log10(m0),pv_error)
axis([-0.5 0.5 0 100])
set(gca,'XTickLabel','inf| | | |8delx| | |4delx|||2delx')
title(['Phase Velocity Error Spectral Distribution, C=' ...
   num2str(C), ', \theta=', num2str(theta) ])
xlabel('\lambda')
ylabel('Phase Velocity Error (%)') ;legend('\gamma = -0.4')
```

Appendix V

TS expansion of amplification factor for TWS^{h} + θTS algorithms in orders of non-D wave number for 2D pure advection

$$G^h = 1 + \frac{(-i\,Ux\,\Delta t\,\Delta y^3\,\mathrm{Cos}[\eta] - i\,Uy\,\Delta t\,\Delta y^3\,\mathrm{Sin}[\eta])\,m}{\Delta y^4} +$$

$$\left(-\frac{1}{\Delta y^4}\left(\frac{2}{27}Ux^2\,Uy^2\,\gamma^2\,\Delta t^4\,\mathrm{Cos}[\eta]^2 - \frac{1}{27}Uy^4\,\gamma^2\,\Delta t^4\,\mathrm{Cos}[\eta]^2 + \frac{4}{27}Ux^2\,\gamma\,\Delta t^2\,\Delta y^2\,\mathrm{Cos}[\eta]^2 - \right.\right.$$

$$\frac{4}{27}Uy^2\,\gamma\,\Delta t^2\,\Delta y^2\,\mathrm{Cos}[\eta]^2 - \frac{4}{27}\Delta y^4\,\mathrm{Cos}[\eta]^2 + Ux^2\,\Delta t^2\,\Delta y^2\,\theta^2\,\mathrm{Cos}[\eta]^2 + 2\,Ux\,Uy\,\Delta t^2\,\Delta y^2\,\theta^2\,\mathrm{Cos}[\eta]\mathrm{Sin}[\eta] -$$

$$\frac{1}{27}Ux^4\,\gamma^2\,\Delta t^4\,\mathrm{Sin}[\eta]^2 + \frac{2}{27}Ux^2\,Uy^2\,\gamma^2\,\Delta t^4\,\mathrm{Sin}[\eta]^2 - \frac{4}{27}Ux^2\,\gamma\,\Delta t^2\,\Delta y^2\,\mathrm{Sin}[\eta]^2 +$$

$$\frac{4}{27}Uy^2\,\gamma\,\Delta t^2\,\Delta y^2\,\mathrm{Sin}[\eta]^2 - \frac{4}{27}\Delta y^4\,\mathrm{Sin}[\eta]^2 + Uy^2\,\Delta t^2\,\Delta y^2\,\theta^2\,\mathrm{Sin}[\eta]^2 + \frac{1}{81}Ux^4\,\gamma^2\,\Delta t^4\,(-\mathrm{Cos}[\eta]^2 - \mathrm{Sin}[\eta]^2) +$$

$$\frac{2}{81}Ux^2\,Uy^2\,\gamma^2\,\Delta t^4\,(-\mathrm{Cos}[\eta]^2 - \mathrm{Sin}[\eta]^2) + \frac{1}{81}Uy^4\,\gamma^2\,\Delta t^4\,(-\mathrm{Cos}[\eta]^2 - \mathrm{Sin}[\eta]^2) -$$

$$\frac{2}{81}Ux^2\,\gamma\,\Delta t^2\,\Delta y^2\,(-\mathrm{Cos}[\eta]^2 - \mathrm{Sin}[\eta]^2) - \frac{2}{81}Uy^2\,\gamma\,\Delta t^2\,\Delta y^2\,(-\mathrm{Cos}[\eta]^2 - \mathrm{Sin}[\eta]^2) +$$

$$\frac{1}{81}\Delta y^4\,(-\mathrm{Cos}[\eta]^2 - \mathrm{Sin}[\eta]^2) - \frac{2}{81}Ux^4\,\gamma^2\,\Delta t^4\left(-\frac{1}{2}\mathrm{Cos}[\eta]^2 - \mathrm{Sin}[\eta]^2\right) +$$

$$\frac{2}{81}Ux^2\,Uy^2\,\gamma^2\,\Delta t^4\left(-\frac{1}{2}\mathrm{Cos}[\eta]^2 - \mathrm{Sin}[\eta]^2\right) + \frac{4}{81}Uy^4\,\gamma^2\,\Delta t^4\left(-\frac{1}{2}\mathrm{Cos}[\eta]^2 - \mathrm{Sin}[\eta]^2\right) -$$

$$\frac{2}{81}Ux^2\,\gamma\,\Delta t^2\,\Delta y^2\left(-\frac{1}{2}\mathrm{Cos}[\eta]^2 - \mathrm{Sin}[\eta]^2\right) - \frac{8}{81}Uy^2\,\gamma\,\Delta t^2\,\Delta y^2\left(-\frac{1}{2}\mathrm{Cos}[\eta]^2 - \mathrm{Sin}[\eta]^2\right) +$$

$$\frac{4}{81}\Delta y^4\left(-\frac{1}{2}\mathrm{Cos}[\eta]^2 - \mathrm{Sin}[\eta]^2\right) + \frac{4}{81}Ux^4\,\gamma^2\,\Delta t^4\left(-\mathrm{Cos}[\eta]^2 - \frac{\mathrm{Sin}[\eta]^2}{2}\right) +$$

$$\frac{2}{81}Ux^2\,Uy^2\,\gamma^2\,\Delta t^4\left(-\mathrm{Cos}[\eta]^2 - \frac{\mathrm{Sin}[\eta]^2}{2}\right) - \frac{2}{81}Uy^4\,\gamma^2\,\Delta t^4\left(-\mathrm{Cos}[\eta]^2 - \frac{\mathrm{Sin}[\eta]^2}{2}\right) -$$

$$\frac{8}{81}Ux^2\,\gamma\,\Delta t^2\,\Delta y^2\left(-\mathrm{Cos}[\eta]^2 - \frac{\mathrm{Sin}[\eta]^2}{2}\right) - \frac{2}{81}Uy^2\,\gamma\,\Delta t^2\,\Delta y^2\left(-\mathrm{Cos}[\eta]^2 - \frac{\mathrm{Sin}[\eta]^2}{2}\right) +$$

$$\frac{4}{81}\Delta y^4\left(-\mathrm{Cos}[\eta]^2 - \frac{\mathrm{Sin}[\eta]^2}{2}\right) - \frac{8}{81}Ux^4\,\gamma^2\,\Delta t^4\left(-\frac{1}{2}\mathrm{Cos}[\eta]^2 - \frac{\mathrm{Sin}[\eta]^2}{2}\right) +$$

$$\frac{2}{81}Ux^2\,Uy^2\,\gamma^2\,\Delta t^4\left(-\frac{1}{2}\mathrm{Cos}[\eta]^2 - \frac{\mathrm{Sin}[\eta]^2}{2}\right) - \frac{8}{81}Uy^4\,\gamma^2\,\Delta t^4\left(-\frac{1}{2}\mathrm{Cos}[\eta]^2 - \frac{\mathrm{Sin}[\eta]^2}{2}\right) -$$

$$\frac{8}{81}Ux^2\,\gamma\,\Delta t^2\,\Delta y^2\left(-\frac{1}{2}\mathrm{Cos}[\eta]^2 - \frac{\mathrm{Sin}[\eta]^2}{2}\right) - \frac{8}{81}Uy^2\,\gamma\,\Delta t^2\,\Delta y^2\left(-\frac{1}{2}\mathrm{Cos}[\eta]^2 - \frac{\mathrm{Sin}[\eta]^2}{2}\right) +$$

$$\left.\left.\frac{16}{81}\Delta y^4\left(-\frac{1}{2}\mathrm{Cos}[\eta]^2 - \frac{\mathrm{Sin}[\eta]^2}{2}\right)\right)\right) +$$

$$\frac{1}{\Delta y^4}\left(\frac{2}{27}\,Ux^2\,Uy^2\,\gamma^2\,\Delta t^4\,\mathrm{Cos}[\eta]^2-\frac{1}{27}\,Uy^4\,\gamma^2\,\Delta t^4\,\mathrm{Cos}[\eta]^2+\frac{4}{27}\,Ux^2\,\gamma\,\Delta t^2\,\Delta y^2\,\mathrm{Cos}[\eta]^2-\right.$$

$$\frac{4}{27}\,Uy^2\,\gamma\,\Delta t^2\,\Delta y^2\,\mathrm{Cos}[\eta]^2-\frac{4}{27}\,\Delta y^4\,\mathrm{Cos}[\eta]^2-Ux^2\,\Delta t^2\,\Delta y^2\,\theta\,\mathrm{Cos}[\eta]^2+Ux^2\,\Delta t^2\,\Delta y^2\,\theta^2\,\mathrm{Cos}[\eta]^2-$$

$$2\,Ux\,Uy\,\Delta t^2\,\Delta y^2\,\theta\,\mathrm{Cos}[\eta]\,\mathrm{Sin}[\eta]+2\,Ux\,Uy\,\Delta t^2\,\Delta y^2\,\theta^2\,\mathrm{Cos}[\eta]\,\mathrm{Sin}[\eta]-\frac{1}{27}\,Ux^4\,\gamma^2\,\Delta t^4\,\mathrm{Sin}[\eta]^2+$$

$$\frac{2}{27}\,Ux^2\,Uy^2\,\gamma^2\,\Delta t^4\,\mathrm{Sin}[\eta]^2-\frac{4}{27}\,Ux^2\,\gamma\,\Delta t^2\,\Delta y^2\,\mathrm{Sin}[\eta]^2+\frac{4}{27}\,Uy^2\,\gamma\,\Delta t^2\,\Delta y^2\,\mathrm{Sin}[\eta]^2-$$

$$\frac{4}{27}\,\Delta y^4\,\mathrm{Sin}[\eta]^2-Uy^2\,\Delta t^2\,\Delta y^2\,\theta\,\mathrm{Sin}[\eta]^2+Uy^2\,\Delta t^2\,\Delta y^2\,\theta^2\,\mathrm{Sin}[\eta]^2+\frac{1}{81}\,Ux^4\,\gamma^2\,\Delta t^4\,\left(-\mathrm{Cos}[\eta]^2-\mathrm{Sin}[\eta]^2\right)+$$

$$\frac{2}{81}\,Ux^2\,Uy^2\,\gamma^2\,\Delta t^4\,\left(-\mathrm{Cos}[\eta]^2-\mathrm{Sin}[\eta]^2\right)+\frac{1}{81}\,Uy^4\,\gamma^2\,\Delta t^4\,\left(-\mathrm{Cos}[\eta]^2-\mathrm{Sin}[\eta]^2\right)-$$

$$\frac{2}{81}\,Ux^2\,\gamma\,\Delta t^2\,\Delta y^2\,\left(-\mathrm{Cos}[\eta]^2-\mathrm{Sin}[\eta]^2\right)-\frac{2}{81}\,Uy^2\,\gamma\,\Delta t^2\,\Delta y^2\,\left(-\mathrm{Cos}[\eta]^2-\mathrm{Sin}[\eta]^2\right)+$$

$$\frac{1}{81}\,\Delta y^4\,\left(-\mathrm{Cos}[\eta]^2-\mathrm{Sin}[\eta]^2\right)-\frac{2}{81}\,Ux^4\,\gamma^2\,\Delta t^4\,\left(-\frac{1}{2}\,\mathrm{Cos}[\eta]^2-\mathrm{Sin}[\eta]^2\right)+$$

$$\frac{2}{81}\,Ux^2\,Uy^2\,\gamma^2\,\Delta t^4\,\left(-\frac{1}{2}\,\mathrm{Cos}[\eta]^2-\mathrm{Sin}[\eta]^2\right)+\frac{4}{81}\,Uy^4\,\gamma^2\,\Delta t^4\,\left(-\frac{1}{2}\,\mathrm{Cos}[\eta]^2-\mathrm{Sin}[\eta]^2\right)-$$

$$\frac{2}{81}\,Ux^2\,\gamma\,\Delta t^2\,\Delta y^2\,\left(-\frac{1}{2}\,\mathrm{Cos}[\eta]^2-\mathrm{Sin}[\eta]^2\right)-\frac{8}{81}\,Uy^2\,\gamma\,\Delta t^2\,\Delta y^2\,\left(-\frac{1}{2}\,\mathrm{Cos}[\eta]^2-\mathrm{Sin}[\eta]^2\right)+$$

$$\frac{4}{81}\,\Delta y^4\,\left(-\frac{1}{2}\,\mathrm{Cos}[\eta]^2-\mathrm{Sin}[\eta]^2\right)+\frac{4}{81}\,Ux^4\,\gamma^2\,\Delta t^4\,\left(-\mathrm{Cos}[\eta]^2-\frac{\mathrm{Sin}[\eta]^2}{2}\right)+$$

$$\frac{2}{81}\,Ux^2\,Uy^2\,\gamma^2\,\Delta t^4\,\left(-\mathrm{Cos}[\eta]^2-\frac{\mathrm{Sin}[\eta]^2}{2}\right)-\frac{2}{81}\,Uy^4\,\gamma^2\,\Delta t^4\,\left(-\mathrm{Cos}[\eta]^2-\frac{\mathrm{Sin}[\eta]^2}{2}\right)-$$

$$\frac{8}{81}\,Ux^2\,\gamma\,\Delta t^2\,\Delta y^2\,\left(-\mathrm{Cos}[\eta]^2-\frac{\mathrm{Sin}[\eta]^2}{2}\right)-\frac{2}{81}\,Uy^2\,\gamma\,\Delta t^2\,\Delta y^2\,\left(-\mathrm{Cos}[\eta]^2-\frac{\mathrm{Sin}[\eta]^2}{2}\right)+$$

$$\frac{4}{81}\,\Delta y^4\,\left(-\mathrm{Cos}[\eta]^2-\frac{\mathrm{Sin}[\eta]^2}{2}\right)-\frac{8}{81}\,Ux^4\,\gamma^2\,\Delta t^4\,\left(-\frac{1}{2}\,\mathrm{Cos}[\eta]^2-\frac{\mathrm{Sin}[\eta]^2}{2}\right)+$$

$$\frac{2}{81}\,Ux^2\,Uy^2\,\gamma^2\,\Delta t^4\,\left(-\frac{1}{2}\,\mathrm{Cos}[\eta]^2-\frac{\mathrm{Sin}[\eta]^2}{2}\right)-\frac{8}{81}\,Uy^4\,\gamma^2\,\Delta t^4\,\left(-\frac{1}{2}\,\mathrm{Cos}[\eta]^2-\frac{\mathrm{Sin}[\eta]^2}{2}\right)-$$

$$\frac{8}{81}\,Ux^2\,\gamma\,\Delta t^2\,\Delta y^2\,\left(-\frac{1}{2}\,\mathrm{Cos}[\eta]^2-\frac{\mathrm{Sin}[\eta]^2}{2}\right)-\frac{8}{81}\,Uy^2\,\gamma\,\Delta t^2\,\Delta y^2\,\left(-\frac{1}{2}\,\mathrm{Cos}[\eta]^2-\frac{\mathrm{Sin}[\eta]^2}{2}\right)+$$

$$\left.\left.\frac{16}{81}\,\Delta y^4\,\left(-\frac{1}{2}\,\mathrm{Cos}[\eta]^2-\frac{\mathrm{Sin}[\eta]^2}{2}\right)\right)\right)m^2+$$

$$
\left(-\frac{1}{\Delta y^8}\left((-i\,Ux\,\Delta t\,\Delta y^3\,\mathrm{Cos}[\eta]-i\,Uy\,\Delta t\,\Delta y^3\,\mathrm{Sin}[\eta])\right.\right.
$$

$$
\left(\frac{2}{27}Ux^2\,Uy^2\,\gamma^2\,\Delta t^4\,\mathrm{Cos}[\eta]^2-\frac{1}{27}Uy^4\,\gamma^2\,\Delta t^4\,\mathrm{Cos}[\eta]^2+\frac{4}{27}Ux^2\,\gamma\,\Delta t^2\,\Delta y^2\,\mathrm{Cos}[\eta]^2-\right.
$$

$$
\frac{4}{27}Uy^2\,\gamma\,\Delta t^2\,\Delta y^2\,\mathrm{Cos}[\eta]^2-\frac{4}{27}\Delta y^4\,\mathrm{Cos}[\eta]^2+Ux^2\,\Delta t^2\,\Delta y^2\,\theta^2\,\mathrm{Cos}[\eta]^2+2\,Ux\,Uy\,\Delta t^2\,\Delta y^2\,\theta^2\,\mathrm{Cos}[\eta]\mathrm{Sin}[\eta]-
$$

$$
\frac{1}{27}Ux^4\,\gamma^2\,\Delta t^4\,\mathrm{Sin}[\eta]^2+\frac{2}{27}Ux^2\,Uy^2\,\gamma^2\,\Delta t^4\,\mathrm{Sin}[\eta]^2-\frac{4}{27}Ux^2\,\gamma\,\Delta t^2\,\Delta y^2\,\mathrm{Sin}[\eta]^2+
$$

$$
\frac{4}{27}Uy^2\,\gamma\,\Delta t^2\,\Delta y^2\,\mathrm{Sin}[\eta]^2-\frac{4}{27}\Delta y^4\,\mathrm{Sin}[\eta]^2+Uy^2\,\Delta t^2\,\Delta y^2\,\theta^2\,\mathrm{Sin}[\eta]^2+
$$

$$
\frac{1}{81}Ux^4\,\gamma^2\,\Delta t^4\left(-\mathrm{Cos}[\eta]^2-\mathrm{Sin}[\eta]^2\right)+\frac{2}{81}Ux^2\,Uy^2\,\gamma^2\,\Delta t^4\left(-\mathrm{Cos}[\eta]^2-\mathrm{Sin}[\eta]^2\right)+
$$

$$
\frac{1}{81}Uy^4\,\gamma^2\,\Delta t^4\left(-\mathrm{Cos}[\eta]^2-\mathrm{Sin}[\eta]^2\right)-\frac{2}{81}Ux^2\,\gamma\,\Delta t^2\,\Delta y^2\left(-\mathrm{Cos}[\eta]^2-\mathrm{Sin}[\eta]^2\right)-
$$

$$
\frac{2}{81}Uy^2\,\gamma\,\Delta t^2\,\Delta y^2\left(-\mathrm{Cos}[\eta]^2-\mathrm{Sin}[\eta]^2\right)+\frac{1}{81}\Delta y^4\left(-\mathrm{Cos}[\eta]^2-\mathrm{Sin}[\eta]^2\right)-
$$

$$
\frac{2}{81}Ux^4\,\gamma^2\,\Delta t^4\left(-\frac{1}{2}\mathrm{Cos}[\eta]^2-\mathrm{Sin}[\eta]^2\right)+\frac{2}{81}Ux^2\,Uy^2\,\gamma^2\,\Delta t^4\left(-\frac{1}{2}\mathrm{Cos}[\eta]^2-\mathrm{Sin}[\eta]^2\right)+
$$

$$
\frac{4}{81}Uy^4\,\gamma^2\,\Delta t^4\left(-\frac{1}{2}\mathrm{Cos}[\eta]^2-\mathrm{Sin}[\eta]^2\right)-\frac{2}{81}Ux^2\,\gamma\,\Delta t^2\,\Delta y^2\left(-\frac{1}{2}\mathrm{Cos}[\eta]^2-\mathrm{Sin}[\eta]^2\right)-
$$

$$
\frac{8}{81}Uy^2\,\gamma\,\Delta t^2\,\Delta y^2\left(-\frac{1}{2}\mathrm{Cos}[\eta]^2-\mathrm{Sin}[\eta]^2\right)+\frac{4}{81}\Delta y^4\left(-\frac{1}{2}\mathrm{Cos}[\eta]^2-\mathrm{Sin}[\eta]^2\right)+
$$

$$
\frac{4}{81}Ux^4\,\gamma^2\,\Delta t^4\left(-\mathrm{Cos}[\eta]^2-\frac{\mathrm{Sin}[\eta]^2}{2}\right)+\frac{2}{81}Ux^2\,Uy^2\,\gamma^2\,\Delta t^4\left(-\mathrm{Cos}[\eta]^2-\frac{\mathrm{Sin}[\eta]^2}{2}\right)-
$$

$$
\frac{2}{81}Uy^4\,\gamma^2\,\Delta t^4\left(-\mathrm{Cos}[\eta]^2-\frac{\mathrm{Sin}[\eta]^2}{2}\right)-\frac{8}{81}Ux^2\,\gamma\,\Delta t^2\,\Delta y^2\left(-\mathrm{Cos}[\eta]^2-\frac{\mathrm{Sin}[\eta]^2}{2}\right)-
$$

$$
\frac{2}{81}Uy^2\,\gamma\,\Delta t^2\,\Delta y^2\left(-\mathrm{Cos}[\eta]^2-\frac{\mathrm{Sin}[\eta]^2}{2}\right)+\frac{4}{81}\Delta y^4\left(-\mathrm{Cos}[\eta]^2-\frac{\mathrm{Sin}[\eta]^2}{2}\right)-
$$

$$
\frac{8}{81}Ux^4\,\gamma^2\,\Delta t^4\left(-\frac{1}{2}\mathrm{Cos}[\eta]^2-\frac{\mathrm{Sin}[\eta]^2}{2}\right)+\frac{2}{81}Ux^2\,Uy^2\,\gamma^2\,\Delta t^4\left(-\frac{1}{2}\mathrm{Cos}[\eta]^2-\frac{\mathrm{Sin}[\eta]^2}{2}\right)-
$$

$$
\frac{8}{81}Uy^4\,\gamma^2\,\Delta t^4\left(-\frac{1}{2}\mathrm{Cos}[\eta]^2-\frac{\mathrm{Sin}[\eta]^2}{2}\right)-\frac{8}{81}Ux^2\,\gamma\,\Delta t^2\,\Delta y^2\left(-\frac{1}{2}\mathrm{Cos}[\eta]^2-\frac{\mathrm{Sin}[\eta]^2}{2}\right)-
$$

$$
\left.\left.\left.\frac{8}{81}Uy^2\,\gamma\,\Delta t^2\,\Delta y^2\left(-\frac{1}{2}\mathrm{Cos}[\eta]^2-\frac{\mathrm{Sin}[\eta]^2}{2}\right)+\frac{16}{81}\Delta y^4\left(-\frac{1}{2}\mathrm{Cos}[\eta]^2-\frac{\mathrm{Sin}[\eta]^2}{2}\right)\right)\right)+
$$

$$\frac{1}{\Delta y^4}\left(-\frac{2}{27}\,i\,Ux^3\,\gamma\Delta t^3\,\Delta y\,Cos[\eta]^3+\frac{2}{27}\,i\,Ux\,Uy^2\,\gamma\Delta t^3\,\Delta y\,Cos[\eta]^3+\frac{4}{27}\,i\,Ux\Delta t\,\Delta y^3\,Cos[\eta]^3+\right.$$
$$\frac{2}{27}\,i\,Ux^2\,Uy\,\gamma\Delta t^3\,\Delta y\,Sin[\eta]^3-\frac{2}{27}\,i\,Uy^3\,\gamma\Delta t^3\,\Delta y\,Sin[\eta]^3+\frac{4}{27}\,i\,Uy\,\Delta t\,\Delta y^3\,Sin[\eta]^3-$$
$$\frac{1}{27}\,i\,Ux^3\,\gamma\Delta t^3\,\Delta y\left(-\frac{1}{6}\,Cos[\eta]^3-Cos[\eta]Sin[\eta]^2\right)+\frac{2}{27}\,i\,Ux\,Uy^2\,\gamma\Delta t^3\,\Delta y\left(-\frac{1}{6}\,Cos[\eta]^3-Cos[\eta]Sin[\eta]^2\right)-$$
$$\frac{2}{27}\,i\,Ux\Delta t\,\Delta y^3\left(-\frac{1}{6}\,Cos[\eta]^3-Cos[\eta]Sin[\eta]^2\right)-\frac{4}{27}\,i\,Ux^3\,\gamma\Delta t^3\,\Delta y\left(-\frac{1}{6}\,Cos[\eta]^3-\frac{1}{2}\,Cos[\eta]Sin[\eta]^2\right)+$$
$$\frac{2}{27}\,i\,Ux\,Uy^2\,\gamma\Delta t^3\,\Delta y\left(-\frac{1}{6}\,Cos[\eta]^3-\frac{1}{2}\,Cos[\eta]Sin[\eta]^2\right)-\frac{8}{27}\,i\,Ux\Delta t\,\Delta y^3\left(-\frac{1}{6}\,Cos[\eta]^3-\frac{1}{2}\,Cos[\eta]Sin[\eta]^2\right)+$$
$$\frac{2}{27}\,i\,Ux^2\,Uy\,\gamma\Delta t^3\,\Delta y\left(-Cos[\eta]^2\,Sin[\eta]-\frac{Sin[\eta]^3}{6}\right)-\frac{1}{27}\,i\,Uy^3\,\gamma\Delta t^3\,\Delta y\left(-Cos[\eta]^2\,Sin[\eta]-\frac{Sin[\eta]^3}{6}\right)-$$
$$\frac{2}{27}\,i\,Uy\,\Delta t\,\Delta y^3\left(-Cos[\eta]^2\,Sin[\eta]-\frac{Sin[\eta]^3}{6}\right)+\frac{2}{27}\,i\,Ux^2\,Uy\,\gamma\Delta t^3\,\Delta y\left(-\frac{1}{2}\,Cos[\eta]^2\,Sin[\eta]-\frac{Sin[\eta]^3}{6}\right)-$$
$$\frac{4}{27}\,i\,Uy^3\,\gamma\Delta t^3\,\Delta y\left(-\frac{1}{2}\,Cos[\eta]^2\,Sin[\eta]-\frac{Sin[\eta]^3}{6}\right)-\frac{8}{27}\,i\,Uy\,\Delta t\,\Delta y^3\left(-\frac{1}{2}\,Cos[\eta]^2\,Sin[\eta]-\frac{Sin[\eta]^3}{6}\right)+$$
$$\frac{1}{27}\,i\,Ux^3\,\gamma\Delta t^3\,\Delta y\left(-\frac{1}{6}\,Cos[\eta]^3+Cos[\eta]\left(-\frac{1}{2}\,Cos[\eta]^2-Sin[\eta]^2\right)\right)+$$
$$\frac{1}{27}\,i\,Ux\,Uy^2\,\gamma\Delta t^3\,\Delta y\left(-\frac{1}{6}\,Cos[\eta]^3+Cos[\eta]\left(-\frac{1}{2}\,Cos[\eta]^2-Sin[\eta]^2\right)\right)-$$
$$\frac{1}{27}\,i\,Ux\Delta t\,\Delta y^3\left(-\frac{1}{6}\,Cos[\eta]^3+Cos[\eta]\left(-\frac{1}{2}\,Cos[\eta]^2-Sin[\eta]^2\right)\right)+$$
$$\frac{1}{27}\,i\,Ux^2\,Uy\,\gamma\Delta t^3\,\Delta y\left(-\frac{1}{6}\,Sin[\eta]^3+Sin[\eta]\left(-Cos[\eta]^2-\frac{Sin[\eta]^2}{2}\right)\right)+$$
$$\frac{1}{27}\,i\,Uy^3\,\gamma\Delta t^3\,\Delta y\left(-\frac{1}{6}\,Sin[\eta]^3+Sin[\eta]\left(-Cos[\eta]^2-\frac{Sin[\eta]^2}{2}\right)\right)-$$
$$\frac{1}{27}\,i\,Uy\,\Delta t\,\Delta y^3\left(-\frac{1}{6}\,Sin[\eta]^3+Sin[\eta]\left(-Cos[\eta]^2-\frac{Sin[\eta]^2}{2}\right)\right)+$$
$$\frac{4}{27}\,i\,Ux^3\,\gamma\Delta t^3\,\Delta y\left(-\frac{1}{6}\,Cos[\eta]^3+Cos[\eta]\left(-\frac{1}{2}\,Cos[\eta]^2-\frac{Sin[\eta]^2}{2}\right)\right)+$$
$$\frac{1}{27}\,i\,Ux\,Uy^2\,\gamma\Delta t^3\,\Delta y\left(-\frac{1}{6}\,Cos[\eta]^3+Cos[\eta]\left(-\frac{1}{2}\,Cos[\eta]^2-\frac{Sin[\eta]^2}{2}\right)\right)-$$
$$\frac{4}{27}\,i\,Ux\Delta t\,\Delta y^3\left(-\frac{1}{6}\,Cos[\eta]^3+Cos[\eta]\left(-\frac{1}{2}\,Cos[\eta]^2-\frac{Sin[\eta]^2}{2}\right)\right)+$$
$$\frac{1}{27}\,i\,Ux^2\,Uy\,\gamma\Delta t^3\,\Delta y\left(-\frac{1}{6}\,Sin[\eta]^3+Sin[\eta]\left(-\frac{1}{2}\,Cos[\eta]^2-\frac{Sin[\eta]^2}{2}\right)\right)+$$
$$\frac{4}{27}\,i\,Uy^3\,\gamma\Delta t^3\,\Delta y\left(-\frac{1}{6}\,Sin[\eta]^3+Sin[\eta]\left(-\frac{1}{2}\,Cos[\eta]^2-\frac{Sin[\eta]^2}{2}\right)\right)-$$
$$\left.\frac{4}{27}\,i\,Uy\,\Delta t\,\Delta y^3\left(-\frac{1}{6}\,Sin[\eta]^3+Sin[\eta]\left(-\frac{1}{2}\,Cos[\eta]^2-\frac{Sin[\eta]^2}{2}\right)\right)\right)m^3+O[m]^4$$

Appendix VI

TS expansion of amplification factor phase error for TWS^{h} + θTS algorithms in orders of non-D wave number for 2D pure advection

$$e^{h}_{k=1} = (i\,Cx\,Cos[\eta] - i\,Ux\,\Delta t\,Cos[\eta] + i\,Cy\,Sin[\eta] - i\,Uy\,\Delta t\,Sin[\eta])\,m +$$

$$
\begin{aligned}
&(i\,Cx\,Cos[\eta] - i\,Ux\,\Delta t\,Cos[\eta] + i\,Cy\,Sin[\eta] - i\,Uy\,\Delta t\,Sin[\eta])\,m + \\
&\Big(-\frac{1}{2}\,Ux^2\,\alpha\,\Delta t^2\,Cos[\eta]^2 - \frac{2}{9}\,Ux^2\,\beta\,\Delta t^2\,Cos[\eta]^2 + \\
&\frac{2}{9}\,Uy^2\,\beta\,\Delta t^2\,Cos[\eta]^2 - \frac{2}{9}\,Ux^2\,Uy^2\,\beta\,\gamma\,\Delta t^4\,Cos[\eta]^2 + \frac{1}{9}\,Uy^4\,\beta\,\gamma\,\Delta t^4\,Cos[\eta]^2 - \\
&Ux^2\,\Delta t^2\,\theta\,Cos[\eta]^2 - \frac{2}{3}\,Ux^2\,Uy^2\,\beta^2\,\Delta t^4\,\theta\,Cos[\eta]^2 + \frac{1}{3}\,Uy^4\,\beta^2\,\Delta t^4\,\theta\,Cos[\eta]^2 - \\
&Ux\,Uy\,\alpha\,\Delta t^2\,Cos[\eta]\,Sin[\eta] - 2\,Ux\,Uy\,\Delta t^2\,\theta\,Cos[\eta]\,Sin[\eta] - \frac{1}{2}\,Uy^2\,\alpha\,\Delta t^2\,Sin[\eta]^2 + \\
&\frac{2}{9}\,Ux^2\,\beta\,\Delta t^2\,Sin[\eta]^2 - \frac{2}{9}\,Uy^2\,\beta\,\Delta t^2\,Sin[\eta]^2 + \frac{1}{9}\,Ux^4\,\beta\,\gamma\,\Delta t^4\,Sin[\eta]^2 - \\
&\frac{2}{9}\,Ux^2\,Uy^2\,\beta\,\gamma\,\Delta t^4\,Sin[\eta]^2 - Uy^2\,\Delta t^2\,\theta\,Sin[\eta]^2 + \frac{1}{3}\,Ux^4\,\beta^2\,\Delta t^4\,\theta\,Sin[\eta]^2 - \\
&\frac{2}{3}\,Ux^2\,Uy^2\,\beta^2\,\Delta t^4\,\theta\,Sin[\eta]^2 - \frac{1}{2}\,(-i\,Cx\,Cos[\eta] - i\,Cy\,Sin[\eta])^2 + \\
&\frac{1}{81}\,(-Cos[\eta]^2 - Sin[\eta]^2) + \frac{1}{27}\,Ux^2\,\beta\,\Delta t^2\,(-Cos[\eta]^2 - Sin[\eta]^2) + \\
&\frac{1}{27}\,Uy^2\,\beta\,\Delta t^2\,(-Cos[\eta]^2 - Sin[\eta]^2) - \frac{2}{27}\,Ux^2\,Uy^2\,\beta\,\gamma\,\Delta t^4\,(-Cos[\eta]^2 - Sin[\eta]^2) - \\
&\frac{2}{9}\,Ux^2\,Uy^2\,\beta^2\,\Delta t^4\,\theta\,(-Cos[\eta]^2 - Sin[\eta]^2) + \frac{1}{27}\,Ux^2\,\beta\,\Delta t^2\,\Big(-\frac{1}{2}\,Cos[\eta]^2 - Sin[\eta]^2\Big) + \\
&\frac{4}{27}\,Uy^2\,\beta\,\Delta t^2\,\Big(-\frac{1}{2}\,Cos[\eta]^2 - Sin[\eta]^2\Big) + \frac{2}{27}\,Ux^4\,\beta\,\gamma\,\Delta t^4\,\Big(-\frac{1}{2}\,Cos[\eta]^2 - Sin[\eta]^2\Big) - \\
&\frac{2}{27}\,Ux^2\,Uy^2\,\beta\,\gamma\,\Delta t^4\,\Big(-\frac{1}{2}\,Cos[\eta]^2 - Sin[\eta]^2\Big) - \frac{4}{27}\,Uy^4\,\beta\,\gamma\,\Delta t^4\,\Big(-\frac{1}{2}\,Cos[\eta]^2 - Sin[\eta]^2\Big) + \\
&\frac{2}{9}\,Ux^4\,\beta^2\,\Delta t^4\,\theta\,\Big(-\frac{1}{2}\,Cos[\eta]^2 - Sin[\eta]^2\Big) - \frac{2}{9}\,Ux^2\,Uy^2\,\beta^2\,\Delta t^4\,\theta\,\Big(-\frac{1}{2}\,Cos[\eta]^2 - Sin[\eta]^2\Big) - \\
&\frac{4}{9}\,Uy^4\,\beta^2\,\Delta t^4\,\theta\,\Big(-\frac{1}{2}\,Cos[\eta]^2 - Sin[\eta]^2\Big) + \frac{4}{27}\,Ux^2\,\beta\,\Delta t^2\,\Big(-Cos[\eta]^2 - \frac{Sin[\eta]^2}{2}\Big) + \\
&\frac{1}{27}\,Uy^2\,\beta\,\Delta t^2\,\Big(-Cos[\eta]^2 - \frac{Sin[\eta]^2}{2}\Big) - \frac{4}{27}\,Ux^4\,\beta\,\gamma\,\Delta t^4\,\Big(-Cos[\eta]^2 - \frac{Sin[\eta]^2}{2}\Big) - \\
&\frac{2}{27}\,Ux^2\,Uy^2\,\beta\,\gamma\,\Delta t^4\,\Big(-Cos[\eta]^2 - \frac{Sin[\eta]^2}{2}\Big) + \frac{2}{27}\,Uy^4\,\beta\,\gamma\,\Delta t^4\,\Big(-Cos[\eta]^2 - \frac{Sin[\eta]^2}{2}\Big) - \\
&\frac{4}{9}\,Ux^4\,\beta^2\,\Delta t^4\,\theta\,\Big(-Cos[\eta]^2 - \frac{Sin[\eta]^2}{2}\Big) - \frac{2}{9}\,Ux^2\,Uy^2\,\beta^2\,\Delta t^4\,\theta\,\Big(-Cos[\eta]^2 - \frac{Sin[\eta]^2}{2}\Big) + \\
&\frac{2}{9}\,Uy^4\,\beta^2\,\Delta t^4\,\theta\,\Big(-Cos[\eta]^2 - \frac{Sin[\eta]^2}{2}\Big) + \frac{4}{27}\,Ux^2\,\beta\,\Delta t^2\,\Big(-\frac{1}{2}\,Cos[\eta]^2 - \frac{Sin[\eta]^2}{2}\Big) + \\
&\frac{4}{27}\,Uy^2\,\beta\,\Delta t^2\,\Big(-\frac{1}{2}\,Cos[\eta]^2 - \frac{Sin[\eta]^2}{2}\Big) + \frac{8}{27}\,Ux^4\,\beta\,\gamma\,\Delta t^4\,\Big(-\frac{1}{2}\,Cos[\eta]^2 - \frac{Sin[\eta]^2}{2}\Big) -
\end{aligned}
$$

$$\frac{2}{27}\,Ux^2\,Uy^2\,\beta\,\gamma\,\Delta t^4\left(-\frac{1}{2}\,\mathrm{Cos}[\eta]^2-\frac{\mathrm{Sin}[\eta]^2}{2}\right)+\frac{8}{27}\,Uy^4\,\beta\,\gamma\,\Delta t^4\left(-\frac{1}{2}\,\mathrm{Cos}[\eta]^2-\frac{\mathrm{Sin}[\eta]^2}{2}\right)+$$
$$\frac{8}{9}\,Ux^4\,\beta^2\,\Delta t^4\,\theta\left(-\frac{1}{2}\,\mathrm{Cos}[\eta]^2-\frac{\mathrm{Sin}[\eta]^2}{2}\right)-\frac{2}{9}\,Ux^2\,Uy^2\,\beta^2\,\Delta t^4\,\theta\left(-\frac{1}{2}\,\mathrm{Cos}[\eta]^2-\frac{\mathrm{Sin}[\eta]^2}{2}\right)+$$
$$\frac{8}{9}\,Uy^4\,\beta^2\,\Delta t^4\,\theta\left(-\frac{1}{2}\,\mathrm{Cos}[\eta]^2-\frac{\mathrm{Sin}[\eta]^2}{2}\right)+\frac{1}{81}\,(\mathrm{Cos}[\eta]^2+\mathrm{Sin}[\eta]^2)+$$
$$\frac{1}{27}\,Ux^4\,\beta\,\gamma\,\Delta t^4\,(\mathrm{Cos}[\eta]^2+\mathrm{Sin}[\eta]^2)+\frac{1}{27}\,Uy^4\,\beta\,\gamma\,\Delta t^4\,(\mathrm{Cos}[\eta]^2+\mathrm{Sin}[\eta]^2)+$$
$$\frac{1}{9}\,Ux^4\,\beta^2\,\Delta t^4\,\theta\,(\mathrm{Cos}[\eta]^2+\mathrm{Sin}[\eta]^2)+\frac{1}{9}\,Uy^4\,\beta^2\,\Delta t^4\,\theta\,(\mathrm{Cos}[\eta]^2+\mathrm{Sin}[\eta]^2)\Big)\,m^2+$$
$$\Big(\frac{4}{27}\,i\,Ux\,\Delta t\,\mathrm{Cos}[\eta]^3+\frac{1}{9}\,i\,Ux^3\,\alpha\,\beta\,\Delta t^3\,\mathrm{Cos}[\eta]^3-\frac{1}{9}\,i\,Ux\,Uy^2\,\alpha\,\beta\,\Delta t^3\,\mathrm{Cos}[\eta]^3-$$
$$\frac{2}{27}\,i\,Ux^3\,\gamma\,\Delta t^3\,\mathrm{Cos}[\eta]^3+\frac{2}{27}\,i\,Ux\,Uy^2\,\gamma\,\Delta t^3\,\mathrm{Cos}[\eta]^3+\frac{4}{27}\,i\,Uy\,\Delta t\,\mathrm{Sin}[\eta]^3-$$
$$\frac{1}{9}\,i\,Ux^2\,Uy\,\alpha\,\beta\,\Delta t^3\,\mathrm{Sin}[\eta]^3+\frac{1}{9}\,i\,Uy^3\,\alpha\,\beta\,\Delta t^3\,\mathrm{Sin}[\eta]^3+$$
$$\frac{2}{27}\,i\,Ux^2\,Uy\,\gamma\,\Delta t^3\,\mathrm{Sin}[\eta]^3-\frac{2}{27}\,i\,Uy^3\,\gamma\,\Delta t^3\,\mathrm{Sin}[\eta]^3-$$
$$\frac{1}{6}\,(-i\,Cx\,\mathrm{Cos}[\eta]-i\,Cy\,\mathrm{Sin}[\eta])^3-\frac{2}{27}\,i\,Ux\,\Delta t\left(-\frac{1}{6}\,\mathrm{Cos}[\eta]^3-\mathrm{Cos}[\eta]\,\mathrm{Sin}[\eta]^2\right)+$$
$$\frac{1}{18}\,i\,Ux^3\,\alpha\,\beta\,\Delta t^3\left(-\frac{1}{6}\,\mathrm{Cos}[\eta]^3-\mathrm{Cos}[\eta]\,\mathrm{Sin}[\eta]^2\right)-$$
$$\frac{1}{9}\,i\,Ux\,Uy^2\,\alpha\,\beta\,\Delta t^3\left(-\frac{1}{6}\,\mathrm{Cos}[\eta]^3-\mathrm{Cos}[\eta]\,\mathrm{Sin}[\eta]^2\right)-$$
$$\frac{1}{27}\,i\,Ux^3\,\gamma\,\Delta t^3\left(-\frac{1}{6}\,\mathrm{Cos}[\eta]^3-\mathrm{Cos}[\eta]\,\mathrm{Sin}[\eta]^2\right)+$$
$$\frac{2}{27}\,i\,Ux\,Uy^2\,\gamma\,\Delta t^3\left(-\frac{1}{6}\,\mathrm{Cos}[\eta]^3-\mathrm{Cos}[\eta]\,\mathrm{Sin}[\eta]^2\right)-$$
$$\frac{8}{27}\,i\,Ux\,\Delta t\left(-\frac{1}{6}\,\mathrm{Cos}[\eta]^3-\frac{1}{2}\,\mathrm{Cos}[\eta]\,\mathrm{Sin}[\eta]^2\right)+$$
$$\frac{2}{9}\,i\,Ux^3\,\alpha\,\beta\,\Delta t^3\left(-\frac{1}{6}\,\mathrm{Cos}[\eta]^3-\frac{1}{2}\,\mathrm{Cos}[\eta]\,\mathrm{Sin}[\eta]^2\right)-$$
$$\frac{1}{9}\,i\,Ux\,Uy^2\,\alpha\,\beta\,\Delta t^3\left(-\frac{1}{6}\,\mathrm{Cos}[\eta]^3-\frac{1}{2}\,\mathrm{Cos}[\eta]\,\mathrm{Sin}[\eta]^2\right)-$$
$$\frac{4}{27}\,i\,Ux^3\,\gamma\,\Delta t^3\left(-\frac{1}{6}\,\mathrm{Cos}[\eta]^3-\frac{1}{2}\,\mathrm{Cos}[\eta]\,\mathrm{Sin}[\eta]^2\right)+$$
$$\frac{2}{27}\,i\,Ux\,Uy^2\,\gamma\,\Delta t^3\left(-\frac{1}{6}\,\mathrm{Cos}[\eta]^3-\frac{1}{2}\,\mathrm{Cos}[\eta]\,\mathrm{Sin}[\eta]^2\right)-$$
$$\frac{2}{27}\,i\,Uy\,\Delta t\left(-\mathrm{Cos}[\eta]^2\,\mathrm{Sin}[\eta]-\frac{\mathrm{Sin}[\eta]^3}{6}\right)-$$
$$\frac{1}{9}\,i\,Ux^2\,Uy\,\alpha\,\beta\,\Delta t^3\left(-\mathrm{Cos}[\eta]^2\,\mathrm{Sin}[\eta]-\frac{\mathrm{Sin}[\eta]^3}{6}\right)+$$
$$\frac{1}{18}\,i\,Uy^3\,\alpha\,\beta\,\Delta t^3\left(-\mathrm{Cos}[\eta]^2\,\mathrm{Sin}[\eta]-\frac{\mathrm{Sin}[\eta]^3}{6}\right)+$$
$$\frac{2}{27}\,i\,Ux^2\,Uy\,\gamma\,\Delta t^3\left(-\mathrm{Cos}[\eta]^2\,\mathrm{Sin}[\eta]-\frac{\mathrm{Sin}[\eta]^3}{6}\right)-\frac{1}{27}\,i\,Uy^3\,\gamma\,\Delta t^3$$

$$\left(-\text{Cos}[\eta]^2\,\text{Sin}[\eta]-\frac{\text{Sin}[\eta]^3}{6}\right)-\frac{8}{27}\,i\,\text{Uy}\,\Delta t\left(-\frac{1}{2}\,\text{Cos}[\eta]^2\,\text{Sin}[\eta]-\frac{\text{Sin}[\eta]^3}{6}\right)-$$
$$\frac{1}{9}\,i\,\text{Ux}^2\,\text{Uy}\,\alpha\,\beta\,\Delta t^3\left(-\frac{1}{2}\,\text{Cos}[\eta]^2\,\text{Sin}[\eta]-\frac{\text{Sin}[\eta]^3}{6}\right)+$$
$$\frac{2}{9}\,i\,\text{Uy}^3\,\alpha\,\beta\,\Delta t^3\left(-\frac{1}{2}\,\text{Cos}[\eta]^2\,\text{Sin}[\eta]-\frac{\text{Sin}[\eta]^3}{6}\right)+$$
$$\frac{2}{27}\,i\,\text{Ux}^2\,\text{Uy}\,\gamma\,\Delta t^3\left(-\frac{1}{2}\,\text{Cos}[\eta]^2\,\text{Sin}[\eta]-\frac{\text{Sin}[\eta]^3}{6}\right)-$$
$$\frac{4}{27}\,i\,\text{Uy}^3\,\gamma\,\Delta t^3\left(-\frac{1}{2}\,\text{Cos}[\eta]^2\,\text{Sin}[\eta]-\frac{\text{Sin}[\eta]^3}{6}\right)-$$
$$\frac{1}{27}\,i\,\text{Ux}\,\Delta t\left(-\frac{1}{6}\,\text{Cos}[\eta]^3+\text{Cos}[\eta]\left(-\frac{1}{2}\,\text{Cos}[\eta]^2-\text{Sin}[\eta]^2\right)\right)-$$
$$\frac{1}{18}\,i\,\text{Ux}^3\,\alpha\,\beta\,\Delta t^3\left(-\frac{1}{6}\,\text{Cos}[\eta]^3+\text{Cos}[\eta]\left(-\frac{1}{2}\,\text{Cos}[\eta]^2-\text{Sin}[\eta]^2\right)\right)-$$
$$\frac{1}{18}\,i\,\text{Ux}\,\text{Uy}^2\,\alpha\,\beta\,\Delta t^3\left(-\frac{1}{6}\,\text{Cos}[\eta]^3+\text{Cos}[\eta]\left(-\frac{1}{2}\,\text{Cos}[\eta]^2-\text{Sin}[\eta]^2\right)\right)+$$
$$\frac{1}{27}\,i\,\text{Ux}^3\,\gamma\,\Delta t^3\left(-\frac{1}{6}\,\text{Cos}[\eta]^3+\text{Cos}[\eta]\left(-\frac{1}{2}\,\text{Cos}[\eta]^2-\text{Sin}[\eta]^2\right)\right)+$$
$$\frac{1}{27}\,i\,\text{Ux}\,\text{Uy}^2\,\gamma\,\Delta t^3\left(-\frac{1}{6}\,\text{Cos}[\eta]^3+\text{Cos}[\eta]\left(-\frac{1}{2}\,\text{Cos}[\eta]^2-\text{Sin}[\eta]^2\right)\right)-$$
$$\frac{1}{27}\,i\,\text{Uy}\,\Delta t\left(-\frac{1}{6}\,\text{Sin}[\eta]^3+\text{Sin}[\eta]\left(-\text{Cos}[\eta]^2-\frac{\text{Sin}[\eta]^2}{2}\right)\right)-$$
$$\frac{1}{18}\,i\,\text{Ux}^2\,\text{Uy}\,\alpha\,\beta\,\Delta t^3\left(-\frac{1}{6}\,\text{Sin}[\eta]^3+\text{Sin}[\eta]\left(-\text{Cos}[\eta]^2-\frac{\text{Sin}[\eta]^2}{2}\right)\right)-$$
$$\frac{1}{18}\,i\,\text{Uy}^3\,\alpha\,\beta\,\Delta t^3\left(-\frac{1}{6}\,\text{Sin}[\eta]^3+\text{Sin}[\eta]\left(-\text{Cos}[\eta]^2-\frac{\text{Sin}[\eta]^2}{2}\right)\right)+$$
$$\frac{1}{27}\,i\,\text{Ux}^2\,\text{Uy}\,\gamma\,\Delta t^3\left(-\frac{1}{6}\,\text{Sin}[\eta]^3+\text{Sin}[\eta]\left(-\text{Cos}[\eta]^2-\frac{\text{Sin}[\eta]^2}{2}\right)\right)+$$
$$\frac{1}{27}\,i\,\text{Uy}^3\,\gamma\,\Delta t^3\left(-\frac{1}{6}\,\text{Sin}[\eta]^3+\text{Sin}[\eta]\left(-\text{Cos}[\eta]^2-\frac{\text{Sin}[\eta]^2}{2}\right)\right)-$$
$$\frac{4}{27}\,i\,\text{Ux}\,\Delta t\left(-\frac{1}{6}\,\text{Cos}[\eta]^3+\text{Cos}[\eta]\left(-\frac{1}{2}\,\text{Cos}[\eta]^2-\frac{\text{Sin}[\eta]^2}{2}\right)\right)-$$
$$\frac{2}{9}\,i\,\text{Ux}^3\,\alpha\,\beta\,\Delta t^3\left(-\frac{1}{6}\,\text{Cos}[\eta]^3+\text{Cos}[\eta]\left(-\frac{1}{2}\,\text{Cos}[\eta]^2-\frac{\text{Sin}[\eta]^2}{2}\right)\right)-$$
$$\frac{1}{18}\,i\,\text{Ux}\,\text{Uy}^2\,\alpha\,\beta\,\Delta t^3\left(-\frac{1}{6}\,\text{Cos}[\eta]^3+\text{Cos}[\eta]\left(-\frac{1}{2}\,\text{Cos}[\eta]^2-\frac{\text{Sin}[\eta]^2}{2}\right)\right)+$$
$$\frac{4}{27}\,i\,\text{Ux}^3\,\gamma\,\Delta t^3\left(-\frac{1}{6}\,\text{Cos}[\eta]^3+\text{Cos}[\eta]\left(-\frac{1}{2}\,\text{Cos}[\eta]^2-\frac{\text{Sin}[\eta]^2}{2}\right)\right)+$$
$$\frac{1}{27}\,i\,\text{Ux}\,\text{Uy}^2\,\gamma\,\Delta t^3\left(-\frac{1}{6}\,\text{Cos}[\eta]^3+\text{Cos}[\eta]\left(-\frac{1}{2}\,\text{Cos}[\eta]^2-\frac{\text{Sin}[\eta]^2}{2}\right)\right)-$$
$$\frac{4}{27}\,i\,\text{Uy}\,\Delta t\left(-\frac{1}{6}\,\text{Sin}[\eta]^3+\text{Sin}[\eta]\left(-\frac{1}{2}\,\text{Cos}[\eta]^2-\frac{\text{Sin}[\eta]^2}{2}\right)\right)-$$
$$\frac{1}{18}\,i\,\text{Ux}^2\,\text{Uy}\,\alpha\,\beta\,\Delta t^3\left(-\frac{1}{6}\,\text{Sin}[\eta]^3+\text{Sin}[\eta]\left(-\frac{1}{2}\,\text{Cos}[\eta]^2-\frac{\text{Sin}[\eta]^2}{2}\right)\right)-$$

$$\frac{2}{9}\,i\,Uy^3\,\alpha\,\beta\,\Delta t^3\left(-\frac{1}{6}\,\mathrm{Sin}[\eta]^3+\mathrm{Sin}[\eta]\left(-\frac{1}{2}\,\mathrm{Cos}[\eta]^2-\frac{\mathrm{Sin}[\eta]^2}{2}\right)\right)+$$

$$\frac{1}{27}\,i\,Ux^2\,Uy\,\gamma\,\Delta t^3\left(-\frac{1}{6}\,\mathrm{Sin}[\eta]^3+\mathrm{Sin}[\eta]\left(-\frac{1}{2}\,\mathrm{Cos}[\eta]^2-\frac{\mathrm{Sin}[\eta]^2}{2}\right)\right)+$$

$$\frac{4}{27}\,i\,Uy^3\,\gamma\,\Delta t^3\left(-\frac{1}{6}\,\mathrm{Sin}[\eta]^3+\mathrm{Sin}[\eta]\left(-\frac{1}{2}\,\mathrm{Cos}[\eta]^2-\frac{\mathrm{Sin}[\eta]^2}{2}\right)\right)+$$

$$(-i\,Ux\,\Delta t\,\mathrm{Cos}[\eta]-i\,Uy\,\Delta t\,\mathrm{Sin}[\eta])$$

$$\left(\frac{4\,\mathrm{Cos}[\eta]^2}{27}-\frac{1}{4}\,Ux^2\,\alpha^2\,\Delta t^2\,\mathrm{Cos}[\eta]^2-\frac{4}{27}\,Ux^2\,\gamma\,\Delta t^2\,\mathrm{Cos}[\eta]^2+\frac{4}{27}\,Uy^2\,\gamma\,\Delta t^2\,\mathrm{Cos}[\eta]^2-\right.$$

$$\frac{2}{27}\,Ux^2\,Uy^2\,\gamma^2\,\Delta t^4\,\mathrm{Cos}[\eta]^2+\frac{1}{27}\,Uy^4\,\gamma^2\,\Delta t^4\,\mathrm{Cos}[\eta]^2-Ux^2\,\alpha\,\Delta t^2\,\theta\,\mathrm{Cos}[\eta]^2-$$

$$\frac{4}{9}\,Ux^2\,\beta\,\Delta t^2\,\theta\,\mathrm{Cos}[\eta]^2+\frac{4}{9}\,Uy^2\,\beta\,\Delta t^2\,\theta\,\mathrm{Cos}[\eta]^2-\frac{4}{9}\,Ux^2\,Uy^2\,\beta\,\gamma\,\Delta t^4\,\theta\,\mathrm{Cos}[\eta]^2+$$

$$\frac{2}{9}\,Uy^4\,\beta\,\gamma\,\Delta t^4\,\theta\,\mathrm{Cos}[\eta]^2-Ux^2\,\Delta t^2\,\theta^2\,\mathrm{Cos}[\eta]^2-\frac{2}{3}\,Ux^2\,Uy^2\,\beta^2\,\Delta t^4\,\theta^2\,\mathrm{Cos}[\eta]^2+$$

$$\frac{1}{3}\,Uy^4\,\beta^2\,\Delta t^4\,\theta^2\,\mathrm{Cos}[\eta]^2-\frac{1}{2}\,Ux\,Uy\,\alpha^2\,\Delta t^2\,\mathrm{Cos}[\eta]\,\mathrm{Sin}[\eta]-$$

$$2\,Ux\,Uy\,\alpha\,\Delta t^2\,\theta\,\mathrm{Cos}[\eta]\,\mathrm{Sin}[\eta]-2\,Ux\,Uy\,\Delta t^2\,\theta^2\,\mathrm{Cos}[\eta]\,\mathrm{Sin}[\eta]+\frac{4\,\mathrm{Sin}[\eta]^2}{27}-$$

$$\frac{1}{4}\,Uy^2\,\alpha^2\,\Delta t^2\,\mathrm{Sin}[\eta]^2+\frac{4}{27}\,Ux^2\,\gamma\,\Delta t^2\,\mathrm{Sin}[\eta]^2-\frac{4}{27}\,Uy^2\,\gamma\,\Delta t^2\,\mathrm{Sin}[\eta]^2+$$

$$\frac{1}{27}\,Ux^4\,\gamma^2\,\Delta t^4\,\mathrm{Sin}[\eta]^2-\frac{2}{27}\,Ux^2\,Uy^2\,\gamma^2\,\Delta t^4\,\mathrm{Sin}[\eta]^2-Uy^2\,\alpha\,\Delta t^2\,\theta\,\mathrm{Sin}[\eta]^2+$$

$$\frac{4}{9}\,Ux^2\,\beta\,\Delta t^2\,\theta\,\mathrm{Sin}[\eta]^2-\frac{4}{9}\,Uy^2\,\beta\,\Delta t^2\,\theta\,\mathrm{Sin}[\eta]^2+\frac{2}{9}\,Ux^4\,\beta\,\gamma\,\Delta t^4\,\theta\,\mathrm{Sin}[\eta]^2-$$

$$\frac{4}{9}\,Ux^2\,Uy^2\,\beta\,\gamma\,\Delta t^4\,\theta\,\mathrm{Sin}[\eta]^2-Uy^2\,\Delta t^2\,\theta^2\,\mathrm{Sin}[\eta]^2+\frac{1}{3}\,Ux^4\,\beta^2\,\Delta t^4\,\theta^2\,\mathrm{Sin}[\eta]^2-$$

$$\frac{2}{3}\,Ux^2\,Uy^2\,\beta^2\,\Delta t^4\,\theta^2\,\mathrm{Sin}[\eta]^2+\frac{2}{81}\,Ux^2\,\gamma\,\Delta t^2\,(-\mathrm{Cos}[\eta]^2-\mathrm{Sin}[\eta]^2)+$$

$$\frac{2}{81}\,Uy^2\,\gamma\,\Delta t^2\,(-\mathrm{Cos}[\eta]^2-\mathrm{Sin}[\eta]^2)-\frac{1}{81}\,Ux^4\,\gamma^2\,\Delta t^4\,(-\mathrm{Cos}[\eta]^2-\mathrm{Sin}[\eta]^2)-$$

$$\frac{2}{81}\,Ux^2\,Uy^2\,\gamma^2\,\Delta t^4\,(-\mathrm{Cos}[\eta]^2-\mathrm{Sin}[\eta]^2)-\frac{1}{81}\,Uy^4\,\gamma^2\,\Delta t^4\,(-\mathrm{Cos}[\eta]^2-\mathrm{Sin}[\eta]^2)+$$

$$\frac{2}{27}\,Ux^2\,\beta\,\Delta t^2\,\theta\,(-\mathrm{Cos}[\eta]^2-\mathrm{Sin}[\eta]^2)+\frac{2}{27}\,Uy^2\,\beta\,\Delta t^2\,\theta\,(-\mathrm{Cos}[\eta]^2-\mathrm{Sin}[\eta]^2)-$$

$$\frac{2}{27}\,Ux^4\,\beta\,\gamma\,\Delta t^4\,\theta\,(-\mathrm{Cos}[\eta]^2-\mathrm{Sin}[\eta]^2)-\frac{4}{27}\,Ux^2\,Uy^2\,\beta\,\gamma\,\Delta t^4\,\theta\,(-\mathrm{Cos}[\eta]^2-\mathrm{Sin}[\eta]^2)-$$

$$\frac{2}{27}\,Uy^4\,\beta\,\gamma\,\Delta t^4\,\theta\,(-\mathrm{Cos}[\eta]^2-\mathrm{Sin}[\eta]^2)-\frac{1}{9}\,Ux^4\,\beta^2\,\Delta t^4\,\theta^2\,(-\mathrm{Cos}[\eta]^2-\mathrm{Sin}[\eta]^2)-$$

$$\frac{2}{9}\,Ux^2\,Uy^2\,\beta^2\,\Delta t^4\,\theta^2\,(-\mathrm{Cos}[\eta]^2-\mathrm{Sin}[\eta]^2)-\frac{1}{9}\,Uy^4\,\beta^2\,\Delta t^4\,\theta^2\,(-\mathrm{Cos}[\eta]^2-\mathrm{Sin}[\eta]^2)-$$

$$\frac{4}{81}\left(-\frac{1}{2}\,\mathrm{Cos}[\eta]^2-\mathrm{Sin}[\eta]^2\right)+\frac{2}{81}\,Ux^2\,\gamma\,\Delta t^2\left(-\frac{1}{2}\,\mathrm{Cos}[\eta]^2-\mathrm{Sin}[\eta]^2\right)+$$

$$\frac{8}{81}\,Uy^2\,\gamma\,\Delta t^2\left(-\frac{1}{2}\,\mathrm{Cos}[\eta]^2-\mathrm{Sin}[\eta]^2\right)+\frac{2}{81}\,Ux^4\,\gamma^2\,\Delta t^4\left(-\frac{1}{2}\,\mathrm{Cos}[\eta]^2-\mathrm{Sin}[\eta]^2\right)-$$

$$\frac{2}{81}\,Ux^2\,Uy^2\,\gamma^2\,\Delta t^4\left(-\frac{1}{2}\,\mathrm{Cos}[\eta]^2-\mathrm{Sin}[\eta]^2\right)-\frac{4}{81}\,Uy^4\,\gamma^2\,\Delta t^4\left(-\frac{1}{2}\,\mathrm{Cos}[\eta]^2-\mathrm{Sin}[\eta]^2\right)+$$

$$\left(-\frac{1}{2}\cos[\eta]^2-\sin[\eta]^2\right)-\frac{4}{81}\,Uy^4\gamma^2\Delta t^4\left(-\frac{1}{2}\cos[\eta]^2-\sin[\eta]^2\right)+$$
$$\frac{2}{27}\,Ux^2\beta\Delta t^2\theta\left(-\frac{1}{2}\cos[\eta]^2-\sin[\eta]^2\right)+\frac{8}{27}\,Uy^2\beta\Delta t^2\theta\left(-\frac{1}{2}\cos[\eta]^2-\sin[\eta]^2\right)+\frac{4}{27}$$
$$Ux^4\beta\gamma\Delta t^4\theta\left(-\frac{1}{2}\cos[\eta]^2-\sin[\eta]^2\right)-\frac{4}{27}\,Ux^2\,Uy^2\beta\gamma\Delta t^4\theta\left(-\frac{1}{2}\cos[\eta]^2-\sin[\eta]^2\right)-$$
$$\frac{8}{27}\,Uy^4\beta\gamma\Delta t^4\theta\left(-\frac{1}{2}\cos[\eta]^2-\sin[\eta]^2\right)+\frac{2}{9}\,Ux^4\beta^2\Delta t^4\theta^2\left(-\frac{1}{2}\cos[\eta]^2-\sin[\eta]^2\right)-$$
$$\frac{2}{9}\,Ux^2\,Uy^2\beta^2\Delta t^4\theta^2\left(-\frac{1}{2}\cos[\eta]^2-\sin[\eta]^2\right)-$$
$$\frac{4}{9}\,Uy^4\beta^2\Delta t^4\theta^2\left(-\frac{1}{2}\cos[\eta]^2-\sin[\eta]^2\right)-\frac{4}{81}\left(-\cos[\eta]^2-\frac{\sin[\eta]^2}{2}\right)+$$
$$\frac{8}{81}\,Ux^2\gamma\Delta t^2\left(-\cos[\eta]^2-\frac{\sin[\eta]^2}{2}\right)+\frac{2}{81}\,Uy^2\gamma\Delta t^2\left(-\cos[\eta]^2-\frac{\sin[\eta]^2}{2}\right)-$$
$$\frac{4}{81}\,Ux^4\gamma^2\Delta t^4\left(-\cos[\eta]^2-\frac{\sin[\eta]^2}{2}\right)-\frac{2}{81}\,Ux^2\,Uy^2\gamma^2\Delta t^4\left(-\cos[\eta]^2-\frac{\sin[\eta]^2}{2}\right)+$$
$$\frac{2}{81}\,Uy^4\gamma^2\Delta t^4\left(-\cos[\eta]^2-\frac{\sin[\eta]^2}{2}\right)+\frac{8}{27}\,Ux^2\beta\Delta t^2\theta\left(-\cos[\eta]^2-\frac{\sin[\eta]^2}{2}\right)+$$
$$\frac{2}{27}\,Uy^2\beta\Delta t^2\theta\left(-\cos[\eta]^2-\frac{\sin[\eta]^2}{2}\right)-\frac{8}{27}\,Ux^4\beta\gamma\Delta t^4\theta\left(-\cos[\eta]^2-\frac{\sin[\eta]^2}{2}\right)-$$
$$\frac{4}{27}\,Ux^2\,Uy^2\beta\gamma\Delta t^4\theta\left(-\cos[\eta]^2-\frac{\sin[\eta]^2}{2}\right)+$$
$$\frac{4}{27}\,Uy^4\beta\gamma\Delta t^4\theta\left(-\cos[\eta]^2-\frac{\sin[\eta]^2}{2}\right)-\frac{4}{9}\,Ux^4\beta^2\Delta t^4\theta^2\left(-\cos[\eta]^2-\frac{\sin[\eta]^2}{2}\right)-$$
$$\frac{2}{9}\,Ux^2\,Uy^2\beta^2\Delta t^4\theta^2\left(-\cos[\eta]^2-\frac{\sin[\eta]^2}{2}\right)+\frac{2}{9}\,Uy^4\beta^2\Delta t^4\theta^2\left(-\cos[\eta]^2-\frac{\sin[\eta]^2}{2}\right)-$$
$$\frac{16}{81}\left(-\frac{1}{2}\cos[\eta]^2-\frac{\sin[\eta]^2}{2}\right)+\frac{8}{81}\,Ux^2\gamma\Delta t^2\left(-\frac{1}{2}\cos[\eta]^2-\frac{\sin[\eta]^2}{2}\right)+$$
$$\frac{8}{81}\,Uy^2\gamma\Delta t^2\left(-\frac{1}{2}\cos[\eta]^2-\frac{\sin[\eta]^2}{2}\right)+\frac{8}{81}\,Ux^4\gamma^2\Delta t^4\left(-\frac{1}{2}\cos[\eta]^2-\frac{\sin[\eta]^2}{2}\right)-$$
$$\frac{2}{81}\,Ux^2\,Uy^2\gamma^2\Delta t^4\left(-\frac{1}{2}\cos[\eta]^2-\frac{\sin[\eta]^2}{2}\right)+$$
$$\frac{8}{81}\,Uy^4\gamma^2\Delta t^4\left(-\frac{1}{2}\cos[\eta]^2-\frac{\sin[\eta]^2}{2}\right)+\frac{8}{27}\,Ux^2\beta\Delta t^2\theta\left(-\frac{1}{2}\cos[\eta]^2-\frac{\sin[\eta]^2}{2}\right)+$$
$$\frac{8}{27}\,Uy^2\beta\Delta t^2\theta\left(-\frac{1}{2}\cos[\eta]^2-\frac{\sin[\eta]^2}{2}\right)+\frac{16}{27}\,Ux^4\beta\gamma\Delta t^4\theta\left(-\frac{1}{2}\cos[\eta]^2-\frac{\sin[\eta]^2}{2}\right)-$$
$$\frac{4}{27}\,Ux^2\,Uy^2\beta\gamma\Delta t^4\theta\left(-\frac{1}{2}\cos[\eta]^2-\frac{\sin[\eta]^2}{2}\right)+$$
$$\frac{16}{27}\,Uy^4\beta\gamma\Delta t^4\theta\left(-\frac{1}{2}\cos[\eta]^2-\frac{\sin[\eta]^2}{2}\right)+\frac{8}{9}\,Ux^4\beta^2\Delta t^4\theta^2$$
$$\left(-\frac{1}{2}\cos[\eta]^2-\frac{\sin[\eta]^2}{2}\right)-\frac{2}{9}\,Ux^2\,Uy^2\beta^2\Delta t^4\theta^2\left(-\frac{1}{2}\cos[\eta]^2-\frac{\sin[\eta]^2}{2}\right)+$$
$$\frac{8}{9}\,Uy^4\beta^2\Delta t^4\theta^2\left(-\frac{1}{2}\cos[\eta]^2-\frac{\sin[\eta]^2}{2}\right)+\frac{1}{81}\left(\cos[\eta]^2+\sin[\eta]^2\right)\Big)\Big)\,m^3+O[m]^4$$

$$\left(\frac{1}{3}+\frac{1}{2}\,(c^2+2\,\text{Deff})-\frac{c^2\gamma}{3}+\frac{1}{2}\left(-\frac{1}{3}+\frac{c^2\gamma}{3}-2\,\text{Deff}\,(1-\theta)-c^2\beta\,(1-\theta)\right)-\right.$$
$$2\,\text{Deff}\,\theta-c^2\beta\,\theta-\left(-\frac{c\alpha}{2}-c\,(1-\theta)\right)\left(\frac{c\alpha}{2}-c\,\theta\right)-$$
$$\left.\left(\frac{c\alpha}{2}-c\,\theta\right)^2+\frac{1}{2}\left(-\frac{1}{3}+\frac{c^2\gamma}{3}+2\,\text{Deff}\,\theta+c^2\beta\,\theta\right)\right)m^2+$$
$$\left(\frac{1}{3}\left(\frac{1}{2}\,i\,c\,(-c^2-2\,\text{Deff})-2\,i\,c\,\text{Deff}\right)+\right.$$
$$i\,(-c\,(1-\theta)-c\,\theta)\left(\frac{1}{3}-\frac{c^2\gamma}{3}-2\,\text{Deff}\,\theta-c^2\beta\,\theta-\left(\frac{c\alpha}{2}-c\,\theta\right)^2\right)+$$
$$i\left(\frac{1}{6}\left(\frac{c\alpha}{2}+c\,(1-\theta)\right)+\frac{1}{2}\left(-\frac{1}{3}+\frac{c^2\gamma}{3}-2\,\text{Deff}\,(1-\theta)-c^2\beta\,(1-\theta)\right)\left(\frac{c\alpha}{2}-c\,\theta\right)+\right.$$
$$\left.\left.\frac{1}{6}\left(-\frac{c\alpha}{2}+c\,\theta\right)+\frac{1}{2}\left(-\frac{c\alpha}{2}-c\,(1-\theta)\right)\left(-\frac{1}{3}+\frac{c^2\gamma}{3}+2\,\text{Deff}\,\theta+c^2\beta\,\theta\right)\right)\right)m^3+$$
$$\left(\frac{1}{4}\left((-c^2-2\,\text{Deff})\,\text{Deff}+\frac{1}{3}\,i\,c\left(-\frac{1}{2}\,i\,c\,(-c^2-2\,\text{Deff})+2\,i\,c\,\text{Deff}\right)\right)+\right.$$
$$\frac{1}{24}\left(\frac{1}{3}-\frac{c^2\gamma}{3}+2\,\text{Deff}\,(1-\theta)+c^2\beta\,(1-\theta)\right)-\frac{1}{6}\left(\frac{c\alpha}{2}+c\,(1-\theta)\right)\left(\frac{c\alpha}{2}-c\,\theta\right)-$$
$$\frac{1}{6}\left(-\frac{c\alpha}{2}-c\,(1-\theta)\right)\left(-\frac{c\alpha}{2}+c\,\theta\right)-\frac{1}{3}\left(\frac{c\alpha}{2}-c\,\theta\right)\left(-\frac{c\alpha}{2}+c\,\theta\right)+$$
$$\frac{1}{24}\left(\frac{1}{3}-\frac{c^2\gamma}{3}-2\,\text{Deff}\,\theta-c^2\beta\,\theta\right)+\frac{1}{12}\left(-\frac{1}{3}+\frac{c^2\gamma}{3}+2\,\text{Deff}\,\theta+c^2\beta\,\theta\right)+$$
$$\frac{1}{4}\left(-\frac{1}{3}+\frac{c^2\gamma}{3}-2\,\text{Deff}\,(1-\theta)-c^2\beta\,(1-\theta)\right)\left(-\frac{1}{3}+\frac{c^2\gamma}{3}+2\,\text{Deff}\,\theta+c^2\beta\,\theta\right)-$$
$$\frac{1}{4}\left(-\frac{1}{3}+\frac{c^2\gamma}{3}+2\,\text{Deff}\,\theta+c^2\beta\,\theta\right)^2+$$
$$\left(-\frac{1}{3}+\frac{c^2\gamma}{3}+2\,\text{Deff}\,\theta+c^2\beta\,\theta+\left(\frac{c\alpha}{2}-c\,\theta\right)^2\right)^2+$$
$$\left(\frac{1}{3}-\frac{c^2\gamma}{3}-2\,\text{Deff}\,\theta-c^2\beta\,\theta-\left(\frac{c\alpha}{2}-c\,\theta\right)^2\right)$$
$$\left(\frac{1}{2}\left(-\frac{1}{3}+\frac{c^2\gamma}{3}-2\,\text{Deff}\,(1-\theta)-c^2\beta\,(1-\theta)\right)-\right.$$
$$\left.\left.\left(-\frac{c\alpha}{2}-c\,(1-\theta)\right)\left(\frac{c\alpha}{2}-c\,\theta\right)+\frac{1}{2}\left(-\frac{1}{3}+\frac{c^2\gamma}{3}+2\,\text{Deff}\,\theta+c^2\beta\,\theta\right)\right)\right)m^4+$$

$$\left(\frac{1}{5}\left(\frac{2}{3}\,\text{Deff}\left(-\frac{1}{2}\,i\,c\,(-c^2-2\,\text{Deff})+2\,i\,c\,\text{Deff}\right)+\right.\right.$$
$$\left.\left.\frac{1}{4}\,i\,c\left(-(-c^2-2\,\text{Deff})\,\text{Deff}-\frac{1}{3}\,i\,c\left(-\frac{1}{2}\,i\,c\,(-c^2-2\,\text{Deff})+2\,i\,c\,\text{Deff}\right)\right)\right)+$$
$$i\left(\frac{1}{3}-\frac{c^2\gamma}{3}-2\,\text{Deff}\,\theta-c^2\beta\theta-\left(\frac{c\alpha}{2}-c\theta\right)^2\right)$$
$$\left(\frac{1}{6}\left(\frac{c\alpha}{2}+c\,(1-\theta)\right)+\frac{1}{2}\left(-\frac{1}{3}+\frac{c^2\gamma}{3}-2\,\text{Deff}\,(1-\theta)-c^2\beta\,(1-\theta)\right)\left(\frac{c\alpha}{2}-c\theta\right)+\right.$$
$$\left.\frac{1}{6}\left(-\frac{c\alpha}{2}+c\theta\right)+\frac{1}{2}\left(-\frac{c\alpha}{2}-c\,(1-\theta)\right)\left(-\frac{1}{3}+\frac{c^2\gamma}{3}+2\,\text{Deff}\,\theta+c^2\beta\theta\right)\right)+$$
$$i\left(\frac{1}{120}\left(-\frac{c\alpha}{2}-c\,(1-\theta)\right)+\frac{1}{120}\left(\frac{c\alpha}{2}-c\theta\right)+\right.$$
$$\frac{1}{24}\left(\frac{1}{3}-\frac{c^2\gamma}{3}+2\,\text{Deff}\,(1-\theta)+c^2\beta\,(1-\theta)\right)\left(\frac{c\alpha}{2}-c\theta\right)+$$
$$\frac{1}{12}\left(-\frac{1}{3}+\frac{c^2\gamma}{3}-2\,\text{Deff}\,(1-\theta)-c^2\beta\,(1-\theta)\right)\left(-\frac{c\alpha}{2}+c\theta\right)+$$
$$\frac{1}{24}\left(-\frac{c\alpha}{2}-c\,(1-\theta)\right)\left(\frac{1}{3}-\frac{c^2\gamma}{3}-2\,\text{Deff}\,\theta-c^2\beta\theta\right)+$$
$$\left.\frac{1}{12}\left(\frac{c\alpha}{2}+c\,(1-\theta)\right)\left(-\frac{1}{3}+\frac{c^2\gamma}{3}+2\,\text{Deff}\,\theta+c^2\beta\theta\right)\right)+$$
$$i\,(-c\,(1-\theta)-c\theta)\left(-\frac{1}{3}\left(\frac{c\alpha}{2}-c\theta\right)\left(-\frac{c\alpha}{2}+c\theta\right)+\right.$$
$$\frac{1}{12}\left(-\frac{1}{3}+\frac{c^2\gamma}{3}+2\,\text{Deff}\,\theta+c^2\beta\theta\right)-\frac{1}{4}\left(-\frac{1}{3}+\frac{c^2\gamma}{3}+2\,\text{Deff}\,\theta+c^2\beta\theta\right)^2+$$
$$\left.\left.\left(-\frac{1}{3}+\frac{c^2\gamma}{3}+2\,\text{Deff}\,\theta+c^2\beta\theta+\left(\frac{c\alpha}{2}-c\theta\right)^2\right)^2\right)\right)m^5+$$

$$\left(\frac{1}{6}\left(\frac{1}{2}\,\text{Deff}\left(-\left(-c^2-2\,\text{Deff}\right)\text{Deff}-\frac{1}{3}\,i\,c\left(-\frac{1}{2}\,i\,c\left(-c^2-2\,\text{Deff}\right)+2\,i\,c\,\text{Deff}\right)\right)+\right.\right.$$
$$\frac{1}{5}\,i\,c\left(-\frac{2}{3}\,\text{Deff}\left(-\frac{1}{2}\,i\,c\left(-c^2-2\,\text{Deff}\right)+2\,i\,c\,\text{Deff}\right)-\right.$$
$$\left.\left.\left.\frac{1}{4}\,i\,c\left(-\left(-c^2-2\,\text{Deff}\right)\text{Deff}-\frac{1}{3}\,i\,c\left(-\frac{1}{2}\,i\,c\left(-c^2-2\,\text{Deff}\right)+2\,i\,c\,\text{Deff}\right)\right)\right)\right)+$$
$$\frac{1}{720}\left(-\frac{1}{3}+\frac{c^2\gamma}{3}-2\,\text{Deff}\,(1-\theta)-c^2\beta\,(1-\theta)\right)-$$
$$\frac{1}{60}\left(-\frac{c\,\alpha}{2}-c\,(1-\theta)\right)\left(\frac{c\,\alpha}{2}-c\,\theta\right)-$$
$$\frac{1}{60}\left(\frac{c\,\alpha}{2}-c\,\theta\right)^2-$$
$$\frac{1}{36}\left(\frac{c\,\alpha}{2}+c\,(1-\theta)\right)\left(-\frac{c\,\alpha}{2}+c\,\theta\right)-$$
$$\frac{1}{36}\left(-\frac{c\,\alpha}{2}+c\,\theta\right)^2+$$
$$\frac{1}{360}\left(\frac{1}{3}-\frac{c^2\gamma}{3}-2\,\text{Deff}\,\theta-c^2\beta\,\theta\right)+$$
$$\frac{1}{48}\left(-\frac{1}{3}+\frac{c^2\gamma}{3}-2\,\text{Deff}\,(1-\theta)-c^2\beta\,(1-\theta)\right)\left(\frac{1}{3}-\frac{c^2\gamma}{3}-2\,\text{Deff}\,\theta-c^2\beta\,\theta\right)+$$
$$\frac{1}{720}\left(-\frac{1}{3}+\frac{c^2\gamma}{3}+2\,\text{Deff}\,\theta+c^2\beta\,\theta\right)+$$
$$\frac{1}{48}\left(\frac{1}{3}-\frac{c^2\gamma}{3}+2\,\text{Deff}\,(1-\theta)+c^2\beta\,(1-\theta)\right)\left(-\frac{1}{3}+\frac{c^2\gamma}{3}+2\,\text{Deff}\,\theta+c^2\beta\,\theta\right)-$$
$$\frac{1}{24}\left(\frac{1}{3}-\frac{c^2\gamma}{3}-2\,\text{Deff}\,\theta-c^2\beta\,\theta\right)\left(-\frac{1}{3}+\frac{c^2\gamma}{3}+2\,\text{Deff}\,\theta+c^2\beta\,\theta\right)+$$
$$\left(\frac{1}{3}-\frac{c^2\gamma}{3}-2\,\text{Deff}\,\theta-c^2\beta\,\theta-\left(\frac{c\,\alpha}{2}-c\,\theta\right)^2\right)$$
$$\left(\frac{1}{24}\left(\frac{1}{3}-\frac{c^2\gamma}{3}+2\,\text{Deff}\,(1-\theta)+c^2\beta\,(1-\theta)\right)-\frac{1}{6}\left(\frac{c\,\alpha}{2}+c\,(1-\theta)\right)\left(\frac{c\,\alpha}{2}-c\,\theta\right)-\right.$$
$$\frac{1}{6}\left(-\frac{c\,\alpha}{2}-c\,(1-\theta)\right)\left(-\frac{c\,\alpha}{2}+c\,\theta\right)+\frac{1}{24}\left(\frac{1}{3}-\frac{c^2\gamma}{3}-2\,\text{Deff}\,\theta-c^2\beta\,\theta\right)+$$
$$\left.\frac{1}{4}\left(-\frac{1}{3}+\frac{c^2\gamma}{3}-2\,\text{Deff}\,(1-\theta)-c^2\beta\,(1-\theta)\right)\left(-\frac{1}{3}+\frac{c^2\gamma}{3}+2\,\text{Deff}\,\theta+c^2\beta\,\theta\right)\right)+$$
$$\left(-\frac{1}{3}+\frac{c^2\gamma}{3}+2\,\text{Deff}\,\theta+c^2\beta\,\theta+\left(\frac{c\,\alpha}{2}-c\,\theta\right)^2\right)\left(\frac{1}{3}\left(\frac{c\,\alpha}{2}-c\,\theta\right)\left(-\frac{c\,\alpha}{2}+c\,\theta\right)+\right.$$
$$\left.\frac{1}{12}\left(\frac{1}{3}-\frac{c^2\gamma}{3}-2\,\text{Deff}\,\theta-c^2\beta\,\theta\right)+\frac{1}{4}\left(-\frac{1}{3}+\frac{c^2\gamma}{3}+2\,\text{Deff}\,\theta+c^2\beta\,\theta\right)^2\right)-$$
$$\left(-\frac{1}{3}+\frac{c^2\gamma}{3}+2\,\text{Deff}\,\theta+c^2\beta\,\theta+\left(\frac{c\,\alpha}{2}-c\,\theta\right)^2\right)\left(-\frac{1}{3}\left(\frac{c\,\alpha}{2}-c\,\theta\right)\left(-\frac{c\,\alpha}{2}+c\,\theta\right)+\right.$$

$$\frac{1}{12}\left(-\frac{1}{3}+\frac{c^2\gamma}{3}+2\,\text{Deff}\,\theta+c^2\beta\theta\right)-\frac{1}{4}\left(-\frac{1}{3}+\frac{c^2\gamma}{3}+2\,\text{Deff}\,\theta+c^2\beta\theta\right)^2+$$
$$\left(-\frac{1}{3}+\frac{c^2\gamma}{3}+2\,\text{Deff}\,\theta+c^2\beta\theta+\left(\frac{c\alpha}{2}-c\theta\right)^2\right)^2\Bigg)+$$
$$\left(\frac{1}{2}\left(-\frac{1}{3}+\frac{c^2\gamma}{3}-2\,\text{Deff}\,(1-\theta)-c^2\beta\,(1-\theta)\right)-\left(-\frac{c\alpha}{2}-c\,(1-\theta)\right)\left(\frac{c\alpha}{2}-c\theta\right)+\right.$$
$$\left.\frac{1}{2}\left(-\frac{1}{3}+\frac{c^2\gamma}{3}+2\,\text{Deff}\,\theta+c^2\beta\theta\right)\right)\left(-\frac{1}{3}\left(\frac{c\alpha}{2}-c\theta\right)\left(-\frac{c\alpha}{2}+c\theta\right)+\right.$$
$$\frac{1}{12}\left(-\frac{1}{3}+\frac{c^2\gamma}{3}+2\,\text{Deff}\,\theta+c^2\beta\theta\right)-\frac{1}{4}\left(-\frac{1}{3}+\frac{c^2\gamma}{3}+2\,\text{Deff}\,\theta+c^2\beta\theta\right)^2+$$
$$\left.\left(-\frac{1}{3}+\frac{c^2\gamma}{3}+2\,\text{Deff}\,\theta+c^2\beta\theta+\left(\frac{c\alpha}{2}-c\theta\right)^2\right)^2\right)\Bigg)\,m^6+O[m]^7$$

Appendix VII

Matlab script for the 1D advection-diffusion

```
clear all;clc;
% TWS algorithm in dimensional form
global X1 elcon;
%********** Geometry **********************************
QL = [1];
%********** Physical Parameters **********************
Xleft = 0; Xright = 40; nnodes = 41;
co = 1.;
%Order of the algorithm: 1)GWS--RG--3)RGm--JLS--5)TG--TWS--Optmiza..
for dd = [1]
if dd == 1
AA = [0 0 0 0.5]
alpha = AA(1,1); beta = AA(1,2); gamma = AA(1,3); theta=AA(1,4);
elseif dd == 2
AA = [2/(sqrt(15)*co) 2/(sqrt(15)*co) 0 0.5]
alpha = AA(1,1); beta = AA(1,2); gamma = AA(1,3); theta=AA(1,4);
elseif dd == 3
AA = [100 100 0 0.5]
alpha = AA(1,1); beta = AA(1,2); gamma = AA(1,3); theta=AA(1,4);
elseif dd == 4
AA = [1 1 0 0.5]
alpha = AA(1,1); beta = AA(1,2); gamma = AA(1,3); theta=AA(1,4);
elseif dd == 5
AA = [0 1 1 0]
alpha = AA(1,1); beta = AA(1,2); gamma = AA(1,3); theta=AA(1,4);
elseif dd == 6
AA = [0 0 -.5 0.5]
alpha = AA(1,1); beta = AA(1,2); gamma = AA(1,3); theta=AA(1,4);
elseif dd == 7
AA = [0.20938 0.15328 -.4799 0.52805]
alpha = AA(1,1); beta = AA(1,2); gamma = AA(1,3); theta=AA(1,4);
end
dq=0;
X1 = linspace(Xleft,Xright,nnodes);
u = ones(nnodes,1);
delta_x = (X1(length(X1))-X1(1))/(nnodes-1);
qleft = 0;
nodeL = ceil(length(X1)/4);
L = X1(nodeL)-X1(1);
XL = X1(1:nodeL);
qinit = zeros(length(X1),1);
qinit(1:nodeL) = (1-cos(2*pi*XL/L))/2;
qFinal = zeros(length(X1),1);
```

```
vel = u(1);
%********** Time Integration Parameters **********
delta_t = co*delta_x/u(1);
start = 1;
inc = 1;
stop = 25;
Pe = 1000;
DifC = 1/Pe;
[Xnodes Ynodes] = size(X1);
%q = qinit;
q_last = qinit;
%unsteady time integration loop.
time_count = 1;
q_store(:,time_count) = qinit;
for timeLoop = start:inc:stop;
q = q_last;

%** Apply Boundary Conditions to Initial Condition for Set 0 ********************
for ii=1:1:length(QL)
q(QL(ii)) = +qleft;
end

%********************** Equations for Set 0*****************

q0 = asres1D(vel*delta_t,[],[],0,'A201L',q)...
   +asres1D(beta*delta_t^2*vel^2/2,[],[],-1,'A211L',q)...
   +asres1D(delta_t*DifC,[],[],-1,'A211L',q);

%Apply Dirichlet boundary condition to boundary QL.
for ii=1:1:length(QL)
q0(QL(ii)) = 0;
end

%***************** Jacobians for Set 0**********
%Equation q by q
q_jac0 = +asjac1D(1,[],[],1,'A200L',[])...
       +asjac1D(-alpha*delta_t*vel/2,[],[],0,'A201L',[])...
       +asjac1D(gamma*delta_t^2*vel^2/6,[],[],-1,'A211L',[])...
       +asjac1D(theta.*delta_t*vel,[],[],0,'A201L',[])...
       +asjac1D(theta.*beta.*delta_t^2*vel^2/2,[],[],-1,'A211L',[])...
       +asjac1D(theta*delta_t*DifC,[],[],-1,'A211L',[]);

%Apply Dirichlet boundary condition to boundary QL.
```

```
for ii=1:1:length(QL)
q_jac0(QL(ii),:) = 0;
q_jac0(:,QL(ii)) = 0;
q_jac0(QL(ii),QL(ii)) = 1;
end

%***************** Solver ********************************************
dq = q_jac0\(-q0);

%************** Solve Iterate ****************************************
q = q + dq;
time_count = time_count + 1;
q_store(:,time_count) = q;
% first entry in q_store is for IC. stop data is stored in stop+1
q_last = q;
end     % end of time integration loop

figure(dd)
hold on
plot(X1,q_store(:,1),'k-')
plot(X1,q_store(:,stop+1),'k-+')
MAXm = max(q_store(:,stop+1))
MINm = min(q_store(:,stop+1))
qstop_plot(:,dd)=q_store(:,stop+1);

xlabel('X1'),ylabel('q')
title(['Pe=' num2str(Pe) ', C=', num2str(co) ', \theta='...
       num2str(theta) ', \alpha=' ...
       num2str(alpha) ', \beta=' ...
       num2str(beta) ', \gamma=' num2str(gamma) ', M='...
      num2str(Xright) ])
legend('t=0','t=25','Location','Best')
%legend('t=0','t=', num2str(dist) ,'t=exact','Location','Best')
%legend(num2str(dist))
  set(gca,'YGrid','on')

end
```

Appendix VIII

Matlab script for the 1D Burgers equation

```
clear all;clc;
global X1 elcon;
%********** Geometry ***********************************
M = 200; nnodes=M+1;
QL = [1]; QR = [nnodes];
timePlot = [ 0 .2 0.6 1.0 1.4 2.0] ; % the time to plot
Re = 1000;
%********** Physical Parameters ***********************
Xleft = 0; Xright = 1;
alpha = -0.25; beta = .5; gamma = 0;
dq=0;
X1 = linspace(Xleft,Xright,nnodes);
delta_x = (X1(length(X1))-X1(1))/(nnodes-1);
uleft = 0;
u0 = zeros(length(X1),1);
u0(1:nnodes) = 0.5*sin(pi*X1)+sin(2*pi*X1);

%********** Time Integration Parameters ***********************
delta_t = 0.05;
theta = 0.5;
start = 1;
inc = 1;
stop = 300; % Max number of time-steps allowed
gammaCoef = gamma*(delta_t^2)/6;
betaCoef = beta*(delta_t^2)/2;
u = u0;
uN = u0;
maxIter = 80; eps = 0.001;
%unsteady time integration loop.
time_count = 1;
time = 0;
Total_Iter = 0;
u_store(:,time_count) = u0;
for timeLoop = start:inc:stop;
   iteration = 0;
%    res_uOld=+asres1D(betaCoef*(1-theta),[],u.^2,-1,'A3011L',u);
%    max_uOld =max(abs(res_uOld))

  for ii = 1:maxIter
    uAvg = (uN+u)/2;
u_res0 = +asres1D(1,[],[],1,'A200L',uN-u)...
       +asres1D(theta*delta_t,[],uN,0,'A3001L',uN)...
       +asres1D(theta*delta_t/Re,[],[],-1,'A211L',uN)...
```

```
        +asres1D(delta_t*(1-theta),[],u,0,'A3001L',u)...
        +asres1D(delta_t*(1-theta)/Re,[],[],-1,'A211L',u)...
        +asres1D(betaCoef*theta,[],uN.^2,-1,'A3011L',uN)...
        +asres1D(gammaCoef,[],uAvg.^2,-1,'A3011L',uN-u)...
        +asres1D(alpha*delta_t/2,[],uAvg,0,'A3010L',uN-u)...
        +asres1D(betaCoef*(1-theta),[],u.^2,-1,'A3011L',u);


%Apply Dirichlet boundary condition to boundary QL.
for ii=1:1:length(QL)
u_res0(QL(ii)) = 0;
end

%Apply Dirichlet boundary condition to boundary QL.
for ii=1:1:length(QR)
u_res0(QR(ii)) = 0;
end
%****************** Jacobians for Set 0**********
%Equation q by q
u_jac0 = +asjac1D(1,[],[],1,'A200L',[])...
        +asjac1D(theta.*delta_t,[],uN,0,'A3001L',[])...
        +asjac1D(theta.*delta_t,[],uN,0,'A3100L',[])...
        +asjac1D(theta.*delta_t/Re,[],[],-1,'A211L',[])...
        +asjac1D(betaCoef*theta,[],uN.^2,-1,'A3011L',[])...
        +asjac1D(betaCoef*theta*2,[],uN,-1,'A3110L',uN)...
         +asjac1D(gammaCoef,[],uAvg.^2,-1,'A3011L',[])...
        +asjac1D(gammaCoef,[],uN-u,-1,'A3110L',uAvg)...
         +asjac1D(alpha*delta_t/2,[],uAvg,0,'A3010L',[])...
         +asjac1D(alpha*delta_t/4,[],uN-u,0,'A3010L',[]);

%Apply Dirichlet boundary condition to boundary QL.
for ii=1:1:length(QL)
u_jac0(QL(ii),:) = 0;
u_jac0(:,QL(ii)) = 0;
u_jac0(QL(ii),QL(ii)) = 1;
end

%Apply Dirichlet boundary condition to boundary QL.
for ii=1:1:length(QR)
u_jac0(QR(ii),:) = 0;
u_jac0(:,QR(ii)) = 0;
u_jac0(QR(ii),QR(ii)) = 1;
end
```

```
%***************** Solver ********************************************
uq = u_jac0\(-u_res0);
uN = uN + uq;
if abs(uq) <= eps
   break
end
   iteration = iteration +1;
end %% end of non-linear loop

%************** Solve Iterate ****************************************
u = uN;
time_count = time_count + 1;
u_store(:,time_count) = uN;
time = time + delta_t
iteration
Total_Iter = Total_Iter+iteration;
if time >= max(timePlot)
   break
end
end %end time integration loop
Total_Iter
figure (1)
PPP = ceil(timePlot/delta_t);
PPP(1) = 1;
axes_handle=plot(X1,u_store(:,PPP),'.-')
xlabel('X1','FontSize',12),ylabel('q','FontSize',12)
title(['M=' num2str(M) ', Re=' num2str(Re) ', \alpha=' num2str(alpha) ...
   ', \beta=' num2str(beta) ...
   ', \gamma=' num2str(gamma) ', \theta=' num2str(theta)],'FontSize',12)
legend(num2str(timePlot(1)),num2str(timePlot(2)),num2str(timePlot(3)),...
   num2str(timePlot(4)),num2str(timePlot(5)),num2str(timePlot(6)))
axes_handle = gca;
set(axes_handle,'YGrid','on')
```

Appendix IX

Matlab script for the rotating cone

```
clear all; clc
global X1 X2 elcon;
%********** Geometry **********************************
eltall=32;
elwide=32;
GenRectMesh('32x32.geom',eltall,elwide,-16,16,-16,16);

%Read geometry from file.
fid = fopen('32x32.geom');

var1 = fscanf(fid,'%s',1);
var2 = fscanf(fid,'%s',1);
if( var1 == 'X1')
      size_X1X2 = fscanf(fid,'%i',[1 2]);
      X1X2 = (fscanf(fid,'%f',[size_X1X2(2) size_X1X2(1)]))';
      X1 = X1X2(:,1);
      X2 = X1X2(:,2);
else
fprinf('Error:The domain variable, X1, has not been identified.')
end

var = fscanf(fid,'%s',1);
if( var == 'elcon')
         size_elcon = fscanf(fid,'%i',[1 2]);
         elcon = (fscanf(fid,'%i',[size_elcon(2) size_elcon(1)]))';
else
fprinf('Error:The element connectivity, elcon, has not been identified.')
end

while(~feof(fid))
var = fscanf(fid,'%s',1);
if(strcmp(var,'XL'))
size_bc = fscanf(fid,'%i',1);
XL = (fscanf(fid,'%i',size_bc))';
elseif(strcmp(var,'XR'))
size_bc = fscanf(fid,'%i',1);
XR = (fscanf(fid,'%i',size_bc))';
elseif(strcmp(var,'YT'))
size_bc = fscanf(fid,'%i',1);
YT = (fscanf(fid,'%i',size_bc))';
elseif(strcmp(var,'YB'))
size_bc = fscanf(fid,'%i',1);
YB = (fscanf(fid,'%i',size_bc))';
```

```
elseif(strcmp(var,'BLANK'))
size_blank = fscanf(fid,'%i',1);
BLANK = (fscanf(fid,'%i',size_blank))';
end
end
fclose(fid);
%********** Physical Parameters **********************
%Pa = 0.01;
%uo = sqrt(2);
%vo = -sqrt(2);
walls = 0;
%********** Iteration Parameters **********************
[Xnodes Ynodes] = size(X1);
q0 = zeros(Xnodes.*Ynodes,1);
for ii=1:1:length(XL)
q0(XL(ii)) = +walls;
end
for ii=1:1:length(XR)
q0(XR(ii)) = +walls;
end
for ii=1:1:length(YT)
q0(YT(ii)) = +walls;
end
for ii=1:1:length(YB)
q0(YB(ii)) = +walls;
end

% 3. Extract the node points where the gaussian wave is to be applied
left = 3;
right = 13;
bottom = -5;
top = 5;
count=1;
for ii=1:1:Xnodes*Ynodes
  if X1(ii) > left & X1(ii) < right & X2(ii) > bottom & X2(ii) < top

      ICxy(count,1) = X1(ii);
      ICxy(count,2) = X2(ii);
      %save the indices for mapping back to the original domain
      index(count,1) = ii;
      count = count + 1;
  end
end
```

```
% 4. Normalize the extracted domain to -pi to pi

Xmax = max(ICxy(:,1));
Xmin = min(ICxy(:,1));
Ymax = max(ICxy(:,2));
Ymin = min(ICxy(:,2));
for ii=1:1:length(ICxy(:,1))
      ICxy_norm(ii,1) = (2*pi)*(ICxy(ii,1)-Xmin)/(Xmax-Xmin) - pi;
      ICxy_norm(ii,2) = (2*pi)*(ICxy(ii,2)-Ymin)/(Ymax-Ymin) - pi;
end

% 5. Apply the gaussian IC to this new domain piece

r = sqrt(ICxy_norm(:,1).^2 + ICxy_norm(:,2).^2);
size_r = size(r);
for ii=1:1:size_r(1)
  for jj=1:1:size_r(2)
      if r(ii,jj)>pi
      q_norm(ii,jj) = 0;
      else
      q_norm(ii,jj) = (1 + cos(r(ii,jj)))/2;
      end
  end
end

size(q0)
% 6. Map the new IC values back to the correct domain locations
for ii=1:1:length(index(:,1))
      q0(index(ii,1),1) = q_norm(ii);
end

start = 1;
inc = 1;
stop = 1;
q = q0;
% u=.1*X2; % u and v are approximately 0.45 at the center of the cone
% v=-.1*X1;
u=(.1*X2)*(10/8); % u and v are approximately 0.45 at the center of the cone
v=(-.1*X1)*(10/8);

delta_t = .2992;theta = 0.5;
gamma=-.5;alpha=0;beta=0;
```

```
%unsteady time integration loop.
time_count = 0;

q_last=q0;
for timeLoop = start:inc:stop;
q = q_last;


%********************** Equations for Set 0*****************
res_0 = asres2D_vel(delta_t,[],u,0,'B3001L',q)...
   +asres2D_vel(delta_t,[],v,0,'B3002L',q)...
   +asres2D_vel(beta*delta_t^2/2,[],u.*u,-1,'B3011L',q)...
   +asres2D_vel(beta*delta_t^2/2,[],v.*v,-1,'B3022L',q)...
   +asres2D_vel(beta*delta_t^2/2,[],u.*v,-1,'B3012L',q)...
   +asres2D_vel(beta*delta_t^2/2,[],u.*v,-1,'B3021L',q);

%Apply Dirichlet boundary condition to boundary XL.
for ii=1:1:length(XL)/2
   res_0(XL(ii)) = 0;
end
%Apply Dirichlet boundary condition to boundary YB.
for ii=1:1:length(YB)/2
   res_0(YB(ii)) = 0;
end
%Apply Dirichlet boundary condition to boundary XR.
for ii=ceil((length(XR)/2)):1:length(XR)
   res_0(XR(ii)) = 0;
end
%Apply Dirichlet boundary condition to boundary YT.
for ii=ceil((length(YT)/2)):1:length(YT)
   res_0(YT(ii)) = 0;
end

%****************** Jacobians for Set 0**********
thdelt = theta.*delta_t;
%Equation q by q
jac_0 = +asjac2D_vel(1,[],[],1,'B200L',[])...
   +asjac2D_vel(thdelt,[],u,0,'B3001L',[])...
   +asjac2D_vel(thdelt,[],v,0,'B3002L',[])...
   +asjac2D_vel(gamma*delta_t^2/6,[],u.*u,-1,'B3011L',[])...
   +asjac2D_vel(gamma*delta_t^2/6,[],v.*v,-1,'B3022L',[])...
   +asjac2D_vel(gamma*delta_t^2/6,[],u.*v,-1,'B3012L',[])...
   +asjac2D_vel(gamma*delta_t^2/6,[],u.*v,-1,'B3021L',[])...
```

```
    +asjac2D_vel(theta*beta*delta_t^2/2,[],u.*u,-1,'B3011L',[])...
    +asjac2D_vel(theta*beta*delta_t^2/2,[],v.*v,-1,'B3022L',[])...
    +asjac2D_vel(theta*beta*delta_t^2/2,[],u.*v,-1,'B3012L',[])...
    +asjac2D_vel(theta*beta*delta_t^2/2,[],u.*v,-1,'B3021L',[])...
    +asjac2D_vel(alpha*delta_t/2,[],u,0,'B3010L',[])...
    +asjac2D_vel(alpha*delta_t/2,[],v,0,'B3020L',[]);

% Apply Dirichlet BC to only top half region of XL
for ii=1:1:length(XL)/2
jac_0(XL(ii),:) = 0;
jac_0(:,XL(ii)) = 0;
jac_0(XL(ii),XL(ii)) = 1;
end
%Apply Dirichlet boundary condition to boundary YB.
for ii=1:1:length(YB)/2
jac_0(YB(ii),:) = 0;
jac_0(:,YB(ii)) = 0;
jac_0(YB(ii),YB(ii)) = 1;
end
%Apply Dirichlet boundary condition to boundary XR.
for ii=ceil(length(XR)/2):1:length(XR)
jac_0(XR(ii),:) = 0;
jac_0(:,XR(ii)) = 0;
jac_0(XR(ii),XR(ii)) = 1;
end
%Apply Dirichlet boundary condition to boundary YB.
for ii=ceil(length(YT)/2):1:length(YT)
jac_0(YT(ii),:) = 0;
jac_0(:,YT(ii)) = 0;
jac_0(YT(ii),YT(ii)) = 1;
end
%****************** Solver ******************************************
dq = jac_0\(-res_0);
q = q + dq;
q_last=q;
q_store(:,timeLoop) = q;

time_count = time_count + 1
end %end time integration loop
```

Appendix X

aPSE model and template file for the NS thermal cavity problem

```
##### **** temp.pns **** {PRES} {U1 U2 TEMP PHI} {OMGA} {PSI} {NORMS}
INTEGRATION FACTORS
   INITIAL_TIME
   FINAL_TIME
   PROBLEM_CONVERGENCE_CRITERIA
   MAXIMUM_CHANGE_IN_Q_(DQ)
   INITIAL_TIME_STEP
   TIME_STEP_MULTIPLIER
   MAXIMUM_TIME_STEP
   CRITERIA_TO_RAISE_MAX_TIME_STEP
   MAXIMUM_NUMBER_OF_STEPS
   MAXIMUM_NUMBER_OF_ITERATIONS_PER_STEP
   ITERATION_CONVERGENCE_CRITERIA
   THETA_IMPLICITNESS_FACTOR
   CONVERGENCE_VARIABLE

TRANSFORMATION ARRAYS
      ETKJ      1.
      DETJ      1
#      DETE      0.

BOUNDARY CONDITIONS
          U1 U2 TEMP PHI PRES OMGA PSI    # ORDER
  FLUX     3  0  0  0  0  0  0     # CONVECTION HEAT FLUX
  HFLUX    4  0  0  0  0  0  0     # HEAT FLUX
  RFLUX    5  0  0  0  0  0  0     # RADIATION HEAT FLUX
  HRFLX    6  0  0  0  0  0  0     # RADIATION HEAT FLUX
  INLT_P   3  0  0  0  0  0  0     # INLET
  WALL_SL  4  0  0  0  0  0  0     # SLIP WALL
  DIRI_U   D  0  0  0  0  0  0     # DIRICHLET U
  DIRI_V   0  D  0  0  0  0  0     # DIRICHLET V
  WALL_NS  D  D  0  0  0  0  D     # NO SLIP WALL
  DIRI_T   0  0  D  0  0  0  0     # WALL TEMPERATURE
  DIRI_PHI 0  0  0  D  0  0  0     # THROUGHFLOW PHI
  DIRI_P   0  0  0  0  D  0  0     # THROUGHFLOW PRESSURE
  DIRI_OMG 0  0  0  0  0  D  0     # DIRICHLET OMGA
  DIRI_PSI 0  0  0  0  0  0  D     # DIRICHLET PSI
  BLANK    D  D  D  D  D  D  D     # BLANK REGION

TITLE
   PHI ALGORITHM,  DELSQ PRESSURE SOLVE

RESIDUALS
  PRES   2   #  VARBL, SET NO.,  --- SPATIAL  SET (PRES)
 ()(U1)(EPMN)(11;-1)(B3011)(U1)
+()(U2)(EPMN)(12;-1)(B3011)(U1)
+()(U1)(EPMN)(21;-1)(B3011)(U2)
+()(U2)(EPMN)(22;-1)(B3011)(U2)
+()(U1)(EPMN)(13;-1)(B3012)(U1)
+()(U2)(EPMN)(14;-1)(B3012)(U1)
+()(U1)(EPMN)(23;-1)(B3012)(U2)
+()(U2)(EPMN)(24;-1)(B3012)(U2)
+()(U1)(EPMN)(31;-1)(B3021)(U1)
```

```
+()(U2)(EPMN)(32;-1)(B3021)(U1)
+()(U1)(EPMN)(41;-1)(B3021)(U2)
+()(U2)(EPMN)(42;-1)(B3021)(U2)
+()(U1)(EPMN)(33;-1)(B3022)(U1)
+()(U2)(EPMN)(34;-1)(B3022)(U1)
+()(U1)(EPMN)(43;-1)(B3022)(U2)
+()(U2)(EPMN)(44;-1)(B3022)(U2)
+(-,GRSH,RE2I)()()(2;0)(B210)(TEMP)
+(-,GRSH,RE2I)()()(4;0)(B220)(TEMP)
  PRES   6   #  VARBL, SET NO.,  --- BOUNDARY  SET (PRES)
 (REI)()(EPMN,RET)(0;-1)(A3011)(U1)
#()(U1)(EPMN)(11;-1)(B3011R)(U1)
  PRES   7   #  VARBL, SET NO.,  --- BOUNDARY  SET (PRES)
 (-,REI)()(EPMN,RET)(0;-1)(A3011)(U1)
  PRES   8   #  VARBL, SET NO.,  --- BOUNDARY  SET (PRES)
 (TWO,REI)()(EPMN,RET)(0;0)(A3001)(U1)
  PRES   9   #  VARBL, SET NO.,  --- BOUNDARY  SET (PRES)
 (-,TWO,REI)()(EPMN,RET)(0;0)(A3001)(U1)

JACOBIANS
  PRES PRES  2  1  #  VARBL, VARDIF, SET, ALL DIRECTIONS
 ()()(EPMN)(1122;-1)(B3011)()
+()()(EPMN)(3344;-1)(B3022)()
+()()(EPMN)(1324;-1)(B3021)()
+()()(EPMN)(1324;-1)(B3012)()

GROUP FREQUENCY
     -1
SOLUTION TYPE
  Q
  ILU_GMRES
  IMPLICIT_EULER
END

TITLE
     PHI CONSTRAINT INS GWS ALGORITHM, 2D, FULL NEWTON JACOBIAN
(12/21/99)

RESIDUALS
  U1   1    #  VARBL, SET NO.,  --- TEMPORAL SET (U1)
 ()()()(0;1)(B200)(-U1)
+()()()(1;0)(B201)(PHI)
+()()()(3;0)(B202)(PHI)
+()()()(1;0)(B201)(SPHI)
+()()()(3;0)(B202)(SPHI)
+(GAMA,HP,HP,HALF)()(U1,U1)(11;-1.0)(B3011)(-U1)
+(GAMA,HP,HP,HALF)()(U1,U2)(12;-1.0)(B3011)(-U1)
+(GAMA,HP,HP,HALF)()(U1,U2)(21;-1.0)(B3011)(-U1)
+(GAMA,HP,HP,HALF)()(U2,U2)(22;-1.0)(B3011)(-U1)
+(GAMA,HP,HP,HALF)()(U1,U1)(13;-1.0)(B3012)(-U1)
+(GAMA,HP,HP,HALF)()(U1,U2)(14;-1.0)(B3012)(-U1)
+(GAMA,HP,HP,HALF)()(U1,U2)(23;-1.0)(B3012)(-U1)
+(GAMA,HP,HP,HALF)()(U2,U2)(24;-1.0)(B3012)(-U1)
```

```
+(GAMA,HP,HP,HALF)()(U1,U1)(31;-1.0)(B3021)(-U1)
+(GAMA,HP,HP,HALF)()(U1,U2)(32;-1.0)(B3021)(-U1)
+(GAMA,HP,HP,HALF)()(U1,U2)(41;-1.0)(B3021)(-U1)
+(GAMA,HP,HP,HALF)()(U2,U2)(42;-1.0)(B3021)(-U1)
+(GAMA,HP,HP,HALF)()(U1,U1)(33;-1.0)(B3022)(-U1)
+(GAMA,HP,HP,HALF)()(U1,U2)(34;-1.0)(B3022)(-U1)
+(GAMA,HP,HP,HALF)()(U1,U2)(43;-1.0)(B3022)(-U1)
+(GAMA,HP,HP,HALF)()(U2,U2)(44;-1.0)(B3022)(-U1)
+(GAMA,HP,HP,HALF)()(U1L,U1L)(11;-1.0)(B3011)(-U1)
+(GAMA,HP,HP,HALF)()(U1L,U2L)(12;-1.0)(B3011)(-U1)
+(GAMA,HP,HP,HALF)()(U1L,U2L)(21;-1.0)(B3011)(-U1)
+(GAMA,HP,HP,HALF)()(U2L,U2L)(22;-1.0)(B3011)(-U1)
+(GAMA,HP,HP,HALF)()(U1L,U1L)(13;-1.0)(B3012)(-U1)
+(GAMA,HP,HP,HALF)()(U1L,U2L)(14;-1.0)(B3012)(-U1)
+(GAMA,HP,HP,HALF)()(U1L,U2L)(23;-1.0)(B3012)(-U1)
+(GAMA,HP,HP,HALF)()(U2L,U2L)(24;-1.0)(B3012)(-U1)
+(GAMA,HP,HP,HALF)()(U1L,U1L)(31;-1.0)(B3021)(-U1)
+(GAMA,HP,HP,HALF)()(U1L,U2L)(32;-1.0)(B3021)(-U1)
+(GAMA,HP,HP,HALF)()(U1L,U2L)(41;-1.0)(B3021)(-U1)
+(GAMA,HP,HP,HALF)()(U2L,U2L)(42;-1.0)(B3021)(-U1)
+(GAMA,HP,HP,HALF)()(U1L,U1L)(33;-1.0)(B3022)(-U1)
+(GAMA,HP,HP,HALF)()(U1L,U2L)(34;-1.0)(B3022)(-U1)
+(GAMA,HP,HP,HALF)()(U1L,U2L)(43;-1.0)(B3022)(-U1)
+(GAMA,HP,HP,HALF)()(U2L,U2L)(44;-1.0)(B3022)(-U1)

  U1   2    #  VARBL, SET NO.,  --- SPATIAL  SET (U1)
 ()()(U1+U2)(1020;0)(B3001)(U1)
+()()(U1+U2)(3040;0)(B3002)(U1)
+()()()(1;0)(B201)(PRES)
+()()()(3;0)(B202)(PRES)
+(REI)()()(1122;-1)(B211)(U1)
+(REI)()()(3344;-1)(B222)(U1)
+(REI)()()(1324;-1)(B221)(U1)
+(REI)()()(1324;-1)(B212)(U1)
+(BETA,HT)()(U1,U1)(11;-1.0)(B3011)(U1)
+(BETA,HT)()(U1,U2)(12;-1.0)(B3011)(U1)
+(BETA,HT)()(U1,U2)(21;-1.0)(B3011)(U1)
+(BETA,HT)()(U2,U2)(22;-1.0)(B3011)(U1)
+(BETA,HT)()(U1,U1)(13;-1.0)(B3012)(U1)
+(BETA,HT)()(U1,U2)(14;-1.0)(B3012)(U1)
+(BETA,HT)()(U1,U2)(23;-1.0)(B3012)(U1)
+(BETA,HT)()(U2,U2)(24;-1.0)(B3012)(U1)
+(BETA,HT)()(U1,U1)(31;-1.0)(B3021)(U1)
+(BETA,HT)()(U1,U2)(32;-1.0)(B3021)(U1)
+(BETA,HT)()(U1,U2)(41;-1.0)(B3021)(U1)
+(BETA,HT)()(U2,U2)(42;-1.0)(B3021)(U1)
+(BETA,HT)()(U1,U1)(33;-1.0)(B3022)(U1)
+(BETA,HT)()(U1,U2)(34;-1.0)(B3022)(U1)
+(BETA,HT)()(U1,U2)(43;-1.0)(B3022)(U1)
+(BETA,HT)()(U2,U2)(44;-1.0)(B3022)(U1)

  U2   1    #  VARBL, SET NO.,  --- TEMPORAL SET (U2)
 ()()()(0;1)(B200)(-U2)
```

```
+()()()(2;0)(B201)(PHI)
+()()()(4;0)(B202)(PHI)
+()()()(2;0)(B201)(SPHI)
+()()()(4;0)(B202)(SPHI)
+(GAMA,HP,HP,HALF)()(U1,U1)(11;-1.0)(B3011)(-U2)
+(GAMA,HP,HP,HALF)()(U1,U2)(12;-1.0)(B3011)(-U2)
+(GAMA,HP,HP,HALF)()(U1,U2)(21;-1.0)(B3011)(-U2)
+(GAMA,HP,HP,HALF)()(U2,U2)(22;-1.0)(B3011)(-U2)
+(GAMA,HP,HP,HALF)()(U1,U1)(13;-1.0)(B3012)(-U2)
+(GAMA,HP,HP,HALF)()(U1,U2)(14;-1.0)(B3012)(-U2)
+(GAMA,HP,HP,HALF)()(U1,U2)(23;-1.0)(B3012)(-U2)
+(GAMA,HP,HP,HALF)()(U2,U2)(24;-1.0)(B3012)(-U2)
+(GAMA,HP,HP,HALF)()(U1,U1)(31;-1.0)(B3021)(-U2)
+(GAMA,HP,HP,HALF)()(U1,U2)(32;-1.0)(B3021)(-U2)
+(GAMA,HP,HP,HALF)()(U1,U2)(41;-1.0)(B3021)(-U2)
+(GAMA,HP,HP,HALF)()(U2,U2)(42;-1.0)(B3021)(-U2)
+(GAMA,HP,HP,HALF)()(U1,U1)(33;-1.0)(B3022)(-U2)
+(GAMA,HP,HP,HALF)()(U1,U2)(34;-1.0)(B3022)(-U2)
+(GAMA,HP,HP,HALF)()(U1,U2)(43;-1.0)(B3022)(-U2)
+(GAMA,HP,HP,HALF)()(U2,U2)(44;-1.0)(B3022)(-U2)
+(GAMA,HP,HP,HALF)()(U1L,U1L)(11;-1.0)(B3011)(-U2)
+(GAMA,HP,HP,HALF)()(U1L,U2L)(12;-1.0)(B3011)(-U2)
+(GAMA,HP,HP,HALF)()(U1L,U2L)(21;-1.0)(B3011)(-U2)
+(GAMA,HP,HP,HALF)()(U2L,U2L)(22;-1.0)(B3011)(-U2)
+(GAMA,HP,HP,HALF)()(U1L,U1L)(13;-1.0)(B3012)(-U2)
+(GAMA,HP,HP,HALF)()(U1L,U2L)(14;-1.0)(B3012)(-U2)
+(GAMA,HP,HP,HALF)()(U1L,U2L)(23;-1.0)(B3012)(-U2)
+(GAMA,HP,HP,HALF)()(U2L,U2L)(24;-1.0)(B3012)(-U2)
+(GAMA,HP,HP,HALF)()(U1L,U1L)(31;-1.0)(B3021)(-U2)
+(GAMA,HP,HP,HALF)()(U1L,U2L)(32;-1.0)(B3021)(-U2)
+(GAMA,HP,HP,HALF)()(U1L,U2L)(41;-1.0)(B3021)(-U2)
+(GAMA,HP,HP,HALF)()(U2L,U2L)(42;-1.0)(B3021)(-U2)
+(GAMA,HP,HP,HALF)()(U1L,U1L)(33;-1.0)(B3022)(-U2)
+(GAMA,HP,HP,HALF)()(U1L,U2L)(34;-1.0)(B3022)(-U2)
+(GAMA,HP,HP,HALF)()(U1L,U2L)(43;-1.0)(B3022)(-U2)
+(GAMA,HP,HP,HALF)()(U2L,U2L)(44;-1.0)(B3022)(-U2)

  U2   2   #  VARBL, SET NO.,  --- SPATIAL  SET (U2)
 ()()(U1+U2)(1020;0)(B3001)(U2)
+()()(U1+U2)(3040;0)(B3002)(U2)
+()()()(2;0)(B201)(PRES)
+()()()(4;0)(B202)(PRES)
+(REI)()()(1122;-1)(B211)(U2)
+(REI)()()(3344;-1)(B222)(U2)
+(REI)()()(1324;-1)(B221)(U2)
+(REI)()()(1324;-1)(B212)(U2)
+(BETA,HT)()(U1,U1)(11;-1.0)(B3011)(U2)
+(BETA,HT)()(U1,U2)(12;-1.0)(B3011)(U2)
+(BETA,HT)()(U1,U2)(21;-1.0)(B3011)(U2)
+(BETA,HT)()(U2,U2)(22;-1.0)(B3011)(U2)
+(BETA,HT)()(U1,U1)(13;-1.0)(B3012)(U2)
+(BETA,HT)()(U1,U2)(14;-1.0)(B3012)(U2)
+(BETA,HT)()(U1,U2)(23;-1.0)(B3012)(U2)
```

```
+(BETA,HT)()(U2,U2)(24;-1.0)(B3012)(U2)
+(BETA,HT)()(U1,U1)(31;-1.0)(B3021)(U2)
+(BETA,HT)()(U1,U2)(32;-1.0)(B3021)(U2)
+(BETA,HT)()(U1,U2)(41;-1.0)(B3021)(U2)
+(BETA,HT)()(U2,U2)(42;-1.0)(B3021)(U2)
+(BETA,HT)()(U1,U1)(33;-1.0)(B3022)(U2)
+(BETA,HT)()(U1,U2)(34;-1.0)(B3022)(U2)
+(BETA,HT)()(U1,U2)(43;-1.0)(B3022)(U2)
+(BETA,HT)()(U2,U2)(44;-1.0)(B3022)(U2)
+(-,GRSH,RE2I)()()(0;1)(B200)(TEMP)

  TEMP   1    #  VARBL, SET NO.,  --- TEMPORAL SET (TEMP)
 ()()()(0;1)(B200)(-TEMP)
+(GAMA,HP,HP,HALF)()(U1,U1)(11;-1.0)(B3011)(-TEMP)
+(GAMA,HP,HP,HALF)()(U1,U2)(12;-1.0)(B3011)(-TEMP)
+(GAMA,HP,HP,HALF)()(U1,U2)(21;-1.0)(B3011)(-TEMP)
+(GAMA,HP,HP,HALF)()(U2,U2)(22;-1.0)(B3011)(-TEMP)
+(GAMA,HP,HP,HALF)()(U1,U1)(13;-1.0)(B3012)(-TEMP)
+(GAMA,HP,HP,HALF)()(U1,U2)(14;-1.0)(B3012)(-TEMP)
+(GAMA,HP,HP,HALF)()(U1,U2)(23;-1.0)(B3012)(-TEMP)
+(GAMA,HP,HP,HALF)()(U2,U2)(24;-1.0)(B3012)(-TEMP)
+(GAMA,HP,HP,HALF)()(U1,U1)(31;-1.0)(B3021)(-TEMP)
+(GAMA,HP,HP,HALF)()(U1,U2)(32;-1.0)(B3021)(-TEMP)
+(GAMA,HP,HP,HALF)()(U1,U2)(41;-1.0)(B3021)(-TEMP)
+(GAMA,HP,HP,HALF)()(U2,U2)(42;-1.0)(B3021)(-TEMP)
+(GAMA,HP,HP,HALF)()(U1,U1)(33;-1.0)(B3022)(-TEMP)
+(GAMA,HP,HP,HALF)()(U1,U2)(34;-1.0)(B3022)(-TEMP)
+(GAMA,HP,HP,HALF)()(U1,U2)(43;-1.0)(B3022)(-TEMP)
+(GAMA,HP,HP,HALF)()(U2,U2)(44;-1.0)(B3022)(-TEMP)
+(GAMA,HP,HP,HALF)()(U1L,U1L)(11;-1.0)(B3011)(-TEMP)
+(GAMA,HP,HP,HALF)()(U1L,U2L)(12;-1.0)(B3011)(-TEMP)
+(GAMA,HP,HP,HALF)()(U1L,U2L)(21;-1.0)(B3011)(-TEMP)
+(GAMA,HP,HP,HALF)()(U2L,U2L)(22;-1.0)(B3011)(-TEMP)
+(GAMA,HP,HP,HALF)()(U1L,U1L)(13;-1.0)(B3012)(-TEMP)
+(GAMA,HP,HP,HALF)()(U1L,U2L)(14;-1.0)(B3012)(-TEMP)
+(GAMA,HP,HP,HALF)()(U1L,U2L)(23;-1.0)(B3012)(-TEMP)
+(GAMA,HP,HP,HALF)()(U2L,U2L)(24;-1.0)(B3012)(-TEMP)
+(GAMA,HP,HP,HALF)()(U1L,U1L)(31;-1.0)(B3021)(-TEMP)
+(GAMA,HP,HP,HALF)()(U1L,U2L)(32;-1.0)(B3021)(-TEMP)
+(GAMA,HP,HP,HALF)()(U1L,U2L)(41;-1.0)(B3021)(-TEMP)
+(GAMA,HP,HP,HALF)()(U2L,U2L)(42;-1.0)(B3021)(-TEMP)
+(GAMA,HP,HP,HALF)()(U1L,U1L)(33;-1.0)(B3022)(-TEMP)
+(GAMA,HP,HP,HALF)()(U1L,U2L)(34;-1.0)(B3022)(-TEMP)
+(GAMA,HP,HP,HALF)()(U1L,U2L)(43;-1.0)(B3022)(-TEMP)
+(GAMA,HP,HP,HALF)()(U2L,U2L)(44;-1.0)(B3022)(-TEMP)

  TEMP   2   #  VARBL, SET NO.,  --- SPATIAL  SET (TEMP)
 ()()(U1+U2)(1020;0)(B3001)(TEMP)
+()()(U1+U2)(3040;0)(B3002)(TEMP)
+(PEI)()()(1122;-1)(B211)(TEMP)
+(PEI)()()(3344;-1)(B222)(TEMP)
+(PEI)()()(1324;-1)(B221)(TEMP)
+(PEI)()()(1324;-1)(B212)(TEMP)
```

```
#+(-)()()(0;1)(B200)(SRCT)
+(BETAT,HT)()(U1,U1)(11;-1.0)(B3011)(TEMP)
+(BETAT,HT)()(U1,U2)(12;-1.0)(B3011)(TEMP)
+(BETAT,HT)()(U1,U2)(21;-1.0)(B3011)(TEMP)
+(BETAT,HT)()(U2,U2)(22;-1.0)(B3011)(TEMP)
+(BETAT,HT)()(U1,U1)(13;-1.0)(B3012)(TEMP)
+(BETAT,HT)()(U1,U2)(14;-1.0)(B3012)(TEMP)
+(BETAT,HT)()(U1,U2)(23;-1.0)(B3012)(TEMP)
+(BETAT,HT)()(U2,U2)(24;-1.0)(B3012)(TEMP)
+(BETAT,HT)()(U1,U1)(31;-1.0)(B3021)(TEMP)
+(BETAT,HT)()(U1,U2)(32;-1.0)(B3021)(TEMP)
+(BETAT,HT)()(U1,U2)(41;-1.0)(B3021)(TEMP)
+(BETAT,HT)()(U2,U2)(42;-1.0)(B3021)(TEMP)
+(BETAT,HT)()(U1,U1)(33;-1.0)(B3022)(TEMP)
+(BETAT,HT)()(U1,U2)(34;-1.0)(B3022)(TEMP)
+(BETAT,HT)()(U1,U2)(43;-1.0)(B3022)(TEMP)
+(BETAT,HT)()(U2,U2)(44;-1.0)(B3022)(TEMP)
  TEMP   3   #  VARBL, SET NO.,  --- BOUNDARY SET (TEMP)
 ()(NUSL)()(0;1)(A200)(TEMP)
+(-)(NUSL)()(0;1)(A200)(TRBC)
  TEMP   5   #  VARBL, SET NO.,  --- BOUNDARY SET (TEMP)
 ()()()(0;1)(A200)(SRCT)

  PHI   1     #  VARBL, SET NO.,  --- SPATIAL  SET (PHI)
 ()()(EPMN)(1;0)(B3001)(U1)
+()()(EPMN)(3;0)(B3002)(U1)
+()()(EPMN)(2;0)(B3001)(U2)
+()()(EPMN)(4;0)(B3002)(U2)
+()()(EPMN)(1122;-1)(B3011)(PHI)
+()()(EPMN)(3344;-1)(B3022)(PHI)
+()()(EPMN)(1324;-1)(B3021)(PHI)
+()()(EPMN)(1324;-1)(B3012)(PHI)

  PHI   3  #  VARBL, SET NO.,-- BOUNDARY SET (PHI)
 (-)()()(1;0)(A200)(U1)
+()()()(2;0)(A200)(U2)

JACOBIANS
  U1  U1  1  1  #  VARBL, VARDIF, SET, DIRECTION 1
 ()()()(;1)(B200)()
+(GAMA,HP,HP,HALF)()(U1,U1)(11;-1.0)(B3011)()
+(GAMA,HP,HP,HALF)()(U1,U2)(12;-1.0)(B3011)()
+(GAMA,HP,HP,HALF)()(U1,U2)(21;-1.0)(B3011)()
+(GAMA,HP,HP,HALF)()(U2,U2)(22;-1.0)(B3011)()
+(GAMA,HP,HP,HALF)()(U1,U1)(13;-1.0)(B3012)()
+(GAMA,HP,HP,HALF)()(U1,U2)(14;-1.0)(B3012)()
+(GAMA,HP,HP,HALF)()(U1,U2)(23;-1.0)(B3012)()
+(GAMA,HP,HP,HALF)()(U2,U2)(24;-1.0)(B3012)()
+(GAMA,HP,HP,HALF)()(U1,U1)(31;-1.0)(B3021)()
+(GAMA,HP,HP,HALF)()(U1,U2)(32;-1.0)(B3021)()
+(GAMA,HP,HP,HALF)()(U1,U2)(41;-1.0)(B3021)()
+(GAMA,HP,HP,HALF)()(U2,U2)(42;-1.0)(B3021)()
+(GAMA,HP,HP,HALF)()(U1,U1)(33;-1.0)(B3022)()
```

```
+(GAMA,HP,HP,HALF)()(U1,U2)(34;-1.0)(B3022)()
+(GAMA,HP,HP,HALF)()(U1,U2)(43;-1.0)(B3022)()
+(GAMA,HP,HP,HALF)()(U2,U2)(44;-1.0)(B3022)()
+(GAMA,HP,HP,HALF)()(U1L,U1L)(11;-1.0)(B3011)()
+(GAMA,HP,HP,HALF)()(U1L,U2L)(12;-1.0)(B3011)()
+(GAMA,HP,HP,HALF)()(U1L,U2L)(21;-1.0)(B3011)()
+(GAMA,HP,HP,HALF)()(U2L,U2L)(22;-1.0)(B3011)()
+(GAMA,HP,HP,HALF)()(U1L,U1L)(13;-1.0)(B3012)()
+(GAMA,HP,HP,HALF)()(U1L,U2L)(14;-1.0)(B3012)()
+(GAMA,HP,HP,HALF)()(U1L,U2L)(23;-1.0)(B3012)()
+(GAMA,HP,HP,HALF)()(U2L,U2L)(24;-1.0)(B3012)()
+(GAMA,HP,HP,HALF)()(U1L,U1L)(31;-1.0)(B3021)()
+(GAMA,HP,HP,HALF)()(U1L,U2L)(32;-1.0)(B3021)()
+(GAMA,HP,HP,HALF)()(U1L,U2L)(41;-1.0)(B3021)()
+(GAMA,HP,HP,HALF)()(U2L,U2L)(42;-1.0)(B3021)()
+(GAMA,HP,HP,HALF)()(U1L,U1L)(33;-1.0)(B3022)()
+(GAMA,HP,HP,HALF)()(U1L,U2L)(34;-1.0)(B3022)()
+(GAMA,HP,HP,HALF)()(U1L,U2L)(43;-1.0)(B3022)()
+(GAMA,HP,HP,HALF)()(U2L,U2L)(44;-1.0)(B3022)()

  U1  U1  2  1  #  VARBL, VARDIF, SET, DIRECTION 1
+()()(U1+U2)(1020;0)(B3001)()
+()()(U1+U2)(3040;0)(B3002)()
+()()(U1)(1;0)(B3100)()
+()()(U1)(3;0)(B3200)()
+(REI)()()(1122;-1)(B211)()
+(REI)()()(1324;-1)(B212)()
+(REI)()()(1324;-1)(B221)()
+(REI)()()(3344;-1)(B222)()
+(BETA,HT)()(U1,U1)(11;-1.0)(B3011)()
+(BETA,HT)()(U1,U2)(12;-1.0)(B3011)()
+(BETA,HT)()(U1,U2)(21;-1.0)(B3011)()
+(BETA,HT)()(U2,U2)(22;-1.0)(B3011)()
+(BETA,HT)()(U1,U1)(13;-1.0)(B3012)()
+(BETA,HT)()(U1,U2)(14;-1.0)(B3012)()
+(BETA,HT)()(U1,U2)(23;-1.0)(B3012)()
+(BETA,HT)()(U2,U2)(24;-1.0)(B3012)()
+(BETA,HT)()(U1,U1)(31;-1.0)(B3021)()
+(BETA,HT)()(U1,U2)(32;-1.0)(B3021)()
+(BETA,HT)()(U1,U2)(41;-1.0)(B3021)()
+(BETA,HT)()(U2,U2)(42;-1.0)(B3021)()
+(BETA,HT)()(U1,U1)(33;-1.0)(B3022)()
+(BETA,HT)()(U1,U2)(34;-1.0)(B3022)()
+(BETA,HT)()(U1,U2)(43;-1.0)(B3022)()
+(BETA,HT)()(U2,U2)(44;-1.0)(B3022)()

  U1  U2  2  1  #
 ()()(U1)(2;0)(B3100)()
+()()(U1)(4;0)(B3200)()

   U1  PHI 1 1 #
 ()()()(1;0)(B201)()
+()()()(3;0)(B202)()
```

```
  U2  U1  2  1  #
 ()()(U2)(1;0)(B3100)()
+()()(U2)(3;0)(B3200)()

  U2  U2  1  1  #
 ()()()(;1)(B200)()
+(GAMA,HP,HP,HALF)()(U1,U1)(11;-1.0)(B3011)()
+(GAMA,HP,HP,HALF)()(U1,U2)(12;-1.0)(B3011)()
+(GAMA,HP,HP,HALF)()(U1,U2)(21;-1.0)(B3011)()
+(GAMA,HP,HP,HALF)()(U2,U2)(22;-1.0)(B3011)()
+(GAMA,HP,HP,HALF)()(U1,U1)(13;-1.0)(B3012)()
+(GAMA,HP,HP,HALF)()(U1,U2)(14;-1.0)(B3012)()
+(GAMA,HP,HP,HALF)()(U1,U2)(23;-1.0)(B3012)()
+(GAMA,HP,HP,HALF)()(U2,U2)(24;-1.0)(B3012)()
+(GAMA,HP,HP,HALF)()(U1,U1)(31;-1.0)(B3021)()
+(GAMA,HP,HP,HALF)()(U1,U2)(32;-1.0)(B3021)()
+(GAMA,HP,HP,HALF)()(U1,U2)(41;-1.0)(B3021)()
+(GAMA,HP,HP,HALF)()(U2,U2)(42;-1.0)(B3021)()
+(GAMA,HP,HP,HALF)()(U1,U1)(33;-1.0)(B3022)()
+(GAMA,HP,HP,HALF)()(U1,U2)(34;-1.0)(B3022)()
+(GAMA,HP,HP,HALF)()(U1,U2)(43;-1.0)(B3022)()
+(GAMA,HP,HP,HALF)()(U2,U2)(44;-1.0)(B3022)()
+(GAMA,HP,HP,HALF)()(U1L,U1L)(11;-1.0)(B3011)()
+(GAMA,HP,HP,HALF)()(U1L,U2L)(12;-1.0)(B3011)()
+(GAMA,HP,HP,HALF)()(U1L,U2L)(21;-1.0)(B3011)()
+(GAMA,HP,HP,HALF)()(U2L,U2L)(22;-1.0)(B3011)()
+(GAMA,HP,HP,HALF)()(U1L,U1L)(13;-1.0)(B3012)()
+(GAMA,HP,HP,HALF)()(U1L,U2L)(14;-1.0)(B3012)()
+(GAMA,HP,HP,HALF)()(U1L,U2L)(23;-1.0)(B3012)()
+(GAMA,HP,HP,HALF)()(U2L,U2L)(24;-1.0)(B3012)()
+(GAMA,HP,HP,HALF)()(U1L,U1L)(31;-1.0)(B3021)()
+(GAMA,HP,HP,HALF)()(U1L,U2L)(32;-1.0)(B3021)()
+(GAMA,HP,HP,HALF)()(U1L,U2L)(41;-1.0)(B3021)()
+(GAMA,HP,HP,HALF)()(U2L,U2L)(42;-1.0)(B3021)()
+(GAMA,HP,HP,HALF)()(U1L,U1L)(33;-1.0)(B3022)()
+(GAMA,HP,HP,HALF)()(U1L,U2L)(34;-1.0)(B3022)()
+(GAMA,HP,HP,HALF)()(U1L,U2L)(43;-1.0)(B3022)()
+(GAMA,HP,HP,HALF)()(U2L,U2L)(44;-1.0)(B3022)()

  U2  U2  2  1  #
+()()(U1+U2)(1020;0)(B3001)()
+()()(U1+U2)(3040;0)(B3002)()
+()()(U2)(2;0)(B3100)()
+()()(U2)(4;0)(B3200)()
+(REI)()()(1122;-1)(B211)()
+(REI)()()(1324;-1)(B212)()
+(REI)()()(1324;-1)(B221)()
+(REI)()()(3344;-1)(B222)()
+(BETA,HT)()(U1,U1)(11;-1.0)(B3011)()
+(BETA,HT)()(U1,U2)(12;-1.0)(B3011)()
+(BETA,HT)()(U1,U2)(21;-1.0)(B3011)()
+(BETA,HT)()(U2,U2)(22;-1.0)(B3011)()
```

```
+(BETA,HT)()(U1,U1)(13;-1.0)(B3012)()
+(BETA,HT)()(U1,U2)(14;-1.0)(B3012)()
+(BETA,HT)()(U1,U2)(23;-1.0)(B3012)()
+(BETA,HT)()(U2,U2)(24;-1.0)(B3012)()
+(BETA,HT)()(U1,U1)(31;-1.0)(B3021)()
+(BETA,HT)()(U1,U2)(32;-1.0)(B3021)()
+(BETA,HT)()(U1,U2)(41;-1.0)(B3021)()
+(BETA,HT)()(U2,U2)(42;-1.0)(B3021)()
+(BETA,HT)()(U1,U1)(33;-1.0)(B3022)()
+(BETA,HT)()(U1,U2)(34;-1.0)(B3022)()
+(BETA,HT)()(U1,U2)(43;-1.0)(B3022)()
+(BETA,HT)()(U2,U2)(44;-1.0)(B3022)()


  U2 TEMP 2  1 #
+(-,GRSH,RE2I)()()(;1)(B200)()

   U2  PHI  1 1 #
 ()()()(2;0)(B201)()
+()()()(4;0)(B202)()

 TEMP U1 2 1 #
()()(TEMP)(1;0)(B3100)()+()()(TEMP)(3;0)(B3200)()

 TEMP U2 2 1 #
()()(TEMP)(2;0)(B3100)()+()()(TEMP)(4;0)(B3200)()

  TEMP TEMP 1  1     #
 ()()()(0;1)(B200)()
 +(GAMA,HP,HP,HALF)()(U1,U1)(11;-1.0)(B3011)()
+(GAMA,HP,HP,HALF)()(U1,U2)(12;-1.0)(B3011)()
+(GAMA,HP,HP,HALF)()(U1,U2)(21;-1.0)(B3011)()
+(GAMA,HP,HP,HALF)()(U2,U2)(22;-1.0)(B3011)()
+(GAMA,HP,HP,HALF)()(U1,U1)(13;-1.0)(B3012)()
+(GAMA,HP,HP,HALF)()(U1,U2)(14;-1.0)(B3012)()
+(GAMA,HP,HP,HALF)()(U1,U2)(23;-1.0)(B3012)()
+(GAMA,HP,HP,HALF)()(U2,U2)(24;-1.0)(B3012)()
+(GAMA,HP,HP,HALF)()(U1,U1)(31;-1.0)(B3021)()
+(GAMA,HP,HP,HALF)()(U1,U2)(32;-1.0)(B3021)()
+(GAMA,HP,HP,HALF)()(U1,U2)(41;-1.0)(B3021)()
+(GAMA,HP,HP,HALF)()(U2,U2)(42;-1.0)(B3021)()
+(GAMA,HP,HP,HALF)()(U1,U1)(33;-1.0)(B3022)()
+(GAMA,HP,HP,HALF)()(U1,U2)(34;-1.0)(B3022)()
+(GAMA,HP,HP,HALF)()(U1,U2)(43;-1.0)(B3022)()
+(GAMA,HP,HP,HALF)()(U2,U2)(44;-1.0)(B3022)()
+(GAMA,HP,HP,HALF)()(U1L,U1L)(11;-1.0)(B3011)()
+(GAMA,HP,HP,HALF)()(U1L,U2L)(12;-1.0)(B3011)()
+(GAMA,HP,HP,HALF)()(U1L,U2L)(21;-1.0)(B3011)()
+(GAMA,HP,HP,HALF)()(U2L,U2L)(22;-1.0)(B3011)()
+(GAMA,HP,HP,HALF)()(U1L,U1L)(13;-1.0)(B3012)()
+(GAMA,HP,HP,HALF)()(U1L,U2L)(14;-1.0)(B3012)()
+(GAMA,HP,HP,HALF)()(U1L,U2L)(23;-1.0)(B3012)()
+(GAMA,HP,HP,HALF)()(U2L,U2L)(24;-1.0)(B3012)()
```

```
+(GAMA,HP,HP,HALF)()(U1L,U1L)(31;-1.0)(B3021)()
+(GAMA,HP,HP,HALF)()(U1L,U2L)(32;-1.0)(B3021)()
+(GAMA,HP,HP,HALF)()(U1L,U2L)(41;-1.0)(B3021)()
+(GAMA,HP,HP,HALF)()(U2L,U2L)(42;-1.0)(B3021)()
+(GAMA,HP,HP,HALF)()(U1L,U1L)(33;-1.0)(B3022)()
+(GAMA,HP,HP,HALF)()(U1L,U2L)(34;-1.0)(B3022)()
+(GAMA,HP,HP,HALF)()(U1L,U2L)(43;-1.0)(B3022)()
+(GAMA,HP,HP,HALF)()(U2L,U2L)(44;-1.0)(B3022)()

  TEMP TEMP 2  1    #
+()()(U1+U2)(1020;0)(B3001)()
+()()(U1+U2)(3040;0)(B3002)()
+(PEI)()()(1122;-1)(B3011)()
+(PEI)()()(3344;-1)(B3022)()
+(PEI)()()(1324;-1)(B3021)()
+(PEI)()()(1324;-1)(B3012)()
+(BETAT,HT)()(U1,U1)(11;-1.0)(B3011)()
+(BETAT,HT)()(U1,U2)(12;-1.0)(B3011)()
+(BETAT,HT)()(U1,U2)(21;-1.0)(B3011)()
+(BETAT,HT)()(U2,U2)(22;-1.0)(B3011)()
+(BETAT,HT)()(U1,U1)(13;-1.0)(B3012)()
+(BETAT,HT)()(U1,U2)(14;-1.0)(B3012)()
+(BETAT,HT)()(U1,U2)(23;-1.0)(B3012)()
+(BETAT,HT)()(U2,U2)(24;-1.0)(B3012)()
+(BETAT,HT)()(U1,U1)(31;-1.0)(B3021)()
+(BETAT,HT)()(U1,U2)(32;-1.0)(B3021)()
+(BETAT,HT)()(U1,U2)(41;-1.0)(B3021)()
+(BETAT,HT)()(U2,U2)(42;-1.0)(B3021)()
+(BETAT,HT)()(U1,U1)(33;-1.0)(B3022)()
+(BETAT,HT)()(U1,U2)(34;-1.0)(B3022)()
+(BETAT,HT)()(U1,U2)(43;-1.0)(B3022)()
+(BETAT,HT)()(U2,U2)(44;-1.0)(B3022)()
 TEMP TEMP 3  1 #
 ()(NUSL)()(0;1)(A200)()

  PHI U1  1 1 #
 ()()(EPMN)(1;0)(B3001)()
+()()(EPMN)(3;0)(B3002)()
  PHI U1  3 1 #
 (-)()()(1;0)(A200)()

  PHI U2 1 1 #
 ()()(EPMN)(2;0)(B3001)()
+()()(EPMN)(4;0)(B3002)()
  PHI U2 3 1 #
 ()()()(2;0)(A200)()

  PHI PHI  1  1  #  VARBL, VARDIF, SET, ALL DIRECTIONS
 ()()(EPMN)(1122;-1)(B3011)()
+()()(EPMN)(3344;-1)(B3022)()
+()()(EPMN)(1324;-1)(B3021)()
+()()(EPMN)(1324;-1)(B3012)()
```

```
GROUP FREQUENCY
      1
SOLUTION TYPE
  DELTA_Q
  ILU_GMRES
  IMPLICIT_EULER
END


TITLE            **** TEMPLATE FILE FFij ****
  2-D  PHI ALGORITHM  RETA  (12/05)

RESIDUALS
  RETA  2  # LOAD SET -{B} FOR RETA
+(-,MULA)()()(0;2.5)(B200)(SSQ2)

JACOBIANS
  RETA  RETA  2  1  # RETA: D(RETA)/D(RETA)
+()()()(0;1)(B200)()

GROUP FREQUENCY
    1
SOLUTION TYPE
  Q
  ILU_GMRES
  IMPLICIT_EULER
END

TITLE            **** TEMPLATE FILE FFij ****
  2-D  PHI ALGORITHM  RETB  (12/05)

RESIDUALS
  RETB  2  # LOAD SET -{B} FOR RETB
+(-,MULB)()()(0;1.5)(B200)(SBQ2)

JACOBIANS
  RETB  RETB  2  1  # RETB: D(RETB)/D(RETB)
+()()()(0;1)(B200)()

GROUP FREQUENCY
    1
SOLUTION TYPE
  Q
  ILU_GMRES
  IMPLICIT_EULER
END

TITLE            **** TEMPLATE FILE FFij ****
  2-D  PHI ALGORITHM  Xij  (12/05)

RESIDUALS
  X11  2  # LOAD SET -{B} FOR X_11
+(-)()(U1)(1122;-1)(B3101)(U1)
```

```
+(-)()(U1)(1324;-1)(B3102)(U1)
+(-)()(U1)(2142;-1)(B3201)(U1)
+(-)()(U1)(3344;-1)(B3202)(U1)

  X12  2  # LOAD SET -{B} FOR X_12
+(-)()(U1)(1122;-1)(B3101)(U2)
+(-)()(U1)(1323;-1)(B3102)(U2)
+(-)()(U1)(3142;-1)(B3201)(U2)
+(-)()(U1)(3344;-1)(B3202)(U2)

  X22  2  # LOAD SET -{B} FOR X_22
+(-)()(U2)(1122;-1)(B3101)(U2)
+(-)()(U2)(1324;-1)(B3102)(U2)
+(-)()(U2)(3142;-1)(B3201)(U2)
+(-)()(U2)(3344;-1)(B3202)(U2)

JACOBIANS
  X11  X11  2  1  # X_11: D(X_11)/D(X_11)
+()()()(0;1)(B200)()
+(SIXTH)()()(1122;0)(B211)()
+(SIXTH)()()(1324;0)(B212)()
+(SIXTH)()()(3142;0)(B221)()
+(SIXTH)()()(3344;0)(B222)()

  X12  X12  2  1  # X_12: D(X_12)/D(X_12)
+()()()(0;1)(B200)()
+(SIXTH)()()(1122;0)(B211)()
+(SIXTH)()()(1324;0)(B212)()
+(SIXTH)()()(3142;0)(B221)()
+(SIXTH)()()(3344;0)(B222)()

  X22  X22  2  1  # X_22: D(X_22)/D(X_22)
+()()()(0;1)(B200)()
+(SIXTH)()()(1122;0)(B211)()
+(SIXTH)()()(1324;0)(B212)()
+(SIXTH)()()(3142;0)(B221)()
+(SIXTH)()()(3344;0)(B222)()

GROUP FREQUENCY
    1
SOLUTION TYPE
  Q
  ILU_GMRES
  IMPLICIT_EULER
END

TITLE            **** TEMPLATE FILE FFij ****
  2-D  PHI ALGORITHM  filter flux  (12/05)

RESIDUALS
  FF11  2  # LOAD SET -{B} FOR FF11
+(THIRD)()()(0;2)(B200)(X11)
```

```
  FF12  2  # LOAD SET -{B} FOR FF12
+(THIRD)()()(0;2)(B200)(X12)

  FF22  2  # LOAD SET -{B} FOR FF22
+(THIRD)()()(0;2)(B200)(X22)

JACOBIANS
  FF11  FF11  2  1  # FF11: D(FF11)/D(FF11)
 ()()()(0;1)(B200)()

  FF12  FF12  2  1  # FF12: D(FF12)/D(FF12)
 ()()()(0;1)(B200)()

  FF22  FF22  2  1  # FF22: D(FF22)/D(FF22)
 ()()()(0;1)(B200)()

GROUP FREQUENCY
    1
SOLUTION TYPE
  Q
  ILU_GMRES
  IMPLICIT_EULER
END

TITLE            **** TEMPLATE FILE FBij ****
  2-D  PHI ALGORITHM   TWS FLUXES  (12/05)

RESIDUALS
  FB11  2  # LOAD SET -{B} FOR FB_11
+(-,HALF,HT)()(U1,U1)(1;0)(B3001)(U1)
+(-,HALF,HT)()(U1,U1)(3;0)(B3002)(U1)
+(-,FOURTH,HT)()(U1,U2)(2;0)(B3001)(U1)
+(-,FOURTH,HT)()(U1,U2)(4;0)(B3002)(U1)
+(-,FOURTH,HT)()(U1,U2)(1;0)(B3001)(U2)
+(-,FOURTH,HT)()(U1,U2)(3;0)(B3002)(U2)

  FB12  2  # LOAD SET -{B} FOR FB_12
+(-,HALF,HT)()(U1,U2)(1;0)(B3001)(U1)
+(-,HALF,HT)()(U1,U2)(3;0)(B3002)(U1)
+(-,FOURTH,HT)()(U2,U2)(2;0)(B3001)(U1)
+(-,FOURTH,HT)()(U2,U2)(4;0)(B3002)(U1)
+(-,FOURTH,HT)()(U2,U2)(1;0)(B3001)(U2)
+(-,FOURTH,HT)()(U2,U2)(3;0)(B3002)(U2)

  FB21  2  # LOAD SET -{B} FOR FB_21
+(-,FOURTH,HT)()(U1,U1)(2;0)(B3001)(U1)
+(-,FOURTH,HT)()(U1,U1)(4;0)(B3002)(U1)
+(-,FOURTH,HT)()(U1,U1)(1;0)(B3001)(U2)
+(-,FOURTH,HT)()(U1,U1)(3;0)(B3002)(U2)
+(-,HALF,HT)()(U1,U2)(2;0)(B3001)(U2)
+(-,HALF,HT)()(U1,U2)(4;0)(B3002)(U2)

  FB22  2  # LOAD SET -{B} FOR FB_22
```

```
+(-,FOURTH,HT)()(U1,U2)(2;0)(B3001)(U1)
+(-,FOURTH,HT)()(U1,U2)(4;0)(B3002)(U1)
+(-,FOURTH,HT)()(U1,U2)(1;0)(B3001)(U2)
+(-,FOURTH,HT)()(U1,U2)(3;0)(B3002)(U2)
+(-,HALF,HT)()(U2,U2)(2;0)(B3001)(U2)
+(-,HALF,HT)()(U2,U2)(4;0)(B3002)(U2)

JACOBIANS
  FB11  FB11  2  1  # FB_11: D(FB_11)/D(FB_11)
 ()()()(0;1)(B200)()

  FB21  FB21  2  1  # FB_21: D(FB_21)/D(FB_21)
 ()()()(0;1)(B200)()

  FB12  FB12  2  1  # FB_12: D(FB_12)/D(FB_12)
 ()()()(0;1)(B200)()

  FB22  FB22  2  1  # FB_22: D(FB_22)/D(FB_22)
 ()()()(0;1)(B200)()

GROUP FREQUENCY
    1
SOLUTION TYPE
  Q
  ILU_GMRES
  IMPLICIT_EULER
END

TITLE            **** TEMPLATE FILE FDij ****
  2-D  PHI ALGORITHM  laminar diffusion flux  (12/05)

RESIDUALS
  FD11  2  # LOAD SET -{B} FOR FD11
+(-,TWO,REI)()()(1;0)(B201)(U1)
+(-,TWO,REI)()()(3;0)(B202)(U1)

  FD12  2  # LOAD SET -{B} FOR FD12
+(-,REI)()()(2;0)(B201)(U1)
+(-,REI)()()(4;0)(B202)(U1)
+(-,REI)()()(1;0)(B201)(U2)
+(-,REI)()()(3;0)(B202)(U2)

  FD22  2  # LOAD SET -{B} FOR FD22
+(-,TWO,REI)()()(2;0)(B201)(U2)
+(-,TWO,REI)()()(4;0)(B202)(U2)

JACOBIANS
  FD11  FD11  2  1  # FD11: D(FD11)/D(FD11)
 ()()()(0;1)(B200)()

  FD12  FD12  2  1  # FD12: D(FD12)/D(FD12)
 ()()()(0;1)(B200)()
```

```
  FD22  FD22  2  1  # FD22: D(FD22)/D(FD22)
 ()()()(0;1)(B200)()

GROUP FREQUENCY
    1
SOLUTION TYPE
  Q
  ILU_GMRES
  IMPLICIT_EULER
END

TITLE            **** TEMPLATE FILE FCij ****
  2-D  PHI ALGORITHM  convective flux  (12/05)

RESIDUALS
  FC11  2  # LOAD SET -{B} FOR FC11
+(-)()(U1)(0;1)(B200)(U1)

  FC12  2  # LOAD SET -{B} FOR FC12
+(-)()(U2)(0;1)(B200)(U1)

  FC22  2  # LOAD SET -{B} FOR FC22
+(-)()(U2)(0;1)(B200)(U2)

JACOBIANS
  FC11  FC11  2  1  # FC11: D(FC11)/D(FC11)
 ()()()(0;1)(B200)()

  FC12  FC12  2  1  # FC12: D(FC12)/D(FC12)
 ()()()(0;1)(B200)()

  FC22  FC22  2  1  # FC22: D(FC22)/D(FC22)
 ()()()(0;1)(B200)()

GROUP FREQUENCY
    1
SOLUTION TYPE
  Q
  ILU_GMRES
  IMPLICIT_EULER
END



TITLE            **** TEMPLATE TEMP.PHI ****
   OMEGA - FROM DELXU  (1/99)

RESIDUALS
  OMGA   2    #  VARBL, SET NO.,  --- SPATIAL  SET (OMGA)
 ()()()(2;0)(B201)(U1)
+()()()(4;0)(B202)(U1)
+(-)()()(1;0)(B201)(U2)
+(-)()()(3;0)(B202)(U2)
```

```
JACOBIANS
  OMGA OMGA  2  1  #  VARBL, VARDIF, SET, ALL DIRECTIONS
 ()()()(0;1)(B200)()

GROUP FREQUENCY
      1
SOLUTION TYPE
  Q
  ILU_GMRES
  IMPLICIT_EULER
END

TITLE            **** TEMPLATE TEMP.PHI ****
   DELSQ PSI FROM OMEGA  (1/99)

RESIDUALS
  PSI   2  #  VARBL, SET NO.,  --- SPATIAL  SET (PSI)
 (-)()()(0;1)(B200)(OMGA)

JACOBIANS
  PSI PSI  2  1 # VARBL, VARDIF, SET, ALL DIRECTIONS
 ()()()(1122;-1)(B211)()
+()()()(3344;-1)(B222)()
+()()()(1324;-1)(B221)()
+()()()(1324;-1)(B212)()

GROUP FREQUENCY
      1
SOLUTION TYPE
  Q
  ILU_GMRES
  IMPLICIT_EULER
END

TITLE            **** TEMPLATE TEMP.PHI ****
  ENERGY NORM COMPUTATIONS, ALL VARIABLES/PARAMETERS  (1/99)

RESIDUALS
  DUNC   1   #                    TEMPORAL TERM IN {F(Q)}
 ()()()(0;1)(B200)(-DUNC)

JACOBIANS
  DUNC DUNC   1 1   #             TIME TERM IN {F(Q)}
 ()()()(0;1)(A200)()
  DUNC DUNC   1 2   #             TIME TERM IN {F(Q)}
 ()()()(0;1)(A200)()

NORMS
  OMGE  1  T                           ENERGY NORM FOR OMGA
 (HALF,REI)()(OMGA)(1122;-1)(B211)(OMGA)
 (HALF,REI)()(OMGA)(1324;-1)(B212)(OMGA)
 (HALF,REI)()(OMGA)(1324;-1)(B221)(OMGA)
```

```
 (HALF,REI)()(OMGA)(3344;-1)(B222)(OMGA)

  PSIE  1  T                              ENERGY NORM FOR PSI
 (HALF)()(PSI)(1122;-2)(B211)(PSI)
 (HALF)()(PSI)(1324;-2)(B212)(PSI)
 (HALF)()(PSI)(1324;-2)(B221)(PSI)
 (HALF)()(PSI)(3344;-2)(B222)(PSI)

  U1E  1  T                              ENERGY NORM FOR U1
 (HALF)()(U1)(1122;-1)(B211)(U1)
 (HALF)()(U1)(1324;-1)(B212)(U1)
 (HALF)()(U1)(1324;-1)(B221)(U1)
 (HALF)()(U1)(3344;-1)(B222)(U1)

  U2E  1  T                              ENERGY NORM FOR U2
 (HALF)()(U2)(1122;-1)(B211)(U2)
 (HALF)()(U2)(1324;-1)(B212)(U2)
 (HALF)()(U2)(1324;-1)(B221)(U2)
 (HALF)()(U2)(3344;-1)(B222)(U2)

  PRSE  1  T                              ENERGY NORM FOR PRES
 (HALF)()(PRES)(1122;-1)(B211)(PRES)
 (HALF)()(PRES)(1324;-1)(B212)(PRES)
 (HALF)()(PRES)(1324;-1)(B221)(PRES)
 (HALF)()(PRES)(3344;-1)(B222)(PRES)

  TMPE  1  T                              ENERGY NORM FOR TEMP
 (HALF,PEI)()(TEMP)(1122;-1)(B211)(TEMP)
 (HALF,PEI)()(TEMP)(1324;-1)(B212)(TEMP)
 (HALF,PEI)()(TEMP)(1324;-1)(B221)(TEMP)
 (HALF,PEI)()(TEMP)(3344;-1)(B222)(TEMP)

  PHIE  1  T                              ENERGY NORM FOR PHI
 (HALF)()(PHI)(1122;-1)(B211)(PHI)
 (HALF)()(PHI)(1324;-1)(B212)(PHI)
 (HALF)()(PHI)(1324;-1)(B221)(PHI)
 (HALF)()(PHI)(3344;-1)(B222)(PHI)

GROUP FREQUENCY
      1
SOLUTION TYPE
  DELTA_Q
  FACTORED_GAUSS_ELIMINATION
  IMPLICIT_EULER

END
```

```
TITLE       **** THERMAL CAVITY  MOD.CAV **** (1/99)
  PHI THERMAL CAVITY
INTEGRATION FACTORS
   0.       $   INITIAL_TIME
   6.E6     $   FINAL_TIME
   1.0E-4   $   PROBLEM_CONVERGENCE_CRITERIA
   0.20     $   MAXIMUM_CHANGE_IN_Q_(DQ)
   0.02   $   INITIAL_TIME_STEP
   1.0     $   TIME_STEP_MULTIPLIER
   .02      $   MAXIMUM_TIME_STEP
   0        $   CRITERIA_TO_RAISE_MAX_TIME_STEP
   500       $   MAXIMUM_NUMBER_OF_STEPS
   10       $   MAXIMUM_NUMBER_OF_ITERATIONS_PER_STEP
   1.0E-3   $   ITERATION_CONVERGENCE_CRITERIA
   0.5      $   THETA_IMPLICITNESS_FACTOR
#  1.0      $   THETA_IMPLICITNESS_FACTOR
   1.       $   CONVERGENCE_VARIABLE
GLOBAL SCALARS
  [ 0. 1. -1. 0. 0.  $  HT ONE MONE REI RE2I
    0. 0. .5 0. 0.0  $  GRSH PEI HALF SPHISW BETAT
    0. 2.0 3. .1666 .3333  $  BETA TWO PLTYPE SIXTH THIRD
    0.08333 0.041666 0.0 0.1 0.0  $  OTI TFI RENO CSS MULS
    0.0 0.17 4.0 0.0 0.17  $  MULA CSL FOUR MULB CSB
    0.25 0. 0. ]  $  FOURTH GAMA HP
MATERIALS
    2      1
  [ 0.  ] $  DUM1
  [ 0.  ] T  DUM1
OTHERS
  0  20  T  ISCALR(20) INVDLT
      1  T  INVDLT 3 = DIVIDE THRU BY HP and modify step size using dq
   0 10            T  ISCALR(10)
   1               T  IETKJA
   0 13            T  ISCALR(13)
   8000            T  ITRMAX
  7.              T VECTOR 7
$     COMMON /CTHERM/
$    1    ALC,       GAMMAF,        AEXT0,        AEXT1,        AEXT2,
       1.          1.4           0.0           0.0           0.       # BGU
$    2   UREF,         AREF,       GASCON,         PREF,        PZERO,
     3.63308E-01  0.          4.972E4     2.1168E3     2.1168E3    # BGU
$    3 CONDCT,       GRAVCN,       SPHEAT,        VISCK,          XMW,
       4.175889E-6  32.17398   .237    1.6617525E-4     28.95748   #
BGU
$    4   TREF,         TMAX,         TMIN,        TZERO,       DELTEM,
#    Ra1.0E6
#        67.4515   .3187800E-0  -.3187800E-0    459.6     0.        #
BGU
#    Ra3.4E6
       67.4515   1.08333E-0    -1.08333E-0    459.6     0.        # BGU
#    Ra3.4E7
#       67.4515   1.08333E+1    -1.08333E+1    459.6     0.        #
BGU
```

```
#    Ra3.4E8
#       67.4515   1.08333E+2    -1.08333E+2    459.6     0.        #
BGU
#    Ra6.2E8
#       67.4515   .3187800E+3    -.3187800E+3    459.6     0.        #
BGU
#    test Ra6.2E8
#       67.4515   .6187800E+4    -.6187800E+4    459.6     0.        #
BGU
$    5    BTU,       XMAREF,        XMAIN,       XMAOUT,       TINTFT,
       778.0       0.           0.           0.           12.         # BGU
$    6     CF,         HREF,        HZERO,        CEXT1,        CEXT2,
       0.          0.           0.           0.           0.          # BGU
$    7   SREF,         SMAX,         SMIN,        SZERO,       DELSAL,
       0.          0.           0.           0.           0.          # BGU
$    8  DEXT1,        DEXT2,        DEXT3,        DEXT4,        DEXT5,
       0.          0.           0.           0.           0.         T
$    9 ZXT(60)
#     You can add (or replace) variables that you have incorporated
#        into your 'hooks' files.
#     Numeric entries are free format.
#     Entries, such as AEXT1 etc. are open for your use.
#  N.B.  ALC is the ONLY variable used in the 'main' subroutines.
#          It is set to 1.0, if you do not set it here.
#          It MUST be in position 1 in this COMMON block.
#   END OF CTHERM
#     COMMON /WALLFN/ TINTPR(100),THKNES(100),SKNFRN(100),TMHICK(100)
PRINT
    41    201     1   # GRID SIZE    TOTAL OF    8241 NODES
                 50   # PRINT INTERVAL (STEPS)
           -1    41    # I WINDOW
            1    201   # J WINDOW
            1     1    # K WINDOW
NONE # VARIABLES IN COUT
NONE # VARIABLES FIRST STEP ONLY
((1P,8(1X,5E14.6/),1X,E14.6)) # FORMAT FOR 33x33
GRAPHICS
#  [ X1 X2 TEMP U1 U2 SPHI PRES OMGA PSI T X11 X12 X22 FF11 FF12 FF22
#    FD11 FD12 FD22 FC11 FC12 FC22 FB11 FB12 FB21 FB22 S11 S12 S22
#    RETS FS11 FS12 FS22 S33 S44 RETA FL11 FL12 FL22 SSQ SSQ2 XB1 XB2
#    SBQ2 RETB SG11 SG12 SG22 ]
   [ X1 X2 TEMP U1 U2 PHI SPHI PRES OMGA PSI OMGE PSIE U1E U2E PRSE
     TMPE  ]
# X1 X2 TEMP U1 U2 PHI SPHI PRES OMGA PSI OMGE PSIE U1E U2E PRSE TMPE
T
THREE_INTEGER    T  INTEGER PRINT FIELD
# [ TEMP U1 U2 SPHI PRES OMGA PSI T X11 X12 X22 FF11 FF12 FF22
#   FD11 FD12 FD22 FC11 FC12 FC22 FB11 FB12 FB21 FB22 S11 S12 S22
#   RETS FS11 FS12 FS22 S33 S44 RETA FL11 FL12 FL22 SSQ SSQ2 SBQ2 XB1
#   XB2 RETB SG11 SG12 SG22 ]
# TEMP U1 U2 PHI SPHI PRES OMGA PSI X1 X2 OMGE PSIE U1E U2E PRSE TMPE
T
  [ TEMP U1 U2 PHI SPHI PRES OMGA PSI X1 X2 OMGE PSIE U1E U2E PRSE
```

```
    TMPE ]
DEBUG
 0 $ STEP NUMBER TO PRINT ALL ITERATIONS
 NONE $ TYPE OF DEBUG PRINT
 1 $ ITERATION NUMBER
 1089,1,1 $ I,J,K  LOCATION, (K=0, ALL PLANES)
 ALL $ VARIABLE OR ALL
 ALL $ TERM NUMBER OR (- FOR SET NO.), OR ALL
BOUNDARY CONDITIONS
 WALL_NS  1 [ 41I1 1 199I41 42 199I41 82 41I-1 8241 ]
 DIRI_T   1 [ 201I41 1 201I41 41 ]
INITIAL CONDITIONS
 [201(41*0.)] $ PRES
 [201(41*0.)] $ U1
 [201(41*0.)] $ U2
# [S 101(1.08333. 6R1.11111 0.069116 4R1.25 0. 4R.8 -0.069116
#   6R0.9 -1.08333) S-10. ] $ TEMP # Ra 3.4
#[S 201(1.08333 39*0.0 -1.08333) S-10. ] $ TEMP # Ra3.4E5
#[S 201(1.08333 20R1.0 0.0 20R1.0 -1.08333) S-10. ] $ TEMP # Ra3.4E5
# [S 201(61.87800 20R1.0 0.0 20R1.0 -61.87800) S+100. ] $ TEMP #
Ra6.2E8
# [S 201(3.187800 20R1.0 0.0 20R1.0 -3.187800) S+100. ] $ TEMP #
Ra6.2E8
 [S 201(1.08333 20R1.0 0.0 20R1.0 -1.08333) S-1. ] $ TEMP # Ra3.4E6
# [S 201(1.08333 20R1.0 0.0 20R1.0 -1.08333) S+10. ] $ TEMP # Ra3.4E7
# [S 201(1.08333 20R1.0 0.0 20R1.0 -1.08333) S+100. ] $ TEMP # Ra3.4E8
 [201(41*0.)] $ PHI
 [201(41*0.)] $ OMGA
 [201(41*0.)] $ PSI
 [201(41*0.)] $ UM11
 [201(41*0.)] $ UM12
 [201(41*0.)] $ UM22
 [201(41*0.)] $ UMAG
 [201(41*0.)] $ NUSL
 [201(41*0.)] $ SPHI
 [201(41*0.)] $ SPHL
 [201(41*0.)] $ TAU2
 [201(41*0.)] $ SRCT
 [201(41*1.)] $ EPMN
 [201(41*1.)] $ RET
 [201(41*0.)] $ OMGE
 [201(41*0.)] $ PSIE
 [201(41*0.)] $ PHIE
 [201(41*0.)] $ U1E
 [201(41*0.)] $ U2E
 [201(41*0.)] $ PRSE
 [201(41*0.)] $ TMPE
 [201(41*0.)] $ SCAL
 [201(41*0.)] $ OTLN
 [201(41*0.)] $ MTRL
 [201(41*0.)] $ DETJ
 [201(41*0.)] $ DETC
 [201(41*0.)] $ ETKJ
```

```
 [201(41*0.)] $ EJK2
 [201(41*0.)] $ EJK3
 [201(41*0.)] $ EJK4
 [201(41*0.)] $ EJK5
 [201(41*0.)] $ EJK6
 [201(41*0.)] $ EJK7
 [201(41*0.)] $ EJK8
 [201(41*0.)] $ EJK9
 [201(41*0.)] $ PREL
 [201(41*0.)] $ U1L
 [201(41*0.)] $ U2L
 [201(41*0.)] $ TEML
 [201(41*0.)] $ PHIL
 [201(41*0.)] $ OMGL
 [201(41*0.)] $ PSIL
 [201(41*0.)] $ DUNL
 [ 201(0. 12R1.11111 .181 8R1.25 .5 8R.8 .819 12R0.9 1.0) ] $ X1    74
 [ -41(0. 30R1.11111 .63 70R1.0 4. 70R1.0 7.37 30R0.9 8.) ] $ X2    75
#[65(0. 32R1.0 .5 32R1.0 1.0)] $ X1 # INTERPOLATED
#[-65(0. 32R1.0 .5 32R1.0 1.0)] $ X2 # INTERPOLATED
 [201(41*0.)] T ONES
END
```

Vita

Sunil Sahu was born in Jabalpur, MP, India on August 1st, 1976. He did his undergraduate in Production Engineering at Manohar Bhai Patel Institute of Engineering and Technology, Gondia, Maharashtra, India graduating in July 1998. Later he joined as a Planning Engineer in Thermal Systems Hyd. Pvt. Ltd., Hyderabad, India. In January 2000 he moved to United States to pursue a Masters degree in Mechanical Engineering at Tennessee Technological University, Cookeville, TN. He finished his Masters degree in December 2001 and joined University of Tennessee in January 2002 to continue with his doctoral studies in Mechanical Engineering.